12. SITE 667[1]

Shipboard Scientific Party[2]

HOLE 667A

Date occupied: 8 April 1986, 1948 UTC

Date departed: 12 April 1986, 1000 UTC

Time on hole: 86.2 hr

Position: 4°34.15′N, 21°54.68′W

Water depth (sea level; corrected m, echo-sounding): 3529.3

Water depth (rig floor; corrected m, echo-sounding): 3539.8

Bottom felt (rig floor; m, drill pipe measurement): 3535.5

Distance between rig floor and sea level (m): 10.5

Total depth (rig floor, m): 3916.8

Penetration (m): 381.3

Number of cores (including cores with no recovery): 41

Total length of cored section (m): 381.3

Total core recovered (m): 309.2

Core recovery (%): 81.0

Oldest sediment cored:
Depth (mbsf): 381.3
Nature: calcareous nannofossil ooze and chalk
Age: Oligocene
Measured velocity (km/s): 1.9

HOLE 667B

Date occupied: 12 April 1986, 1125 UTC

Date departed: 13 April 1986, 0800 UTC

Time on hole: 21.6 hr

Position: 4°34.15′N, 21°54.68′W

Water depth (sea level; corrected m, echo-sounding): 3529.3

Water depth (rig floor; corrected m, echo-sounding): 3539.8

Bottom felt (rig floor; m, drill pipe measurement): 3535.2

Distance between rig floor and sea level (m): 10.5

Total depth (rig floor, m): 3674.3

Penetration (m): 139.1

Number of cores (including cores with no recovery): 15

Total length of cored section (m): 139.1

Total core recovered (m): 128.6

Core recovery (%): 92.4

Oldest sediment cored:
Depth (mbsf): 139.1
Nature: slump deposit; calcareous nannofossil silty clay
Age: late Miocene (~10–9 Ma)
Measured velocity (km/s): 1.54

Principal results: Site 667 is located in the eastern equatorial Atlantic at 4°34.15′N, 21°54.68′W, at a water depth of 3525.0 m in a small, flat-floored basin lying on the western margin of the Sierra Leone Rise (see "Background and Scientific Objectives" section, this chapter). The acoustic layering is moderately stratified and reflective, and the sediments are draped over the underlying basement (see "Background and Scientific Objectives" section, this chapter). Our primary objective was to obtain a Pliocene–Pleistocene sequence from relatively shallow water depths for use as part of a depth transect to study deep-water isolation in the eastern equatorial Atlantic. A secondary objective was to use this set of cores for monitoring long-term fluxes in $CaCO_3$ from surface waters, along with $CaCO_3$ dissolution and downslope redistribution. We also planned to core a single, deeper hole to retrieve a long Neogene sequence for biostratigraphic and paleomagnetic studies.

From Hole 667A, we recovered 23 advanced piston corer (APC) cores and 18 extended-core-barrel (XCB) cores to a total penetration depth of 381.3 mbsf, with average recovery of 81.0%. From Hole 667B, we cored 15 APC cores to a total depth of 139.1 mbsf, with average recovery of 92.4%.

Hole 667A contains six lithologic units (Fig. 1). *Unit I* (0–20.3 mbsf) is Pleistocene foraminifer-nannofossil ooze, clay-bearing foraminifer-nannofossil ooze, and foraminifer-nannofossil ooze, with secondary amounts of clay and lesser amounts of opal. *Unit II* (20.3–66.5 mbsf) is upper-Pliocene to lower-Pleistocene, clay-bearing foraminifer-nannofossil ooze and foraminifer-bearing nannofossil ooze, with secondary amounts of clay and accessory minerals and trace amounts of opal. *Unit III* (66.5–124.3 mbsf) is upper-Miocene to lower-Pliocene, foraminifer-nannofossil ooze; clay-bearing, foraminifer-bearing nannofossil ooze; and brownish-red, clay-bearing nannofossil ooze, with secondary clay and accessory minerals. *Unit IV* (124.3–148.3 mbsf) is an upper-Miocene slump deposit consisting of a mixture of lithologies similar to lithologic Units III and VI. *Unit V* (148.3–198.8 mbsf) is middle-Miocene, mud-bearing nannofossil ooze; foraminifer-bearing, clayey nannofossil ooze; and foraminifer-bearing nannofossil ooze, with substantial amounts of clay and lesser amounts of quartz and accessory minerals.

Unit VI (198.8–376.5 mbsf) is Oligocene to middle-Miocene, silt-bearing, clay-bearing nannofossil ooze; muddy nannofossil ooze; and clayey nannofossil chalk interbedded with silt-bearing, siliceous-bearing, clay-bearing nannofossil ooze; nannofossil-bearing, siliceous-

[1] Ruddiman, W., Sarnthein, M., Baldauf, J., et al., 1988. *Proc., Init. Repts. (Pt. A), ODP*, 108.

[2] William Ruddiman (Co-Chief Scientist), Lamont-Doherty Geological Observatory, Palisades, NY 10964; Michael Sarnthein (Co-Chief Scientist), Geologisch-Paläontologisches Institut, Universität Kiel, Olshausenstrasse 40, D-2300 Kiel, Federal Republic of Germany; Jack Baldauf, ODP Staff Scientist, Ocean Drilling Program, Texas A&M University, College Station, TX 77843; Jan Backman, Department of Geology, University of Stockholm, S-106 91 Stockholm, Sweden; Jan Bloemendal, Graduate School of Oceanography, University of Rhode Island, Narragansett, RI 02882-1197; William Curry, Woods Hole Oceanographic Institution, Woods Hole, MA 02543; Paul Farrimond, School of Chemistry, University of Bristol, Cantocks Close, Bristol BS8 1TS, United Kingdom; Jean Claude Faugeres, Laboratoire de Géologie-Océanographie, Université de Bordeaux I, Avenue des Facultés Talence 33405, France; Thomas Janacek, Lamont-Doherty Geological Observatory, Palisades, NY 10964; Yuzo Katsura, Institute of Geosciences, University of Tsukuba, Ibaraki 305, Japan; Hélène Manivit, Laboratoire de Stratigraphie des Continents et Océans, (UA 319) Université Paris VI, 4 Place Jussieu, 75230 Paris Cedex, France; James Mazzullo, Department of Geology, Texas A&M University, College Station, TX 77843; Jürgen Mienert, Geologisch-Paläontologisches Institut, Universität Kiel, Olshausenstrasse 40, D-2300 Kiel, Federal Republic of Germany, and Woods Hole Oceanographic Institution, Woods Hole, MA 02543; Edward Pokras, Lamont-Doherty Geological Observatory, Palisades, NY 10964; Maureen Raymo, Lamont-Doherty Geological Observatory, Palisades, NY 10964; Peter Schultheiss, Institute of Oceanographic Sciences, Brook Road, Wormley, Godalming, Surrey GU8 5UG, United Kingdom; Rüdiger Stein, Geologisch-Paläontologisches Institut, Universität Giessen, Senckenbergstrasse 3, 6300 Giessen, Federal Republic of Germany; Lisa Tauxe, Scripps Institution of Oceanography, La Jolla, CA 92093; Jean-Pierre Valet, Centre des Faibles Radioactivités, CNRS, Avenue de la Terrasse, 91190 Gif-sur-Yvette, France; Philip Weaver, Institute of Oceanographic Sciences, Brook Road, Wormley, Godalming, Surrey GU8 5UG, United Kingdom; Hisato Yasuda, Department of Geology, Kochi University, Kochi 780, Japan.

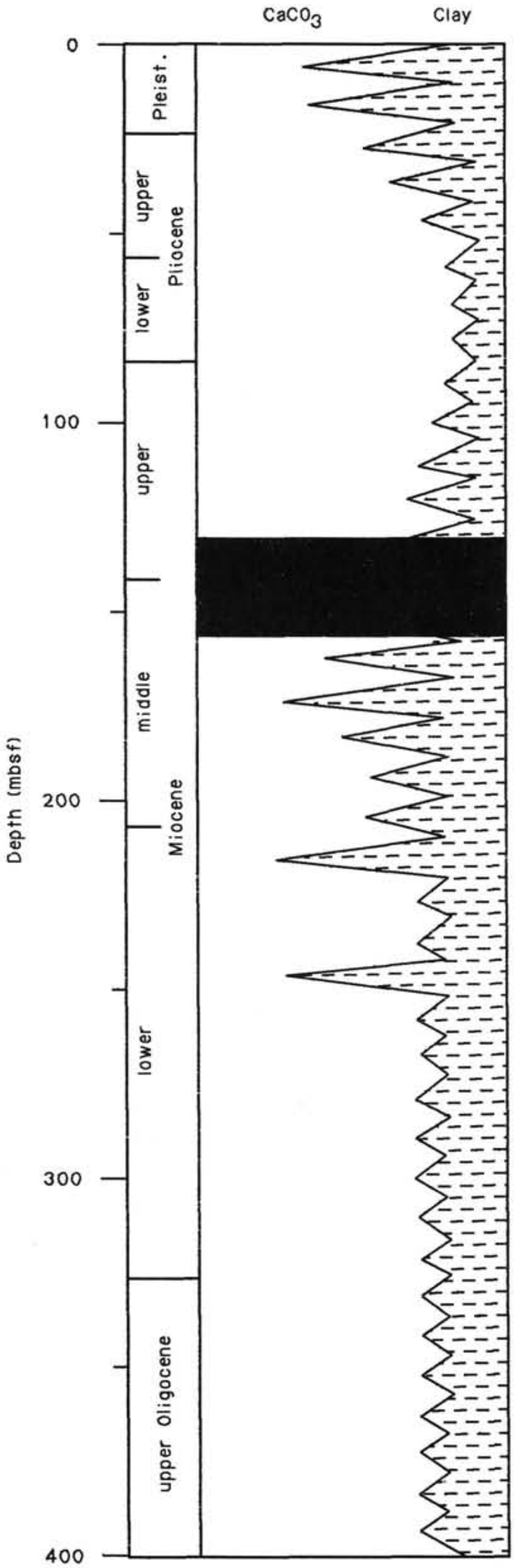

Figure 1. Biostratigraphic and lithostratigraphic summary of Site 667. Black layer indicates slump unit. Below 200 mbsf, clay facies contains higher silica content, and sediments are far more indurated. Schematic $CaCO_3$ cycles show general range of $CaCO_3$ variations.

bearing claystone; and silt-bearing siliceous clay. Quartz is a secondary component. Below 210 mbsf, the degree of induration increases markedly.

The calcareous microfossils showed good-to-moderate preservation throughout the section, whereas preservation of diatoms fluctuated greatly. Paleomagnetic stratigraphy at Site 667 provided only three datum levels because of strong overprinting at depth. Nannofossils and planktonic foraminifers provided 37 additional levels for chronostratigraphic constraints. One-half these datums occur in the well-defined upper Miocene to Holocene part of the section (8.8–0 Ma). The biostratigraphic coverage is much poorer before a middle-Miocene hiatus or interval of slow deposition (14.0–8.8 Ma). Aside from this interval, sedimentation rates throughout the entire section vary within a narrow range (13 to 20 m/m.y.).

The long-term depositional history at Site 667 reflects the northward plate-tectonic movement of the site. The higher concentrations of biogenic opal in the upper Oligocene to the middle Miocene suggest a location under the high-productivity, surface-water conditions that occur at the equatorial divergence, and the subsequent loss of silica then may reflect drift of the site into lower-productivity waters (Stein, 1985). The possible middle to upper Miocene hiatus at Site 667 partly overlaps similar hiatuses at Site 366 (see DSDP Leg 41, Site 366 chapter). Pelagic deposition was disrupted in the late Miocene by a slump.

Cyclic variations of clay and carbonate over depth scales of about 60–70 cm were typical of all intervals from the upper Miocene to the lower Pliocene and are similar to cycles reported from Site 366 (Dean et al., 1978). High concentrations of foraminifers in lower Pliocene to lower Pleistocene sediments (4.0–1.5 Ma) suggest winnowing of the coarse fraction, although turbidite deposition of some of these layers also is possible. Increased percentages of clay in the Pleistocene sediments agree with trends observed in most preceding sites.

BACKGROUND AND SCIENTIFIC OBJECTIVES

Site 667 (target Site Eq-4b) was the third site in the Sierra Leone Rise depth transect (see Fig. 2, "Background and Scientific Objectives" section, Site 665 chapter). Two groups of objectives were planned for this site: one group was related to the large bathymetric gradients in this limited area (for a full discussion see "Background and Scientific Objectives" section, Site 665 chapter), and the other group was based on the role of this site in the total paleoenvironmental coverage provided by all Leg 108 sites. For our paleoenvironmental objectives, the deeper penetration planned for this site was intended to extend the Neogene record obtained at other Sierra Leone Rise sites back into the late Paleogene.

The depth-related late Neogene objectives were as follows:

1. To determine the history of relative isolation of eastern Atlantic deep waters, based on depletion of $\delta^{13}C$ ratios in benthic foraminifers and on organic-carbon content. Although Site 667 lies well above the 3800- to 4000-m depth at which partial isolation of the eastern basins becomes apparent, it is positioned to record unusually shallow manifestations of this phenomenon.
2. To assess the flux of $CaCO_3$ from the surface waters, the dissolution of $CaCO_3$ by deep waters, and the redistribution of all sediment components by bottom currents. Dean et al. (1981) found strong cyclicity in records of percentages of $CaCO_3$ from Sierra Leone Rise Site 366, with periods of 30,000 to 50,000 yr dominant from the Oligocene to middle Miocene, and periods of 7,000 to 21,000 yr dominant during the Eocene. We planned to determine any periodicity in the Site 667 $CaCO_3$ record of the late Miocene to Holocene, an interval thoroughly deformed by rotary drilling at Site 366. In addition, we planned to refine the early Miocene and late Paleogene $CaCO_3$ signals, based on improved stratigraphy.

Regional paleoenvironmental objectives were as follows:

1. To measure fluxes of eolian dust and freshwater diatoms as indicators of continental source-area aridity and of wind strength during the late Paleogene and Neogene.

2. To monitor late Neogene changes in surface-water temperature using assemblages of planktonic foraminifers and other indicators.

3. To obtain a high-quality late Paleogene and Neogene reference section of $CaCO_3$-rich equatorial sediments for detailed biostratigraphic and paleomagnetic studies.

4. To monitor the late Paleogene and Neogene deposition of opaline silica to see whether the decrease in opaline silica deposition after the middle Miocene at Site 366 also was recorded here. Stein (1985) interpreted this change as indicating a northward plate-tectonic drift of this site out of the equatorial high-productivity area.

Geologic and Topographic Setting

Site 667 is located in the eastern equatorial Atlantic in a small, flat-floored basin lying on the western margin of the Sierra Leone Rise (Figs. 2 and 3; see also Fig. 2 in Site 665 chapter). Air-gun records from this region show at least 1.2 s of sediment above acoustic basement (Fig. 3). Layering is well-stratified and moderately reflective and is draped over the underlying basement in the style characteristic of pelagic sediments. Little variation in thickness of the basin sediment fill is apparent in the seismic records, except for thinning around the steep-walled margins, where basement rises to or close to the surface. Site 667 was chosen at a point where the upper 0.5 s of sediment was slightly thicker than average and the sub-bottom reflectors particularly flat-lying (Fig. 2). The echogram character from this region has strong, nearly flat-lying, sub-bottom reflectors, and small swales in the near-surface relief. These features suggest some redistribution of sediment, but indicate predominant pelagic deposition.

The basement age at Site 667 is Cretaceous (about 80 Ma), based on the ages obtained at Site 366. The sediment section from the upper 400 m is lower Oligocene to Holocene nannofossil oozes and marls, with possible middle-Miocene unconformities.

OPERATIONS

After departing Site 666, we steamed at 13 kt to a way point at 4°27′N, 21°34′W, where we slowed to 5 kt at 0535 UTC on 8 April 1986, and streamed out our geophysical gear (80-in.^3 water guns and a magnetometer) to begin surveying Site 667. We followed a course of 243° to a second point at 4°22′N, 21°44′W, turning at 0730 UTC to a course of 320°. (All times are expressed as UTC, Universal Time Coordinated, formerly GMT, Greenwich Mean Time.) We held that course to a third way point at 4°35′N, 21°55′W, where we turned at 1051 to a course of 270°. We then held a westward course to a final way point at 4°35′N, 21°59.5′W, where we turned at 1146 to a course of 096°. We kept to that course to the eventual location of Site 667 at 4°34.15′N, 21°54.68′W (3529.3 m water depth by the precision depth recorder).

On our first pass over the site location, we dropped a homemade "poor-boy" buoy as a marker at 1245, turned and pulled in our geophysical gear, and then returned to this buoy marker, dropping a beacon at 1329 on 8 April. By 1345, we were positioned over the beacon at Site 667, and we began running drill pipe into Hole 667A.

We finished running pipe into Hole 667A at 1915; the first advanced piston corer (APC) core (108-667A-1H), which established the mud line at a 3525.0-m water depth, came on deck at 2003 on 8 April. We then cored continuously with the APC un-

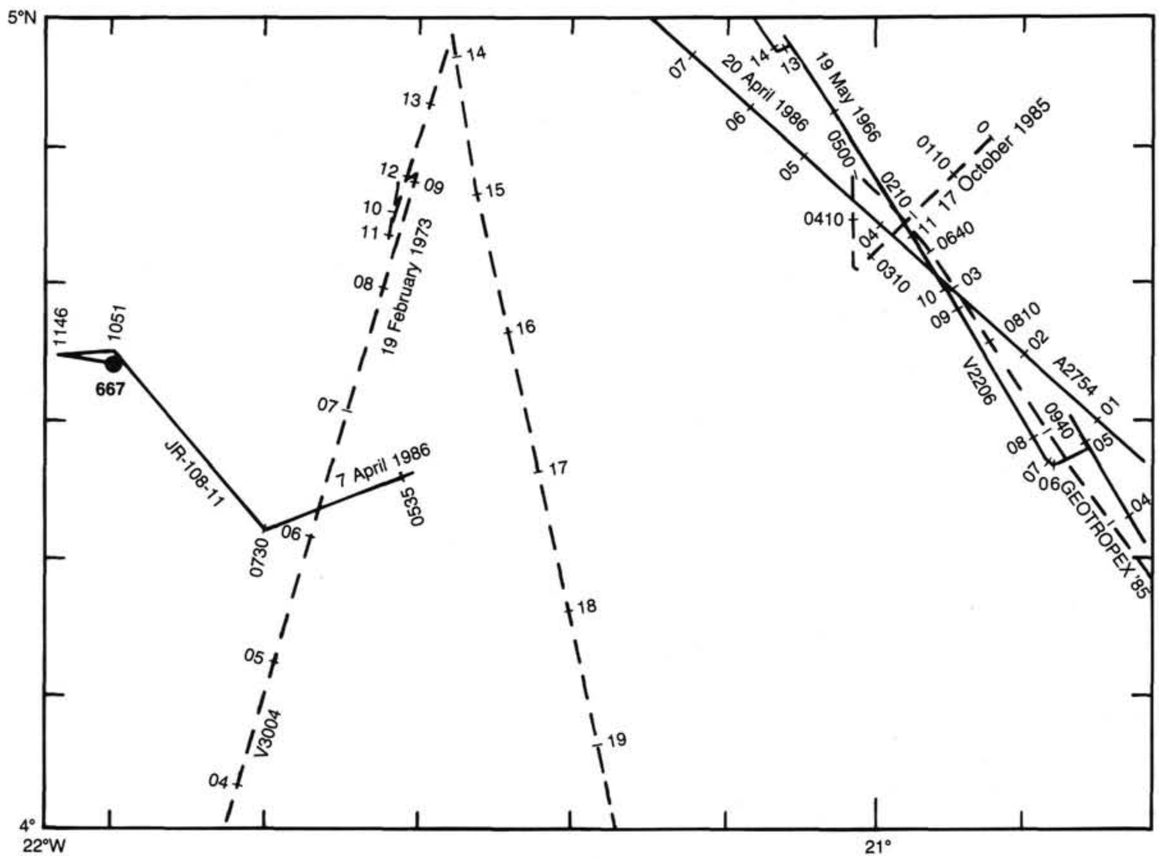

Figure 2. Seismic track lines near Site 667.

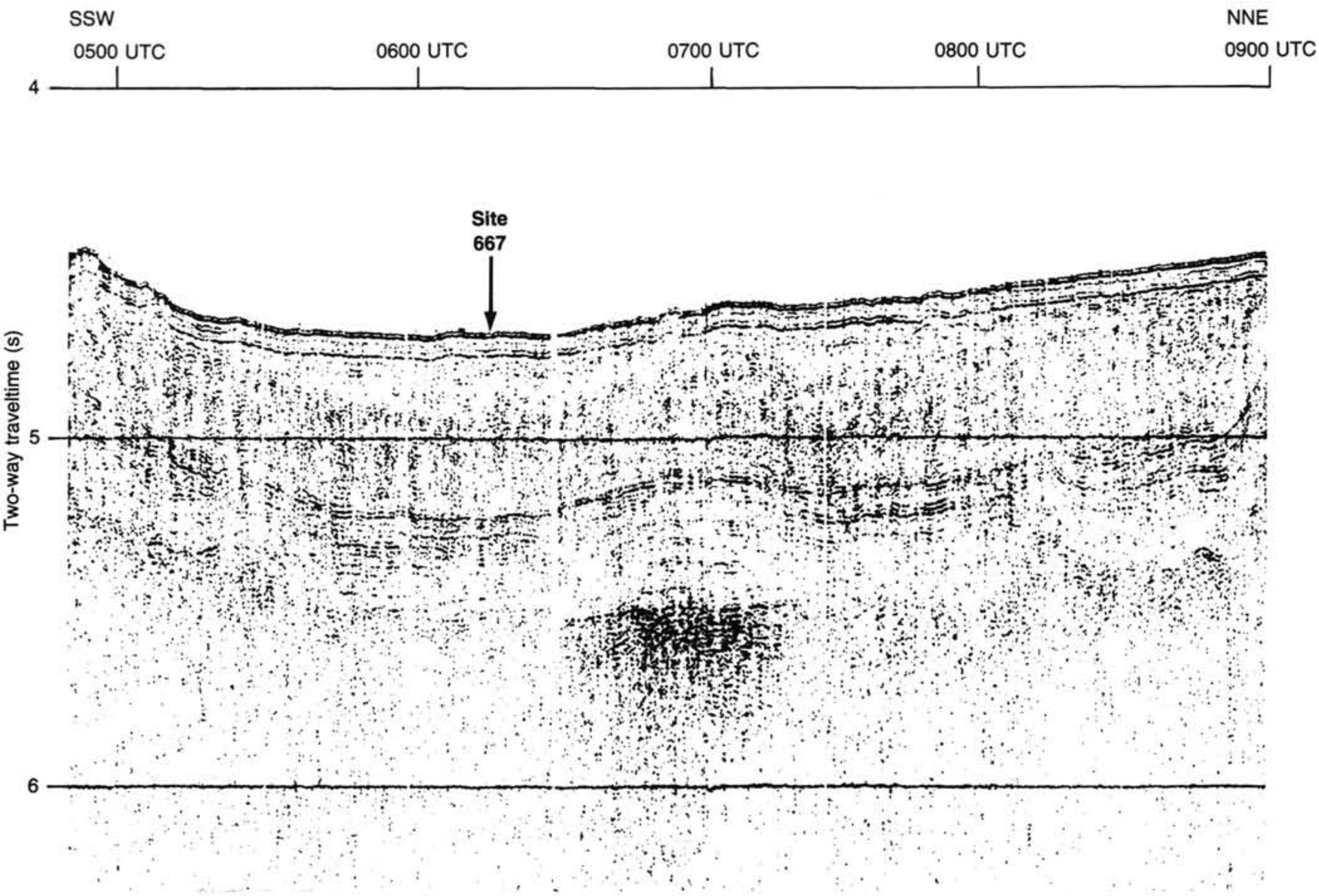

Figure 3. Seismic-reflection record from cruise V3004 near Site 667.

til Core 108-667A-23H came aboard at 1755 on 9 April (Table 1). We then switched to XCB coring. We cored continuously with the XCB until Core 108-667A-36X came on deck at 1434 on 10 April.

From 1445 to 1600 on 10 April, the hole was swept with mud and several stands of pipe pulled to position the drill string near the mud line. At 1600, we began a combined test of a side-entry sub and logging of Hole 667A. Sheaves for the side-entry sub were rigged, and a dummy tool was run to a 3675-m water depth. In our first attempt with the logging tool from 0000 to 0100 on 11 April, the tool failed at 500 m and was retrieved. The problem was traced to a swivel (slip ring) on top of this tool.

In a second attempt from 0745 to 0900, the tool failed at a 3360-m water depth, and this time the problem was traced to a short circuit in the logging-tool cable. The tool then was retrieved from 0900 to 1330. At this point, concern over the inability of a line clamp in the side-entry sub to hold the weight of the logging tool ended testing.

At 1330, we began running drill pipe back down into Hole 667A to start XCB coring at the depth where we previously had stopped (333.8 mbsf). Core 108-667A-36X came on deck at 1619 on 11 April, and we XCB-cored continuously through the last core (108-667A-41X), which came on deck at 2305.

From 2315 to 2400 on 11 April, we swept the hole with mud to condition it for additional logging. From 0000 to 0045 on 12 April, we pulled several stands of pipe to position the drill string near the mud line (3525.0 m). From 0045 to 0115, we rigged for conventional logging (without the side-entry sub). From 0115 to 0800, we ran in with the logging tool, which failed once more at 3667 m (142 mbsf). The logging tool then was retrieved; we ran the drill bit into the hole to fill it with mud and were finished by 0930 on 12 April.

From 0930 to 1000, we pulled out of Hole 667A and offset drill pipe 15 m to the south for Hole 667B. Our first attempt brought back Core 667B-1H at 1145 on 12 April and established the mud line at 3524.7 m. We then APC-cored continuously and measured heat flow for Cores 108-667B-6H, -667B-8H, -667B-11H, and -667B-14H. The final APC core (108-667B-15H) came on deck at 0020 on 13 April. We then began pulling out of Hole 667B, had the drill string back on deck, and were under way to Site 668 by 0800 on 13 April.

LITHOSTRATIGRAPHY AND SEDIMENTOLOGY

On the basis of sedimentology and color, Site 667 can be divided into six lithologic units. Unit I consists of alternating layers of foraminifer-nannofossil ooze; clay-bearing, foraminifer-nannofossil ooze; and foraminifer-bearing, muddy nannofossil ooze. Unit II consists of coarser-grained foraminifer-nannofossil oozes interbedded with foraminifer sands. Unit III consists of beds of white to light gray foraminifer-nannofossil ooze and nannofossil ooze interbedded with light yellowish brown to pale brown muddy nannofossil ooze. Unit IV is a slump (approximately 10 m thick) composed of lithologies similar to those found in Unit III. Unit V consists of beds of nannofossil oozes and clayey nannofossil oozes interbedded with silty clay. Unit VI consists of muddy nannofossil ooze and clayey nannofossil chalk interbedded with siliceous-bearing nannofossil ooze and claystone. Each unit is described in detail next.

Table 1. Site 667 coring summary (drilling depths).

Core no.	Date (April 1986)	Time (UTC)	Depths (mbsf)	Length cored (m)	Length recovered (m)	Recovery (%)
Hole 667A						
1H	8	2003	0-1.3	1.3	1.4	105.0
2H	8	2045	1.3-10.8	9.5	9.3	97.9
3H	8	2142	10.8-20.3	9.5	9.5	100.0
4H	8	2233	20.3-29.8	9.5	9.0	94.4
5H	8	2335	29.8-39.3	9.5	9.0	94.2
6H	9	0115	39.3-48.8	9.5	8.7	91.0
7H	9	0235	48.8-58.3	9.5	8.1	84.9
8H	9	0340	58.3-67.8	9.5	8.2	85.8
9H	9	0445	67.8-77.3	8.5	8.4	98.5
10H	9	0535	77.3-86.8	9.5	8.2	86.5
11H	9	0625	86.8-96.3	9.5	7.9	82.8
12H	9	0720	96.3-105.8	9.5	7.9	83.6
13H	9	0810	105.8-115.3	9.5	9.1	95.9
14H	9	0904	115.3-124.8	9.5	9.0	95.1
15H	9	1025	124.8-134.3	9.5	9.6	101.0
16H	9	1118	134.3-143.8	9.5	9.1	95.3
17H	9	1216	143.8-153.3	9.5	7.6	79.7
18H	9	1313	153.3-162.8	9.5	9.7	102.0
19H	9	1414	162.8-172.3	9.5	7.7	81.1
20H	9	1510	172.3-181.8	9.5	9.2	96.8
21H	9	1608	181.8-191.3	9.5	9.6	101.0
22H	9	1700	191.3-200.8	9.5	9.5	100.0
23H	9	1755	200.8-210.3	9.5	9.9	104.0
24X	9	2007	210.3-219.8	9.5	4.7	49.7
25X	9	2138	219.8-229.3	9.5	5.4	57.0
26X	9	2305	229.3-238.8	9.5	4.7	49.9
27X	10	0040	238.8-248.3	9.5	6.0	63.1
28X	10	0125	248.3-257.8	9.5	4.8	50.5
29X	10	0330	257.8-267.3	9.5	9.2	97.1
30X	10	0445	267.3-276.8	9.5	8.0	84.4
31X	10	0600	276.8-286.3	9.5	5.4	57.0
32X	10	0700	286.3-295.8	9.5	8.6	90.6
33X	10	0905	295.8-305.3	9.5	6.0	62.8
34X	10	1048	305.3-314.8	9.5	6.9	72.7
35X	10	1248	314.8-324.3	9.5	6.0	62.7
36X	10	1434	324.3-333.8	9.5	5.6	59.2
37X	11	1619	333.8-343.3	9.5	7.9	82.8
38X	11	1755	343.3-352.8	9.5	6.7	70.1
39X	11	1934	352.8-362.3	9.5	4.3	45.0
40X	11	2105	362.3-371.8	9.5	8.8	92.9
41X	11	2305	371.8-381.3	9.5	4.7	49.3
Hole 667B						
1H	12	1145	0-6.1	6.1	6.1	100.0
2H	12	1234	6.1-15.6	9.5	8.5	89.0
3H	12	1323	15.6-25.1	9.5	6.0	63.5
4H	12	1409	25.1-34.6	9.5	4.5	47.8
5H	12	1455	34.6-44.1	9.5	8.2	86.2
6H	12	1557	44.1-53.6	9.5	9.8	102.0
7H	12	1642	53.6-63.1	9.5	9.3	97.3
8H	12	1740	63.1-72.6	9.5	8.8	92.1
9H	12	1829	72.6-82.1	9.5	9.6	100.0
10H	12	1931	82.1-91.6	9.5	9.7	102.0
11H	12	2041	91.6-101.1	9.5	9.7	102.0
12H	12	2150	101.1-110.6	9.5	9.8	103.0
13H	12	2233	110.6-120.1	9.5	9.6	101.0
14H	12	2325	120.1-129.6	9.5	9.8	103.0
15H	13	0020	129.6-139.6	10.0	9.4	93.6

H = hydraulic piston. X = extended-core barrel. UTC = Universal Time Coordinated.

Unit I

Cores 108-667A-1H through -667A-3H, CC; depth, 0-20.3 mbsf; age, Pleistocene (1.5-0 Ma).
Core 108-667B-1H through Section 108-667B-3H-4, 37 cm; depth, 0-19.0 mbsf; age, Pleistocene (1.5-0 Ma).

Unit I consists of interbedded foraminifer-nannofossil ooze; clay-bearing, foraminifer-nannofossil ooze; and foraminifer-bearing, muddy nannofossil ooze, which vary in color from dark brown to light yellowish brown. This unit generally is weakly bioturbated. The carbonate content of this unit varies from 20% to 80% (Fig. 4). The principal noncarbonate dilutant is clay, whereas opal concentrations generally range from trace amounts up to 10%. Quartz is a minor component (0%-10%) within this unit.

Unit II

Cores 108-667A-4H through -667A-8H, CC; depth, 20.3-66.5 mbsf; age, early Pliocene to early Pleistocene (approximately 4-1.5 Ma).
Sections 108-667B-3H-4, 37 cm, through -667B-9H-4, 100 cm; depth, 19.0-78.1 mbsf; age, early Pliocene to early Pleistocene.

Unit II consists of clay-bearing, foraminifer-bearing nannofossil ooze and foraminifer-nannofossil ooze, generally light gray to white. Coarse foraminifer sands, generally white, are interbedded in this unit. The foraminifer-nannofossil ooze and clay-bearing, foraminifer-bearing nannofossil ooze exhibit both graded and reverse-graded bedding. Contacts with the foraminifer sands are sharp, often at both the upper and lower contacts. Bioturbation within this unit varies from weak to moderate in the nannofossil ooze, is generally weaker in the foraminifer-nannofossil ooze, and is absent in the foraminifer sands.

Carbonate content for this unit varies from 60% to 80% (Fig. 4). Biogenic opal is rare to absent throughout this unit. The principal noncarbonate dilutants are clay (5% to 35%) and accessory minerals (up to 10%).

Unit III

Cores 108-667A-9H through -667A-14H, CC; depth, 66.5-124.3 mbsf; age, late Miocene to early Pliocene.
Sections 108-667B-9H-4, 100 cm, through -667B-14H-2, 130 cm; depth, 78.1-122.9 mbsf; age, late Miocene to early Pliocene.

Unit III consists of white foraminifer-nannofossil ooze; clay-bearing, foraminifer-bearing nannofossil ooze; and clay-bearing nannofossil ooze interbedded with very pale brown to light yellowish brown, muddy nannofossil ooze. The unit shows cyclic bedding of the white and brown beds and is weakly to moderately bioturbated throughout. The cycles appear to be from 60 to 90 cm long. Within this unit, a small slump occurs in Cores 108-667A-10H-2 through -667A-10H-3, 60 cm, and Cores 108-667B-10H-5, 110 cm, through -667B-10H-6, 110 cm.

The carbonate content of this unit varies from 70% to 80% (Fig. 4). The principal noncarbonate dilutant is clay (up to 20%) and accessory minerals (up to 5%). Biogenic opal, calcite, and dolomite are present as trace components within this unit.

Unit IV

Core 108-667A-15H through Section -667A-17H-3, 150 cm; depth, 124.3-148.3 mbsf; age, late Miocene.
Sections 108-667B-14H-2, 130 cm, through -667B-15H, CC; depth 122.9-139.6 mbsf; age, late Miocene.

Unit IV is a slump deposit. This unit is a mixture of sediments similar in lithology to Unit III that have been extremely distorted because of the slump. A debris flow within this unit appears to consist of sediments similar in lithology to Unit VI. The slump is composed of blocks and pebbles of light greenish gray to greenish gray nannofossil silty clay. The bedding is extremely contorted, and most of the primary structures have been lost.

Unit V

Sections 108-667A-17H-4 to -667A-22H-5, 150 cm; depth, 148.3-198.8 mbsf; age, middle Miocene.

Unit V consists of white to very pale brown, mud-bearing nannofossil ooze; foraminifer-bearing, clayey nannofossil ooze; and foraminifer-bearing nannofossil ooze interbedded with yel-

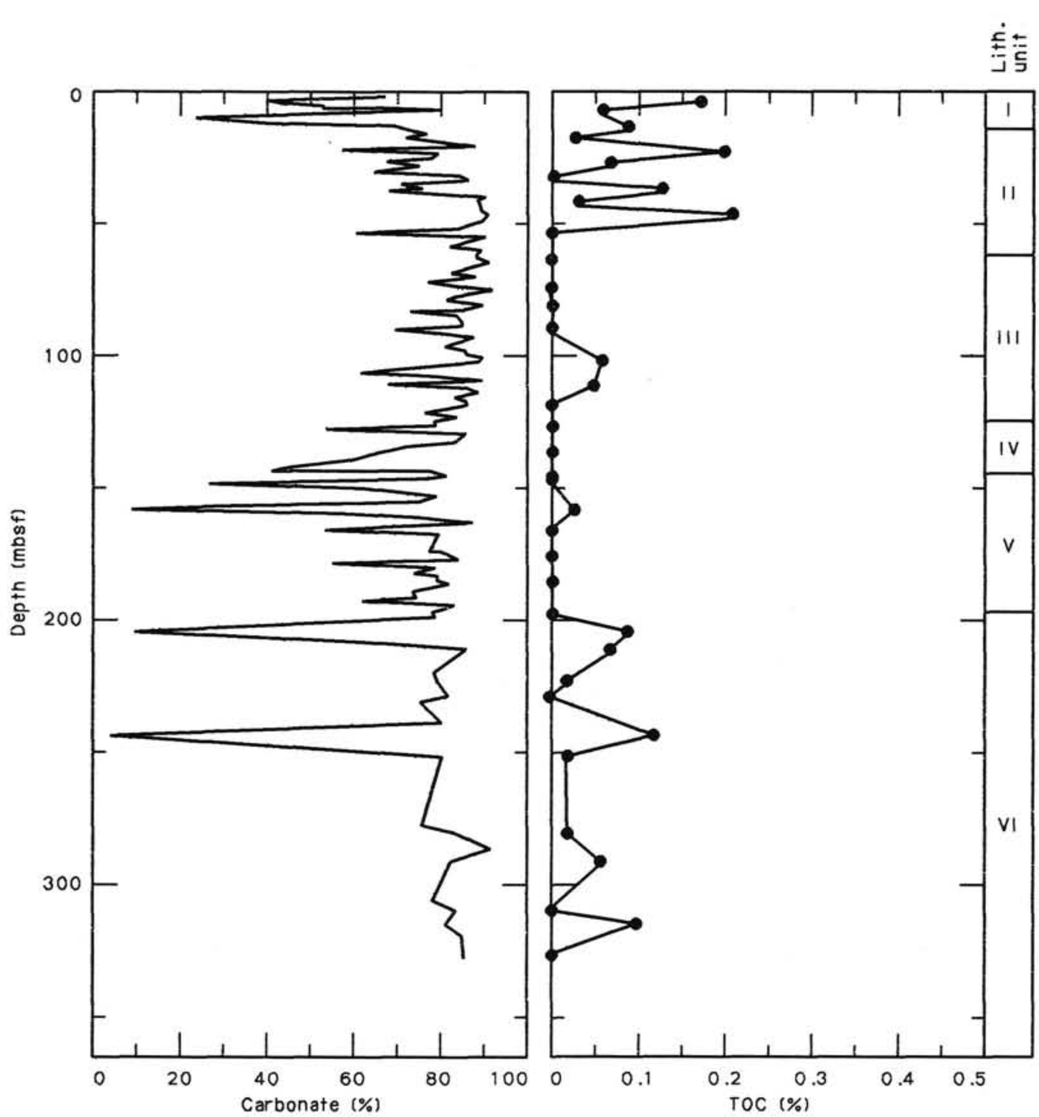

Figure 4. Percentages of carbonate and total organic carbon (TOC) for Site 667.

low and brownish yellow, nannofossil-bearing silty clay. The lithologies occur in uniform cycles that vary in thickness from 60 to 70 cm. The unit is moderately to severely bioturbated throughout.

The carbonate content of this unit varies from less than 20% to greater than 80% (Fig. 4). Clay concentrations up to 85% cause the lowest carbonate concentrations. Quartz concentrations vary up to 10%, whereas accessory minerals occur in concentrations up to 15%. Biogenic opal occurs only in trace amounts.

Unit VI

Cores 108-667A-22H-6 through -667A-41X, CC; depth, 198.8-376.5 mbsf; age, late Oligocene to middle Miocene.

Unit VI consists of light greenish gray, silt-bearing, clay-bearing nannofossil ooze; muddy nannofossil ooze; and clayey nannofossil chalk interbedded with greenish gray to grayish green, silt-bearing, siliceous-bearing, clay-bearing, nannofossil ooze; nannofossil-bearing, siliceous-bearing claystone; and silt-bearing siliceous clay. Below Core 108-667A-24X (219.8 mbsf), sediments are extremely indurated. This unit is moderately bioturbated throughout, and well-preserved planulites, chrondrites, and *Zoophycus* burrows are abundant. The unit has been brecciated by drilling disturbance caused by the XCB.

The carbonate content of this unit varies from near 0% to greater than 80% (Fig. 4). The lowest carbonate values occur in clays and claystones, although biogenic opal is a significant component (up to 45%) of this unit. Clay concentrations reach 50% in this unit, and quartz concentrations vary up to about 15%.

Depositional Environment

The sedimentation history at this site reflects changes in geographic position relative to the equatorial high-productivity zone and changes in the reworking of sediments because of bottom-current scouring. From the late Oligocene to the middle Miocene, high concentrations of biogenic opal in these sediments show that the productivity in the surface water above this site was generally high. Continuous pelagic deposition occurred throughout the middle Miocene, but the concentration of biogenic opal decreased significantly. At this time, sediment deposition was cyclic with average cycle thicknesses of 60 to 70 cm. Pelagic deposition was interrupted in the late Miocene by a slump that mixed older, more siliceous material with clay-rich deposits. Cyclic deposition of clay-rich and clay-poor nannofossil ooze resumed in the late Miocene and continued until the early Pliocene (approximately 4 Ma). From the early Pliocene to the early Pleistocene (approximately 4 to 1.5 Ma), sediments at this site have significantly higher concentrations of foraminifers. Foraminifer sands are common and may be the result of either winnowing or turbidite deposition. At this time, bottom-current scouring may have removed significant portions of the finer material (both clays and nannofossils). Normal pelagic sedimentation resumed at about 1.5 Ma and continued throughout the Quaternary. Throughout this interval, increased clay concentrations suggest that eolian material became a significant component in the sediments deposited at this site.

BIOSTRATIGRAPHY

Two holes were drilled at Site 667 on the southern slope of the Sierra Leone Rise in a water depth of 3525.0 m. Forty-one cores were retrieved from Hole 667A, and 15 cores were recovered from Hole 667B. The recovered sediments are early Oligocene through Holocene in age and display continuous deposition from the early to late Miocene through Holocene and from the late to early Oligocene through the early to middle Miocene (Figs. 5 and 6). Just over 5 m.y. of the middle Miocene is represented by a hiatus (8.7–14.0 Ma). The depth of the hiatus coincides with obvious slump deposits (Cores 108-667A-15H through -667A-17H), which consist of lower Miocene and early to middle Miocene sediment.

Calcareous microfossils show good-to-moderate preservation in most of the samples investigated and occur throughout the entire sequence. Roughly one-half of the core-catcher samples were barren of diatoms, and strong variations in preservation were observed over relatively short stratigraphic distances. Both planktonic foraminifers and nannofossils show greater diversity in the shallow cores. Together, these three groups provide 38 biochronologic datums that were used to establish the sediment-accumulation rate patterns (see "Sediment-Accumulation Rates" section, this chapter). Of these 38 datums, 19 occur between 0 Ma and 8.85 Ma, and 19 occur in the 20 m.y. interval recovered below the middle Miocene hiatus. Thus, the biostratigraphic resolution is poor during pre-middle Miocene times and good during post-middle Miocene times. Similar differences exist regarding the chronological reliability of the datums, with the largest uncertainties in the pre-middle Miocene group of datums.

Calcareous Nannofossils

The 41 cores retrieved from Hole 667A yielded Oligocene through Holocene nannofossil assemblages, most of which show moderate preservation. The Pliocene–Pleistocene assemblages are similar in composition to those cored earlier during Leg 108, with geophyrocapsids and small reticulofenestrids as dominating elements in the Pliocene and Pleistocene, respectively. *Helicosphaera carteri* and *Umibilicosphaera mirabilis* were abundant in some Pleistocene samples. Pliocene discoasters occur in great abundance.

Color cycles in the upper Miocene sediment reflect differences in nannofossil preservation, with the whitish cycles displaying moderately dissolved placolith assemblages and moderately to badly overgrown discoasters. The reddish cycles show severely dissolved placoliths and well-preserved discoasters. The entry and exit of *Discoaster quinqueramus* could be determined precisely in the reddish, but not in the whitish, layers because samples taken from the latter sediment facies typically contained specimens from which all finer morphological detail (e.g., the central knob) were obscured by calcite overgrowth. Besides discoasters, reticulofenestrids are the dominant assemblage component in the upper Miocene sediment.

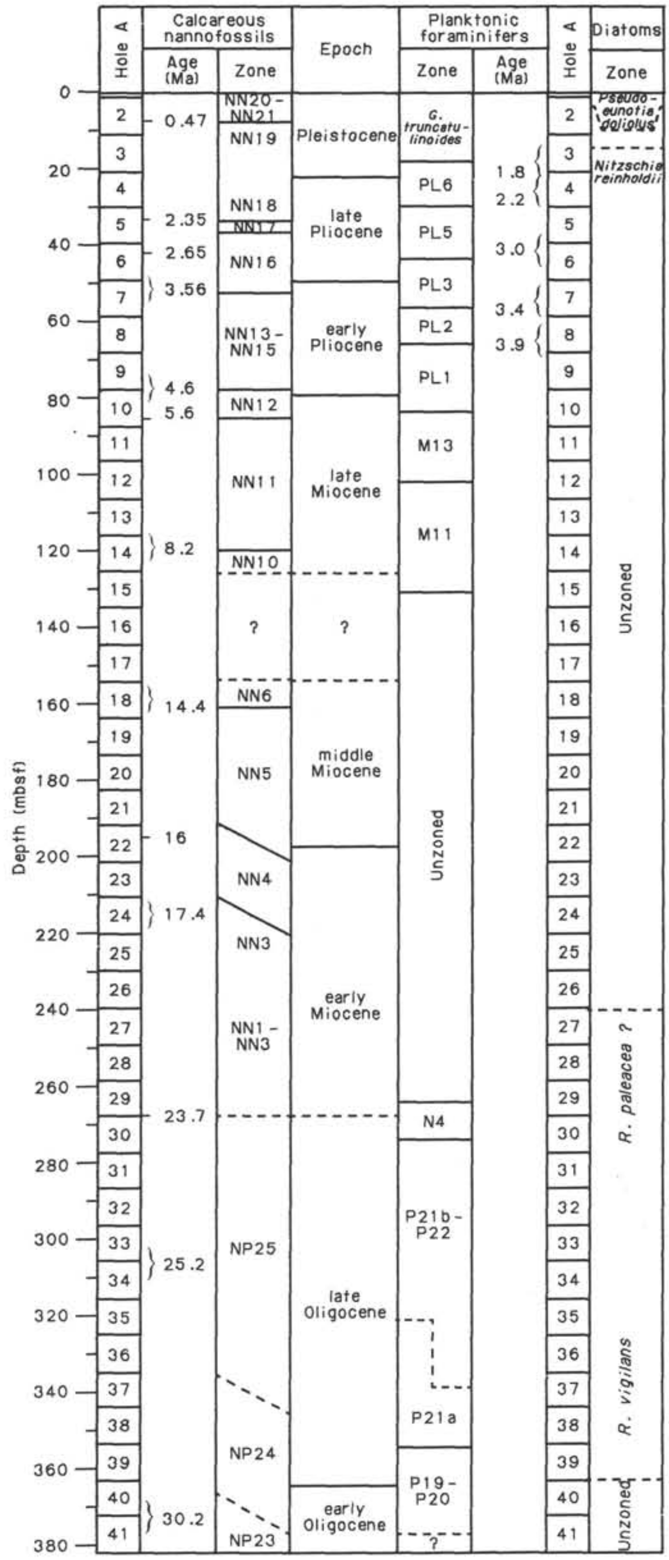

Figure 5. Zonal assignments for cores recovered from Hole 667A.

Generally, the lower Miocene assemblages are dominated completely by *Cyclicargolithus floridanus*; *Coccolithus pelagicus Discoaster deflandrei*, the *Sphenolithus moriformis* plexus, and *Triquetrohabdulus carinatus* also were prominent in certain inter-

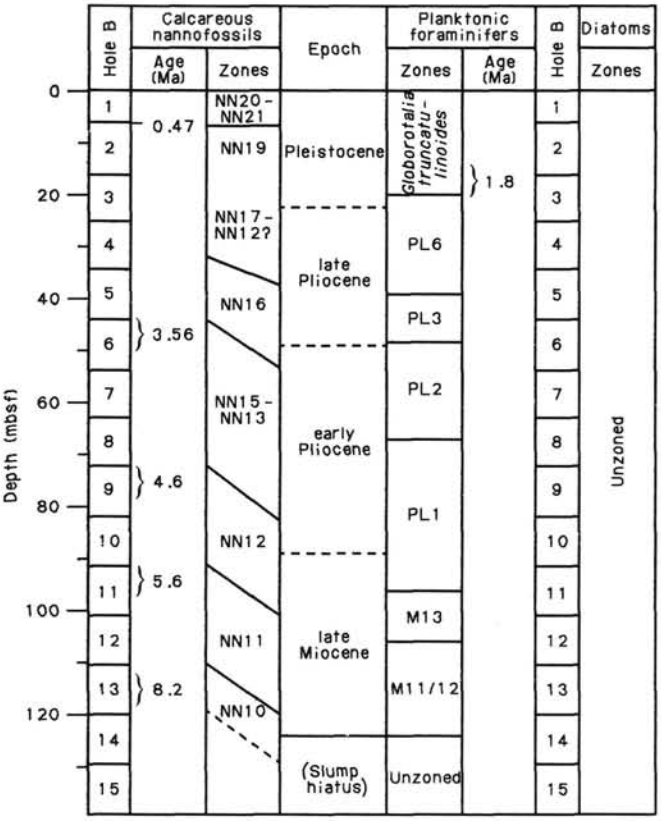

Figure 6. Zonal assignments for cores recovered from Hole 667B.

vals. Placoliths show good-to-moderate preservation, whereas the discoasters, in particular *Discoaster deflandrei*, were overgrown. *Coccolithus miopelagicus–Coccolithus eopelagicus, Coronocyclus nitescens, Reticulofenestra daviesi*, and helicosphaerids generally were sparse. Apart from observations of the early Miocene helicosphaerids (*Helicosphaera ampliaperta, Helicosphaera euphratis, Helicosphaera granulata, Helicosphaera intermedia*, and *Helicosphaera obliqua*), we also noticed the presence of the large *Helicosphaera truempyi* in the basal Miocene.

The Oligocene assemblages are broadly similar to the lower Miocene ones in composition and abundance (strong dominance of *C. floridanus* and *S. moriformis*), except that the former contain common *Ericsonia fenestratus* and rare occurrences of uniquely Oligocene sphenoliths and helicosphaerids. In his low-latitude zonation, Bukry (1973) used the extinction of *Dictyococcites bisectus* for approximate recognition of the Paleogene/Neogene boundary. Therefore, the total absence of *D. bisectus* in the Oligocene assemblages was surprising.

Pleistocene

Glacial and interglacial cycles are represented by alternating dark and white oozes, and *Pseudoemiliania lacunosa* disappears in one of the dark cycles between Samples 108-667A-2H-4, 80 cm, and 108-667A-2H-4, 110 cm, and in the uppermost meter in Section 108-667B-2H-1. Small gephyrocapsids are present in great abundance in Sample 108-667A-3H-4, 120 cm, possibly indicating the "small *Gephyrocapsa* acme Zone" of Gartner (1977) and a level that correlates to the Jaramillo geomagnetic event. For Hole 667B, this bloom was observed in Sample 108-667B-3H-2, 140 cm. The core-catcher sample of Core 108-667A-3H contained common Pliocene discoasters and placoliths, as well as some early Miocene placoliths and discoasters. *Discoaster brouweri* was common in Sample 108-667A-4H, CC, together with few *D. triradiatus* and rare *Triquetrorhadbulus rugosus*, indicating that this assemblage also in part reflects reworking. Subsampling of Core 108-667A-4H did not provide unambiguous information regarding the true extinction levels of either *C. macintyrei* or *D. brouweri.*

Slightly less ambiguous results were obtained from Hole 667B. An assemblage containing *Helicosphaera sellii*, but not *C. macintyrei*, was observed in Sample 108-667B-3H-4, 100 cm. The core-catcher samples of Core 108-667B-3H and Section 108-667B-4H-1 were characterized by reworked Pliocene discoasters, but the interval between Samples 108-667B-4H-2, 100 cm, and 667B-4H-3, 100 cm, held upper Pliocene–lower Pleistocene assemblages that lacked discoasters but contained *H. sellii* and *C. macintyrei.*

Pliocene

The acme interval of *Discoaster triradiatus* was not observed in any of the samples investigated from either Cores 108-667A-4H or -667A-5H, suggesting a hiatus with a duration in excess of 0.2 m.y. *Discoaster pentaradiatus* was rare below Section 108-667A-5H-3, and *D. surculus* was rare below Section 108-667A-5H-4. Closer sampling intervals, coupled with counts of these two species, eventually may lead to better results regarding their extinction levels. Likewise, the disappearance of *Discoaster tamalis* is poorly constrained because of few occurrences in the upper part of its range, which was observed in Core 108-667A-6H.

Rare-to-few *D. brouweri, D. triradiatus*, and *Discoaster pentaradiatus* were observed in Sample 108-667B-4H-CC, 10 cm, followed by abundant late Pliocene discoasters, including common *Discoaster surculus, Discoaster asymmetricus*, and *D. tamalis* in Section 108-667B-5H-1 (Zone NN16). Sample 108-667B-5H-2, 40 cm, provided a discoaster assemblage belonging to Zone NN16, although above the range of *D. tamalis* and *D. asymmetricus*, indicating that the assemblage in Section 108-667B-5H-1 represents reworking. Rare *D. tamalis* and *D. asymmetricus* occurred together with other typical late Pliocene discoasters in Samples 108-667B-5H-2, 110 cm, and -667B-5H-3, 120 cm, thus presumably representing the true extinction levels of *D. tamalis.*

The early to late Pliocene boundary is determined approximately by the disappearance of sphenoliths in Section 108-667A-7H-1. *Reticulofenestra pseudoumbilica* is rare at the bottom of Section 108-667A-7H-1 and common in Section 108-667A-7H-4. Sphenoliths are absent in Sections 108-667B-6H-2 and -667B-6H-1, rare to few in Section 108-667B-6H-3, and common in Section 108-667B-6H-4. Few to common *Reticulofenestra pseudoumbilica* occurred in Section 108-667B-6H-5, but the species was not observed above this section.

The next older, reliable nannofossil event is represented by the first occurrence (FO) of *Ceratolithus rugosus*. Typical *C. rugosus* were present in Section 108-667A-9H-6 but not at stratigraphically lower levels, whereas typical *Ceratolithus acutus* have a short range in the upper one-half of Core 108-667A-10H. Rare occurrences of *C. rugosus* were observed in Sample 108-667B-9H-2, 100 cm, but not below this level. The upper limit of *C. acutus* occurred in Sample 108-667B-9H-3, 120 cm.

A lower Pliocene assemblage displaying *T. rugosus* but not *Discoaster quinqueramus* characterized Samples 108-667A-10H-5, 86 cm, and -667B-10H, CC. *Discoaster quinqueramus* was present in Sample 108-667A-10H-6, 31 cm, and in Core 108-667B-11H.

Miocene

Discoaster quinqueramus is common in Cores 108-667A-11H and -667A-12H but decreases in abundance in Core 108-667A-13H. *Amaurolithus* spp. were rare in these cores but present down to Sample 108-667A-13H-1, 100 cm. In several of the upper Miocene samples, the amaurolithid to total assemblage ratio was less than 1/10,000, which suggests that the FO of amaurolithids can be missed easily. The last occurrence (LO) of *Discoaster neohamatus* was observed in Sample 108-667A-13H-2, 100 cm. Transitional forms between, on the one hand, *Discoaster bellus* and, on the other, *Discoaster berggrenii/D. quinqueramus* were noticed in the reddish oozes at the top of Core 108-667A-14H. The lowermost occurrence of morphotypes referable to *D. berggrenii/D. quinqueramus* was observed in Section 108-667A-14H-4. With the exception of *D. berggrenii/D. quinqueramus*, the assemblage present in Section 108-667A-14H-4 continues down to the core-catcher sample of Core 108-667A-14H.

Poorly preserved specimens of *D. quinqueramus/D. berggrenii* occur in Sample 108-667B-13H, CC. The core-catcher samples of Cores 108-667B-14H and -667B-15H are early Miocene in age, with the latter sample representing the deepest penetration of Hole 667B.

All sections of Cores 108-667A-15H and -667A-16H, as well as the upper three sections of Core 108-667A-17H, represent obvious slump deposits. The nannofossil assemblages are composed of mixtures of early to middle and early Miocene taxa. Sections 108-667A-17H-4 and 108-667A-17H-5 probably are also slumped because they contain middle Miocene assemblages belonging to Zone NN6 that overlie the Zone NN7 assemblage present in Section 108-667A-17H, CC.

Section 108-667A-18H-1 contained a lower middle-Miocene assemblage (e.g., *C. macintyrei, C. miopelagicus, Discoaster exilis, H. granulata*, and *R. pseudoumbilica*) but lacked *C. floridanus* and *S. heteromorphus*, and is referred to Zone NN6. *Cyclicargolithus floridanus* is present in Sections 108-667A-18H-3, -667A-18H-4, and in the upper part of 108-667A-18H-5 without being accompanied by *S. heteromorphus*. The disappearance of this last species was observed in the bottom of Section 108-667A-18H-5. One specimen of *H. ampliaperta* was observed in Samples 108-667A-19H-5, 100 cm, and -667A-20H, CC, but it was not present in Sample 108-667A-21H, CC. Rare *H. ampliaperta* occurred in Samples 108-667A-22H, CC and -667A-23H, CC. The core-catcher samples of Cores 108-667A-18H through -667A-22H contained common-to-abundant *S. heteromorphus*. The abundance of this species decreased profoundly in Core 108-667A-23H, and its FO was noticed in Sample 108-667A-23H, CC. This sample also showed the LO of the distinct *Reticulofenestra daviesi*.

Sphenolithus belemnos occured in Sample 108-667A-24X, CC, together with a typical lower Miocene assemblage. The only atypical element was a single specimen of one of the Oligocene/Miocene boundary markers, *H. recta*. The lowermost occurrence of *S. belemnos* was observed in Sample 108-667A-25X, CC. Calcite overgrowth of discoasters prevented accurate identifications of *D. druggii*. Its lowermost observed occurrence, however, was recorded in Section 108-667A-28X-2.

Triquetrorhabdulus carinatus was rare in the core-catcher samples of Cores 108-667A-25X through -667A-27X. A sharp increase in abundance (at least one order of magnitude going downhole) of *T. carinatus* occurred between Samples 108-667A-28-2, 60 cm, and -667A-28-3, 2 cm, which probably represents a better biostratigraphic indication than its last occurrence. Parker et al. (1985) also recorded a similar sharp decline in frequency, followed by a long trail of rare occurrences in the mid-latitudes of the North Atlantic at DSDP Sites 558 and 563.

The high-abundance interval of *T. carinatus* continues down to Sample 108-667A-32X, CC, but rare-to-few specimens occur down to Sample 108-667A-36X, CC. Although many samples were investigated from Cores 108-667A-28X through -667A-35X, we did not observe consistent occurrences of Oligocene species in that interval, except for one specimen of *H. recta* in Samples 108-667A-32X-5, 90 cm, and 108-667A-35X, CC, as well as rare specimens of *Dictyococcites bisectus* in Core 108-667A-33X (which is the only sample investigated showing *D. bisectus*).

Bukry (1973) placed the Oligocene/Miocene boundary at the end of the acme interval of *Cyclicargolithus abisectus*. We did not observe distinctly high abundances of *C. abisectus*, followed by sharply decreased abundance, in any of the samples investigated, despite the equatorial location of Site 667 and, consequently, cannot apply Bukry's zonal concept.

Oligocene

In the absence of *D. bisectus* and *Helicosphaera recta*, the Oligocene/Miocene boundary had to be determined approximately by the LO of *Sphenolithus ciperoensis*. Unfortunately, the Oligocene sphenolith marker species, *S. ciperoensis, Sphenolithus distentus*, and *Sphenolithus predistentus*, occur only in sporadic numbers. Preliminary counts of *S. ciperoensis* from the core-catcher samples of Cores 108-667A-33X through -667A-38X (using a view-field diameter of 0.2 mm, a nannofossil density of about 200 specimens per view-field, and counting 25 view-fields per sample) gave no *S. ciperoensis* in Core 108-667A-33X, one specimen in Core 108-667A-34X, two specimens in Core 108-667A-35X, and >10 specimens in Cores 108-667A-36X through 108-667A-38X. Sample 108-667A-36X, CC also shows relatively more diagenetic calcite and an increased abundance of small *C. floridanus* relative to shallower cores. One likely suggestion for the placement of the Oligocene/Miocene boundary thus appears to be within Core 108-667A-36X, based on the marked decrease in abundance of *S. ciperoensis*. Another possibility is that the boundary may occur as high as Core 108-667A-32X if reliance is placed on a single specimen of *H. recta*.

The first downhole co-occurrence of *S. ciperoensis* and *S. predistentus* in Sample 108-667A-37X-5, 137 cm, indicates Zone NP24. Rare *S. ciperoensis* occurred in Section 108-667A-40X-2, whereas *S. distentus* and *S. predistentus* occur without *S. ciperoensis* in Section 108-667A-41X-3. The interval between these two sections, therefore, probably marks the NP23/NP24 zonal boundary. *Helicosphaera compacta* was fairly common in Cores 108-667A-40X and -667A-41X but not at shallower levels.

Rare specimens of forms belonging to the *Ericsonia obruta/Ericsonia subdisticha* group were observed throughout the Oligocene interval cored at Site 667. In the absence of obvious reworking of early Oligocene-late Eocene species, we have to consider the possibility that this group continues its range to the top of the Oligocene.

Planktonic Foraminifers

The close proximity of Sites 666 and 667 is reflected by similarities in their faunal makeup. Preservation is better at Site 667 than at Site 666, with abundant and well-preserved specimens throughout most of the Pliocene and Pleistocene. Preservation in the lowermost Pliocene and uppermost Pleistocene is moderate, with some signs of dissolution. With few exceptions, foraminifers are abundant and moderately well preserved throughout the Oligocene and Miocene. The faunal makeup is tropical, with *Globigerinoides trilobus, Globigerinoides ruber, Globigerinoides sacculifer* all common in the Pliocene and Pleistocene, and *Globorotalia limbata* and *Globigerinoides obliquus* common in the Pliocene. High species abundances are found in the Pliocene–Pleistocene, with 20 to 30 species per sample, whereas in the Miocene they decrease to around 10 to 15 per sample, and in the Oligocene decrease to less than 10 per sample.

The base of the *Globorotalia truncatulinoides* Zone is marked by the LO of *G. obliquus*, which occurs between Samples 108-667A-3H-3, 110 cm, and -667A-3H-5, 126 cm, in Hole 667A and between Samples 108-667B-2H, CC and -667B-3H, CC in Hole 667B. The most common species in the Pleistocene are *G.*

trilobus, G. ruber, Globorotalia menardii/tumida, and *G. sacculifer.* At the top of the PL6 Zone, there is a short overlap of *G. obliquus* with *G. truncatulinoides.* The base of Zone PL6 lies between Samples 108-667A-4H-5, 110 cm, and -667A-4H, CC in Hole 667A, and between Samples 108-667B-4H, CC and -667B-5H, CC in Hole 667B. The base of Zone PL5 lies between 108-667A-6H-1, 126 cm, and 108-667A-6H-3, 126 cm, in Hole 667A, and presumably within Core 108-667B-4H. Zone PL4 was not identified in either hole, but as this zone is only 0.1 m.y. long, it would be very short at a site with such a low accumulation rate. This zone presumably lies within Cores 108-667A-6H and -667B-5H. The base of Zone PL3 lies between Samples 108-667A-7H-3, 110 cm, and -667A-7H-5, 110 cm, in Hole 667A, and between 108-667B-5H, CC and -667B-6H, CC in Hole 667B. In the late Pliocene zones, *G. trilobus, G. ruber, G. sacculifer, Globorotalia miocenica*, and *G. obliquus* are the most common species, but the fauna is diverse.

Early Pliocene Zones PL2 and PL1 contain diverse assemblages, with *G. trilobus, G. obliquus*, and *G. limbata* being the most common species. The base of Zone PL2 lies between Samples 108-667A-8H-3, 109 cm, and -667A-8H-5, 109 cm, in Hole 667A, and between Samples 108-667B-7H, CC and -667B-8H, CC in Hole 667B. The base of the PL1 Zone is between Samples 108-667A-9H, CC and -667A-10H, CC in Hole 667A, and between Samples 108-667B-10H, CC and -667B-11H, CC in Hole 667B.

As at previous Leg 108 sites, several of the late Miocene zonal markers used by Berggren et al. (1985) are missing. The base of Zone M13 can be recognized between Samples 108-667A-11H, CC and -667A-12H, CC and between Samples 108-667B-11H, CC and -667B-12H, CC, based on the FO of *Globorotalia margaritae.* Zone M12 cannot be recognized because of the absence of *Globorotalia conomiozea*, but the base of the M11 Zone, based on the FO of *Neogloboquadrina acostaensis*, occurs between Samples 108-667A-14H, CC and -667A-15H, CC. Hole 667B does not extend this far. *Globigerinoides trilobus, Dentogloboquadrina altispira, Sphaeroidinellopsis seminulina*, and *Globigerina nepenthes* are the most common species in the late Miocene.

Compared with the fauna described by Berggren et al. (1983) from the Rio Grande Rise, the lower and middle Miocene fauna at Site 667 are impoverished. The only zonal boundaries that can be recognized are the top and base of Zone M1 (equal to Zone N4 of Blow, 1969), by the LO and FO, respectively, of *Globorotalia kugleri.* The LO of this species lies between Samples 108-667A-28X, CC and -667A-29X, CC. According to K. Miller and A. Brower (pers. comm., 1986), the FO of *Globorotalia kugleri* at Hole 667A corresponds to a depth between 272.16 and 270.8 mbsf (between Samples 108-667A-30X-4, 36–39 cm, and -667A-30X-3, 50–53 cm), indicating the base of Zone N4 at this level. The presence of the late Oligocene/early Miocene boundary (within the same interval) is supported by the first occurrence of abundant *Globigerinoides* spp.

The following information was supplied by K. Miller and A. Brower (pers. comm., 1986). The LO of *Chiloguembelina* spp. in Hole 667A corresponds to a depth of 319.65 mbsf (Sample 108-667A-35X-3, 35–38 cm), with the last common occurrence being at 337.15 mbsf (Sample 108-667A-37X-3, 35–38 cm). The possibility of reworking in the interval between these two levels is reflected by the dashed nature of the zonal boundary in Figure 5. This suggests that Zone P21a is, indeed, present in this hole. The overlapping of this taxon with the *Globigerina angulisuturalis* FO at 353.16 mbsf (Sample 108-667A-39X-1, 36–40 cm) also indicates the presence of Zone P21a.

The apparent lack of *Globorotalia opima opima* in the interval from 340.16 to 267.66 mbsf (Samples 108-667A-37X-5, 36–39 cm, through -667A-30X-1, 36–39 cm) suggests that Zone P21b is absent in Hole 667A. K. Miller (pers. comm., 1986) suggests that Zone P21b also is absent at nearby DSDP Site 366 (located at the Sierra Leone Rise).

Benthic Foraminifers

Benthic foraminifers occur in all core-catcher samples examined from Hole 667A. Core-catcher Samples 108-667A-1H through -667A-9H contain common-to-few, well-preserved specimens. The characteristic species are similar throughout this interval. The common species are *Pyrgo murrhina, Planulina wuellerstorfi, Uvigerina hispida, Pullenia bulloides*, and *Epistominella exigua.* Core-catcher Samples 108-667A-10H through -667A-17H contain rare-to-few, moderately well-preserved specimens. The characteristic species are *Epistominella umbonifera, Pleurostomella* spp., and *Stilostomella* spp. *Oridorsalis tener, Globocassidulina subglobosa*, and *Eggerella bradyi* occur in Samples 108-667A-1H, CC through -667A-17H, CC. In addition, *Karreriella bradyi, Cibicidoides kullenbergi*, and *Gyroidinoides soldanii* occur sporadically throughout this interval. Core-catcher Samples 108-667A-18H through -667A-41X contain rare, poorly preserved specimens. *Stilostomella* sp., *Gyroidinoides* sp., and *Dentalina* spp. are found in this interval.

Hoeglundina elegans was observed only in Sample 108-667A-1H. The FO of this species was recognized in middle-Pleistocene sediments at the subtropical sites (Sites 657 through 661), but this species was not observed in the sediments of the same age at the equatorial sites (Sites 662 through 666). *Bulimina alazanensis* disappears above Core 108-667A-12H.

Diatoms

Diatoms are common in Samples 108-667A-1H, CC and -667A-2H, CC, with moderate-to-poor preservation. The flora is tropical in character. The occurrence of *Pseudoeunotia doliolus* in both samples and of *Nitzschia reinholdii* in Sample 108-667A-2H, CC allows Sample 108-667A-1H, CC to be assigned to the *Pseudoeunotia doliolus* Zone and Sample 108-667A-2H, CC to be assigned to the *Nitzschia reinholdii* Zone. Sample 108-667A-2H, CC has an age of 0.65 Ma. Sample 667B-1H, CC, at a sub-bottom depth intermediate between Samples 108-667A-1H, CC and -667A-2H, CC, contains only rare, freshwater diatoms. The lack of marine species may reflect Pleistocene productivity cycles, although any such suggestion is highly tentative because of the scarceness of samples.

Samples 108-667A-3H, CC through -667A-18H, CC, 108-667A-20, CC, and 108-667B-2H, CC through 108-667A-15H, CC are barren of diatoms. In addition, Samples 108-667A-19H, CC, -667A-21H, CC, and -667A-22H, CC contain only rare diatoms with poor preservation. This interval is characterized by calcareous oozes with relatively coarse grain sizes (see "Lithostratigraphy and Sedimentology" section, this chapter). Thus, it is likely that these sediments were subjected to winnowing, with the resulting loss of fine-grained sediments, including any fine-grained, siliceous component that originally existed.

Diatoms are present in Samples 108-667A-23H, CC through -667A-31X, CC, and 108-667A-33X, CC through -667A-39X, CC. The assemblage is similar to that described from the equatorial Pacific. Abundances vary from rare to abundant, and preservation is poor to moderate. Variations in abundance and preservation between samples may be related to the degree of induration of the sediments, with opal being more poorly preserved in more indurated sediments because of diagenetic alteration.

Samples 108-667A-24X, CC through -667A-26X, CC possess too few marker taxa for definite zonal assignment. However, the occurrence of *Coscinodiscus oligocenicus, Craspedodiscus elegans*, and *Craspedodiscus* s. ampl. in one or more of these samples suggests possible placement into the *Rossiella paleacea* Zone. Samples 108-667A-27X, CC and -667A-28X, CC are assigned to the upper portion of Subzone A of the *Rossiella paleacea* Zone, based on the co-occurrence of *Bogorovia veniamini, Thalassiosira primalabiata*, and *Rosiella paleacea*. The presence of *Coscinodiscus lewisianus* var. *similis, B. veniamini*, and *Rocella vigilans* without *R. paleacea* and *Rocella gelida* in Sample 108-667A-35X, CC suggests placement of this sample into the *Bogorovia veniamini* Zone. This assumes that these species have stratigraphic ranges at this site similar to those in the equatorial Pacific.

Because of the poor preservation, the zonal assignment of Sample 108-667A-36X, CC is difficult. The occurrence of *Coscinodiscus lewisianus* var. *similis* suggests a zonal assignment no younger than the lower portion of Subzone A of the *Rossiella paleacea* Zone and the presence of *Coscinodiscus rhombicus* and *R. vigilans* without *R. gelida* or *B. veniamini* suggest a zonal assignment equivalent to, or younger than, Subzone B of the *Rocella vigilans* Zone. It is possible, however, that *R. gelida* and/or *B. veniamini* are excluded from this sample because of preservation. Additional samples will be required to accurately place samples from Core 108-667A-36X into the appropriate diatom zone.

Sample 108-667A-37X, CC, which contains only rare diatoms, cannot be zoned. Sample 108-667A-38X, CC is tentatively placed in Subzone A of the *Rocella vigilans* Zone, based on the occurrence of common *R. vigilans* and rare *Cestodiscus muhinge*. Sample 108-667A-39X, CC contains only rare diatoms, and Samples 108-667A-40X, CC and -667A-41X, CC are barren of diatoms.

PALEOMAGNETISM

Magnetostratigraphy

The paleomagnetic results for sediments from Site 667 were as good as expected. We attribute this to strong overprinting and decreased downhole stability of magnetization. Continuous core measurements were obtained for Cores 108-667A-1H through 667A-23H and for Cores 108-667B-1H through -667B-5H. One sample per section from 667A was routinely subjected to alternating-current demagnetization.

In Figure 7, we plot the data from the archive halves of Cores 108-667A-1H through -667A-10H. In this same figure, we also show the results obtained from measuring the discrete samples. All APC cores from Hole 667A were oriented, and the declinations were corrected so that a normal declination plot is near 90°, and a reverse one near 270°. Following the same procedure as at Site 666, the upper layers of every core were deleted, as well as the data associated with disturbed layers.

A striking feature that appeared at some levels in the declination record is the disagreement of results from the continuous core measurements and the discrete samples. In the upper 30 mbsf, this discrepancy results from the presence of a strong secondary component. The demagnetization plot in Figure 8B shows that its direction is near the present geomagnetic field and, thus, is probably of viscous origin. The secondary component is not removed after 50 Oe, and it masks the Matuyama-Brunhes transition in the continuous record, which is revealed only by the discrete-sample results at 11.5 mbsf. The same is true for the record from Hole 667B presented in Figure 9. Discrete samples from Cores 108-667B-1H through -667B-6H were saved for post-cruise measurements in a low magnetic field environment.

No coherent pattern is found in the data obtained below 30 mbsf. The highly scattered directions do not show any clearly defined reversed or normal polarities. No stable magnetism was found at these levels, and any interpretation of the results would be speculative. Farther downhole, the cores were entirely remagnetized. In most cases, the archive and working halves of these cores were found to be identical and probably were remagnetized either during or shortly after splitting. Furthermore, these discrete samples were characterized by incoherent behavior during demagnetization. No definite explanation has been found so far for this phenomenon, which was mentioned in the Site 661 chapter (this volume). It may be due to mechanical reorientation of the grains inside the water-filled voids (favored by the low shear strength of the sediment in the last cores and their high water content). It also could reflect the presence of extremely unstable magnetic grains (e.g., multidomain or superparamagnetic). It is, of course, also possible that both phenomena are occurring simultaneously. We conclude that the magnetostratigraphy obtained from this site currently is limited to the upper 30 m of both holes.

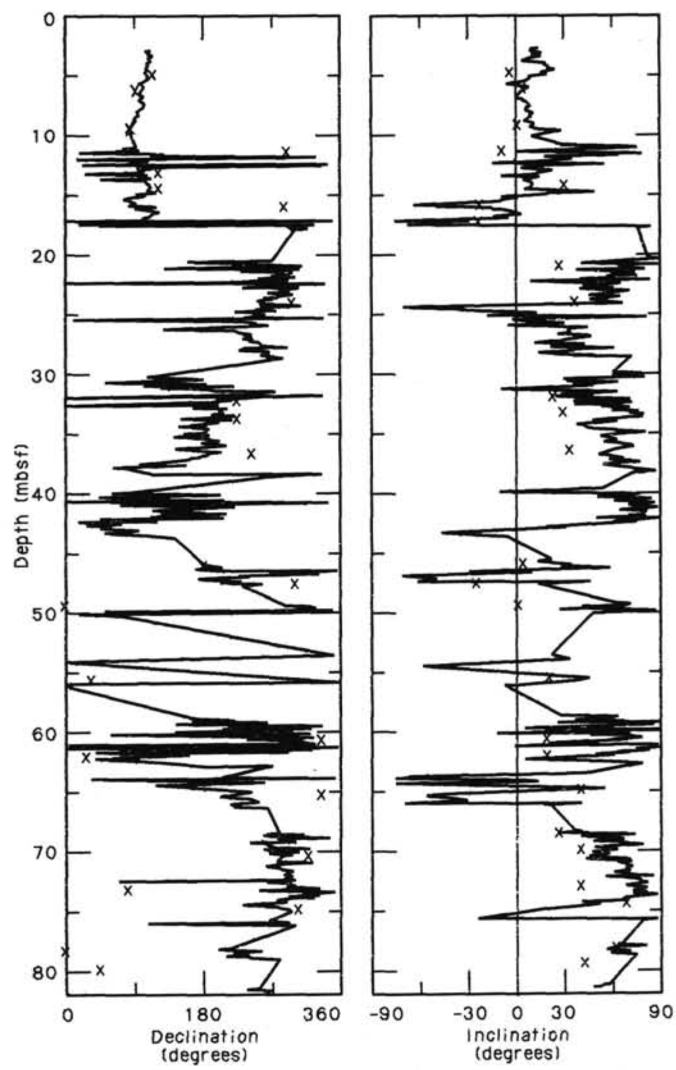

Figure 7. Declination and inclination data from archive halves demagnetized to 50 Oe. Crosses represent data for the discrete samples.

Magnetic Susceptibility

Whole-core volume susceptibilities were measured at 3-cm intervals throughout Holes 667A and 667B. Detailed between-hole correlations are possible between about 0–19 mbsf (Fig. 10) and about 40–95 mbsf.

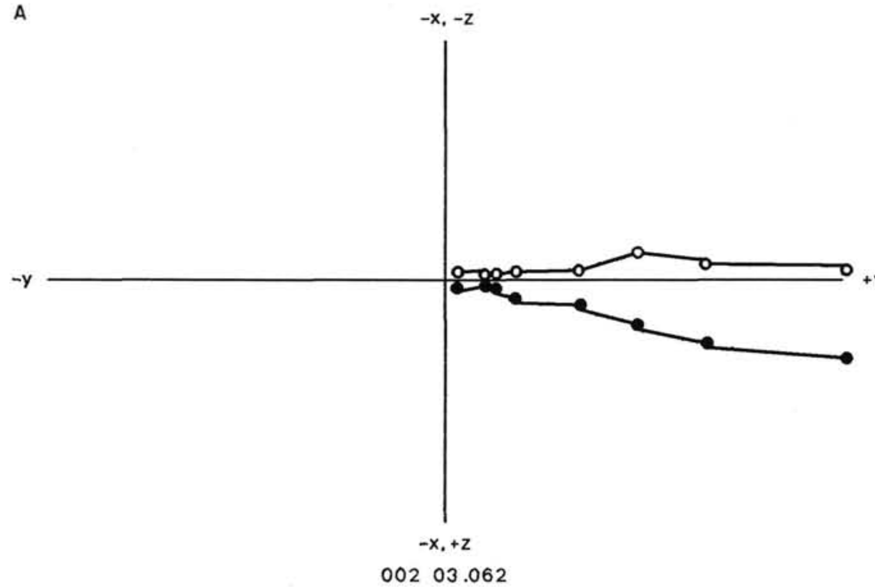

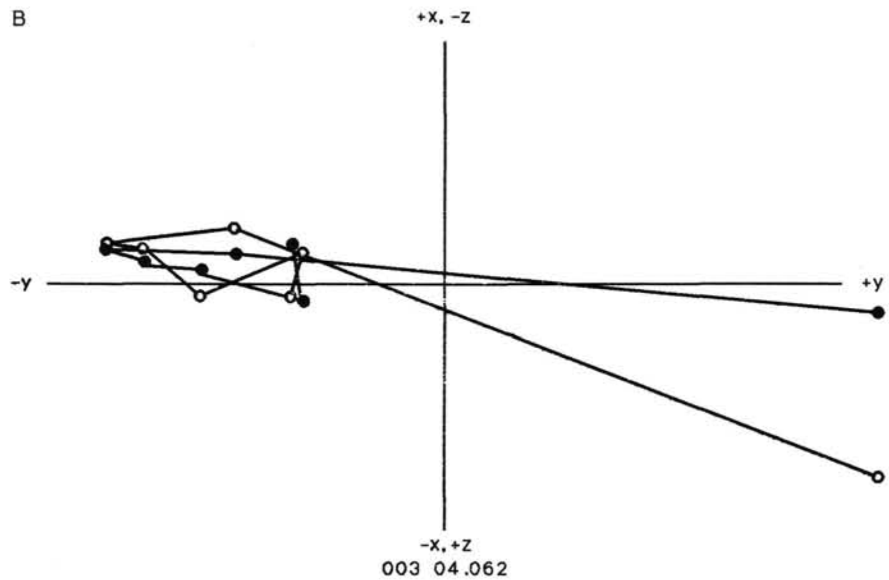

Figure 8. Typical demagnetization diagrams obtained from samples with original normal (*a*) and reverse (*b*) polarities.

SEDIMENT-ACCUMULATION RATES

The sediment-accumulation rates calculated for Hole 667A illustrate the difficulties to reconstruct accurately the depositional histories without adequate magnetostratigraphic control. Biostratigraphic/biochronologic control points are important for assessing sedimentary histories; however, the lack of magnetostratigraphy and the resulting loss in precision of the age-depth control points restrict our ability to recognize fully the variability in accumulation rates.

Although several good datum events exist for the late Miocene and Pliocene, the scatter of the available datums in Hole 667A allows at least two equally reasonable interpretations of sedimentary history. The scatter of the pre-middle Miocene datums reflects their imprecise calibration to the geomagnetic polarity time scale.

The accumulation rates at Hole 667A were established using three magnetostratigraphic and 37 biostratigraphic/biochronologic data points (Figs. 11 through 13 and Table 2). Figure 11 shows the age-depth markers for the entire Oligocene through Holocene sequence. The rates were not corrected for compaction or slump deposits. One major slump unit occurs in Cores 108-667A-15H through -667A-17H (124.8–153.3 mbsf). The middle Miocene is largely lost because of a hiatus. Figure 11 clearly shows the scatter of pre-middle Miocene data points, emphasizing the need for improved correlation between biostratigraphy and magnetostratigraphy in the Oligocene to lower Miocene interval.

The accumulation rates during late Miocene through Pleistocene time are shown in Figure 12. From 0 Ma to 2.2 Ma (0–29.8 mbsf), rates appear well constrained, with the one deviating point representing the LO of *Globigerinoides obliquus*, a datum that has proved unreliable at most Leg 108 sites. Two alternative rates are shown for the interval below 29.8 mbsf; the first is based on the last occurrences of *Globorotalia margaritae* and *Globigerina nepenthes* and the first occurrences of *Ceratolithus*

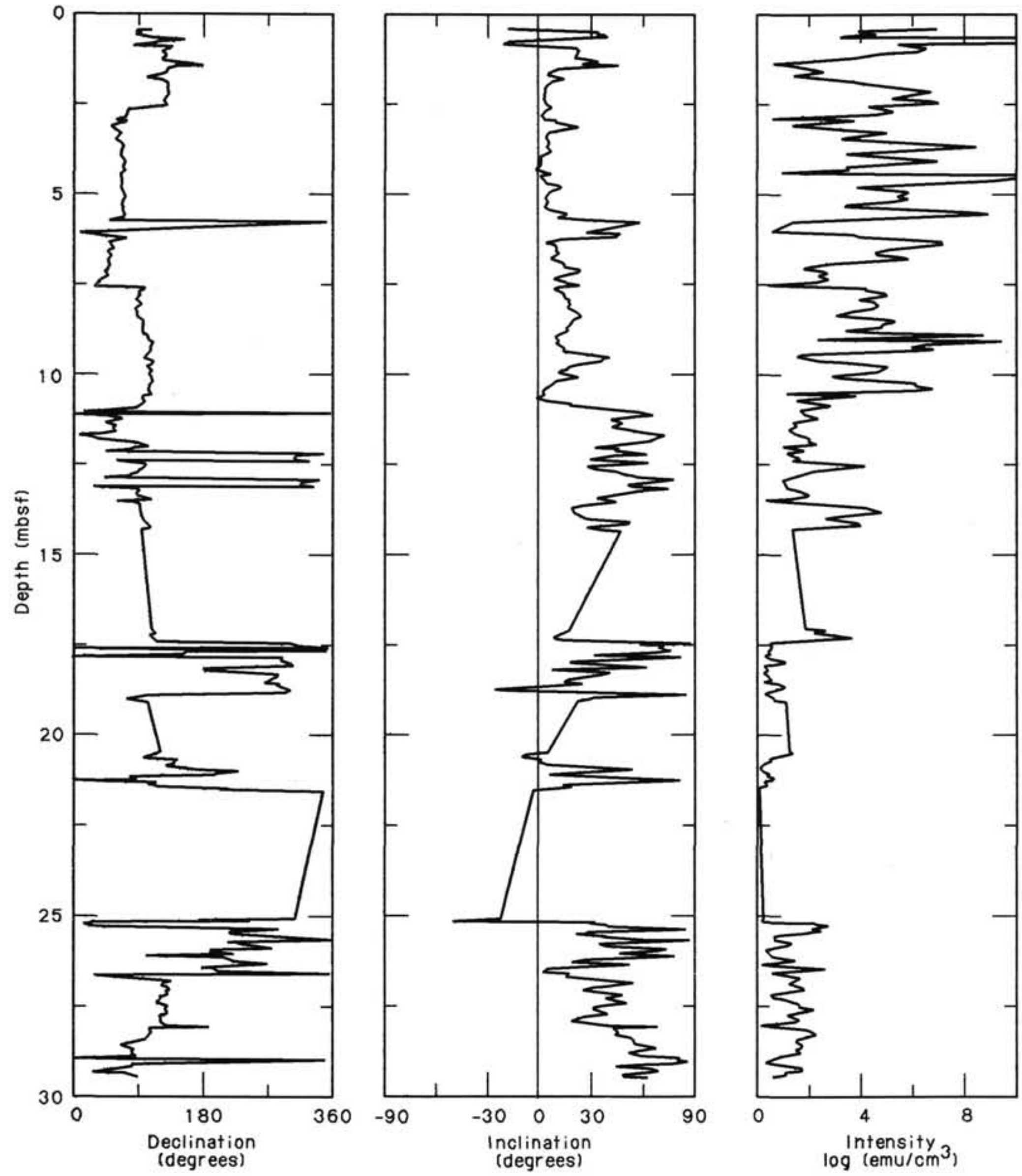

Figure 9. Data obtained from measuring continuous cores for Hole 667B.

rugosus and *G. margaritae.* These datums give a rate of 20 m/m.y. between 29.8 and 102 mbsf, with sharply decreased accumulation rates at about 5.9 Ma required to incorporate the three deepest control points.

The second alternative is based on the last occurrences of *Sphaeroidinellopsis seminulina, Reticulofenestra pseudoumbilica, Globoquadrina dehiscens, Discoaster quinqueramus,* and the FO of *D. quinqueramus.* These datums give a constant accumulation rate of 16.0 m/m.y. from the latest Miocene (5.6 Ma) through the late Pliocene (2.2 Ma), and a slightly lower rate of 13.1 m/m.y. during the late Miocene.

Neither interpretation suggests a change in depositional pattern during early Pliocene time, as has been the case at all previous Leg 108 sites. This implies that (1) either the depositional conditions differed in the area of Site 667 or (2) the accumulation rates in Figure 12 were misinterpreted.

The late Oligocene through early-middle Miocene accumulation rates are plotted in Figure 13. One cluster of control points occurs between 191.3 and 219.8 mbsf, and another group of datums occurs between 305.3 and 376.0 mbsf. We chose the simplest solution by assuming a constant sedimentation rate and connecting the two clusters with a straight age-depth line. A number of the intermediate datums, which fall off the lines, have not been correlated directly to magnetostratigraphy in the equatorial Atlantic Ocean. The slow, but uniform, late Oligocene to early Miocene sedimentation rate of 13 m/m.y would be higher if compaction were taken into account. The Oligocene/Miocene boundary (23.7 Ma) is recognized at the first occurrence level of *Globorotalia kugleri* (271.5 mbsf).

INORGANIC GEOCHEMISTRY

Interstitial-water samples were squeezed from eight sediment samples routinely recovered approximately every 50 m at Hole 667A. Values for pH and alkalinity were measured in conjunction, using a Metrohm 605 pH-meter, followed by titration with 0.1N HCl, and salinities were measured using an optical refractometer. Cl^-, Ca^{2+}, and Mg^{2+} concentrations were determined using the titrations described in Gieskes and Peretsman (1986).

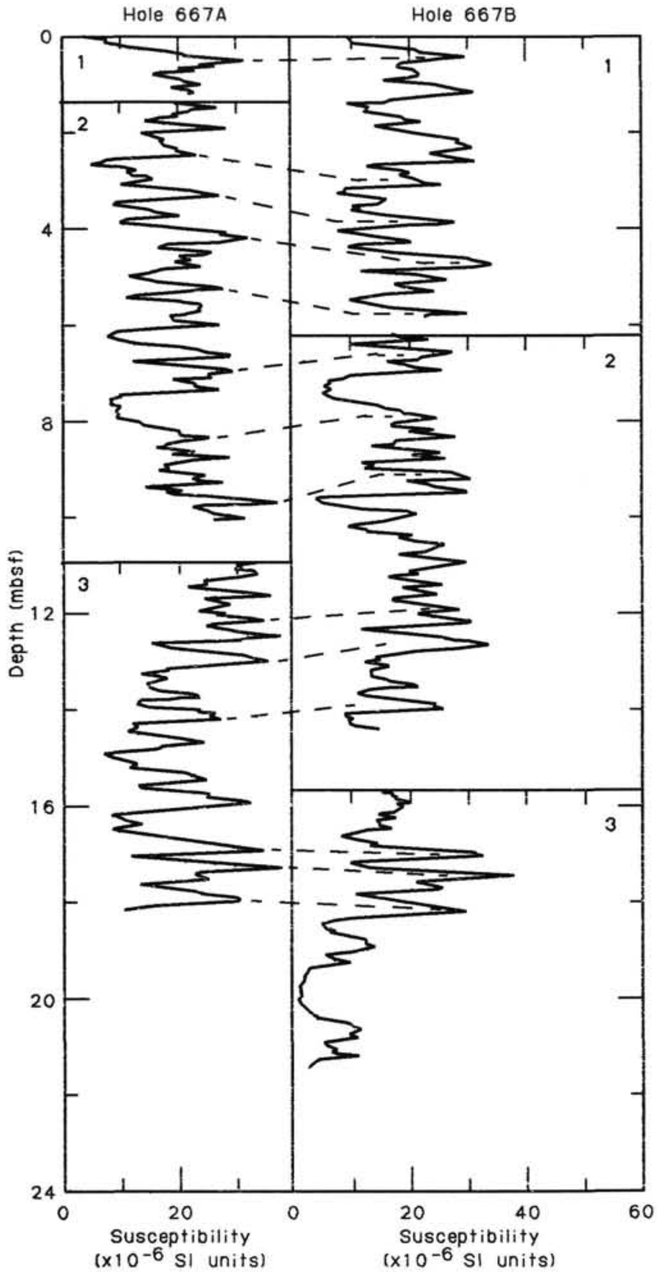

Figure 10. Magnetic-susceptibility correlations between Holes 667A and 667B.

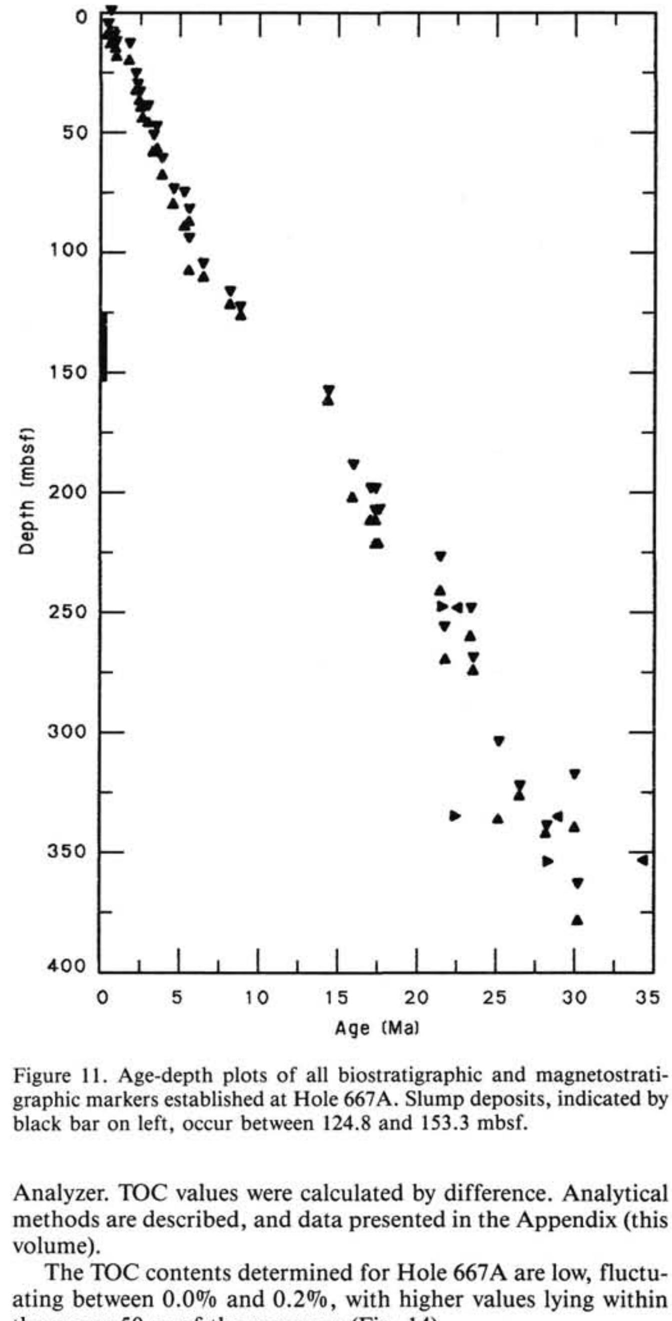

Figure 11. Age-depth plots of all biostratigraphic and magnetostratigraphic markers established at Hole 667A. Slump deposits, indicated by black bar on left, occur between 124.8 and 153.3 mbsf.

SO_4^{2-} analyses were conducted by ion chromatography using a Dionex 2120i instrument. Results from all analyses are presented in Table 3.

ORGANIC GEOCHEMISTRY

At Site 667, Hole 667A, the carbonate contents of 140 physical-property and smear-slide samples were determined. Of these, 39 samples from throughout the sequence also were analyzed for total organic carbon (TOC). Because of the low organic carbon content, no Rock-Eval analyses were performed. No samples were analyzed from Hole 667B.

Organic and Inorganic Carbon

Inorganic-carbon (IC) contents were measured using the Coulometrics Carbon Dioxide Coulometer, while total-carbon (TC) values were determined using the Perkin Elmer 240C Elemental Analyzer. TOC values were calculated by difference. Analytical methods are described, and data presented in the Appendix (this volume).

The TOC contents determined for Hole 667A are low, fluctuating between 0.0% and 0.2%, with higher values lying within the upper 50 m of the sequence (Fig. 14).

The carbonate content is highly variable, ranging from 3% to 93%, although much of the sequence displays values ranging from 70% to 90% (Fig. 14). Unit I (see "Lithostratigraphy and Sedimentology" section, this chapter, for division of units) is relatively poor in carbonate, with values between 23% and 81%. Units II through IV are considerably richer, with all samples containing at least 50% carbonate. In addition, these units display low-amplitude variations that appear to be pseudocyclic. Unit V is characterized by a wide range of carbonate contents (9% to 87%), varying in a quasiperiodic manner. In contrast, Unit VI displays a uniformly high carbonate content (75% to 92%), except for two samples with extremely low carbonate concentrations.

Discussion

Site 667 sediments are characterized by the low organic-carbon contents typical of open-marine environments (Müller et

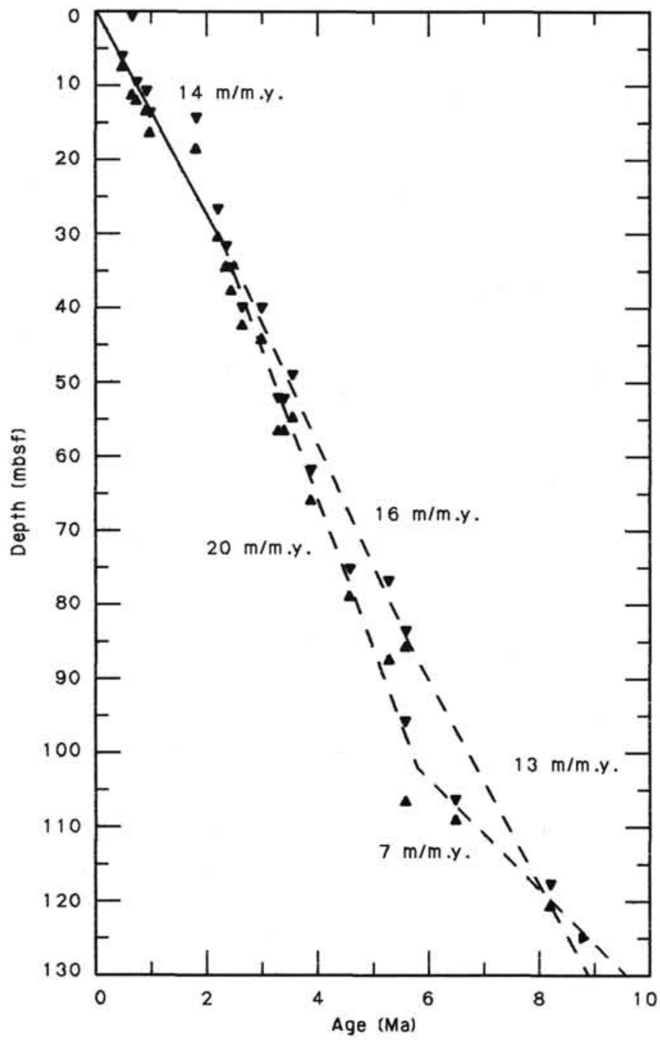

Figure 12. Age-depth plots of late Miocene through Pleistocene biostratigraphic and magnetostratigraphic markers.

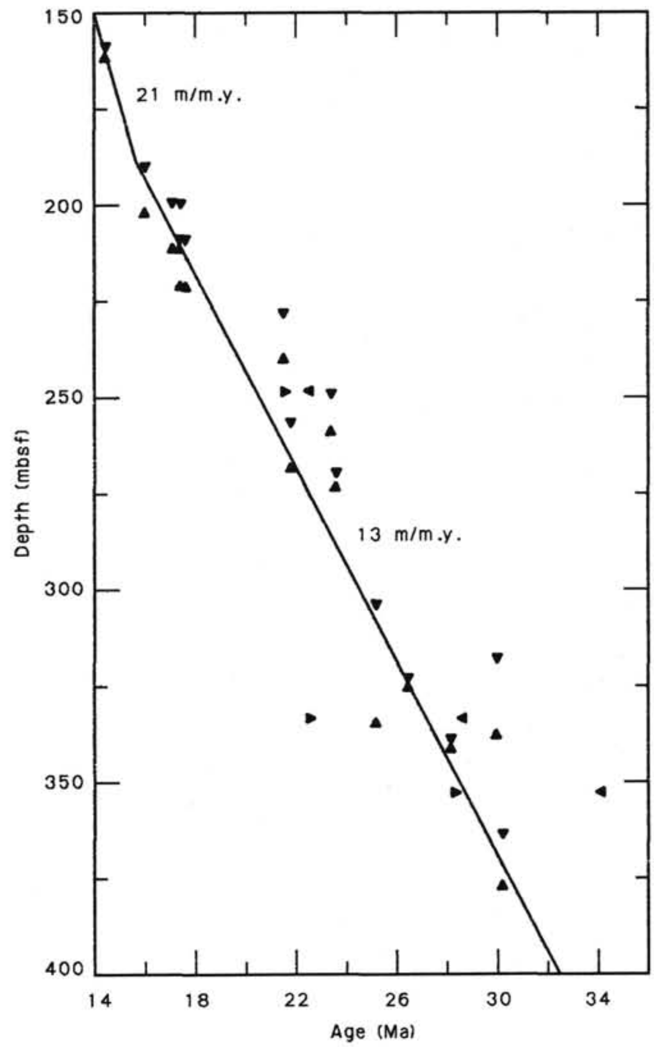

Figure 13. Age-depth plots of late Oligocene through early-middle Miocene biostratigraphic markers.

al., 1983). These values are somewhat lower than those for Sites 665 and 666; this may be a function of either regional productivity differences or winnowing. High carbonate contents characterize the sequence at Site 667, although superimposed quasi-periodic variations and isolated short intervals of low carbonate accumulation occur.

PHYSICAL PROPERTIES

The techniques used for shipboard physical-property measurements at Site 667 are outlined in the "Introduction and Explanatory Notes" (this volume). Both index properties and vane shear strength were measured throughout Holes 667A and 667B. Data for Holes 667A and 667B are shown in Tables 4 through 6 and plotted in Figures 15 through 22. A profile of the calcium carbonate content is shown in Figure 18. Both holes were logged continuously using the *P*-wave logger (PWL) and the GRAPE. A synthesis of the PWL data for Hole 667A is given in Table 5. The *in-situ* temperature gradient was measured in Hole 667B, and thermal conductivity also was measured for some cores from this hole. These data (Table 7) are plotted in Figure 19. No data presented here were screened for bad data points.

The wet-bulk-density profile (Fig. 15) can be divided into three units. In Unit I (0–110 mbsf), the wet-bulk density increases steadily from about 1.4 g/cm^3 to about 1.7 g/cm^3. Unit II (110–260 mbsf) is subdivided. In Unit IIA (110–200 mbsf), the average density remains constant at about 1.7 g/cm^3, with only minor fluctuations. In Unit IIB (200–260 mbsf), the density fluctuates markedly as the calcium carbonate content (Fig. 18) varies between 10% and 90%. In Unit III (260–375 mbsf), the density increases steadily from about 1.7 g/cm^3 to about 2.0 g/cm^3. Other index properties also reflect this behavior (Figs. 15 through 17).

The grain-density profile (Fig. 17) clearly shows the change between Units IIA and IIB, while the grain density of the low-carbonate intervals is lower than those intervals in Units IIA and I (0–200 mbsf). This might be related to an increase in the degree of diagenesis of the opaline-bearing sediments (see "Lithostratigraphy and Sedimentology" section, this chapter). The vane shear strength (Fig. 17) increases from about 10 kPa near the mud line to about 60 kPa at the base of Unit I (110 mbsf) and to a maximum of 140 kPa in Unit II. Below 200 mbsf, increased lithification prevented any further "Torvane" measurements.

The *P*-wave-velocity profile (Fig. 18) shows a small gradient over the upper 200 mbsf from a velocity of about 1.53 km/s at the mud line to about 1.6 km/s at 200 mbsf. The fluctuations in velocity correlate to some extent with both wet-bulk density and vane shear strength, indicating that increased rigidity, resulting

Table 2. Depth ranges and age estimates of biostratigraphic and magnetostratigraphic indicators used to establish accumulation rates for Hole 667A.

Datum	Depth (mbsf)	Age (Ma)
LO *Pseudoemiliania lacunosa*	6.6-6.9	0.47
LO *Nitzschia reinholdii*	1.3-10.8	0.65
Brunhes/Matuyama	10.5-11.5	0.73
Matuyama/Jaramillo	11.4-12.9	0.91
Jaramillo/Matuyama	14.4-15.9	0.98
LO *Globigerinoides obliquus*	14.9-18.1	1.80
LO *Globigerina miocenica*	27.3-29.8	2.20
LO *Discoaster pentaradiatus*	32.2-33.8	2.35
LO *D. surculus*	35.1-37.0	2.45
LO *D. tamalis*	40.5-41.7	2.65
LO *Sphaeroidinellopsis seminulina*	40.6-43.6	3.00
LO *Pulleniatina* spp.	52.9-55.9	3.30
LO *Globorotalia margaritae*	52.9-55.9	3.40
LO *Reticulofenestra pseudoumbilica*	49.6-54.2	3.56
LO *Globigerina nepenthes*	62.4-65.4	3.90
FO *Ceratolithus rugosus*	75.8-78.3	4.60
LO *Globoquadrina dehiscens*	77.3-86.8	5.30
LO *Discoaster quinqueramus*	84.2-85.1	5.60
FO *Globorotalia margaritae*	96.3-105.8	5.60
FO *Amaurolithus* spp.	106.8-108.3	6.50
FO *Discoaster quinqueramus*	118.3-120.0	8.20
within Zone NN10	124.8	8.85
LO *Sphenolithus heteromorphus*	159.8-160.4	14.40
LO *Helicosphaera ampliaperta*	191.3-200.8	16.00
FO *S. heteromorphus*	200.8-210.3	17.10
LO *Catapsydrax stainforthi*	200.8-210.3	17.40
LO *Sphenolithus belemnos*	210.3-219.8	17.40
LO *Catapsydrax dissimilis*	210.3-219.8	17.60
FO *S. belemnos*	229.3-238.8	21.50
upper part of Subzone A of *Rossiella paleacea* Zone	248.3	21.70-22.30
above *D. druggii*	250.4-257.8	23.40
LO *Globorotalia kugleri*	257.8-267.3	21.80
FO *G. kugleri*	270.8-272.2	23.60
LO *Sphenolithus ciperoensis*	305.3-333.8	25.20
LO *Chiloguembelina*	319.6-337.1	30.00
above base *Bogorovia veniamini* Zone	324.3	26.50
below top *Rocella gelida* Zone/ above base of Subzone B of *Rocella vigilans* Zone	333.8	22.70-28.50
LO *Globorotalia opima*	340.2	28.20
Within Subzone A of *Rocella vigilans* Zone	352.8	28.50-34.00
FO *Sphenolithus ciperoensis*	364.8-376.0	30.20

FO = first occurrence. LO = last occurrence.

from early diagenesis, is a significant contributing factor for velocity as depth increases. Below 200 mbsf, the velocity increases rapidly to nearly 2 km/s at more than 300 mbsf.

The *in-situ* temperature gradient (Fig. 19) was measured as 0.077°C/m, which is relatively high compared with the temperature gradients measured at other sites during this leg.

SEISMIC STRATIGRAPHY

Site 667 was cored to a depth of 381.3 mbsf. The water-gun seismic profiler records obtained during the approach to Site 667 indicate two seismic units (Fig. 23) within this depth range:

Seismic unit 1, 0-0.04 s, is an upper unit with a false acoustic signal caused by the water guns. This unit should equate to the upper 31 m of sediment.

Seismic unit 2, 0.04-0.46 s, is a middle unit with a series of somewhat diffuse reflectors of moderate strength. Individual reflectors in this unit vary markedly along the track line shown in Figure 23, with little lateral continuity. Some increase in reflectivity occurs at about 0.25 to 0.35 s, but reflectors in this interval also are more jumbled and chaotic, suggesting erosion or highly differential deposition.

Three seismic units lie below the cored interval (Fig. 23):

Seismic unit 1, 0.46-0.64 s, is a lower unit of stronger reflectors, nearly flat-lying except for a gentle dip to the east toward the center of the basin.

Seismic unit 2, 0.64-0.8 s, is a unit of relatively transparent reflectors with little relief.

Seismic unit 3, >0.8 s, is a group of strong reflectors representing acoustic basement.

The lithologic units in Hole 667A are shown in Figure 23 (see also "Lithostratigraphy and Sedimentology" section, this chapter). To evaluate possible correlations of the seismic units with lithologic units (Fig. 23), we converted the lithologic units in Hole 667A to seconds of two-way traveltime using the following mean (two-way) sound velocities: 765 m/s for the upper 100 mbsf, 780 m/s for the interval at 100-200 mbsf, 875 m/s for the interval at 200-300 mbsf, and 950 m/s for the interval at 300-381.3 mbsf (see "Physical Properties" section, this chapter).

Lithologic Unit I is roughly equivalent to seismic unit 1, but this comparison is meaningless because the latter is an artifact of the source characteristics of the water gun used aboard the *JOIDES Resolution*. Seismic unit 2 encompasses the five remaining lithologic units (Units II through VI), and, thus, no further correlation of the boundaries is possible. An apparent link between the increased reflectivity at 0.23-0.35 s exists within seismic unit 2 and the onset of higher *P*-wave velocities at 200-250 mbsf in direct measurements conducted for the sediments (see "Physical Properties" section, this chapter).

Based on results from DSDP Site 366, it is likely that the strong, flat-lying reflectors in seismic unit 3 just beyond the depths drilled at Site 667 represent upper Eocene cherts and highly indurated limestones. We also note that the acoustic character of the water-gun records obtained during approaches to Site 667 at different azimuths varied substantially; this suggests that, in this region, severe limitations exist for the use of conventional seismic records to infer lithologic characteristics.

Table 3. Results of inorganic-geochemical analyses conducted for Site 667.

Core/ section	pH	Alkalinity (mmol/L)	Salinity (‰)	Chlorinity (mmol/L)	SO_4^{2-} (mmol/L)	Mg^{2+} (mmol/L)	Ca^{2+} (mmol/L)
2H-5	7.51	4.30	34.2	559	26.44	51.05	12.30
7H-5	7.40	4.33	33.9	562	23.86	47.83	15.44
12H-4	7.44	4.66	34.1	568	22.68	44.45	18.51
17H-4	7.54	5.71	34.0	567	21.51	42.31	23.43
22H-5	7.15	5.23	34.2	564	20.57	39.74	24.80
27H-2	7.19	4.66	34.1	548	20.57	30.93	28.03
32H-5	7.25	4.42	34.3	567	19.16	34.79	30.79
37H-4	7.37	5.19	34.3	571	16.81	33.13	33.16

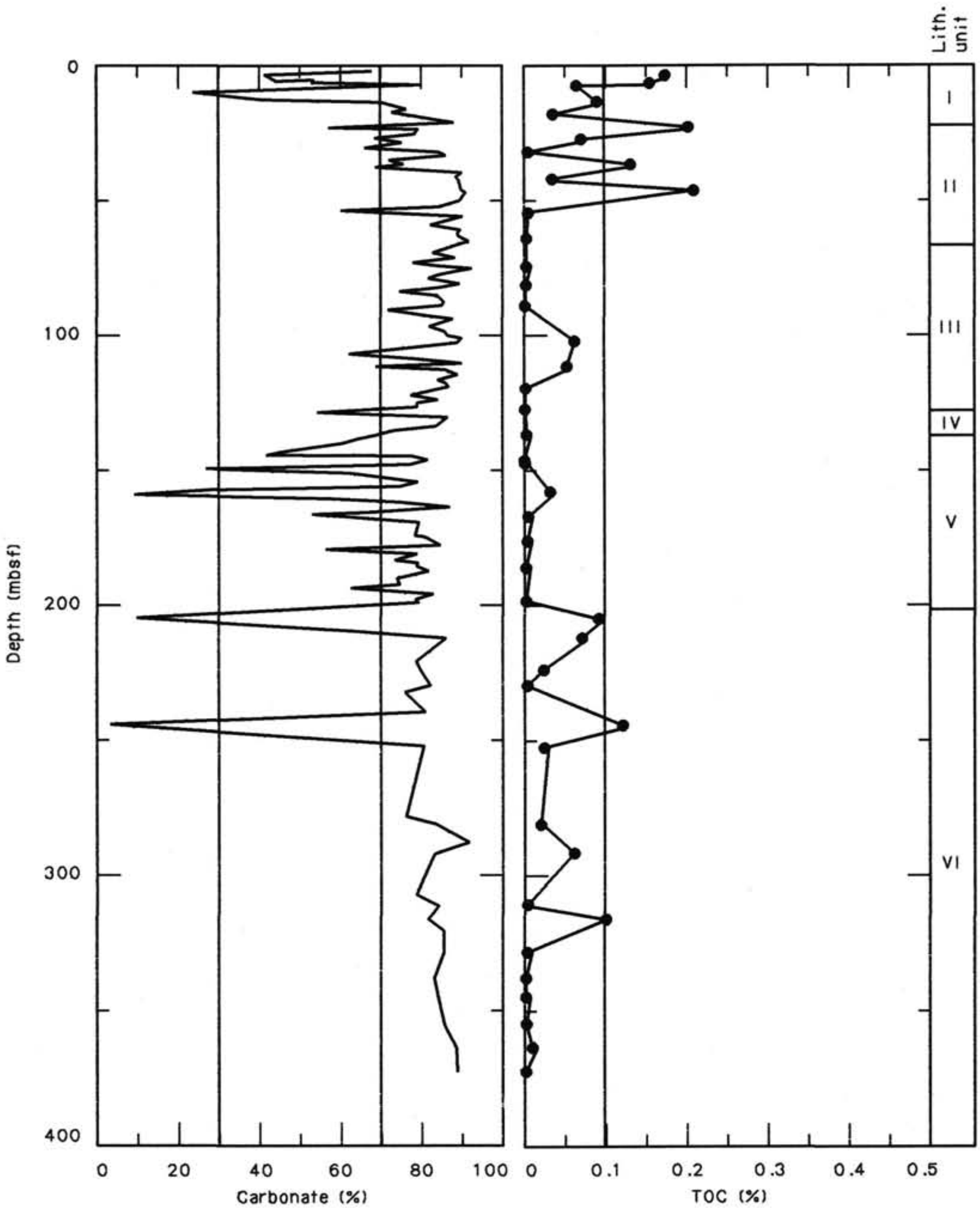

Figure 14. Organic carbon and carbonate records for Hole 667A.

COMPOSITE-DEPTH SECTION

Correlations between Holes 667A and 667B were possible for two portions of the sediment section above Cores 108-667A-11H and -667B-10H. The correlations shown in Tables 8 and 9 were based on magnetic-susceptibility data. Table 8 uses short sections from Hole 667B to span core breaks between longer sequences in Hole 667A; Table 9 uses the opposite approach. A continuous sequence can be traced through the upper 19 m, equivalent to the upper 1.0 Ma of the Pleistocene. A second continuous sequence covers the depth interval of 40 to 93 mbsf, equivalent to the time interval from latest Miocene to late Pliocene. An intervening uncorrelated interval occurs from late Miocene to early Pleistocene.

REFERENCES

Berggren, W. A., Aubrey, M. P., and Hamilton, N., 1983. Neogene magnetobiostratigraphy of Deep Sea Drilling Project Site 516 (Rio Grande Rise, South Atlantic). *In* Barker, P. F., Carlson, R. L., Johnson, D. A., et al., *Init. Repts. DSDP*, 72: Washington (U.S. Govt. Printing Office), 675–713.

Berggren, W. A., Kent, D. V., and Van Couvering, J. A., 1985. Neogene geochronology and chronostratigraphy. *In* Snelling, N. J. (Ed.), *The Chronology of the Geological Record*: London (Blackwell Scientific Publications), 211–259.

Blow, W. H., 1969. Late middle Eocene to Recent planktonic foraminiferal biostratigraphy. *Proc. 1st Int. Conf. on Planktonic Microfossils*, 1:199–422.

Bukry, D., 1973. Low-latitude coccolith biostratigraphic zonation. *In* Edgar, N. T., Saunders, J. B., et al., *Init. Repts. DSDP*, 15: Washington (U.S. Govt. Printing Office), 685-703.

Dean, W. E., Gardner, J. V., and Čepek, P., 1981. Tertiary carbonate-dissolution cycles on the Sierra Leone Rise, eastern equatorial Atlantic Ocean. *Mar. Geol.*, 39:81-101.

Dean, W. E., Gardner, J. V., Jansa, L. F., Čepek, P., and Seibold, E., 1978. Cyclic sedimentation along the continental margin of Northwest Africa. *In* Lancelot, Y., Seibold, E., et al., *Init. Repts. DSDP*, 41: Washington (U.S. Govt. Printing Office), 965-989.

Gartner, S., Jr., 1977. Calcareous nannofossil biostratigraphy and revised zonation of the Pleistocene. *Mar. Micropaleontol.*, 2:1-25.

Gieskes, J. M., and Peretsman, G., 1986. Water chemistry procedures aboard the *JOIDES Resolution*. OPD Technical Note No. 5.

Müller, P., Erlenkeuser, H., and von Grafenstein, R., 1983. Glacial-interglacial cycles in oceanic productivity inferred from organic carbon contents in eastern North Atlantic sediment cores. *In* Thiede, J., and Suess, E. (Eds.), *Coastal Upwelling: Its Sediment Record*, Part B: New York (Plenum Press), 365-398.

Parker, M. E., Clark, M., and Wise, S. W., Jr., 1985. Calcareous nannofossils of Deep Sea Drilling Project Sites 558 and 563, North Atlantic Ocean: biostratigraphy and the distribution of Oligocene braarudosphaerids. *In* Bougault, H., Cande, S. C., et al., *Init. Repts. DSDP*, 82: Washington (U.S. Govt. Printing Office), 559-589.

Stein, R., 1985. The post-Eocene sediment record of DSDP Site 366: implications for African climate and plate tectonic drift. *Geol. Soc. Am. Mem.*, 163:305-315.

Table 4. Index-properties and vane-shear-strength data for Hole 667A.

Core/ section	Interval (cm)	Depth (mbsf)	Grain density (g/cm^3)	Wet-water content (%)	Dry-water content (%)	Wet-bulk density (g/cm^3)	Dry-bulk density (g/cm^3)	Porosity (%)	Vane shear strength (kPa)
2H-1	121	2.51	2.56	52.22	109.30	1.43	0.74	73.50	12.00
2H-2	121	4.01	2.62	58.48	129.79	1.39	0.64	77.15	17.00
2H-3	121	5.51	2.60	53.63	115.64	1.42	0.70	74.90	16.00
2H-4	121	7.01	2.65	51.72	107.12	1.45	0.74	73.77	17.00
2H-5	121	8.51	2.59	51.09	104.47	1.45	0.75	72.83	16.00
2H-6	111	9.91	2.49	56.48	129.78	1.37	0.64	76.26	17.00
3H-1	121	12.01	2.54	60.81	155.16	1.33	0.57	79.71	24.00
3H-2	121	13.46	2.55	48.66	94.77	1.47	0.80	70.50	27.00
3H-3	121	14.96	2.65	49.94	99.77	1.47	0.78	72.36	25.00
3H-4	111	16.36	2.82	46.65	87.46	1.55	0.85	70.96	10.00
3H-5	121	17.96	2.57	47.35	89.93	1.49	0.84	69.60	14.00
4H-1	121	21.51	2.72	46.80	87.98	1.53	0.85	70.34	15.00
4H-2	121	23.01	2.68	47.95	92.12	1.51	0.82	70.99	20.00
4H-3	121	24.51	2.61	45.70	84.16	1.52	0.87	68.52	14.00
4H-4	121	26.01	2.61	44.13	79.00	1.55	0.91	67.11	19.00
4H-5	121	27.51	2.63	45.75	84.32	1.53	0.87	68.72	19.00
4H-6	121	28.94	2.71	42.70	74.53	1.59	0.94	66.64	20.00
5H-1	121	31.01	2.62	42.23	75.11	1.58	0.95	65.43	24.00
5H-2	121	32.51	2.62	43.96	78.44	1.55	0.90	67.05	22.00
5H-3	121	34.01	2.59	41.89	72.07	1.57	0.96	64.62	19.00
5H-4	121	35.51	2.49	44.30	79.53	1.52	0.91	66.19	20.00
5H-5	121	37.01	2.45	45.47	83.39	1.50	0.87	66.08	31.00
5H-6	121	38.51	2.68	44.57	80.42	1.55	0.91	66.08	31.00
6H-1	121	40.51	2.55	47.08	88.96	1.49	0.84	69.17	22.00
6H-2	121	42.01	2.69	44.36	79.73	1.56	0.90	67.92	31.00
6H-3	121	43.44	2.72	46.28	86.17	1.53	0.87	69.83	14.00
6H-5	99	46.22	2.56	47.90	91.93	1.49	0.81	69.99	20.00
6H-6	93	47.66	2.62	46.73	87.74	1.51	0.84	69.49	12.00
7H-1	121	50.01	2.73	48.81	95.35	1.50	0.81	72.00	6.00
7H-3	121	53.01	2.62	44.58	60.45	1.54	0.89	67.58	10.00
7H-4	99	54.29	2.54	42.27	76.21	1.56	0.96	64.76	25.00
7H-5	121	58.01	2.79	45.17	82.38	1.56	0.90	69.48	14.00
8H-1	121	59.51	2.60	43.06	75.62	1.56	0.92	66.00	16.00
8H-2	121	61.01	2.64	45.83	84.61	1.53	0.86	66.86	14.00
8H-3	121	62.51	2.38	43.87	78.17	1.50	0.88	64.84	21.00
8H-4	121	64.01	2.64	41.92	72.17	1.58	0.97	65.31	20.00
8H-5	121	65.51	2.65	39.66	65.73	1.62	1.02	63.25	30.00
9H-1	121	70.01	2.62	40.56	68.23	1.60	1.00	63.87	32.00
9H-2	121	71.51	2.60	40.66	68.51	1.60	0.98	63.78	45.00
9H-3	121	73.01	2.59	38.47	62.53	1.63	1.05	61.58	39.00
9H-4	121	74.51	2.60	38.71	63.16	1.62	1.05	61.83	40.00
9H-5	99	75.79	2.68	41.08	69.73	1.61	1.00	64.84	52.00
9H-6	51	76.81	2.37	45.88	84.78	1.47	0.84	65.51	40.00
10H-1	121	78.41	2.62	38.34	62.19	1.64	1.06	61.72	35.00
10H-2	121	79.91	2.72	38.22	61.87	1.66	1.07	62.46	45.00
10H-3	121	81.41	2.60	40.37	67.71	1.60	1.01	63.50	32.00
10H-4	121	82.91	2.69	38.02	61.35	1.66	1.06	61.96	36.00
10H-5	121	84.41	2.67	35.07	54.02	1.70	1.15	58.78	59.00
10H-6	49	85.19	2.63	37.81	60.79	1.65	1.07	61.27	32.00
11H-1	121	88.01	2.65	37.93	61.12	1.65	1.06	61.51	34.00
11H-2	121	89.51	2.54	37.95	61.16	1.62	1.05	60.53	31.00
11H-3	121	91.01	2.57	37.80	60.76	1.63	1.07	60.65	35.00
11H-4	121	92.51	2.57	36.98	58.67	1.65	1.09	59.86	41.00
11H-5	121	94.01	2.56	38.74	58.07	1.65	1.10	59.53	44.00
12H-1	123	97.53	2.55	35.29	54.53	1.67	1.13	57.83	41.00
12H-2	121	99.01	2.68	37.42	59.78	1.67	1.09	61.32	41.00
12H-3	121	100.51	2.61	33.67	50.76	1.71	1.17	56.69	44.00
12H-4	121	100.01	2.67	35.30	57.00	1.68	1.10	60.05	38.00

Table 4 (continued).

Core/ section	Interval (cm)	Depth (mbsf)	Grain density (g/cm^3)	Wet-water content (%)	Dry-water content (%)	Wet-bulk density (g/cm^3)	Dry-bulk density (g/cm^3)	Porosity (%)	Vane shear strength (kPa)
12H-5	121	103.51	2.69	35.21	58.77	1.69	1.12	60.10	40.00
13H-1	121	107.01	2.64	31.43	45.84	1.76	1.25	54.39	58.00
13H-2	121	108.51	2.58	33.28	49.87	1.71	1.18	55.91	38.00
13H-3	121	110.01	2.65	34.49	52.65	1.71	1.15	57.93	17.00
13H-4	121	111.51	2.60	32.72	48.63	1.72	1.20	55.48	32.00
13H-5	121	113.01	2.61	37.48	59.94	1.65	1.08	66.74	13.00
13H-6	121	114.51	2.63	40.18	67.18	1.61	1.01	63.59	20.00
14H-1	121	116.47	2.46	36.29	56.96	1.63	1.10	58.10	21.00
14H-2	121	117.97	2.62	33.01	49.29	1.72	1.20	55.99	32.00
14H-3	121	119.47	2.60	34.22	52.03	1.70	1.16	57.19	27.00
14H-4	121	120.97	2.60	35.88	55.95	1.67	1.12	58.94	39.00
14H-5	121	122.47	2.55	37.76	60.66	1.63	1.07	60.47	18.00
14H-6	121	123.97	2.55	38.75	63.28	1.61	1.03	61.46	23.00
15H-1	121	126.01	2.72	35.30	54.56	1.71	1.16	59.40	88.00
15H-2	121	127.51	2.59	33.21	49.72	1.71	1.20	55.98	64.00
15H-3	121	129.01	0.00	35.66	55.42	1.70	1.10	58.44	85.00
15H-4	121	130.51	0.00	37.32	59.53	1.67	1.06	60.14	45.00
15H-5	111	131.91	0.00	38.73	63.20	1.65	1.02	61.53	35.00
15H-6	121	133.51	0.00	39.67	65.75	1.64	1.00	62.44	30.00
16H-2	121	137.01	2.75	37.99	61.27	1.67	1.10	62.44	100.00
16H-3	121	138.51	2.58	35.76	55.66	1.67	1.12	58.66	47.00
16H-4	121	140.01	2.70	37.36	59.64	1.67	1.10	61.36	30.00
16H-6	121	143.01	2.53	36.48	57.44	1.64	1.09	58.92	112.50
16H-7	111	144.41	2.53	35.22	54.37	1.66	1.14	57.57	95.00
17H-1	121	145.01	2.71	35.54	55.14	1.71	1.15	59.59	45.00
17H-2	121	146.51	2.53	34.79	53.36	1.67	1.15	57.12	35.00
17H-3	121	148.01	2.52	33.24	49.78	1.69	1.08	55.32	82.50
17H-4	121	149.51	2.60	35.11	54.11	1.68	0.54	56.14	102.50
17H-5	121	151.01	2.66	33.52	50.42	1.73	1.18	56.99	55.00
18H-1	121	154.51	0.00	34.49	52.65	1.72	1.13	57.21	62.50
18H-2	121	156.01	0.00	35.89	55.98	1.70	1.09	58.68	90.00
18H-3	121	157.51	0.00	42.27	73.21	1.60	0.93	64.87	127.50
18H-4	121	159.01	0.00	43.13	75.83	1.58	0.91	65.64	107.50
18H-5	111	160.41	0.00	38.17	61.73	1.66	1.03	60.98	95.00
18H-6	121	162.01	0.00	34.93	53.69	1.71	1.12	57.68	72.50
19H-1	121	164.01	2.62	37.54	60.11	1.65	1.07	60.90	25.00
19H-2	121	165.33	2.61	34.08	51.69	1.70	1.18	57.10	80.00
19H-3	121	166.83	2.57	36.29	56.96	1.66	1.08	59.16	137.50
19H-4	121	168.33	2.61	33.02	49.31	1.72	1.20	55.95	55.00
20H-2	121	173.96	2.60	36.58	57.68	1.66	1.11	59.69	70.00
20H-3	121	175.46	2.56	38.40	57.22	1.65	1.10	59.15	50.00
20H-4	121	178.96	2.54	34.71	53.17	1.67	1.16	57.12	52.50
20H-5	121	178.46	2.66	35.12	54.14	1.70	1.14	58.70	100.00
20H-6	121	179.96	2.64	34.63	52.98	1.70	1.18	58.04	65.00
21H-1	121	183.01	2.55	34.88	53.56	1.68	1.14	57.46	80.00
21H-2	121	184.51	2.67	34.78	53.32	1.71	1.16	55.44	70.00
21H-3	119	185.95	2.69	33.16	49.61	1.74	1.21	56.85	84.00
21H-4	119	187.41	2.71	33.86	51.20	1.74	1.19	57.79	82.00
21H-6	119	190.13	2.64	34.67	53.54	1.70	1.16	58.24	78.00
22H-1	121	192.51	2.59	36.58	57.67	1.66	1.10	59.60	90.00
22H-2	121	194.01	2.41	40.30	67.50	1.56	1.00	61.71	97.00
22H-3	121	195.51	2.59	35.52	50.41	1.71	1.18	56.30	80.00
22H-4	121	197.01	2.60	39.59	65.54	1.61	1.02	62.73	87.50
22H-5	121	198.51	2.61	35.83	55.83	1.67	1.12	58.97	97.50
22H-6	121	200.01	2.63	39.21	64.51	1.63	1.04	62.67	100.40
23H-3	132	203.79	2.39	55.90	126.77	1.36	0.65	73.05	106.00
23H-6	121	206.95	2.46	41.48	70.89	1.55	0.95	63.28	120.00
23H-9	4	209.55	2.58	40.27	67.41	1.60	1.00	63.20	0.00
24H-1	131	211.61	2.23	41.12	69.84	1.50	0.96	60.70	25.00
25H-1	45	220.25	2.63	36.08	61.50	1.64	1.06	61.53	0.00
25H-3	122	224.02	2.59	36.36	54.71	1.68	1.12	58.30	0.00
26H-1	56	229.86	2.57	41.61	71.25	1.58	0.95	64.45	0.00
26H-2	121	232.01	2.58	33.73	50.91	1.70	1.19	56.45	0.00
27H-1	104	239.84	2.67	38.45	62.47	1.65	1.06	62.23	27.00
27H-4	115	244.45	1.99	60.61	153.87	1.26	0.53	75.35	0.00
28H-2	110	250.83	2.35	31.50	45.99	1.67	1.24	51.68	0.00
28H-3	111	252.34	2.51	31.03	44.99	1.73	1.24	52.69	0.00
31H-1	115	277.95	0.00	30.61	44.11	1.79	1.25	52.91	31.00
31H-1	115	277.95	0.00	30.61	44.11	1.79	1.25	52.91	0.00
31H-3	120	281.00	0.00	32.49	48.13	1.76	1.19	55.04	0.00
32H-1	121	287.51	0.00	29.84	42.53	1.80	1.27	52.02	0.00
32H-4	121	292.01	0.00	27.94	38.77	1.84	1.33	49.73	0.00
34H-1	121	306.51	0.00	25.08	35.28	1.88	1.39	47.41	0.00
34H-4	121	311.01	0.00	25.81	34.79	1.89	1.40	47.06	0.00
35H-1	121	316.01	0.00	24.11	31.77	1.92	1.46	44.63	0.00

Table 4 (continued).

Core/ section	Interval (cm)	Depth (mbsf)	Grain density (g/cm^3)	Wet-water content (%)	Dry-water content (%)	Wet-bulk density (g/cm^3)	Dry-bulk density (g/cm^3)	Porosity (%)	Vane shear strength (kPa)
35H-4	121	320.51	0.00	25.28	33.83	1.90	1.42	46.38	0.00
36H-3	121	328.21	0.00	27.22	37.40	1.86	1.36	48.85	0.00
37H-3	83	337.63	0.00	22.70	29.37	1.95	1.51	42.92	0.00
38H-2	37	345.17	0.00	25.65	34.49	1.89	1.41	46.85	0.00
39H-2	119	355.49	0.00	24.48	32.41	1.91	1.45	45.32	0.00
40H-1	121	363.51	0.00	24.61	32.64	1.91	1.44	45.50	0.00
41H-1	141	373.21	0.00	21.15	26.82	1.99	1.57	40.73	0.00

Table 5. Synthesis of *P*-wave-logger velocity data for Hole 667A.

Depth (mbsf)	*P*-wave velocity (km/s)	Depth (mbsf)	*P*-wave velocity (km/s)	Depth (mbsf)	*P*-wave velocity (km/s)
0.50	1.511	95.30	1.543	166.90	1.572
1.80	1.552	87.80	1.550	168.70	1.609
2.30	1.520	88.70	1.523	169.80	1.595
3.80	1.541	90.80	1.545	171.30	1.561
4.10	1.512	91.80	1.531	173.30	1.620
5.30	1.511	93.70	1.553	175.30	1.582
6.30	1.537	96.80	1.540	177.30	1.662
6.80	1.538	99.30	1.525	179.30	1.580
8.30	1.521	100.70	1.581	181.30	1.620
9.90	1.511	102.90	1.531	183.00	1.654
11.70	1.545	107.00	1.576	184.30	1.560
13.70	1.512	109.20	1.527	185.80	1.650
16.10	1.531	110.50	1.550	186.80	1.636
17.90	1.510	112.30	1.526	186.90	1.550
19.90	1.563	113.80	1.553	187.80	1.570
21.30	1.550	115.60	1.640	188.00	1.638
23.30	1.519	116.60	1.545	189.10	1.665
25.90	1.560	118.50	1.605	190.80	1.580
27.30	1.540	119.80	1.540	195.00	1.612
29.10	1.533	122.00	1.646	199.00	1.623
30.80	1.567	122.30	1.538	199.30	1.552
32.90	1.521	123.30	1.583	200.50	1.635
35.90	1.539	125.80	1.563	202.80	1.750
37.80	1.536	128.70	1.600	211.30	1.750
39.30	1.537	129.80	1.530	214.30	1.560
40.30	1.531	131.80	1.556	224.30	1.695
42.30	1.537	133.80	1.550	230.00	1.700
42.70	1.645	135.30	1.545	232.30	1.760
43.30	1.532	137.30	1.548	239.80	1.680
44.80	1.560	139.90	1.583	241.60	1.800
47.30	1.540	140.30	1.550	242.60	1.780
49.80	1.530	142.30	1.565	242.80	1.550
51.80	1.551	144.30	1.546	244.10	1.740
53.80	1.524	145.80	1.536	249.30	1.560
56.30	1.545	147.10	1.598	250.60	1.740
60.30	1.526	148.20	1.615	251.50	1.743
61.50	1.554	148.60	1.543	252.50	1.785
63.30	1.540	149.80	1.575	258.40	1.800
64.70	1.573	150.80	1.570	260.10	1.797
66.30	1.535	154.30	1.563	263.00	1.800
69.30	1.549	156.30	1.563	265.60	1.842
71.80	1.540	158.30	1.569	277.80	1.820
73.80	1.539	159.80	1.567	290.30	1.862
75.80	1.525	161.60	1.678	300.40	1.920
77.70	1.600	162.20	1.550	306.00	1.900
79.30	1.544	163.80	1.552	310.10	1.980
81.30	1.530	164.80	1.576	318.30	1.890
83.40	1.565	166.10	1.540	327.30	1.940

Table 6. Index-properties and vane-shear-strength data for Hole 667B.

Core/ section	Interval (cm)	Depth (mbsf)	Grain density (g/cm³)	Wet-water content (%)	Dry-water content (%)	Wet-bulk density (g/cm³)	Dry-bulk density (g/cm³)	Porosity (%)	Vane shear strength (kPa)
1H-1	121	1.21	2.51	52.71	111.44	1.42	0.71	73.50	6.20
1H-2	121	2.71	2.69	54.20	118.35	1.42	0.69	75.92	5.40
1H-3	121	4.21	2.61	55.38	124.09	1.40	0.67	76.30	11.20
1H-4	111	5.62	2.63	57.79	136.90	1.37	0.62	78.12	13.40
2H-1	121	7.31	2.60	47.79	91.53	1.49	0.82	70.17	14.00
2H-2	121	8.81	2.57	52.12	108.84	1.43	0.71	73.51	13.00
2H-3	121	10.31	2.58	54.75	120.98	1.40	0.68	75.59	17.00
2H-4	121	11.81	2.50	61.20	157.75	1.32	0.55	79.69	23.00
2H-5	121	13.31	2.60	47.41	90.16	1.50	0.83	69.91	28.00
3H-1	121	16.81	2.56	51.24	105.10	1.44	0.74	72.72	17.00
3H-2	121	18.31	2.63	48.35	93.62	1.49	0.81	70.90	8.00
3H-3	121	19.81	2.50	60.14	150.87	1.34	0.59	78.97	0.00
3H-4	121	21.31	2.31	46.07	85.44	1.46	0.86	66.20	8.00
4H-1	121	26.31	2.53	51.24	105.10	1.44	0.75	72.54	21.00
4H-2	121	27.81	2.63	48.82	95.38	1.48	0.81	71.26	81.00
4H-3	121	29.31	2.54	46.21	85.92	1.50	0.84	68.33	29.00
5H-1	121	35.81	2.60	44.57	80.41	1.54	0.90	67.37	19.00
5H-2	121	37.31	2.60	42.39	73.58	1.57	0.93	65.46	28.00
5H-3	121	38.81	2.70	43.90	78.26	1.57	0.91	67.65	32.00
5H-4	121	40.31	2.46	45.48	83.41	1.50	0.88	67.05	35.00
5H-5	121	41.81	2.25	50.67	102.71	1.40	0.74	69.67	29.00
6H-1	121	45.31	2.61	46.87	88.20	1.51	0.83	69.47	10.00
6H-2	121	46.81	2.55	57.43	134.89	1.37	0.64	77.38	0.00
6H-3	121	48.31	2.77	51.17	104.77	1.48	0.80	74.22	17.00
6H-4	121	49.81	2.78	48.45	93.97	1.51	0.82	72.12	8.00
6H-5	121	51.31	2.66	43.05	75.60	1.57	0.93	66.50	19.00
6H-6	121	52.81	2.63	51.42	105.83	1.45	0.75	73.42	0.00
7H-1	127	54.87	2.58	46.14	85.66	1.51	0.86	68.66	17.00
7H-2	121	56.31	2.64	50.51	102.08	1.46	0.76	72.76	0.00
7H-3	121	57.81	2.14	56.04	127.50	1.33	0.72	73.11	15.00
7H-4	121	59.31	2.65	43.30	76.35	1.57	0.93	66.64	17.00
7H-5	121	60.81	2.61	46.47	86.80	1.51	0.85	69.14	24.00
8H-2	121	65.81	2.58	42.89	75.11	1.56	0.94	65.69	24.00
8H-3	121	67.31	2.61	39.94	66.49	1.61	1.01	63.13	39.00
8H-4	121	68.81	3.87	12.53	14.33	2.87	1.43	35.28	38.00
8H-5	121	70.31	2.70	41.14	69.90	1.61	1.00	65.12	29.00
9H-1	121	73.81	2.55	42.46	73.78	1.56	0.94	65.05	20.00
9H-2	121	75.31	2.55	41.19	70.04	1.58	0.97	63.87	28.00
9H-3	121	76.80	2.60	43.32	76.42	1.56	0.92	66.29	29.00
9H-4	121	78.31	2.60	40.12	67.00	1.60	1.00	63.22	25.00
9H-5	121	79.81	2.69	40.71	68.66	1.61	0.99	64.57	31.00
9H-6	121	81.31	2.58	39.09	64.17	1.61	1.04	62.05	28.00
10H-1	121	83.31	2.60	38.89	63.64	1.62	1.04	62.04	42.00
10H-2	121	84.81	2.61	38.06	61.46	1.64	1.05	61.35	40.00
10H-3	121	86.31	2.58	42.31	73.34	1.57	0.96	65.18	35.00
10H-4	121	87.81	2.61	40.91	69.23	1.59	0.98	64.08	36.00
10H-5	121	89.31	2.66	39.29	64.71	1.63	1.03	62.97	40.00
10H-6	121	90.81	2.57	38.85	63.54	1.61	1.04	61.71	41.00
11H-1	121	92.81	2.73	39.91	66.42	1.63	1.02	64.15	11.00
11H-2	121	94.31	2.61	35.89	55.98	1.67	1.10	59.04	51.00
11H-3	121	95.81	2.61	37.06	58.88	1.65	1.08	60.25	52.00
11H-4	121	97.31	2.63	32.94	49.13	1.73	1.21	58.01	53.00
11H-5	121	98.81	2.61	35.59	55.24	1.68	1.13	58.76	62.00
11H-6	121	100.31	2.64	34.15	51.85	1.71	1.17	57.51	36.00
12H-1	121	102.31	2.66	33.50	50.37	1.73	1.19	56.90	48.00
12H-2	121	103.81	2.57	37.43	59.81	1.64	1.06	60.29	22.00
12H-3	121	105.31	2.63	35.23	54.38	1.69	1.15	58.51	30.00
12H-4	121	106.81	2.65	39.35	64.87	1.63	1.03	62.97	29.00
12H-5	121	108.31	2.65	31.35	45.66	1.77	1.26	54.45	44.00
12H-6	121	109.81	2.65	33.33	49.98	1.73	1.19	56.64	25.00
13H-1	121	111.81	2.61	34.95	53.73	1.69	1.14	58.03	26.00
13H-2	121	113.31	2.80	40.03	66.76	1.65	1.03	64.91	22.00
13H-3	121	114.81	2.46	35.33	54.63	1.64	1.11	57.03	52.00
13H-4	121	116.31	2.58	39.77	63.33	1.62	1.03	61.78	25.00
13H-5	121	117.81	2.67	41.99	72.39	1.59	0.97	65.61	26.00
13H-6	121	119.31	2.68	43.60	77.30	1.57	0.94	67.23	0.00
14H-1	121	121.31	2.51	39.56	65.44	1.59	1.01	61.87	34.00
14H-2	121	122.81	2.64	36.49	57.45	1.67	1.09	58.95	67.00
14H-3	121	124.31	2.61	36.82	58.29	1.66	1.10	60.01	101.00
14H-4	121	125.81	2.59	37.84	60.87	1.64	1.06	60.89	135.00
14H-5	121	127.31	2.52	37.13	59.06	1.63	1.09	58.49	112.50
14H-6	121	128.81	2.51	35.98	56.20	1.64	1.16	58.19	97.50
15H-1	121	130.81	2.53	47.09	89.00	1.49	0.83	69.01	40.00
15H-2	121	132.31	2.35	43.60	77.32	1.50	0.92	64.26	102.50
15H-3	121	133.81	2.75	42.86	75.01	1.59	0.97	67.07	125.00

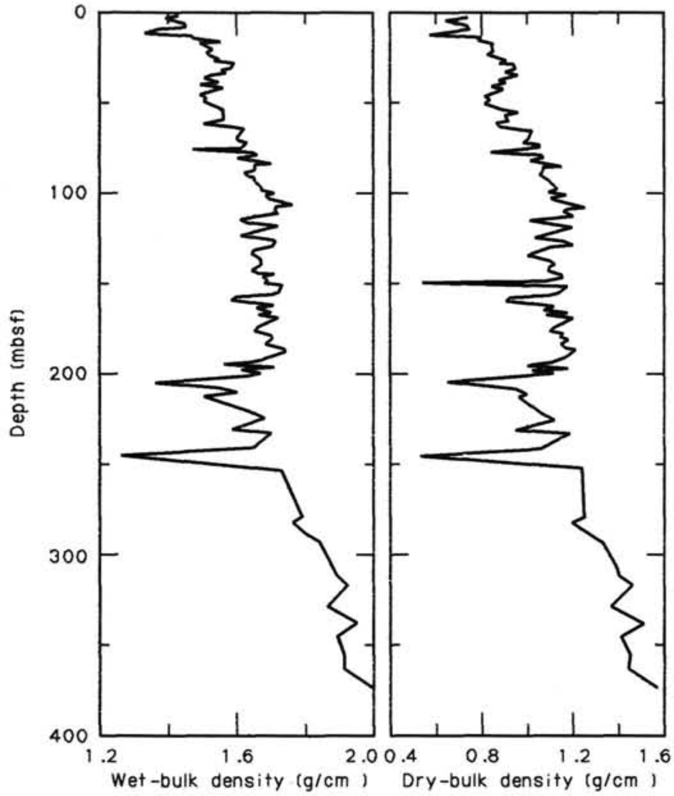

Figure 15. Wet- and dry-bulk-density profiles for Hole 667A.

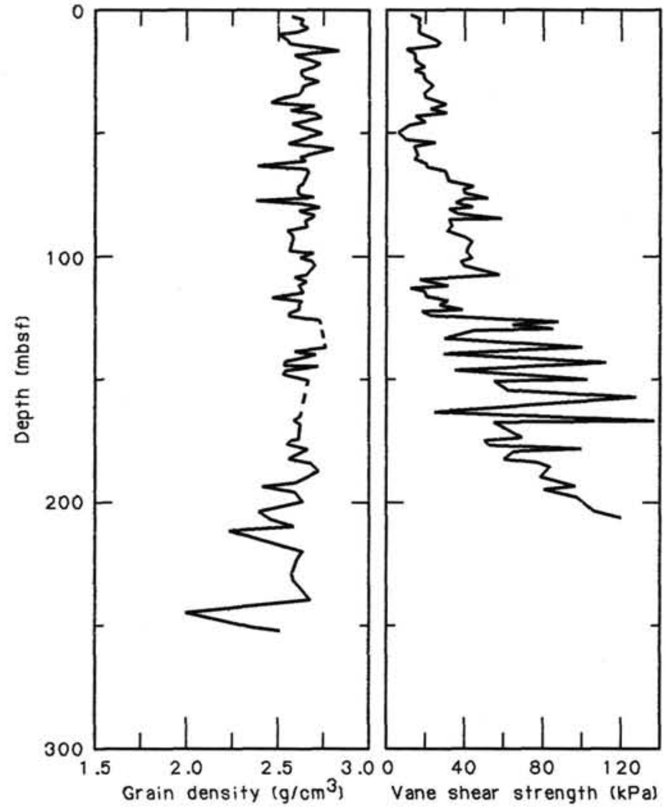

Figure 17. Grain-density and vane-shear-strength profiles for Hole 667A.

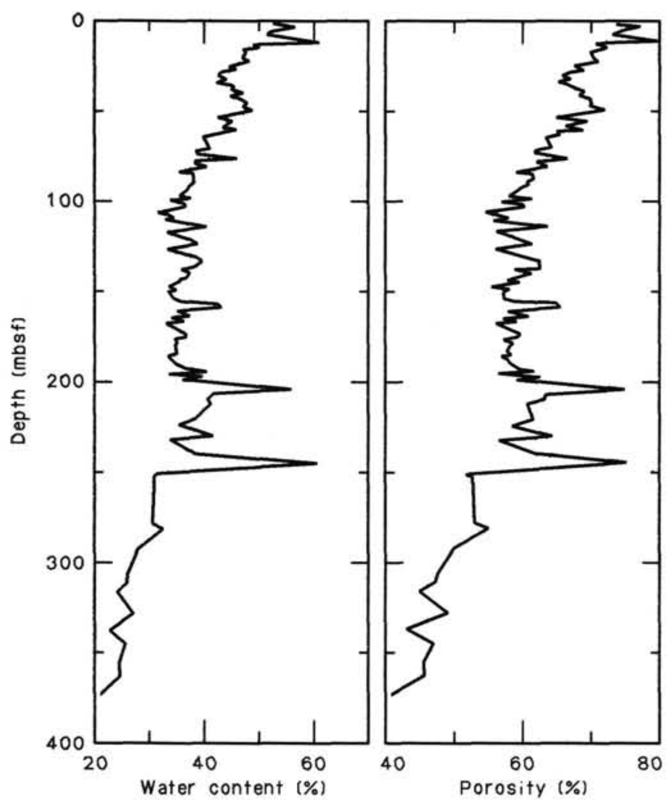

Figure 16. Water-content and porosity profiles for Hole 667A.

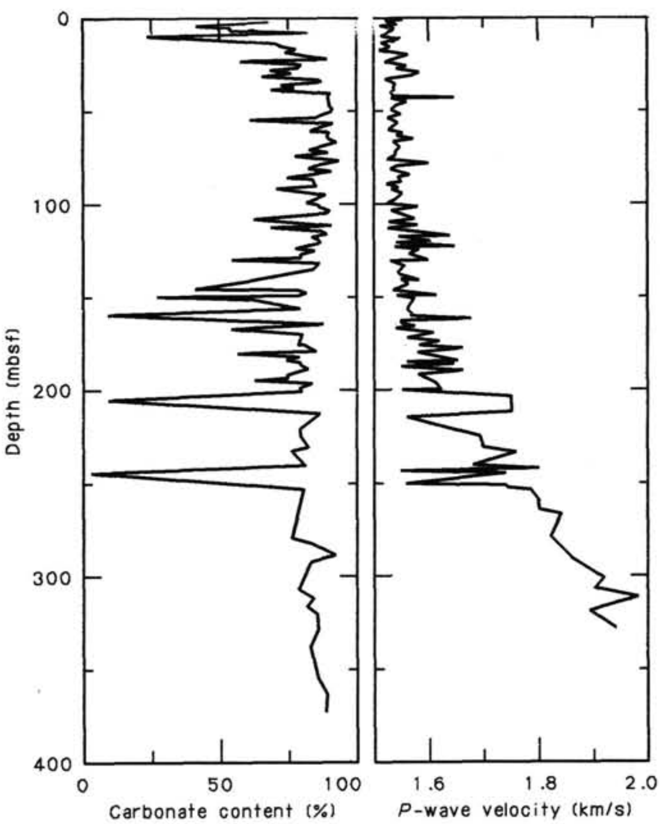

Figure 18. Profiles of carbonate content and *P*-wave velocity for Hole 667A.

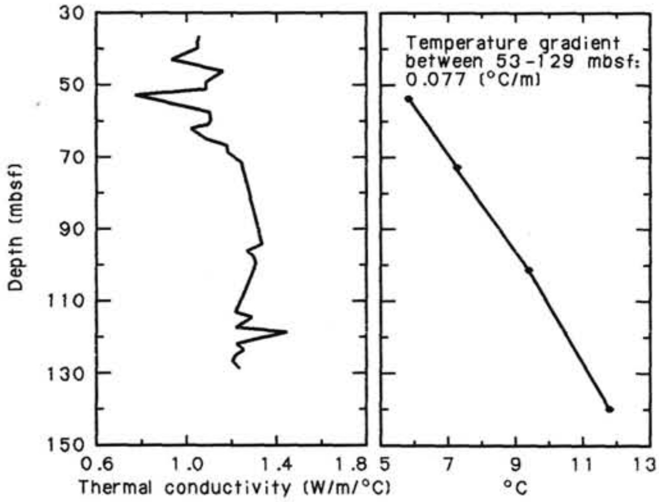

Figure 19. Profiles of thermal conductivity and *in-situ* temperature for Hole 667B.

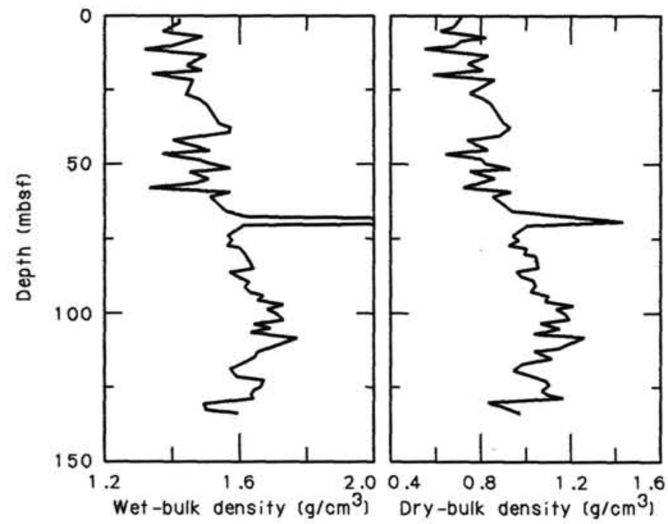

Figure 20. Wet- and dry-bulk-density profiles for Hole 667B.

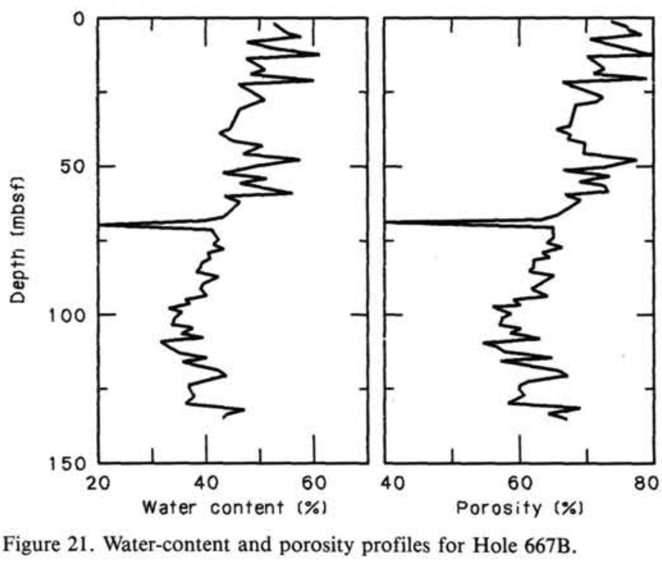

Figure 21. Water-content and porosity profiles for Hole 667B.

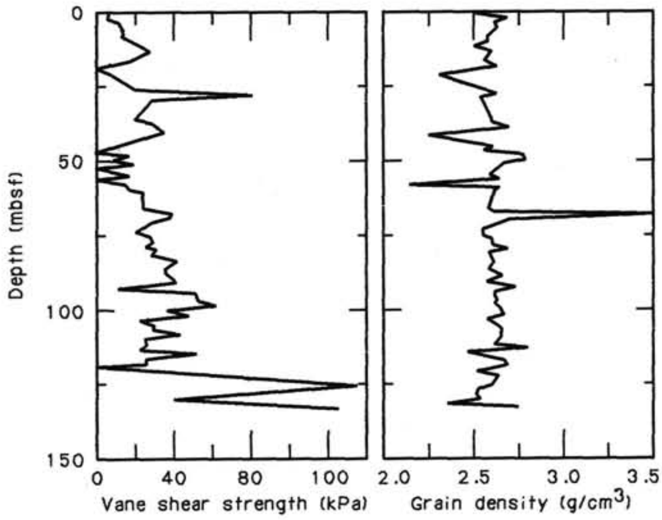

Figure 22. Vane-shear-strength and grain-density profiles for Hole 667B.

Table 7. Thermal-conductivity data for Hole 667B.

Core/ section	Int. (cm)	Depth (mbsf)	Thermal conductivity (W/m/°C)
5H-2	40	36.5	1.050
5H-3	40	38.0	1.044
5H-4	40	39.5	1.644
5H-5	40	41.0	0.998
5H-6	40	42.5	0.982
6H-2	40	46.0	1.161
6H-3	40	47.5	1.114
6H-4	40	49.0	1.051
6H-5	40	50.5	1.081
6H-6	40	52.0	0.770
7H-2	40	55.5	1.047
7H-3	40	57.0	1.100
7H-4	40	58.5	1.102
7H-5	40	60.0	1.096
7H-6	40	61.5	1.015
8H-2	40	65.0	1.106
8H-3	40	66.5	1.132
8H-4	40	68.0	1.133
8H-5	40	69.5	1.214
8H-6	40	71.0	1.238
11H-2	120	94.3	1.335
11H-3	120	95.8	1.259
11H-4	120	97.3	1.292
11H-5	120	98.8	1.302
11H-6	120	100.3	1.300
13H-2	120	113.3	1.212
13H-3	120	114.8	1.291
13H-4	120	116.8	1.242
13H-5	120	117.8	1.215
13H-6	120	119.8	1.407
14H-2	120	122.8	1.218
14H-3	120	124.3	1.258
14H-4	120	125.8	1.215
14H-5	120	127.3	1.200
14H-6	120	128.8	1.230

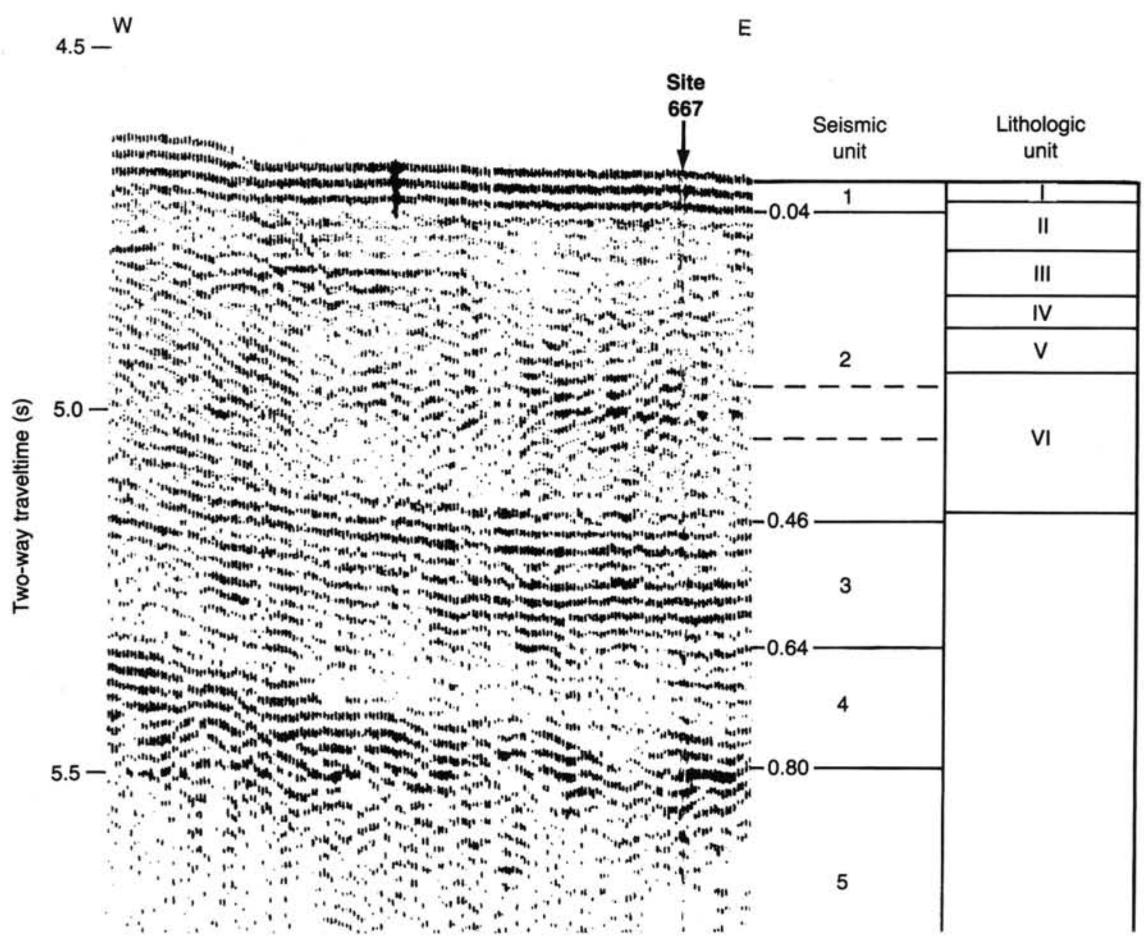

Figure 23. Comparison of Site 667 seismic units with lithologic units. All depths in seconds of two-way traveltime.

Table 8. Composite-depth levels used to correlate cores from Holes 667A and 667B.

Hole 667A Interval (cm)		Hole 667B Interval (cm)	Composite depth (mbsf)
1-1, 0			0
1-1, 80	.........>	1-1, 40	0.80
2-1, 67	<.........	1-2, 119	3.09
2-6, 115	.........>	2-3, 34	11.07
3-1, 28	<.........	2-4, 31	12.54
3-4, 112	.........>	3-1, 103	17.88
		3-2, 106	19.41
	Gap		
6-1, 92			40.22
6-6, 70	.........>	6-3, 52	47.50
7-1, 56	<.........	6-4, 76	49.24
7-5, 139	.........>	7-2, 22	56.07
8-1, 130	<.........	7-4, 79	59.64
8-6, 28	.........>	8-3, 58	66.12
9-1, 52	<.........	8-5, 10	68.64
9-6, 67	.........>	9-5, 19	76.29
10-1, 37	<.........	9-6, 28	77.88
10-6, 14	.........>	10-2, 94	85.15
11-1, 76	<.........	10-3, 40	86.11
11-5, 82			92.17

Note: Composite depths equal to those at Hole 667B.

Table 9. Composite-depth levels used to correlate cores from Holes 667A and 667B.

Hole 667B Interval (cm)		Hole 667A Interval (cm)	Composite depth (mbsf)
1-1, 0			0
1-4, 121	.........>	2-3, 88	5.71
2-1, 28	<.........	2-4, 91	7.24
2-6, 55	.........>	3-3, 49	15.01
3-1, 103	<.........	3-4, 112	17.14
3-2, 106			18.67
	Gap		
5-4, 37			39.47
5-5, 97	.........>	6-2, 94	41.57
6-2, 4	<.........	6-5, 34	45.47
6-6, 4	.........>	7-2, 127	51.47
7-2, 22	<.........	7-5, 139	56.09
7-6, 55	.........>	8-3, 31	62.42
8-2, 0	<.........	8-4, 131	64.92
8-6, 67	.........>	9-2, 61	71.59
9-1, 52	<.........	9-3, 52	73.00
9-7, 25	.........>	10-2, 76	81.73
10-1, 55	<.........	10-4, 76	84.73
10-6, 145			93.13

Note: Composite depths equal to those at Hole 667B.

SITE 667 HOLE A CORE 1H CORED INTERVAL 3525.0-3526.3 mbsl; 0-1.30 mbsf

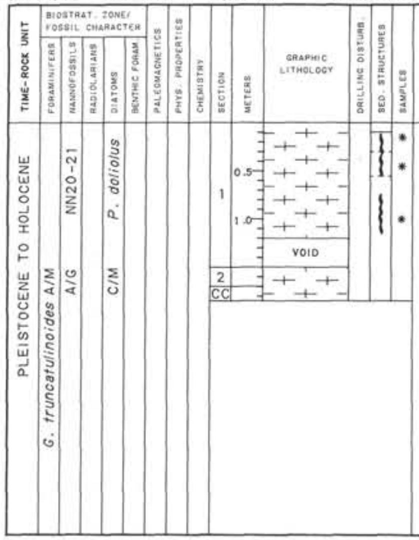

LITHOLOGIC DESCRIPTION

CLAY-BEARING FORAMINIFER-NANNOFOSSIL OOZE to FORAMINIFER-NANNOFOSSIL OOZE

Clay-bearing foraminifer-nannofossil ooze, yellowish-brown (10YR 5/8), to foraminifer-nannofossil ooze, yellowish-brown (10YR 5/6); weakly bioturbated.

Minor lithology: nannofossil-foraminifer ooze, dark-brown (10YR 3/3).

SMEAR SLIDE SUMMARY (%):

	1, 8 M	1, 50 D	1, 106 M
TEXTURE:			
Sand	40	20	30
Silt	20	10	20
Clay	40	70	50
COMPOSITION:			
Quartz	Tr	Tr	Tr
Clay	—	15	Tr
Accessory Minerals	5	—	Tr
Foraminifers	50	30	40
Nannofossils	40	55	50
Diatoms		Tr	Tr
Radiolarians	5	5	Tr
Sponge spicules		Tr	Tr

Chemistry: IC here refers to weight % $CaCO_3$.

SITE 667 HOLE A CORE 2H CORED INTERVAL 3526.3-3835.8 mbsl; 1.30-10.80 mbsf

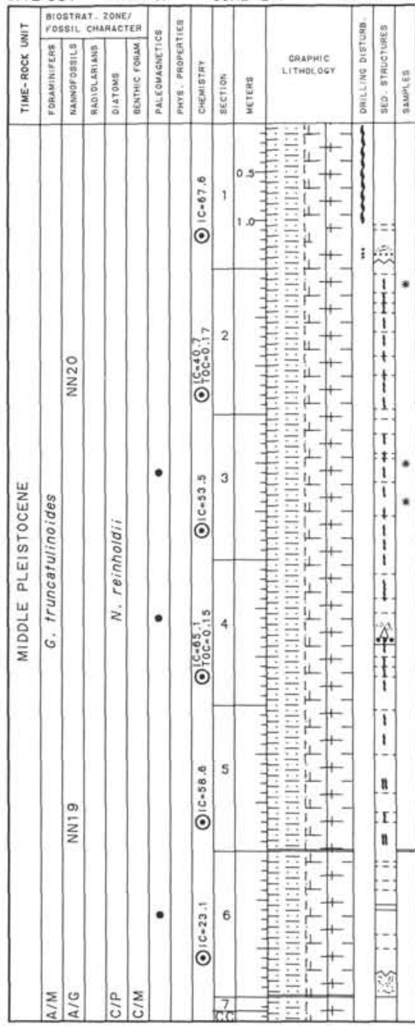

LITHOLOGIC DESCRIPTION

MUD-BEARING, FORAMINIFER-NANNOFOSSIL OOZE and FORAMINIFER-NANNOFOSSIL OOZE, alternating with FORAMINIFER-BEARING, MUDDY NANNOFOSSIL OOZE

Mud-bearing, foraminifer-nannofossil ooze, pale-brown (10YR 6/3) to light-yellowish-brown (10YR 6/4), and foraminifer-nannofossil ooze, very pale-brown (10YR 7/4) to light-gray (10YR 7/2), alternating with foraminifer-bearing, muddy nannofossil ooze, pale-brown (10YR 6/4) to dark-grayish-brown (10YR 4/2); weak bioturbation; turbidites or graded bedding with sharp contacts in Section 1, 130–140 cm; Section 4, 80–90 cm, and Section 6, 120–145 cm. Minor void in Section 6, 149–150 cm.

SMEAR SLIDE SUMMARY (%):

	2, 19 D	3, 59 D	3, 85 D
TEXTURE:			
Sand	20	10	—
Silt	20	20	30
Clay	60	70	70
COMPOSITION:			
Quartz	5	10	20
Clay	10	—	15
Foraminifers	30	30	10
Nannofossils	50	60	55
Radiolarians	5	Tr	Tr
Sponge spicules	—	—	Tr

SITE 667 HOLE A CORE 3H CORED INTERVAL 3535.8-3545.3 mbsl; 10.8-20.3 mbsf

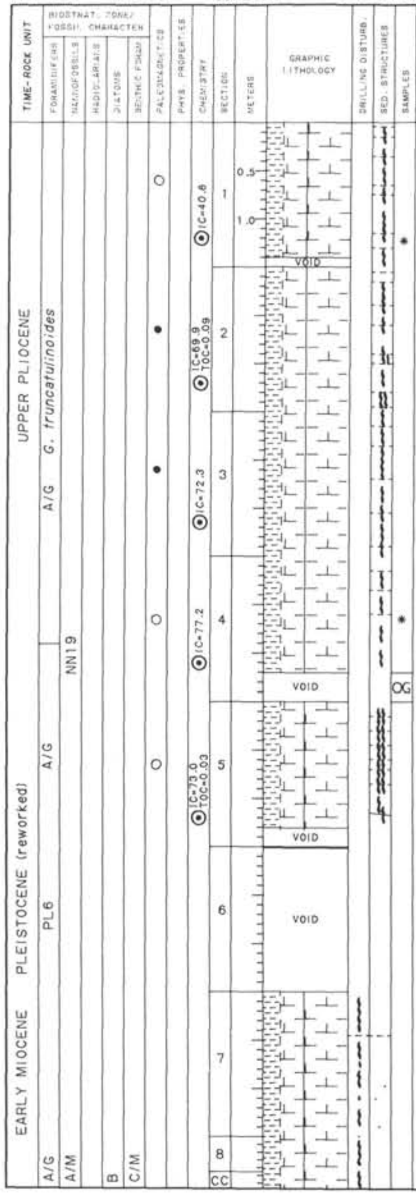

LITHOLOGIC DESCRIPTION

CLAYEY NANNOFOSSIL OOZE, *alternating with* SILT-BEARING, FORAMINIFER-BEARING NANNOFOSSIL OOZE

Clayey nannofossil ooze, very pale-brown (10YR 7/4), light-yellowish-brown (10YR 6/4), and yellowish-brown (10YR 6/6), alternating with silt-bearing, foraminifer-bearing nannofossil ooze, pale-brown (10YR 6/3) or light-gray (10YR 7/2, 7/1); moderately bioturbated. Large sandy foraminifer turbidite in Section 7 through CC. Thin layer of clayey nannofossil ooze/silty, foraminifer-bearing nannofossil ooze in Section 6, 0–5 cm.

SMEAR SLIDE SUMMARY (%):

	1, 120 D	4, 70 D
TEXTURE:		
Sand	10	15
Silt	15	15
Clay	75	70
COMPOSITION:		
Quartz	—	Tr
Clay	35	5
Accessory Minerals	5	10
Foraminifers	5	15
Nannofossils	55	65
Diatoms	Tr	5

SITE 667 HOLE A CORE 4H CORED INTERVAL 3545.3-3554.8 mbsl; 20.3-29.8 mbsf

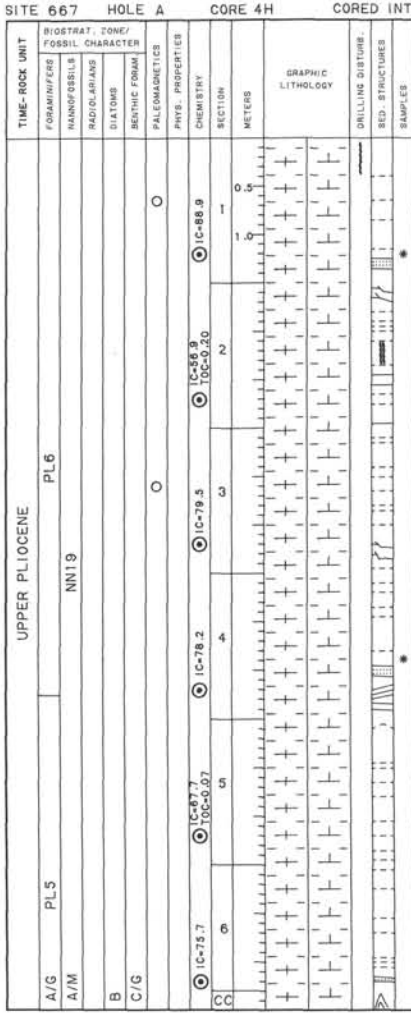

LITHOLOGIC DESCRIPTION

CLAY-BEARING FORAMINIFER-BEARING NANNOFOSSIL OOZE, *alternating with* FORAMINIFER-NANNOFOSSIL OOZE

Clay-bearing, foraminifer-bearing nannofossil ooze, light-gray (2.5Y 7/2) to light-brownish-gray (2.5Y 6/2), alternating with foraminifer-nannofossil ooze, white (2.5Y 8/1) to light-gray (5Y 7/1, 7/2); very weakly bioturbated with small turbidites(?) in Section 1, 125–130 cm; Section 4, 87–91 cm, and Section 6, 6, 116–120 cm.

SMEAR SLIDE SUMMARY (%):

	1, 120 D	4, 70 D
TEXTURE:		
Sand	15	25
Silt	15	20
Clay	70	55
COMPOSITION:		
Quartz	5	5
Clay	10	5
Accessory Minerals	5	5
Foraminifers	15	30
Nannofossils	65	55

SITE 667 HOLE A CORE 5H CORED INTERVAL 3554.8-3564.3 mbsl; 29.8-39.3 mbsf

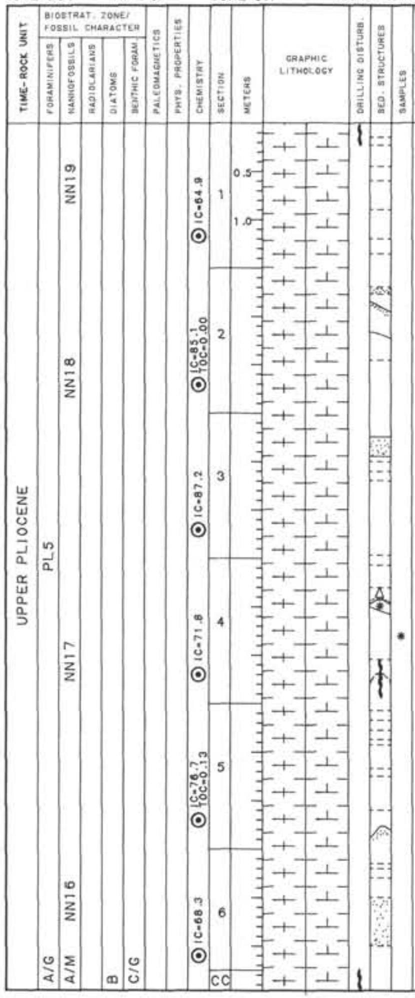

LITHOLOGIC DESCRIPTION

SILT-BEARING, CLAY-BEARING NANNOFOSSIL OOZE, alternating with CLAY-BEARING, FORAMINIFER-NANNOFOSSIL OOZE

Silt-bearing, clay-bearing nannofossil ooze, light-gray (2.5Y 7/2) or light-greenish-gray (5GY 7/1), alternating with clay-bearing, foraminifer-nannofossil ooze, white (10YR 8/1) or light-gray (10YR 7/2); weak bioturbation. Thin, 5–20 cm, coarse-grained layers with sharp contacts in Sections 2 through 6.

SMEAR SLIDE SUMMARY (%):

	4, 40 D	4, 70 D
TEXTURE:		
Sand	5	25
Silt	15	15
Clay	80	60
COMPOSITION:		
Quartz	Tr	Tr
Clay	10	10
Accessory Minerals	10	5
Foraminifers	5	25
Nannofossils	75	55
Diatoms	Tr	5

SITE 667 HOLE A CORE 6H CORED INTERVAL 3564.3-3573.8 mbsl; 39.3-48.8 mbsf

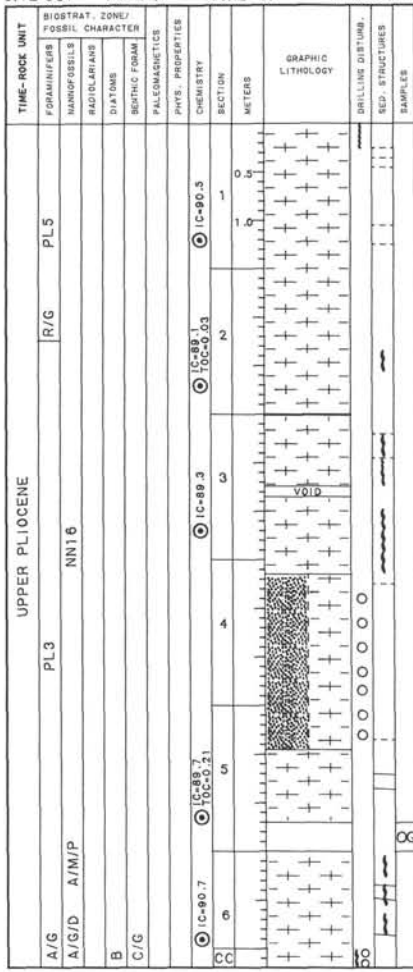

LITHOLOGIC DESCRIPTION

CLAY-BEARING FORAMINIFER-NANNOFOSSIL OOZE

Clay-bearing foraminifer-nannofossil ooze, white (10YR 8/1, 5Y 8/1) or light-gray (5Y 7/1, 7/2); very weak bioturbation; soupy foraminifer sand in Section 4, 15 cm, and Section 5, 44 cm. Minor void in Section 3, 0–5 cm.

SITE 667 HOLE A CORE 7H CORED INTERVAL 3573.8-3583.3 mbsl; 48.8-58.3 mbsf

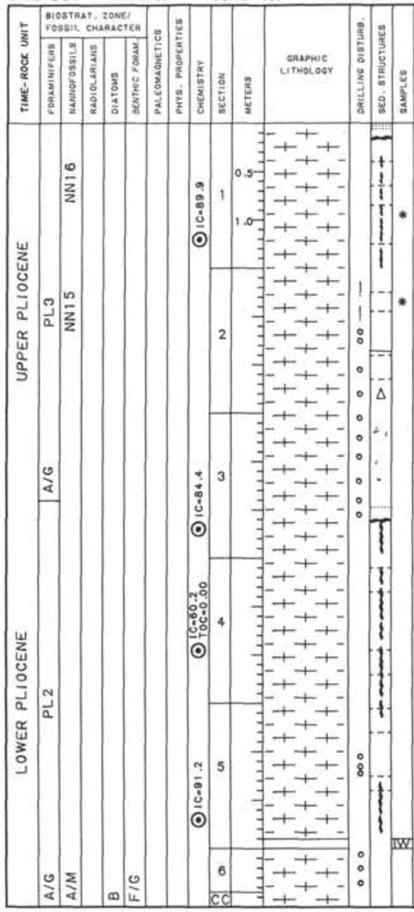

LITHOLOGIC DESCRIPTION

FORAMINIFER-NANNOFOSSIL OOZE and CLAY-BEARING FORAMINIFER-NANNOFOSSIL OOZE

Foraminifer-nannofossil ooze, white (5Y 8/1, 10YR 8/1), and clay-bearing foraminifer-nannofossil ooze, white (5Y 8/1) to light-gray (5Y 7/2); weakly bioturbated. Several soupy intervals, possibly the result of coring disturbance. Minor void in Section 5, 143–150 cm.

SMEAR SLIDE SUMMARY (%):

	1, 100 D	2, 30 D
TEXTURE:		
Sand	30	30
Silt	20	20
Clay	50	50
COMPOSITION:		
Quartz	—	Tr
Rock Fragments	—	Tr
Clay	5	10
Accessory Minerals	Tr	Tr
Foraminifers	40	35
Nannofossils	55	55

SITE 667 HOLE A CORE 8H CORED INTERVAL 3583.3-3592.8 mbsl; 58.3-67.8 mbsf

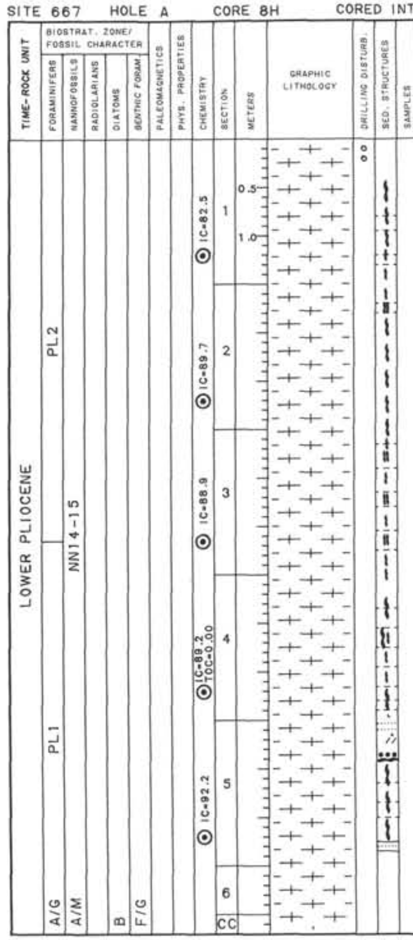

LITHOLOGIC DESCRIPTION

FORAMINIFER-NANNOFOSSIL OOZE and CLAY-BEARING FORAMINIFER-NANNOFOSSIL OOZE

Foraminifer-nannofossil ooze, white (5Y 8/1, 10YR 8/1), and clay-bearing foraminifer-nannofossil ooze, white (5Y 8/1) to light-gray (5Y 7/2); weakly bioturbated. coarse foraminifer sandy turbidites(?) in Section 5.

SITE 667 HOLE A CORE 9H CORED INTERVAL 3592.8-3602.3 mbsl; 68.8-77.3 mbsf

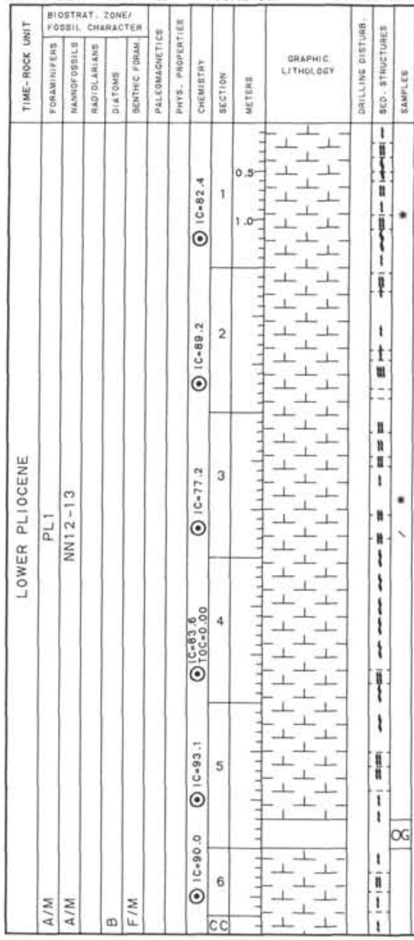

LITHOLOGIC DESCRIPTION

FORAMINIFER-BEARING NANNOFOSSIL OOZE and CLAY-BEARING NANNOFOSSIL OOZE

Foraminifer-bearing nannofossil ooze, white (5Y 8/1), and clay-bearing nannofossil ooze, white (5Y 8/1) to pale-yellow (5Y 7/3); moderately bioturbated.

SMEAR SLIDE SUMMARY (%):

	1, 90 D	3, 90 D
TEXTURE:		
Sand	—	—
Silt	10	10
Clay	90	90
COMPOSITION:		
Quartz	Tr	Tr
Clay	10	5
Accessory Minerals	Tr	Tr
Foraminifers	5	10
Nannofossils	85	85

SITE 667 HOLE A CORE 10H CORED INTERVAL 3602.3-3611.8 mbsl; 77.3-86.8 mbsf

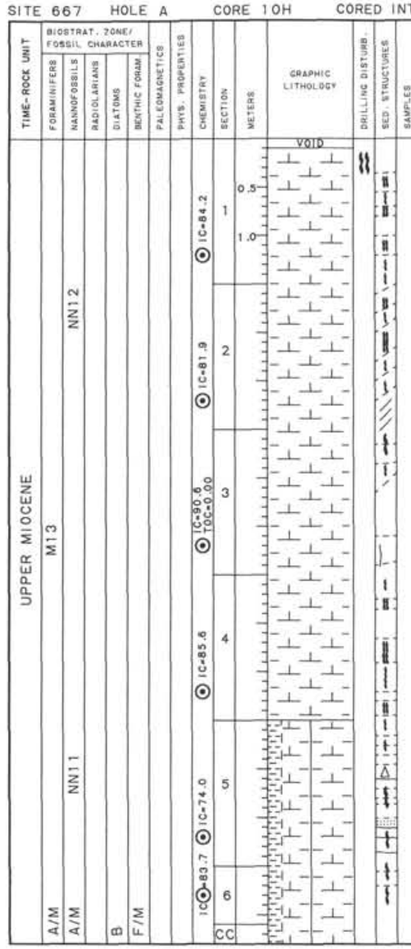

LITHOLOGIC DESCRIPTION

FORAMINIFER-BEARING NANNOFOSSIL OOZE and CLAY-BEARING NANNOFOSSIL OOZE, alternating with CLAYEY NANNOFOSSIL OOZE

Foraminifer-bearing nannofossil ooze, white (10YR 8/1), and clay-bearing nannofossil ooze, white (5Y 8/1) to pale-yellow (5Y 7/3) in Section 1 throughout Section 4.

Foraminifer-bearing nannofossil ooze, white (10YR 8/1), and clayey nannofossil ooze, white (5Y 8/1) to pale-yellow (5Y 7/3) alternating with clayey nannofossil ooze, pale-brown (10YR 6/3) to yellowish-brown (10YR 5/6), in Section 4 through CC; moderate bioturbation throughtout core. Most of Section 2 and upper half of Section 3 may be part of slump. Coarse foraminifer sand with erosional contacts in Section 5, 59 and 110 cm.

SITE 667 HOLE A CORE 11H CORED INTERVAL 3611.8-3621 mbsl; 86.80-96.30 mbsf

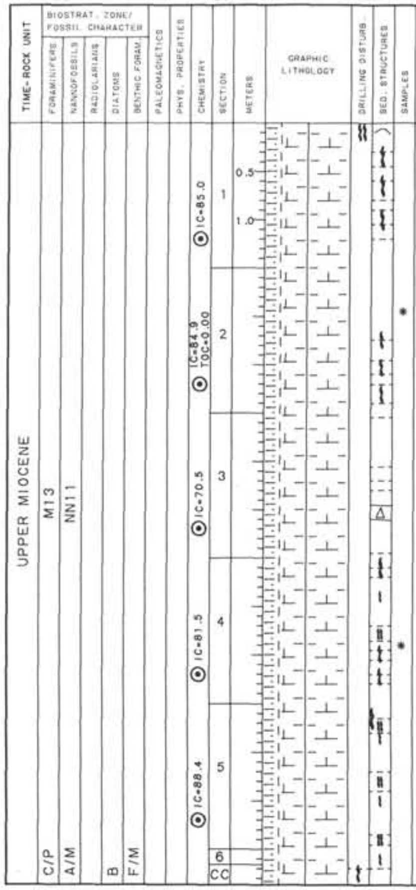

LITHOLOGIC DESCRIPTION

CLAY-BEARING, FORAMINIFER-BEARING NANNOFOSSIL OOZE, alternating with MUDDY NANNOFOSSIL OOZE

Clay-bearing, foraminifer-bearing nannofossil ooze, white (5Y 8/2, 10YR 8/1), alternating with muddy nannofossil ooze, very pale-brown (10YR 7/3), light-yellowish-brown (10YR 6/4), or light-gray (10YR 7/2); weak to moderate bioturbation; coarse foraminifer sand layer with sharp upper and lower contacts in Section 3, 100–110 cm.

SMEAR SLIDE SUMMARY (%):

	2, 40 D	4, 80 D
TEXTURE:		
Sand	20	5
Silt	10	15
Clay	70	80
COMPOSITION:		
Quartz	Tr	Tr
Clay	10	20
Accessory Minerals	Tr	5
Foraminifers	20	5
Nannofossils	70	70
Radiolarians	Tr	—

SITE 667 HOLE A CORE 12H CORED INTERVAL 3621.3-3630.8 mbsl; 96.30-105.80 mbsf

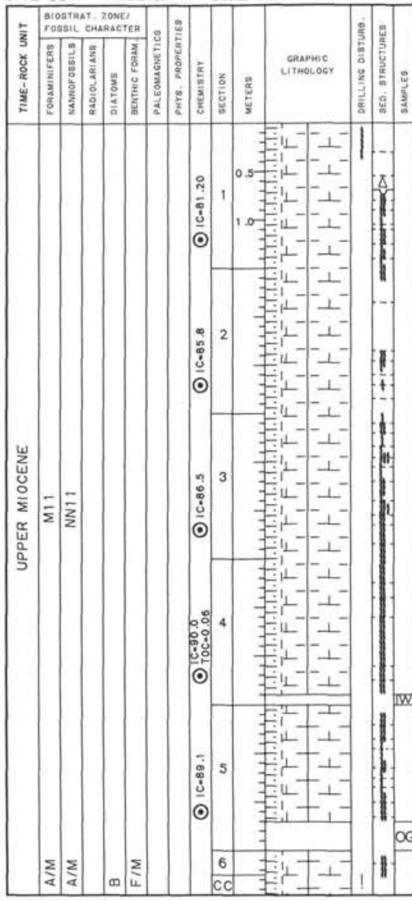

LITHOLOGIC DESCRIPTION

CLAY-BEARING, FORAMINIFER-BEARING NANNOFOSSIL OOZE, alternating with MUDDY NANNOFOSSIL OOZE

Clay-bearing, foraminifer-bearing nannofossil ooze, white (5Y 8/2, 10YR 8/1), alternating with muddy nannofossil ooze, very pale-brown (10YR 7/3), light-yellowish-brown (10YR 6/4), or light-gray (10YR 7/2); moderate bioturbation; graded bedding in Section 1, 60–70 cm.

SITE 667 HOLE A CORE 13H CORED INTERVAL 3630.8-3640.3 mbsl; 105.80-115.30 mbsf

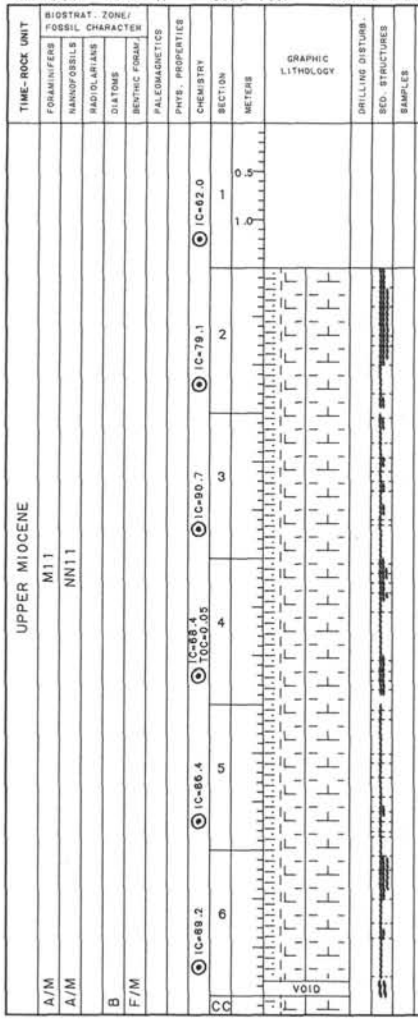

LITHOLOGIC DESCRIPTION

CLAY-BEARING, FORAMINIFER-BEARING NANNOFOSSIL OOZE, alternating with MUDDY NANNOFOSSIL OOZE

Clay-bearing, foraminifer-bearing nannofossil ooze, white (5Y 8/2, 10YR 8/1), alternating with muddy nannofossil ooze, very pale-brown (10YR 7/3), light-yellowish-brown (10YR 6/4), or light-gray (10YR 7/2); moderately bioturbated; contacts dip slightly between Section 5, 100 cm, and Section 6, 30 cm.

SITE 667 HOLE A CORE 14H CORED INTERVAL 3640.3-3649.8 mbsl; 115.30-124.80 mbsf

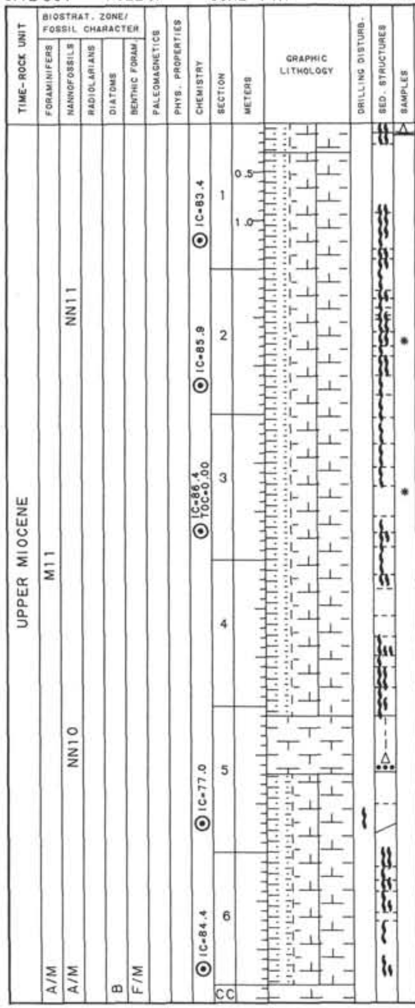

LITHOLOGIC DESCRIPTION

CLAY-BEARING, FORAMINIFER-BEARING NANNOFOSSIL OOZE to NANNOFOSSIL OOZE, alternating with MUDDY NANNOFOSSIL OOZE

Clay-bearing, foraminifer-bearing nannofossil ooze to nannofossil ooze, white (5Y 8/2, 10YR 8/1), alternating with muddy nannofossil ooze, very pale-brown (10YR 7/3), light-yellowish-brown (10YR 6/4), or light-gray (10YR 7/2); weak to moderate bioturbation; erosional contact in Section 1, 10 cm. Coarse foraminifer ooze with erosional(?) lower contact in Section 5, 10–70 cm. Minor void in Section 1, 33–37 cm.

SMEAR SLIDE SUMMARY (%):

	1, 8 D	2, 76 D	3, 91 D
TEXTURE:			
Sand	—	—	—
Silt	5	15	10
Clay	95	85	90
COMPOSITION:			
Quartz	1	2	Tr
Clay	—	20	—
Calcite	2	3	Tr
Accessory Minerals	2	3	Tr
Foraminifers	5	Tr	10
Nannofossils	90	75	90

SITE 667 HOLE A CORE 15H CORED INTERVAL 3649.8-3659.3 mbsl; 124.80-134.30 mbsf

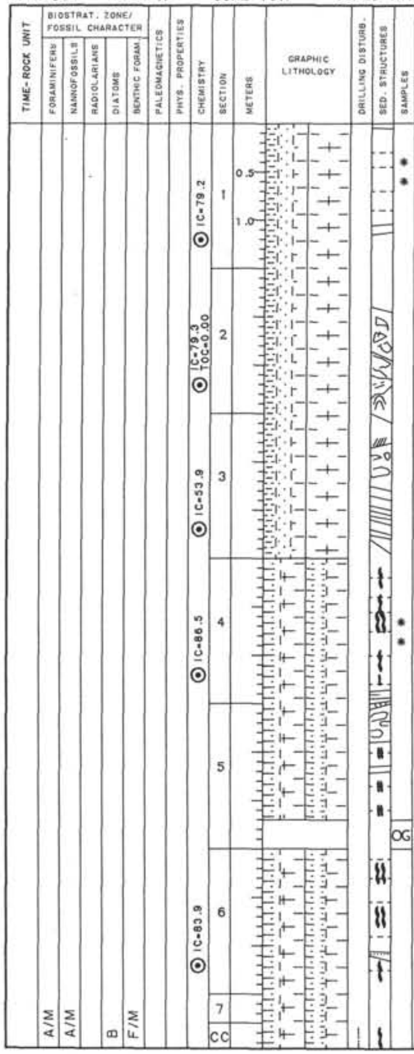

LITHOLOGIC DESCRIPTION

SILT-BEARING, FORAMINIFER-NANNOFOSSIL OOZE, alternating with NANNOFOSSIL silty clay; and MUDDY NANNOFOSSIL OOZE, alternating with MUDDY FORAMINIFER-NANNOFOSSIL OOZE

Silt-bearing foraminifer-nannofossil ooze, light-greenish-gray (5G 7/1) in Section 1 through 3, 150 cm, alternating with nannofossil silty clay, light-greenish-gray (5GY 7/1, 5G 7/1) or greenish-gray (5G 6/1); bedding planes and laminations controt, fold, and dip; interval part of a slump.

Muddy nannofossil ooze, pinkish-gray (7.5YR 7/2) or light-brown (7.5YR 6/4) in Section 3 through CC, alternating with muddy foraminifer nannofossil ooze, white (10YR 8/1, 8/2); moderately bioturbated; coarse foraminifer 2- to 5-cm thick sand with erosional contacts in Sections 4, 5, and 6. Small debris flow in Section 4, 140 cm, and Section 5, 40 cm.

SMEAR SLIDE SUMMARY (%):

	1, 66 D	1, 40 D	4, 68 D	4, 95 D
TEXTURE:				
Sand	15	5	—	10
Silt	25	10	15	30
Clay	60	85	85	60
COMPOSITION:				
Quartz	10	10	15	15
Clay	—	60	25	10
Foraminifers	30	5	Tr	25
Nannofossils	60	25	60	50
Sponge Spicules	Tr	—	—	—

SITE 667 HOLE A CORE 16H CORED INTERVAL 3659.3-3668.8 mbsl; 134.30-143.80 mbsf

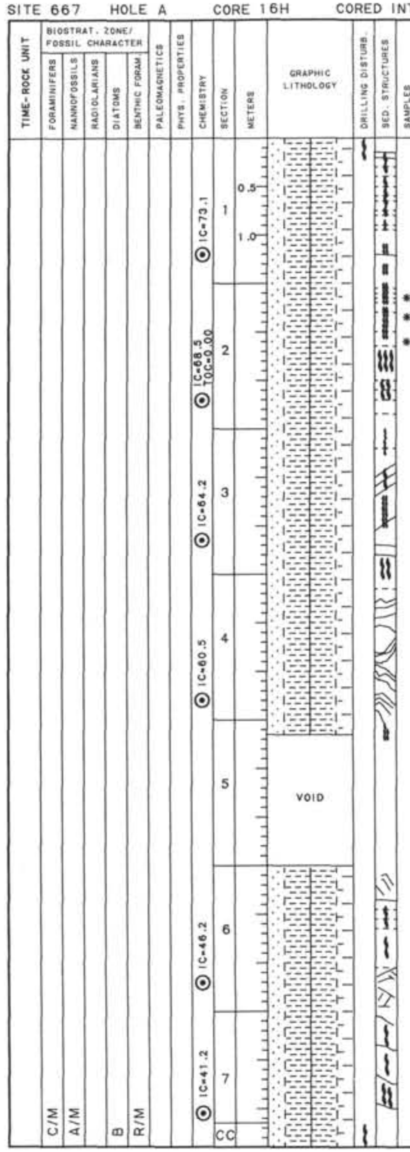

LITHOLOGIC DESCRIPTION

NANNOFOSSIL-BEARING SILTY CLAY, alternating with FORAMINIFER-BEARING, CLAYEY NANNOFOSSIL OOZE

Nannofossil-bearing silty clay, light-brown (7.5YR 6/4) or brown (7.5YR 5/4), alternating with foraminifer-bearing, clayey nannofossil ooze, white (10YR 8/2) and pink (10YR 8/4); moderately to extensively bioturbated in Sections 1 and 2. Section 3 through CC has folded, contorted, and dipping bedding planes and laminations. Slide planes occur in Sections 3 and 6; interval part of a slump.

SMEAR SLIDE SUMMARY (%):

	2, 12 D	2, 36 D	2, 69 D
TEXTURE:			
Sand	—	—	5
Silt	15	20	10
Clay	85	80	85
COMPOSITION:			
Quartz	15	20	Tr
Clay	65	60	30
Accessory Minerals	—	Tr	—
Foraminifers	—	—	10
Nannofossils	20	20	60

SITE 667 HOLE A CORE 17 CORED INTERVAL 3668.8-3678.3 mbsl; 143.8-153.3 mbsf

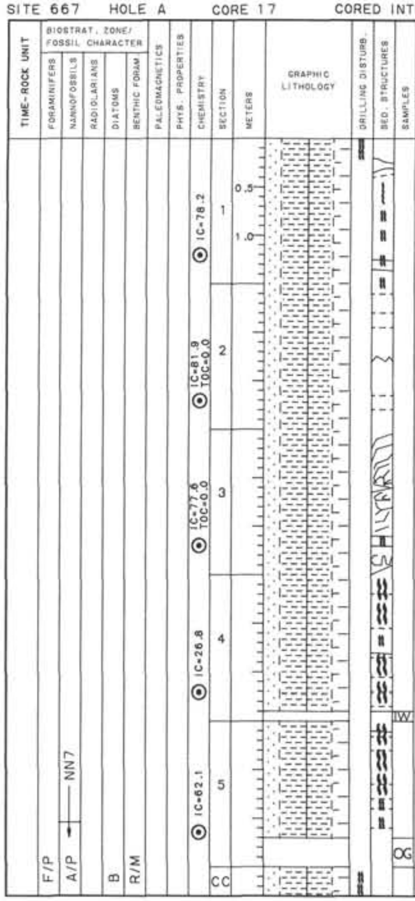

LITHOLOGIC DESCRIPTION

NANNOFOSSIL-BEARING SILTY CLAY, alternating with FORAMINIFER-BEARING, CLAYEY NANNOFOSSIL OOZE

Nannofossil-bearing silty clay, reddish-yellow (7.5YR 6/6) to strong-brown (7.5YR 5/6), alternating with foraminifer-bearing, clayey nannofossil ooze, very pale-brown (10YR 8/3); moderately bioturbated. Section 3 has folded and dipping bedding planes; part of slump.

SITE 667 HOLE A CORE 18H CORED INTERVAL 3678.3-3687.8 mbsl; 153.3-162.8 mbsf

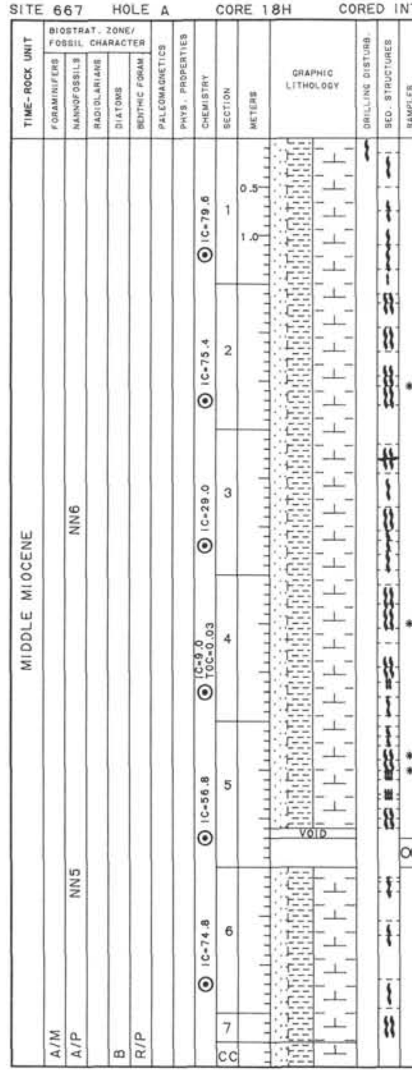

LITHOLOGIC DESCRIPTION

NANNOFOSSIL OOZE, alternating with SILTY CLAY

Nannofossil ooze, very pale-brown (10YR 8/3), alternating with silty clay, pink (7.5YR 7/4), reddish-yellow (7.5YR 6/6), or strong-brown (7.5YR 5/8); moderately bioturbated.

SMEAR SLIDE SUMMARY (%):

	2, 108 D	4, 51 D	5, 35 D	5, 49 D
TEXTURE:				
Sand	—	—	—	—
Silt	15	10	20	10
Clay	85	90	80	90
COMPOSITION:				
Quartz	10	3	15	3
Clay	85	5	80	—
Calcite/Dolomite	—	2	—	2
Accessory Minerals	5	—	4	—
Foraminifers	—	5	—	<5
Nannofossils	Tr	80	Tr	90
Diatoms	—			
Radiolarians	—	2	1	1
Sponge Spicules	—			

SITE 667 HOLE A CORE 19H CORED INTERVAL 3687.8-3697.3 mbsl; 162.8-172.3 mbsf

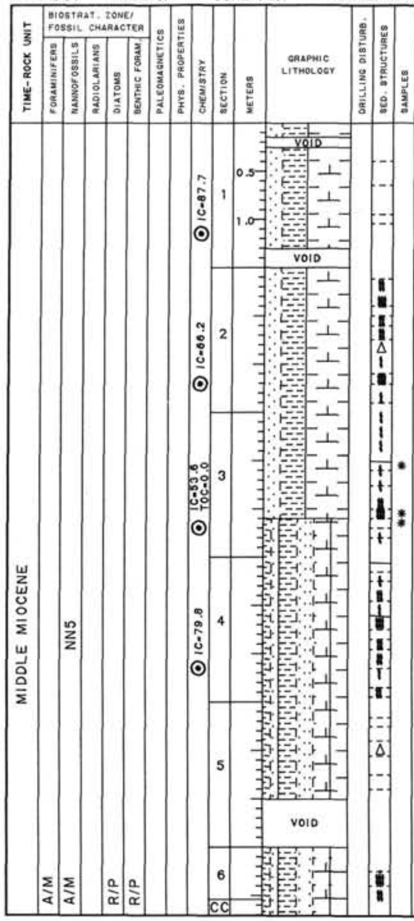

LITHOLOGIC DESCRIPTION

FORAMINIFER-BEARING NANNOFOSSIL OOZE, alternating with SILTY CLAY, and FORAMINIFER-BEARING NANNOFOSSIL OOZE, alternating with SILTY CLAY and NANNOFOSSIL SILTY CLAY

Foraminifer-bearing nannofossil ooze, white (10YR 8/1) in Section 1 through Section 3, 110 cm, alternating with silty clay, very pale-brown (10YR 7/4) or light-yellowish-brown (10YR 6/4); moderately bioturbated; graded bedding in Section 2, 75–90 cm.

Foraminifer-bearing nannofossil ooze, white (10YR 8/1) in Section 3, 110 cm through CC, alternating with silty clay, very pale-brown (10YR 7/4) or light-yellowish-brown (10YR 6/4), and nannofossil silty clay, pale-yellow (5Y 7/3); moderately bioturbated; graded bedding in Section 5 at 45–60 cm.

SMEAR SLIDE SUMMARY (%):

	3, 63 D	2, 108 D	3, 116 D
TEXTURE:			
Sand	10	—	—
Silt	20	15	15
Clay	70	85	85
COMPOSITION:			
Quartz	Tr	10	15
Clay	—	85	45
Calcite/Dolomite	3	—	—
Accessory Minerals	Tr	4	Tr
Foraminifers	22	—	—
Nannofossils	75	Tr	40
Diatoms	Tr		
Radiolarians	Tr	1	1
Sponge spicules	Tr		

SITE 667 HOLE A CORE 20H CORED INTERVAL 3697.3-3706.8 mbsl; 172.3-181.8 mbsf

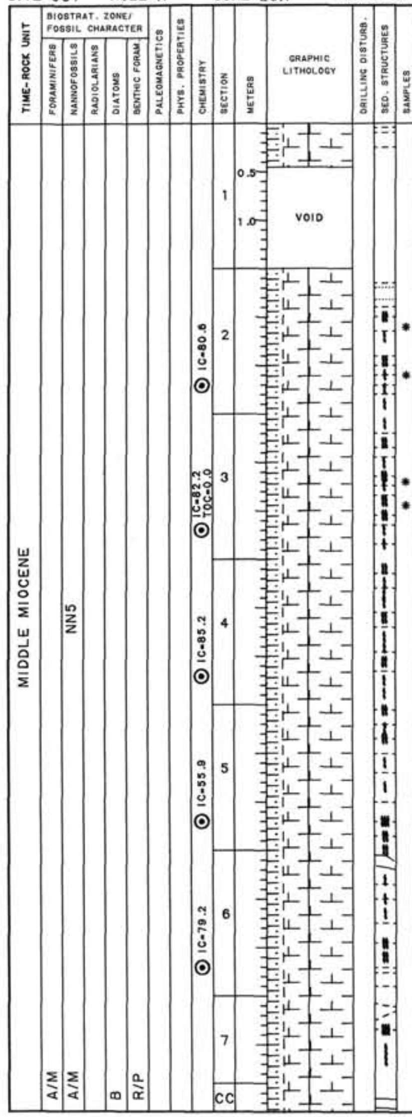

LITHOLOGIC DESCRIPTION

MUDDY NANNOFOSSIL OOZE, alternating with SILT-BEARING, CLAYEY NANNOFOSSIL OOZE

Muddy nannofossil ooze, white (5Y 8/1), alternating with silt-bearing, clayey nannofossil ooze, very pale-brown (10YR 7/3) or light-yellowish-brown (10YR 6/4), moderately bioturbated; coarse-grained intervals with erosional contacts in Section 2, 18–38 cm, and Section 6, 3–15 cm.

SMEAR SLIDE SUMMARY (%):

	2, 55 D	2, 110 D	3, 70 D	3, 90 D
TEXTURE:				
Sand	5	—	5	20
Silt	15	20	20	15
Clay	80	80	75	65
COMPOSITION:				
Quartz	—	Tr	5	—
Clay	20	30	20	10
Accessory Minerals	5	10	15	10
Foraminifers	5	Tr	5	20
Nannofossils	70	60	55	60

SITE 667 HOLE A CORE 21H CORED INTERVAL 3706.8-3716.3 mbsl; 181.8-191.3 mbsf

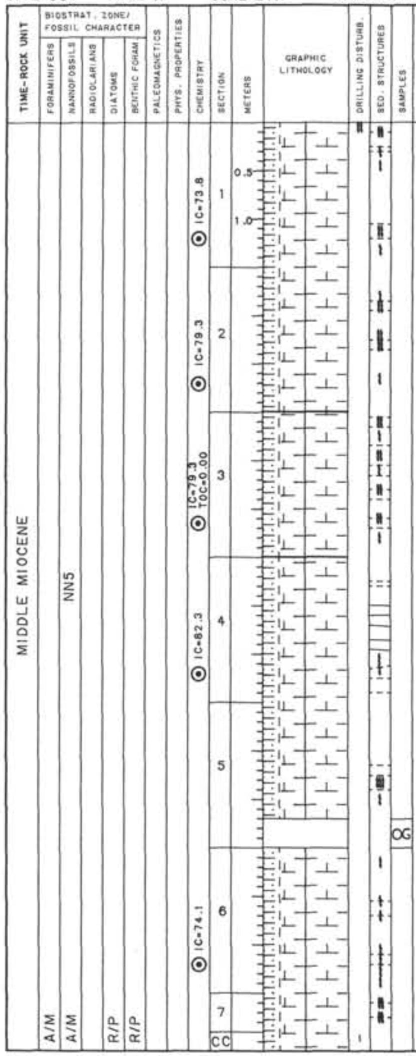

LITHOLOGIC DESCRIPTION

MUDDY NANNOFOSSIL OOZE, alternating with SILT-BEARING, CLAY-BEARING NANNOFOSSIL OOZE

Muddy nannofossil ooze, white (5Y 8/1), alternating with silt-bearing, clay-bearing nannofossil ooze, very pale-brown (10YR 7/3) or light-yellowish-brown (10YR 6/4), weakly to moderately bioturbated. Foraminifer-turbidite in Section 4, 103–111 cm. Minor voids in Section 2, 143–150 cm; Section 3, 149–150 cm; and Section 4, 38 cm.

SITE 667 HOLE A CORE 22H CORED INTERVAL 3716.3-3725.8 mbsl; 191.3-200.8 mbsf

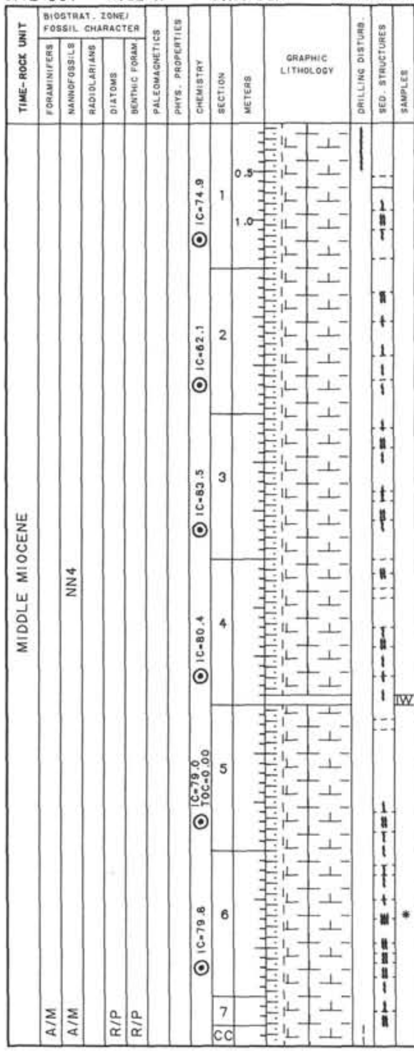

LITHOLOGIC DESCRIPTION

MUDDY NANNOFOSSIL OOZE, alternating with SILT-BEARING, CLAY-BEARING NANNOFOSSIL OOZE

Muddy nannofossil ooze, white (5Y 8/1), alternating with silt-bearing, clay-bearing nannofossil ooze, very pale-brown (10YR 7/3) or light-yellowish-brown (10YR 6/4), weakly to moderately bioturbated. Foraminifer sand with an erosional contact in Section 1, 50–65cm.

SMEAR SLIDE SUMMARY (%):

	6, 60 D
TEXTURE:	
Sand	—
Silt	5
Clay	95
COMPOSITION:	
Clay	10
Accessory Minerals	10
Foraminifers	Tr
Nannofossils	80

SITE 667 HOLE A CORE 23H CORED INTERVAL 3725.8-3735.3 mbsl; 200.8-210.3 mbsf

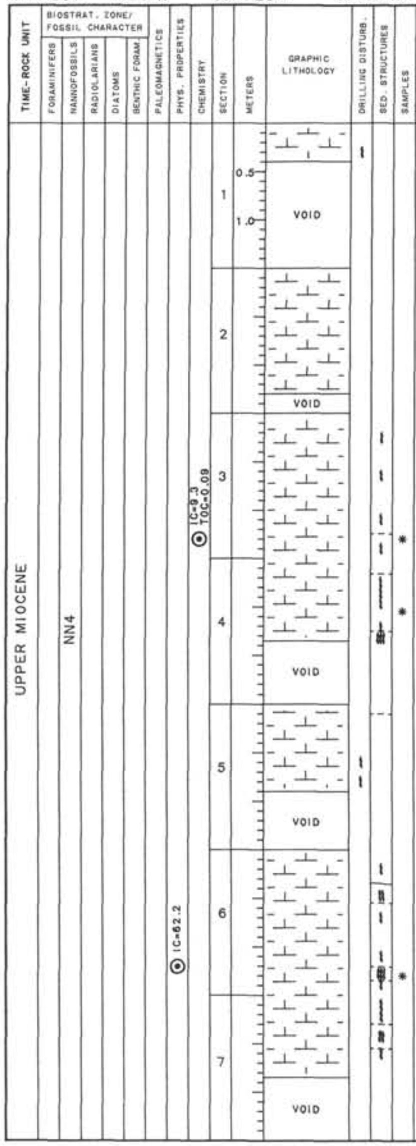

LITHOLOGIC DESCRIPTION

SILT-BEARING, CLAY-BEARING, SILICEOUS-BEARING NANNOFOSSIL OOZE to CLAY-BEARING, SILT-BEARING FORAMINIFER-BEARING NANNOFOSSIL OOZE

Silt-bearing, clay-bearing, siliceous-bearing nannofossil ooze to clay-bearing, silt-bearing foraminifer-bearing nannofossil ooze, light-greenish-gray (5GY 7/1, 5G 7/1); weakly bioturbated.

SMEAR SLIDE SUMMARY (%):

	3, 135 D	4, 50 D	6, 130 D
TEXTURE:			
Sand	Tr	5	—
Silt	20	15	20
Clay	80	80	80
COMPOSITION:			
Quartz	15	Tr	Tr
Clay	20	10	15
Accessory Minerals	15	15	10
Foraminifers	—	10	Tr
Nannofossils	5	65	65
Diatoms		Tr	10
Radiolarians	45	—	
Sponge spicules		—	—

cont.

SITE 667 HOLE A CORE 23 CORED INTERVAL 3725.8-3735.3 mbsl; 200.8-210.3 mbsf

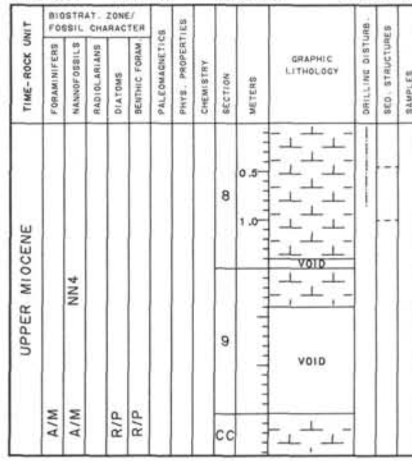

LITHOLOGIC DESCRIPTION

cont.

SILT-BEARING, CLAY-BEARING, SILICEOUS-BEARING NANNOFOSSIL OOZE to CLAY-BEARING, SILT-BEARING FORAMINIFER-BEARING NANNOFOSSIL OOZE

Silt-bearing, clay-bearing, siliceous-bearing nannofossil ooze to clay-bearing, silt-bearing foraminifer-bearing nannofossil ooze, light-greenish-gray (5GY 7/1, 5G 7/1); weakly bioturbated.

SITE 667 HOLE A CORE 24X CORED INTERVAL 3735.3-3744.8 mbsl; 210.3-219.8 mbsf

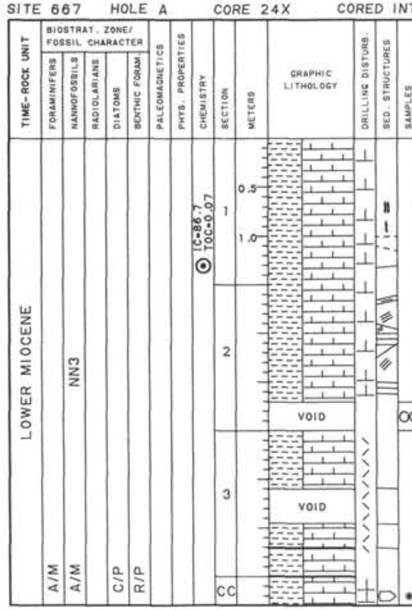

LITHOLOGIC DESCRIPTION

CLAYEY NANNOFOSSIL CHALK

Clayey nannofossil chalk, light-greenish-gray (5G 7/1); weakly bioturbated and highly indurated. Section 2 has dipping laminations and bedding planes; part of a slump. Turbidite in Section 1, 120–142 cm. Minor voids in Section 3, 122–131 and 143–150 cm.

SMEAR SLIDE SUMMARY (%):

	CC, 10 D
TEXTURE:	
Sand	Tr
Silt	15
Clay	85
COMPOSITION:	
Clay	30
Accessory Minerals	5
Foraminifers	Tr
Nannofossils	65
Diatoms	Tr
Radiolarians	Tr
Sponge spicules	Tr

SITE 667 HOLE A CORE 25X CORED INTERVAL 3744.8-3754.3 mbsl; 219.8-229.3 mbsf

TIME-ROCK UNIT	FORAMINIFERS	NANNOFOSSILS	RADIOLARIANS	DIATOMS	BENTHIC FORAM.	PALEOMAGNETICS	PHYS. PROPERTIES	CHEMISTRY	SECTION	METERS
LOWER MIOCENE	A/M	NN2-NN3 A/P		R/P	R/P			⊙ IC=79.0	1	0.5, 1.0
									2	
								⊙ IC=79.6 TOC=0.02	3	
									4	
									CC	

GRAPHIC LITHOLOGY / DRILLING DISTURB. / SED. STRUCTURES / SAMPLES

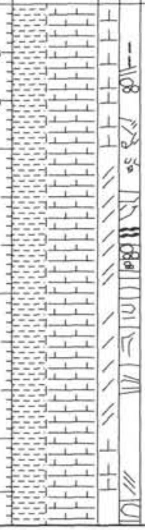

LITHOLOGIC DESCRIPTION

CLAYEY NANNOFOSSIL CHALK

Clayey nannofossil chalk, light-greenish-gray (5G 7/1) or greenish-gray (5G 6/1); severely brecciated and slumped.

SITE 667 HOLE A CORE 26X CORED INTERVAL 3754.3-3763.8 mbsl; 229.3-238.8 mbsf

TIME-ROCK UNIT	FORAMINIFERS	NANNOFOSSILS	RADIOLARIANS	DIATOMS	BENTHIC FORAM.	PALEOMAGNETICS	PHYS. PROPERTIES	CHEMISTRY	SECTION	METERS
LOWER MIOCENE	C/M	NN2 A/P		F/P	R/P			⊙ IC=82.2 TOC=0.00	1	0.5, 1.0
								⊙ IC=75.6	2	
									3	
									4	
									CC	

GRAPHIC LITHOLOGY / DRILLING DISTURB. / SED. STRUCTURES / SAMPLES

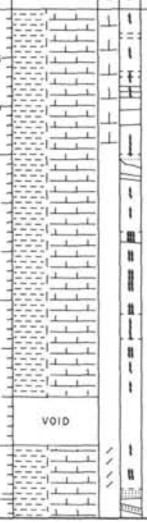

LITHOLOGIC DESCRIPTION

CLAYEY NANNOFOSSIL CHALK

Clayey nannofossil chalk, light-greenish-gray (5G 7/1) or greenish-gray (5G 6/1); slighty deformed and moderately fragmented. Turbidite in Section 2 0–10 cm. Sections 2 and 3 moderately bioturbated.

SMEAR SLIDE SUMMARY (%):

	1, 65 D
TEXTURE:	
Sand	—
Silt	15
Clay	85
COMPOSITION:	
Quartz	Tr
Clay	30
Accessory Minerals	5
Foraminifers	Tr
Nannofossils	60
Diatoms	
Radiolarians	5
Sponge spicules	

SITE 667 HOLE A CORE 27X CORED INTERVAL 3763.8-3773.3 mbsl; 238.8-248.3 mbsf

TIME-ROCK UNIT	FORAMINIFERS	NANNOFOSSILS	RADIOLARIANS	DIATOMS	BENTHIC FORAM.	PALEOMAGNETICS	PHYS. PROPERTIES	CHEMISTRY	SECTION	METERS
LOWER MIOCENE	A/M	NN1-2 A/P		subzone A. *R. paleacea* A/M	R/P			⊙ IC=81.2	1	0.5, 1.0
									2	
									3	
								⊙ IC=3.25 TOC=0.12	4	
									CC	

GRAPHIC LITHOLOGY / DRILLING DISTURB. / SED. STRUCTURES / SAMPLES

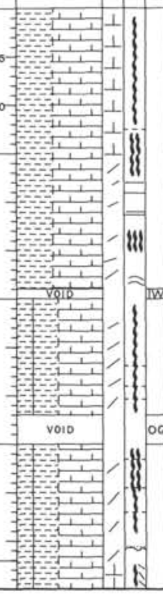

LITHOLOGIC DESCRIPTION

CLAYEY NANNOFOSSIL CHALK, and CLAYEY NANNOFOSSIL CHALK alternating with NANNOFOSSIL-BEARING, SILICEOUS-BEARING CLAY(STONE)

Clayey nannofossil chalk, light-greenish-gray (5G 7/1) or greenish-gray (5G 6/1) in Section 1 and Section 2, 150 cm; weak to moderate bioturbation; moderately to highly fragmented and indurated. Clayey nannofossil chalk, light-greenish-gray (5G 7/1) in Section 3 through CC, alternating with nannofossil-bearing, siliceous-bearing clay(stone), grayish-green (5G 5/2) or gray (5Y 5/1); weakly to moderately bioturbated; slightly fractured; highly indurated; erosional contact in Section 4, 110 cm.

SMEAR SLIDE SUMMARY (%):

	3, 95 D
TEXTURE:	
Sand	—
Silt	25
Clay	75
COMPOSITION:	
Clay	50
Accessory Minerals	10
Foraminifers	20
Nannofossils	
Diatoms	20
Radiolarians	

SITE 667 HOLE A CORE 28X CORED INTERVAL 3773.3-3782.8 mbsl; 248.3-257.8 mbsf

TIME-ROCK UNIT	FORAMINIFERS	NANNOFOSSILS	RADIOLARIANS	DIATOMS	BENTHIC FORAM.	PALEOMAGNETICS	PHYS. PROPERTIES	CHEMISTRY	SECTION	METERS
LOWER MIOCENE	C/M	NN1-2 A/P		subzone A *R. paleacea* A/M	R/P				1	0.5, 1.0
									2	
								⊙ IC=80.6 TOC=0.02	3	
									CC	

GRAPHIC LITHOLOGY / DRILLING DISTURB. / SED. STRUCTURES / SAMPLES

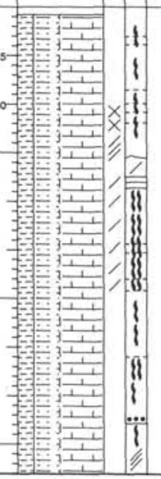

LITHOLOGIC DESCRIPTION

CLAYEY NANNOFOSSIL CHALK, alternating with NANNOFOSSIL-BEARING, SILICEOUS-BEARING CLAY(STONE)

Clayey nannofossil chalk, light-greenish-gray (5G 7/1), alternating with nannofossil-bearing, siliceous-bearing clay(stone), grayish-green (5G 5/2) or gray (5Y 5/1); weakly to moderately bioturbated; slightly fractured; highly indurated. Erosional contact and graded bedding in Section 3, 125–130 cm.

SITE 667 HOLE A CORE 29X CORED INTERVAL 3782.8-3792.3 mbsl; 257.8-267.3 mbsf

TIME-ROCK UNIT	BIOSTRAT. ZONE/ FOSSIL CHARACTER: FORAMINIFERS	NANNOFOSSILS	RADIOLARIANS	DIATOMS	BENTHIC FORAM	PALEOMAGNETICS	PHYS. PROPERTIES	CHEMISTRY	SECTION	METERS	GRAPHIC LITHOLOGY	DRILLING DISTURB.	SED. STRUCTURES	SAMPLES	LITHOLOGIC DESCRIPTION
LOWER MIOCENE	*G. kugleri*	NN1-NN2							1	0.5, 1.0					CLAYEY NANNOFOSSIL CHALK, alternating with NANNOFOSSIL-BEARING, SILICEOUS-BEARING CLAY(STONE)
									2						Clayey nannofossil chalk, light-greenish-gray (5G 7/1), alternating with nannofossil-bearing, siliceous-bearing clay(stone), grayish-green (5G 5/2) or gray (5Y 5/1); weakly to moderately bioturbated; slightly fractured; highly indurated. Composite and nested burrows of *Zoophycos* and *Chondrites* common. Minor void in CC, 8–12 cm.
									3						
									4						
									5		VOID				
									6						
									7		VOID				
	A/M	A/M		F/P	R/P				CC						

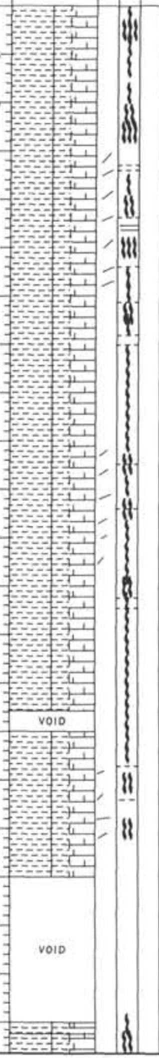

SITE 667 HOLE A CORE 30X CORED INTERVAL 3792.3-3801.8 mbsl; 267.3-276.8 mbsf

TIME-ROCK UNIT	BIOSTRAT. ZONE/ FOSSIL CHARACTER: FORAMINIFERS	NANNOFOSSILS	RADIOLARIANS	DIATOMS	BENTHIC FORAM	PALEOMAGNETICS	PHYS. PROPERTIES	CHEMISTRY	SECTION	METERS	GRAPHIC LITHOLOGY	DRILLING DISTURB.	SED. STRUCTURES	SAMPLES	LITHOLOGIC DESCRIPTION
LOWER MIOCENE	*G. kugleri*	NN1-NN2							1	0.5, 1.0					CLAYEY NANNOFOSSIL CHALK, alternating with NANNOFOSSIL-BEARING, SILICEOUS-BEARING CLAY(STONE)
									2						Clayey nannofossil chalk, light-greenish-gray (5G 7/1), alternating with nannofossil-bearing, siliceous-bearing clay(stone), grayish-green (5G 5/2) or gray (5Y 5/1); weakly to moderately bioturbated; slightly fractured; highly indurated; laminations and/or ripple marks in Sections 2 and 3. *Zoophycos* burrows common.
									3						
									4		VOID			OG	
									5						
									6						
	A/M	A/P		F/P	R/P				CC						

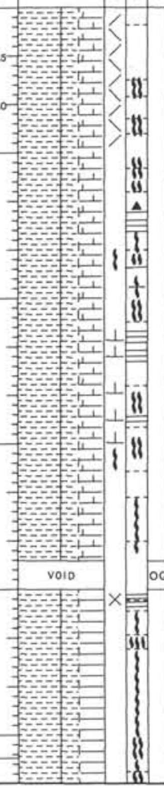

SITE 667 HOLE A CORE 31X CORED INTERVAL 3801.8-3811.3 mbsl; 276.8-286.3 mbsf

TIME-ROCK UNIT: LOWER MIOCENE

BIOSTRAT. ZONE/FOSSIL CHARACTER: FORAMINIFERS A/M; NANNOFOSSILS NN1, A/D; RADIOLARIANS R/P

CHEMISTRY: IC=76.0

SECTION: 1, 2, 3, 4, CC

METERS: 0.5, 1.0

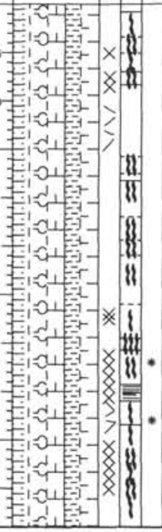

LITHOLOGIC DESCRIPTION

CLAYEY NANNOFOSSIL OOZE, alternating with MUDDY, SILICEOUS NANNOFOSSIL OOZE

Clayey nannofossil ooze, light-greenish-gray (5GY 7/1) or greenish-gray (5G 6/1), alternating with muddy, siliceous nannofossil ooze, bluish-gray (5B 6/1); weakly bioturbated; moderately fragmented in Sections 1 and 2; highly brecciated in Sections 3 and 4.

SMEAR SLIDE SUMMARY (%):

	3, 63 D	3, 86 D
TEXTURE:		
Sand	—	—
Silt	20	2
Clay	80	98
COMPOSITION:		
Quartz	5	—
Clay	20	40
Foraminifers	5	—
Nannofossils	45	58
Diatoms	Tr	—
Radiolarians	20	Tr
Sponge spicules	5	2

SITE 667 HOLE A CORE 32X CORED INTERVAL 3811.3-3820.8 mbsl; 286.3-295.8 mbsf

TIME-ROCK UNIT: LOWER MIOCENE

BIOSTRAT. ZONE/FOSSIL CHARACTER: FORAMINIFERS F/P; NANNOFOSSILS NN1, A/P; DIATOMS B; BENTHIC FORAM. R/P

CHEMISTRY: IC=92.3; IC=83.0, TOC=0.06

SECTION: 1, 2, 3, 4, 5, 6, CC

METERS: 0.5, 1.0

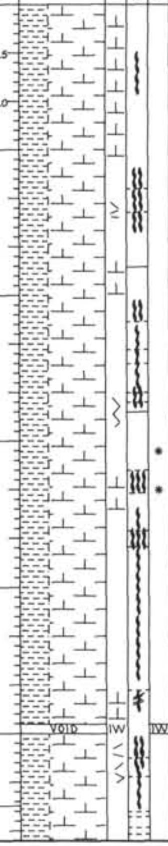

LITHOLOGIC DESCRIPTION

CLAYEY NANNOFOSSIL OOZE and SILICEOUS-BEARING, CLAYEY NANNOFOSSIL OOZE

Clayey nannofossil ooze, light-greenish-gray (5G 7/1), and siliceous-bearing nannofossil ooze, greenish-gray (5GY 6/1); weakly bioturbated and moderately fragmented; highly indurated.

SMEAR SLIDE SUMMARY (%):

	4, 15 D	4, 42 D
TEXTURE:		
Sand	—	—
Silt	5	20
Clay	95	80
COMPOSITION:		
Quartz	Tr	Tr
Clay	30	30
Calcite	Tr	—
Accessory Minerals	5	5
Foraminifers	5	5
Nannofossils	65	50
Diatoms	—	10
Radiolarians	—	

SITE 667 HOLE A CORE 33X CORED INTERVAL 3820.8-3830.3 mbsl; 295.8-305.3 mbsf

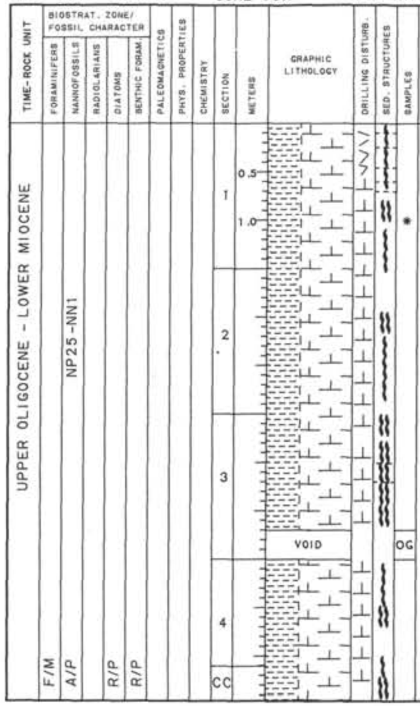

LITHOLOGIC DESCRIPTION

ZEOLITE-BEARING, CLAYEY NANNOFOSSIL OOZE

Zeolite-bearing, clayey nannofossil ooze, light-greenish-gray (5GY 7/1, 5G 7/1), greenish-gray (5GY 6/1), or light-gray (5Y 7/1); weakly to moderately bioturbated; moderately fragmented and highly indurated. *Zoophycos* burrows and green laminations common.

SMEAR SLIDE SUMMARY (%):

	1, 100 D
TEXTURE:	
Sand	—
Silt	10
Clay	90
COMPOSITION:	
Clay	40
Zeolites	10
Nannofossils	50

SITE 667 HOLE A CORE 34X CORED INTERVAL 3830.3-3839.8 mbsl; 305.3-314.8 mbsf

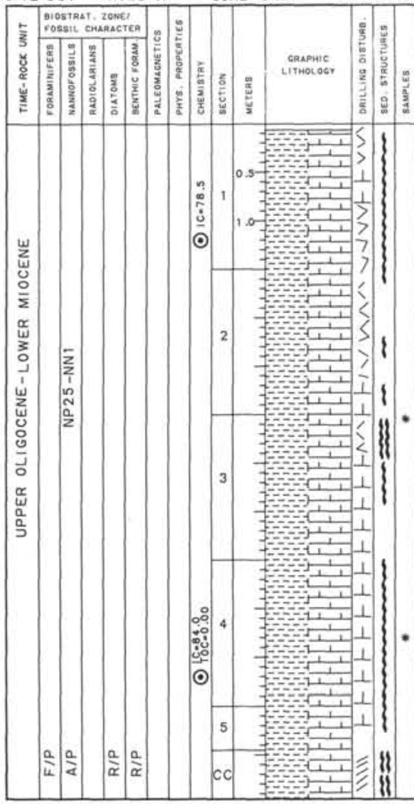

LITHOLOGIC DESCRIPTION

FORAMINIFER-BEARING, CLAYEY NANNOFOSSIL CHALK

Foraminifer-bearing, clayey nannofossil chalk, light-greenish-gray (5G 7/1), greenish-gray (5GY 6/1), or white (5Y 8/1); weakly to moderately bioturbated; moderately to highly fragmented, highly indurated. Minor void in Section 1, 0–7 cm.

SMEAR SLIDE SUMMARY (%):

	3, 8 D	4, 77 D
TEXTURE:		
Sand	—	5
Silt	10	15
Clay	90	80
COMPOSITION:		
Quartz	Tr	Tr
Clay	30	—
Foraminifers	—	10
Nannofossils	60	88
Diatoms		
Radiolarians	10	2
Sponge spicules		

SITE 667 HOLE A CORE 35X CORED INTERVAL 3839.8-3849.3 mbsl; 314.8-324.3 mbsf

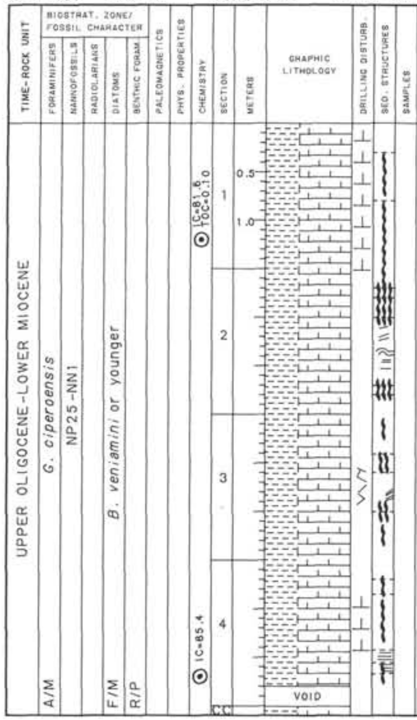

LITHOLOGIC DESCRIPTION

SILICEOUS-BEARING, CLAYEY NANNOFOSSIL CHALK

Siliceous-bearing, clayey nannofossil chalk, light-greenish-gray (5G 7/1), greenish-gray (5GY 6/1), white (5Y 8/1), or gray (10YR 6/1); moderately to highly bioturbated; highly indurated. Black, purple, and green laminations common. Sediments moderately to highly fractured.

SMEAR SLIDE SUMMARY (%):

	2, 46
	D
TEXTURE:	
Sand	—
Silt	20
Clay	80
COMPOSITION:	
Quartz	Tr
Clay	30
Accessory Minerals	Tr
Nannofossils	50
Diatoms	5
Radiolarians	10
Sponge spicules	5

SITE 667 HOLE A CORE 36X CORED INTERVAL 3849.3-3858.8 mbsl; 324.3-333.8 mbsf

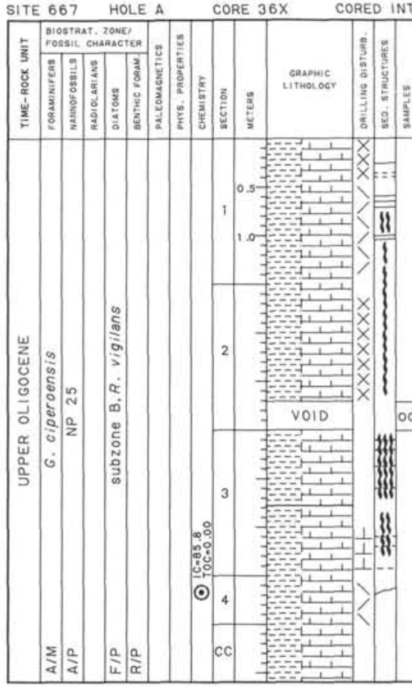

LITHOLOGIC DESCRIPTION

SILICEOUS-BEARING, CLAYEY NANNOFOSSIL CHALK

Siliceous-bearing, clayey nannofossil chalk, light-greenish-gray (5G 7/1) or greenish-gray (5GY 6/1); highly fractured and brecciated; individual biscuits highly bioturbated; black laminations common. Minor void in Section 3, 73–77 cm.

SITE 667 HOLE A CORE 37X CORED INTERVAL 3858.8-3868.3 mbsl; 333.8-343.3 mbsf

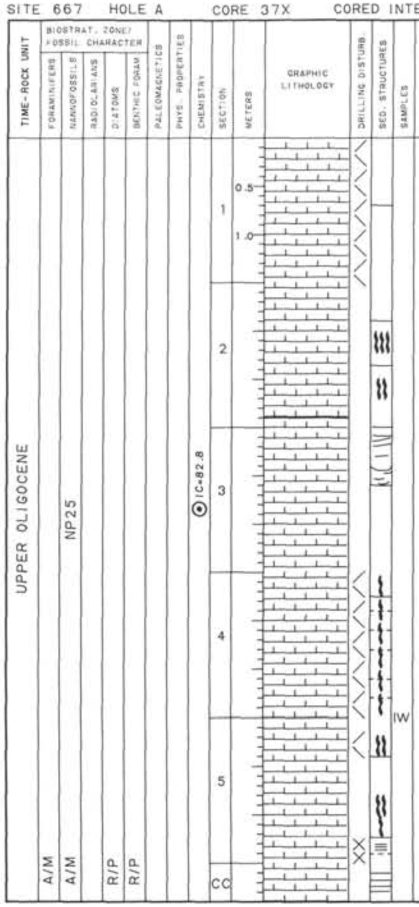

LITHOLOGIC DESCRIPTION

SILICEOUS-BEARING, NANNOFOSSIL CHALK

Siliceous-bearing, nannofossil chalk, light-greenish-gray (5G 7/1) or greenish-gray (5GY 6/1); highly fractured and brecciated; individual biscuits highly bioturbated; black laminations common. Minor void in Section 2, 130–139 cm.

SITE 667 HOLE A CORE 38X CORED INTERVAL 3868.3-3877.8 mbsl; 343.3-352.8 mbsf

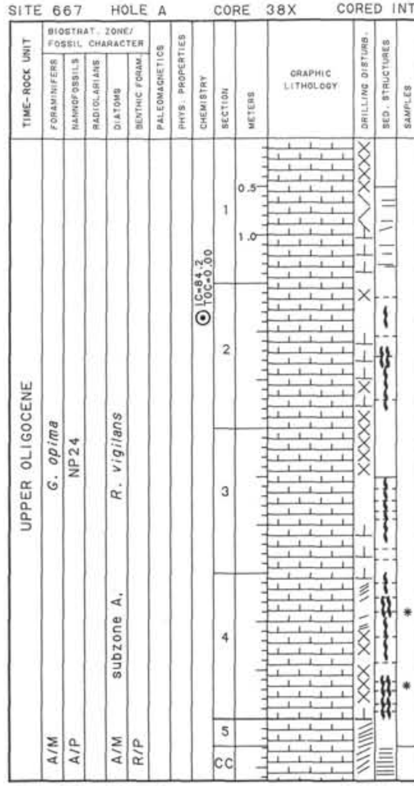

LITHOLOGIC DESCRIPTION

FORAMINIFER-BEARING NANNOFOSSIL CHALK

Foraminifer-bearing nannofossil chalk, light-greenish-gray (5GY 7/1, 5G 7/1); highly fractured, brecciated, and indurated. Individual biscuits moderately bioturbated. Many biscuits have purple and green laminations.

SMEAR SLIDE SUMMARY (%):

	4, 53 D	4, 120 D
TEXTURE:		
Sand	—	5
Silt	15	15
Clay	85	80
COMPOSITION:		
Quartz	Tr	—
Clay	—	5
Calcite	2	2
Foraminifers	13	15
Nannofossils	85	75
Diatoms	—	
Radiolarians	—	3
Sponge spicules	Tr	

SITE 667 HOLE A CORE 39X CORED INTERVAL 3877.8-3887.3 mbsl; 352.8-362.3 mbsf

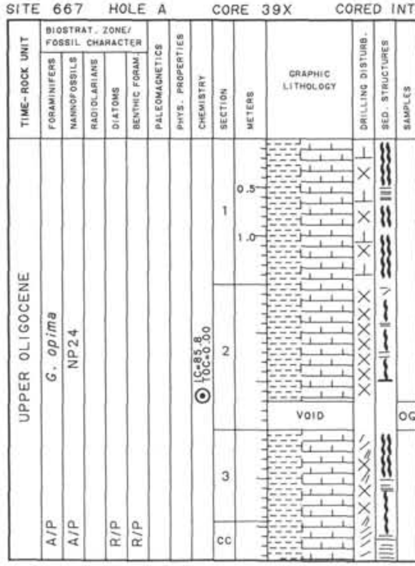

LITHOLOGIC DESCRIPTION

CLAYEY NANNOFOSSIL CHALK

Clayey nannofossil chalk, white (5Y 8/1), light-greenish-gray (5GY 7/1; 5G 7/1), or gray (5Y 6/1); highly fractured, brecciated, and indurated. Individual biscuits moderately bioturbated. Many biscuits have purple and green laminations.

SITE 667 HOLE A CORE 40X CORED INTERVAL 3887.3-3896.8 mbsl; 362.3-371.8 mbsf

TIME-ROCK UNIT: UPPER OLIGOCENE

BIOSTRAT. ZONE/FOSSIL CHARACTER: FORAMINIFERS: G. opima, A/M; NANNOFOSSILS: NP24, A/M; RADIOLARIANS; DIATOMS: B; BENTHIC FORAM.: R/P

PALEOMAGNETICS; PHYS. PROPERTIES; CHEMISTRY: IC=88.8

SECTION: 1, 2, 3, 4, 5, 6, CC

METERS: 0.5, 1.0

GRAPHIC LITHOLOGY; DRILLING DISTURB.; SED. STRUCTURES; SAMPLES

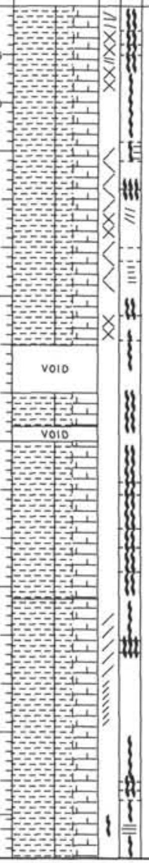

LITHOLOGIC DESCRIPTION

CLAYEY NANNOFOSSIL CHALK, alternating with NANNOFOSSIL-BEARING, SILICEOUS-BEARING CLAY

Clayey nannofossil chalk, white (5Y 8/1)), alternating with nannofossil-bearing, siliceous-bearing clay, light-greenish-gray (5GY 7/1), greenish-gray (5GY 6/1); highly fractured and brecciated; highly indurated. Individual biscuits moderately bioturbated. Many biscuits have purple and green laminations. Minor void in Section 5, 11–16 cm.

SITE 667 HOLE A CORE 41X CORED INTERVAL 3896.8-3906.3 mbsl; 371.8-381.3 mbsf

TIME-ROCK UNIT: UPPER OLIGOCENE

BIOSTRAT. ZONE/FOSSIL CHARACTER: FORAMINIFERS: F/P; NANNOFOSSILS: NP23, A/M; RADIOLARIANS; DIATOMS: B; BENTHIC FORAM.: R/P

PALEOMAGNETICS; PHYS. PROPERTIES; CHEMISTRY: IC=88.6

SECTION: 1, 2, 3, CC

METERS: 0.5, 1.0

GRAPHIC LITHOLOGY; DRILLING DISTURB.; SED. STRUCTURES; SAMPLES

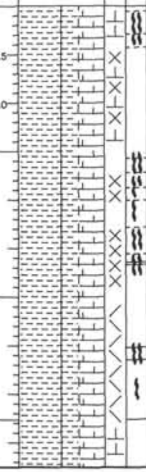

LITHOLOGIC DESCRIPTION

CLAYEY NANNOFOSSIL CHALK, alternating with NANNOFOSSIL-BEARING, SILICEOUS-BEARING CLAY

Clayey nannofossil chalk, white (5Y 8/1)), alternating with nannofossil-bearing, siliceous-bearing clay, light-greenish-gray (5GY 7/1), greenish-gray (5GY 6/1); moderately fractured and brecciated; highly indurated; individual biscuits moderately bioturbated.

SITE 667 HOLE B CORE 1H CORED INTERVAL 3524.7-3530.8 mbsl; 0-6.1 mbsf

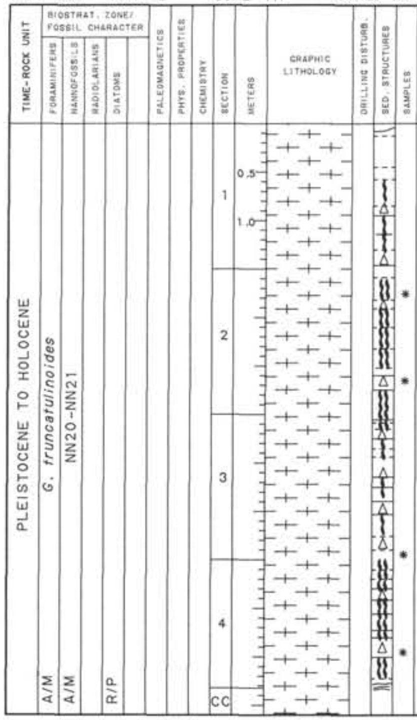

LITHOLOGIC DESCRIPTION

FORAMINIFER-NANNOFOSSIL OOZE and CLAY-BEARING FORAMINIFER-NANNOFOSSIL OOZE

Foraminifer-nannofossil ooze and clay-bearing foraminifer-nannofossil ooze, very pale-brown (10YR 7/3), light-brownish-gray (10YR 6/2), or brownish-yellow (10YR 6/6); weakly to moderately bioturbated throughout; fining-upward sequences common. Some graded beds have sharp lower contacts.

SMEAR SLIDE SUMMARY (%):

	2, 24 D	2, 115 D	3, 141 D	4, 92 D
TEXTURE:				
Sand	25	15	10	15
Silt	20	20	30	15
Clay	55	65	60	70
COMPOSITION:				
Quartz	—	Tr	—	—
Clay	10	15	20	15
Foraminifers	45	30	40	30
Nannofossils	45	50	40	55
Diatoms	—	5	—	—
Radiolarians	—		—	Tr

SITE 667 HOLE B CORE 2H CORED INTERVAL 3530.8-3540.3 mbsl; 6.1-15.6 mbsf

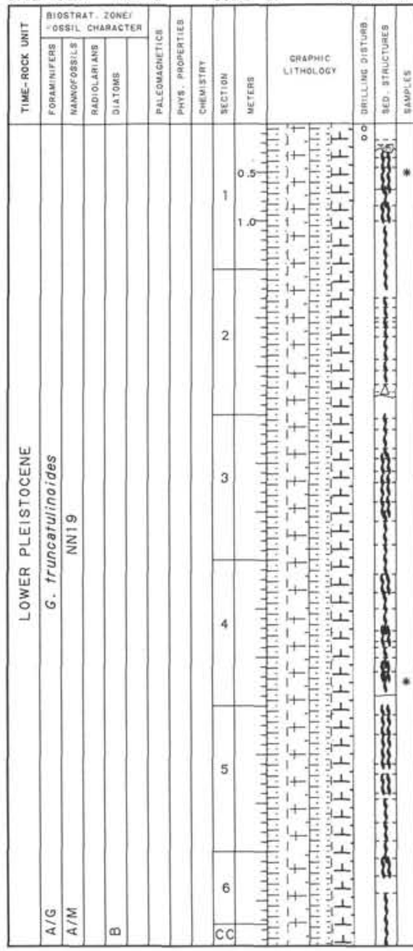

LITHOLOGIC DESCRIPTION

FORAMINIFER-BEARING, MUDDY NANNOFOSSIL OOZE, alternating with SILICEOUS, MUDDY FORAMINIFER-NANNOFOSSIL OOZE

Foraminifer-bearing, muddy nannofossil ooze, alternating with siliceous, muddy foraminifer-nannofossil ooze, pale-brown, light-yellowish-brown, or reddish-yellow (10YR 6/3, 6/4; 7.5YR 6/6); weakly to moderately bioturbated throughout.

SMEAR SLIDE SUMMARY (%):

	4, 50 D	4, 120 D
TEXTURE:		
Sand	5	10
Silt	30	35
Clay	65	35
COMPOSITION:		
Quartz	15	10
Clay	20	15
Foraminifers	15	25
Nannofossils	45	40
Diatoms	—	10
Radiolarians	—	

SITE 667 HOLE B CORE 3H CORED INTERVAL 3540.3-3549.8 mbsl; 15.6-25.1 mbsf

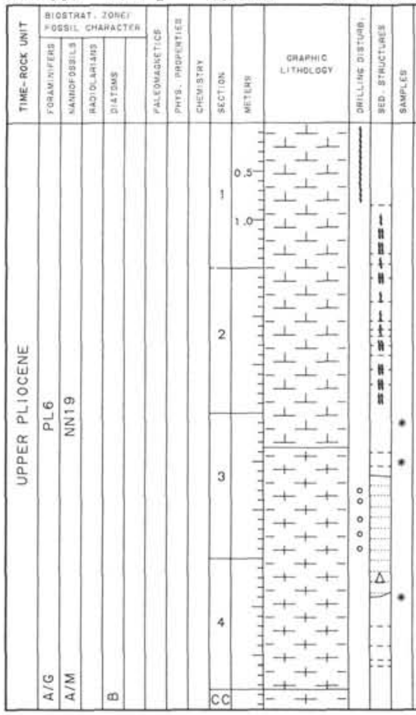

LITHOLOGIC DESCRIPTION

FORAMINIFER-BEARING NANNOFOSSIL OOZE and FORAMINIFER-NANNOFOSSIL OOZE

Foraminifer-bearing nannofossil ooze, yellowish-brown, light-gray to gray (10YR 5/6, 7/2, 8/1), and foraminifer-nannofossil ooze, white (10YR 8/2). Sections 1 and 2 weakly to moderately bioturbated. Turbidites present in Section 4, 37 cm, and Section 3, 63 cm.

SMEAR SLIDE SUMMARY (%):

	3, 10 D	3, 42 D	4, 36 D
TEXTURE:			
Sand	5	15	45
Silt	20	25	30
Clay	75	60	25
COMPOSITION:			
Quartz	2	Tr	—
Clay	Tr	Tr	—
Calcite/Dolomite	2	—	—
Accessory Minerals	1	—	—
Foraminifers	20	35	75
Nannofossils	75	65	25
Diatoms	Tr	Tr	—
Radiolarians	Tr	Tr	—
Sponge spicules	Tr	Tr	—

SITE 667 HOLE B CORE 4H CORED INTERVAL 3549.8-3553.8 mbsl; 25.1-34.6 mbsf

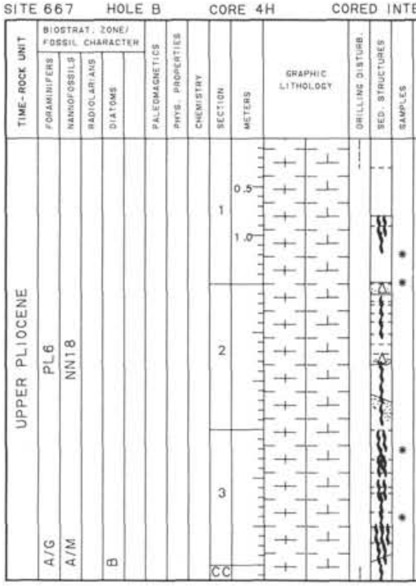

LITHOLOGIC DESCRIPTION

MUD-BEARING, FORAMINIFER-NANNOFOSSIL OOZE and FORAMINIFER-NANNOFOSSIL OOZE, alternating with MUD-BEARING, FORAMINIFER-BEARING NANNOFOSSIL OOZE and CLAY-BEARING, FORAMINIFER-BEARING NANNOFOSSIL OOZE

Mud-bearing, foraminifer-nannofossil ooze and foraminifer-nannofossil ooze, white (2.5Y 8/2; 5Y 8/2, 8/1), alternating with mud-bearing, foraminifer-bearing nannofossil ooze and clay-bearing, foraminifer-bearing nannofossil ooze, pale-olive to greenish-gray (5Y 6/3, 5GY 6/1). Contacts between the nannofossil oozes and foraminifer-nannofossil oozes often gradational. Possible turbidites in Section 2, 10 and 115 cm. Sections 2 and 3 weakly to moderately bioturbated.

SMEAR SLIDE SUMMARY (%):

	1, 117 D	1, 142 D	3, 20 D	3, 87 D
TEXTURE:				
Sand	15	20	5	5
Silt	25	30	20	15
Clay	60	50	75	80
COMPOSITION:				
Quartz	Tr	3	5	Tr
Clay	—	5	10	10
Calcite/Dolomite	—	—	—	5
Accessory Minerals	—	2	Tr	—
Foraminifers	30	40	15	15
Nannofossils	60	60	70	70
Sponge Spicules	10	—	—	—

SITE 667 HOLE B CORE 5H CORED INTERVAL 3553.8-3567.8 mbsl; 34.6-44.1 mbsf

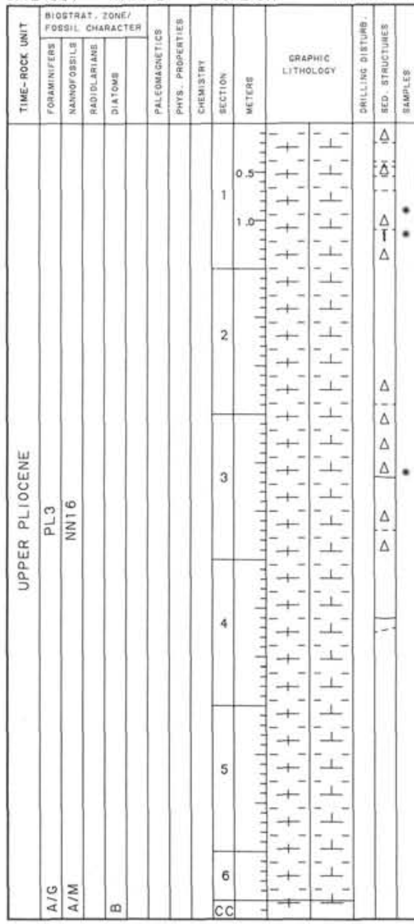

LITHOLOGIC DESCRIPTION

MUD-BEARING, FORAMINIFER-BEARING NANNOFOSSIL OOZE, alternating with FORAMINIFER-NANNOFOSSIL OOZE and NANNOFOSSIL-FORAMINIFER OOZE

Mud-bearing, foraminifer-bearing nannofossil ooze, light-gray (5Y 7/1), alternating with foraminifer-nannofossil ooze, white (5Y 8/1); repeated fining-upward cycles, both with and without sharp lower contacts. Unit is massive throughout with little evidence of bioturbation.

SMEAR SLIDE SUMMARY (%):

	1, 86 D	1, 116 D	3, 55 D
TEXTURE:			
Sand	25	—	50
Silt	35	20	30
Clay	40	80	20
COMPOSITION:			
Quartz	Tr	3	—
Clay	—	10	—
Accessory Minerals	—	2	—
Foraminifers	40	15	20
Nannofossils	60	70	30

SITE 667 HOLE B CORE 6H CORED INTERVAL 3567.8-3577.3 mbsl; 44.1-53.6 mbsf

TIME-ROCK UNIT	FORAMINIFERS	NANNOFOSSILS	RADIOLARIANS	DIATOMS	PALEOMAGNETICS	PHYS. PROPERTIES	CHEMISTRY	SECTION	METERS	GRAPHIC LITHOLOGY	DRILLING DISTURB.	SED. STRUCTURES	SAMPLES
LOWER PLIOCENE	PL2	NN15						1, 2, 3, 4, 5, 6, 7, CC	0.5, 1.0				
	A/G	A/M		B									

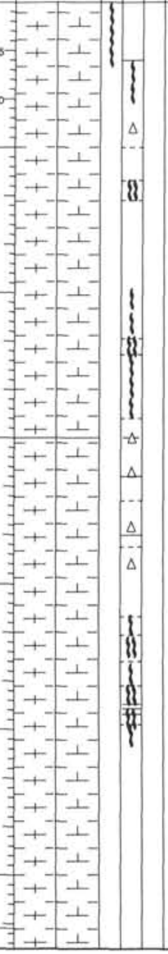

LITHOLOGIC DESCRIPTION

MUD-BEARING, FORAMINIFER-BEARING NANNOFOSSIL OOZE, alternating with FORAMINIFER-NANNOFOSSIL OOZE and NANNOFOSSIL-FORAMINIFER OOZE

Mud-bearing, foraminifer-bearing nannofossil ooze, light-gray (5Y 7/1), alternating with foraminifer-nannofossil ooze, white (5Y 8/1); repeated fining-upward cycles, both with and without sharp lower contacts in Section 4. Unit is massive throughout Sections 6 and 7 with little evidence of bioturbation. Bioturbation weak to moderate throughout remainder of core. Minor voids in Sections 3, 148–150 cm, and Section 4, 0–2 cm.

SITE 667 HOLE B CORE 7H CORED INTERVAL 3577.3-3586.8 mbsl; 53.6-63.1 mbsf

TIME-ROCK UNIT	FORAMINIFERS	NANNOFOSSILS	RADIOLARIANS	DIATOMS	PALEOMAGNETICS	PHYS. PROPERTIES	CHEMISTRY	SECTION	METERS	GRAPHIC LITHOLOGY	DRILLING DISTURB.	SED. STRUCTURES	SAMPLES
LOWER PLIOCENE	PL2	NN13-NN15						1, 2, 3, 4, 5, 6, 7, CC	0.5, 1.0	VOID			
	A/G	A/G		B									

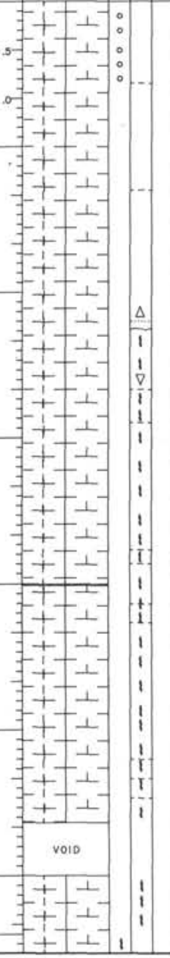

LITHOLOGIC DESCRIPTION

MUD-BEARING, FORAMINIFER-BEARING NANNOFOSSIL OOZE, alternating with FORAMINIFER-NANNOFOSSIL OOZE and NANNOFOSSIL-FORAMINIFER OOZE

Mud-bearing, foraminifer-bearing nannofossil ooze, light-gray (5Y 7/1), alternating with foraminifer-nannofossil ooze, white (5Y 8/1), and nannofossil-foraminifer ooze, white (5Y 8/1); graded and reverse-graded beds present in Section 3. Bioturbation weak throughout core. Minor void in Section 5, 0–3 cm.

SITE 667 HOLE B CORE 8H CORED INTERVAL 3586.8-3596.3 mbsl; 63.1-72.6 mbsf

TIME-ROCK UNIT	BIOSTRAT. ZONE/FOSSIL CHARACTER: FORAMINIFERS	NANNOFOSSILS	RADIOLARIANS	DIATOMS	PALEOMAGNETICS	PHYS. PROPERTIES	CHEMISTRY	SECTION	METERS	GRAPHIC LITHOLOGY	DRILLING DISTURB.	SED. STRUCTURES	SAMPLES
	PL1	NN13-NN15						1, 2, 3, 4, 5, 6, CC	0.5, 1.0				
	A/G	A/M		B									

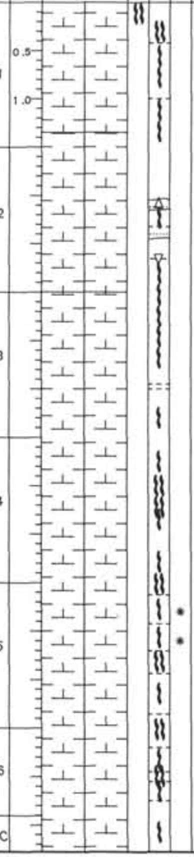

LITHOLOGIC DESCRIPTION

FORAMINIFER-BEARING NANNOFOSSIL OOZE, alternating with CLAY-BEARING NANNOFOSSIL OOZE

Foraminifer-bearing nannofossil ooze, white (10YR 8/1, 5Y 8/1), alternating with clay-bearing nannofossil ooze, light-gray to white (5Y 7/1, 8/2); weakly to moderately bioturbated throughout. Turbidite in Section 2, 50–60 cm. Section 2, 110–120 cm, shows reverse-graded beds. Minor voids in Section 1, 51–55 and 132–137 cm, and Section 2, 143–150 cm.

SMEAR SLIDE SUMMARY (%):

	5, 30 D	5, 60 D
TEXTURE:		
Sand	10	5
Silt	15	15
Clay	75	80
COMPOSITION:		
Quartz	Tr	—
Clay	5	10
Accessory Minerals	5	5
Foraminifers	15	5
Nannofossils	75	80
Diatoms	—	Tr

SITE 667 HOLE B CORE 9H CORED INTERVAL 3596.3-3605.8 mbsl; 72.6-82.1 mbsf

TIME-ROCK UNIT	BIOSTRAT. ZONE/FOSSIL CHARACTER: FORAMINIFERS	NANNOFOSSILS	RADIOLARIANS	DIATOMS	PALEOMAGNETICS	PHYS. PROPERTIES	CHEMISTRY	SECTION	METERS	GRAPHIC LITHOLOGY	DRILLING DISTURB.	SED. STRUCTURES	SAMPLES
LOWER PLIOCENE	PL1	NN12						1, 2, 3, 4, 5, 6, 7, CC	0.5, 1.0				
	A/G	A/M		B									

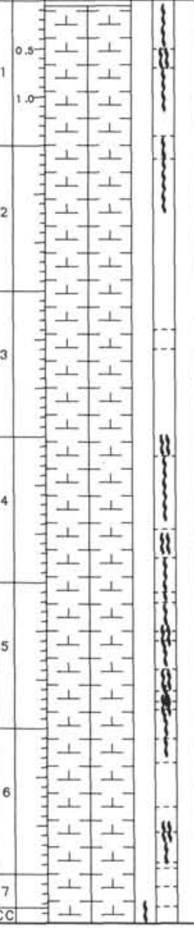

LITHOLOGIC DESCRIPTION

FORAMINIFER-BEARING NANNOFOSSIL OOZE, alternating with CLAY-BEARING NANNOFOSSIL OOZE

Foraminifer-bearing nannofossil ooze, white (10YR 8/1, 5Y 8/1), alternating with clay-bearing nannofossil ooze, light-gray and white (5Y 7/1, 8/2), to very pale-brown (10YR 7/3). Sections 1, 4, 5, and 6 weakly to moderately bioturbated.

SITE 667 HOLE B CORE 10H CORED INTERVAL 3605.8-3615.3 mbsl; 82.1-91.6 mbsf

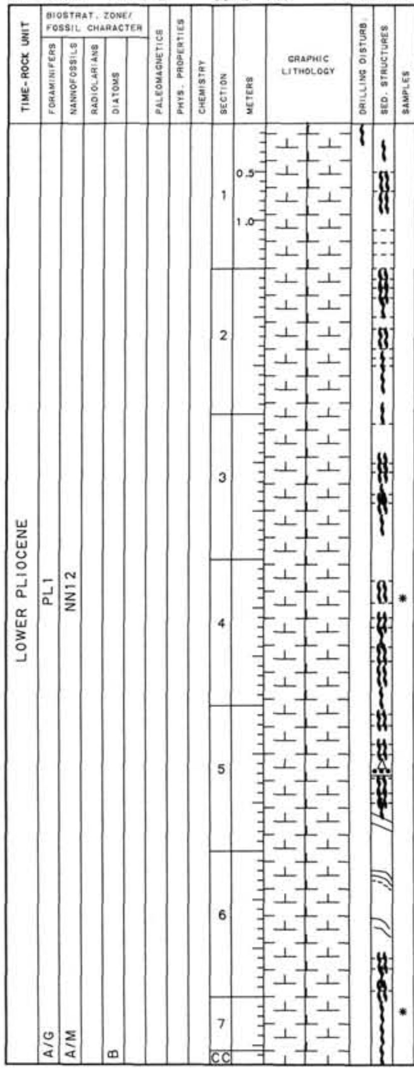

LITHOLOGIC DESCRIPTION

CLAY-BEARING NANNOFOSSIL OOZE, alternating with CLAY-BEARING, FORAMINIFER-BEARING NANNOFOSSIL OOZE

Clay-bearing nannofossil ooze, light-yellowish-brown (10YR 6/4), alternating with clay-bearing, foraminifer-bearing nannofossil ooze, light-gray to white (2.5Y 7/2, 8/2); weakly to moderately bioturbated throughout. Tilted beds between Section 5, 100 cm, and Section 6, 100 cm. Turbidite in Section 5, 60 cm.

SMEAR SLIDE SUMMARY (%):

	4, 40 D	7, 20 D
TEXTURE:		
Sand	5	15
Silt	10	15
Clay	55	70
COMPOSITION:		
Clay	10	20
Accessory Minerals	5	25
Foraminifers	5	20
Nannofossils	80	55
Diatoms	Tr	—

SITE 667 HOLE B CORE 11H CORED INTERVAL 3615.3-3624.8 mbsl; 91.6-101.1 mbsf

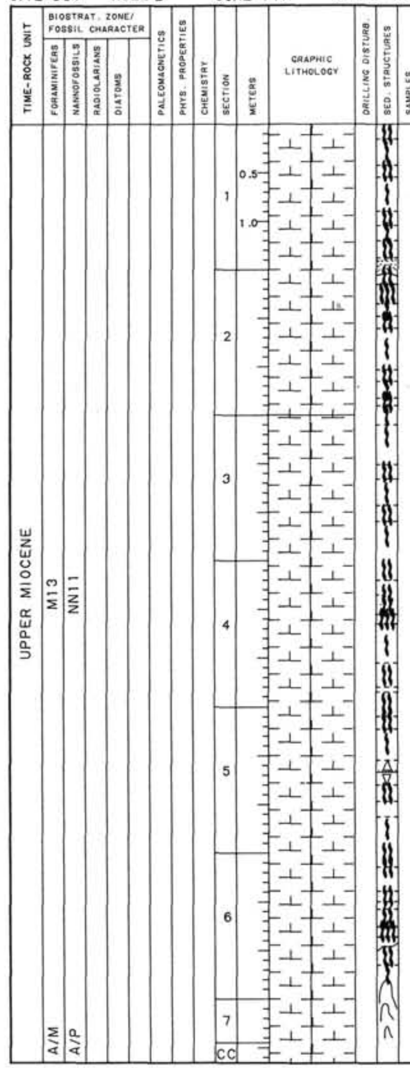

LITHOLOGIC DESCRIPTION

CLAY-BEARING NANNOFOSSIL OOZE, alternating with CLAY-BEARING, FORAMINIFER-BEARING NANNOFOSSIL OOZE

Clay-bearing nannofossil ooze, light-yellowish-brown to very pale-brown (10YR 6/4, 7/3, 8/3), alternating with clay-bearing, foraminifer-bearing nannofossil ooze, white (10YR 8/2); moderately to severely bioturbated throughout. Minor void in Section 2, 147–150 cm.

SITE 667 HOLE B CORE 12H CORED INTERVAL 3624.8-3634.3 mbsl; 101.1-110.6 mbsf

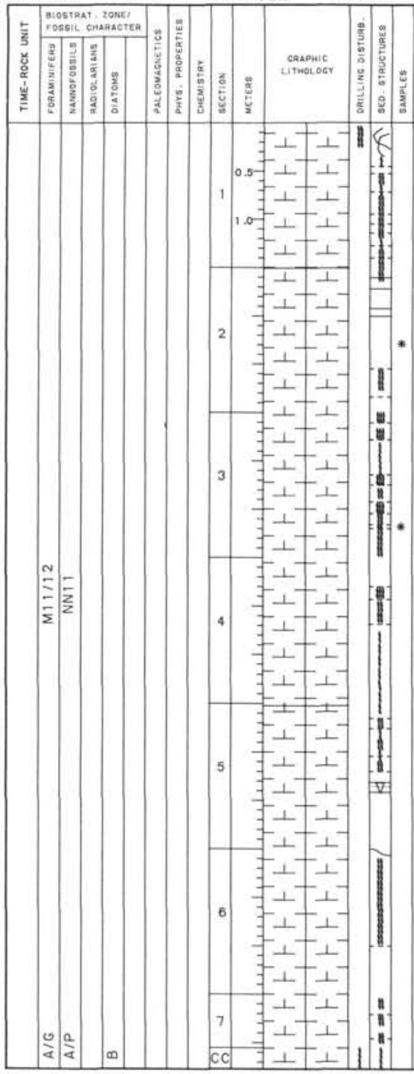

LITHOLOGIC DESCRIPTION

CLAY-BEARING NANNOFOSSIL OOZE, alternating with CLAY-BEARING, FORAMINIFER-BEARING NANNOFOSSIL OOZE

Clay-bearing nannofossil ooze, light-yellowish-brown to very pale-brown (10YR 6/4, 7/3, 8/3), alternating with clay-bearing, foraminifer-bearing nannofossil ooze, white (10YR 8/2); moderately to severely bioturbated throughout. Minor voids in Section 2, 0–2 cm, and Section 5, 0–3 cm.

SMEAR SLIDE SUMMARY (%):

	2, 80 D	3, 115 D
TEXTURE:		
Sand	5	—
Silt	10	10
Clay	85	90
COMPOSITION:		
Quartz	—	Tr
Clay	15	20
Accessory Minerals	—	5
Foraminifers	10	—
Nannofossils	75	75

SITE 667 HOLE B CORE 13H CORED INTERVAL 3634.3-3643.8 mbsl; 110.6-120.5 mbsf

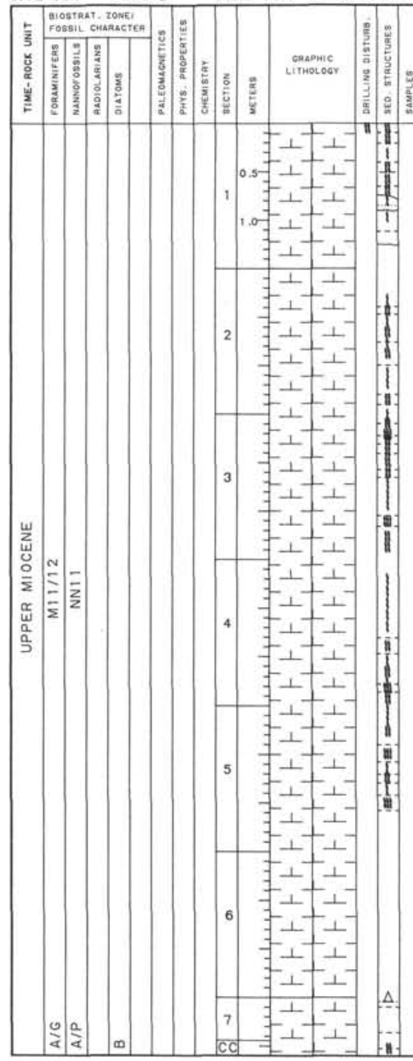

LITHOLOGIC DESCRIPTION

CLAY-BEARING NANNOFOSSIL OOZE, alternating with FORAMINIFER-BEARING, CLAY-BEARING NANNOFOSSIL OOZE

Clay-bearing nannofossil ooze, light-yellowish-brown to very pale-brown (10YR 6/4, 7/3, 8/3), alternating with foraminifer-bearing, clay-bearing nannofossil ooze, white to very pale-brown (10YR 8/1, 8/2, 8/3); generally weakly to moderately bioturbated throughout; Section 6 is massive, containing more foraminifers. Minor void in Section 6, 145–150 cm.

SITE 667 HOLE B CORE 14H CORED INTERVAL 3643.8-3653.3 mbsl; 120.1-129.6 mbsf

TIME-ROCK UNIT | BIOSTRAT. ZONE/FOSSIL CHARACTER: FORAMINIFERS, NANNOFOSSILS, RADIOLARIANS, DIATOMS | PALEOMAGNETICS | PHYS. PROPERTIES | CHEMISTRY | SECTION | METERS | GRAPHIC LITHOLOGY | DRILLING DISTURB. | SED. STRUCTURES | SAMPLES | LITHOLOGIC DESCRIPTION

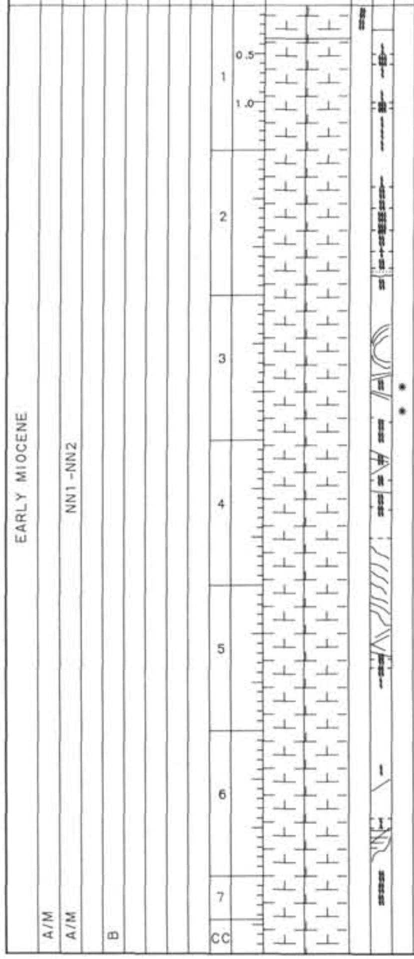

CLAY-BEARING NANNOFOSSIL OOZE, alternating with FORAMINIFER-BEARING, CLAY-BEARING NANNOFOSSIL OOZE and CLAY-BEARING NANNOFOSSIL OOZE

Clay-bearing nannofossil ooze, light-yellowish-brown to very pale-brown (10YR 6/4, 7/3, 8/3), in Section 1, 0–150 cm, and Section 2, 0–150 cm, alternating with foraminifer-bearing, clay-bearing nannofossil ooze, white to very pale-brown (10YR 8/1, 8/2, 8/3), and clay-bearing nannofossil ooze, light-greenish-gray (5G 7/8, 8/1; 5GY 7/1, 8/1) in Section 3, 0–150 cm, through CC. Sections 1 and 2 show cyclic beds similar to those observed in 108-667B-13H. Section 3 through CC exhibit a slump deposit. Both sections moderately bioturbated. Minor void in Section 1, 33–37 cm. *Chondrites* burrows are common.

SMEAR SLIDE SUMMARY (%):

	3, 46 D	3, 120 D
TEXTURE:		
Sand	—	—
Silt	10	10
Clay	90	90
COMPOSITION:		
Quartz	—	Tr
Clay	20	15
Accessory Minerals	5	5
Foraminifers	<5	Tr
Nannofossils	70	80

SITE 667 HOLE B CORE 15H CORED INTERVAL 3653.3-3662.8 mbsl; 129.6-139.6 mbsf

TIME-ROCK UNIT | BIOSTRAT. ZONE/FOSSIL CHARACTER: FORAMINIFERS, NANNOFOSSILS, RADIOLARIANS, DIATOMS | PALEOMAGNETICS | PHYS. PROPERTIES | CHEMISTRY | SECTION | METERS | GRAPHIC LITHOLOGY | DRILLING DISTURB. | SED. STRUCTURES | SAMPLES | LITHOLOGIC DESCRIPTION

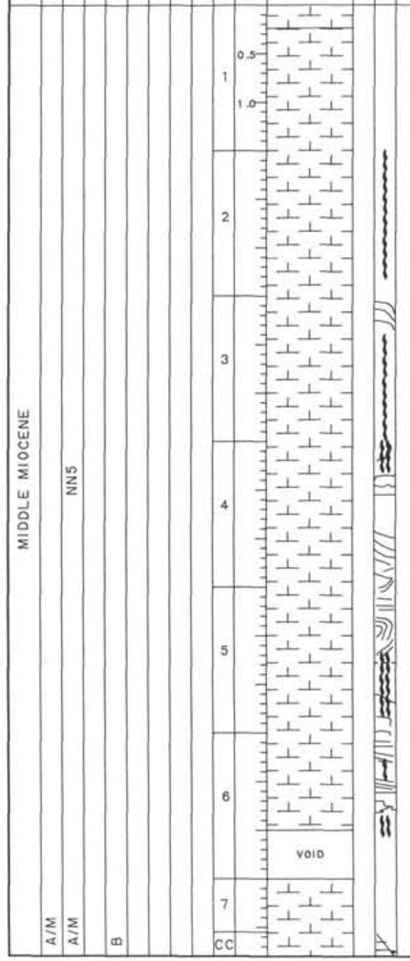

CLAY-BEARING NANNOFOSSIL OOZE

Slump deposit mixture of clay-bearing nannofossil ooze, light-greenish-gray (5G 7/8, 8/1), and clay nannofossil ooze, light-yellowish-brown to very pale-brown (10YR 6/4, 7/3, 8/3); extremely contorted bedding; *Zoophycos* burrows common in Section 3. Minor void in Section 1, 26–27 cm.

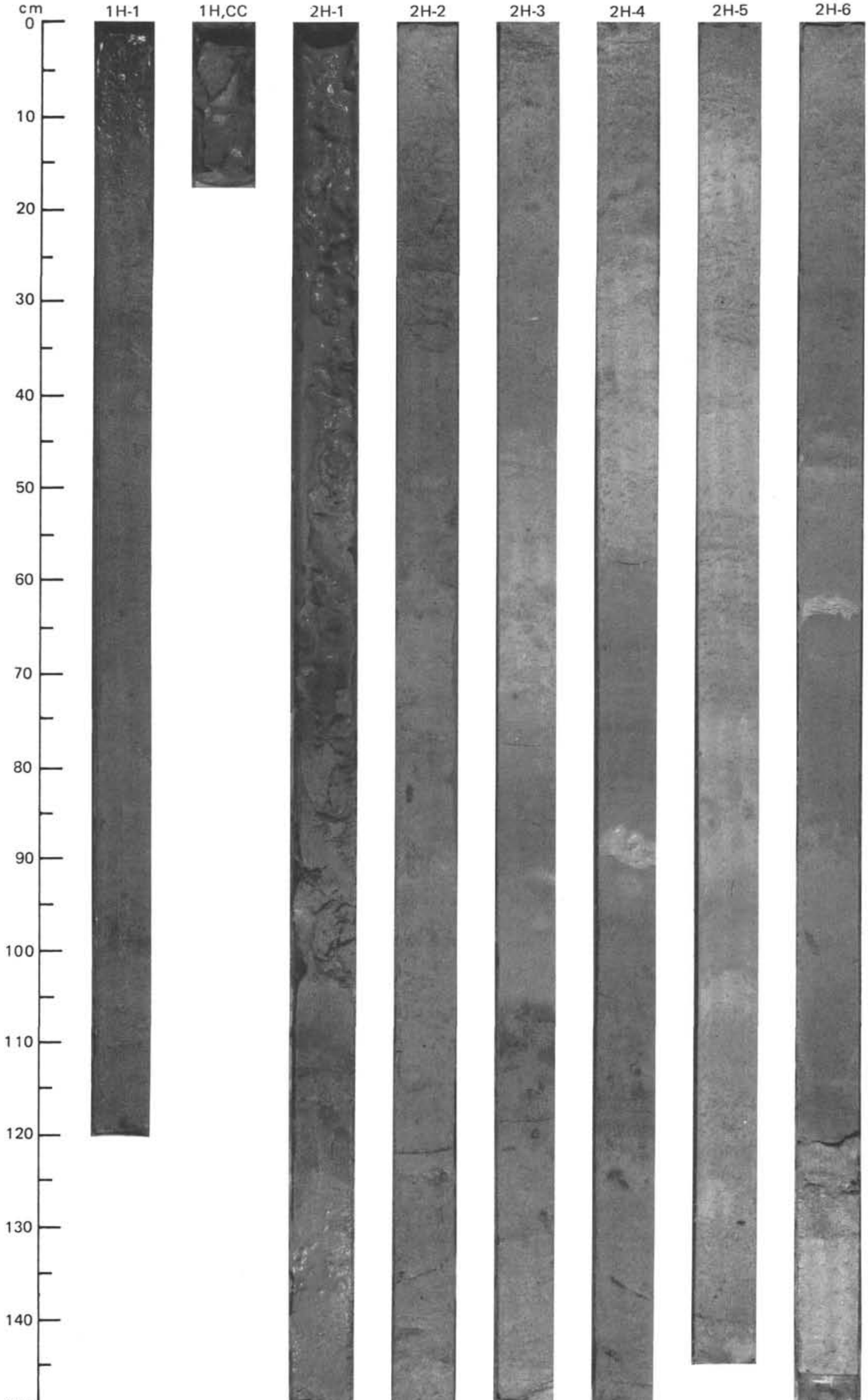
cm
0
10
20
30
40
50
60
70
80
90
100
110
120
130
140
150
1H-1
1H,CC
2H-1
2H-2
2H-3
2H-4
2H-5
2H-6

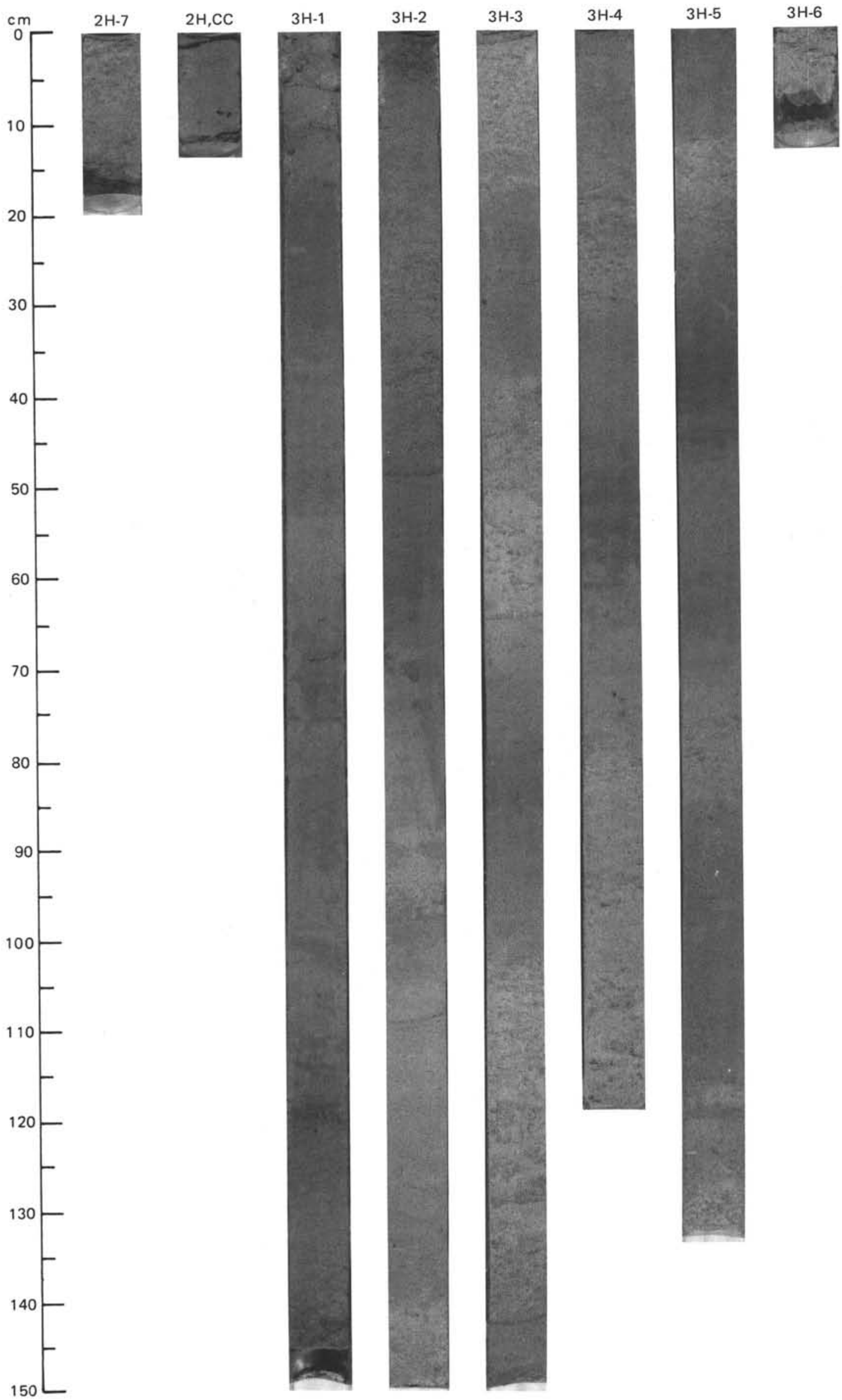
cm
0
10
20
30
40
50
60
70
80
90
100
110
120
130
140
150
2H-7
2H,CC
3H-1
3H-2
3H-3
3H-4
3H-5
3H-6

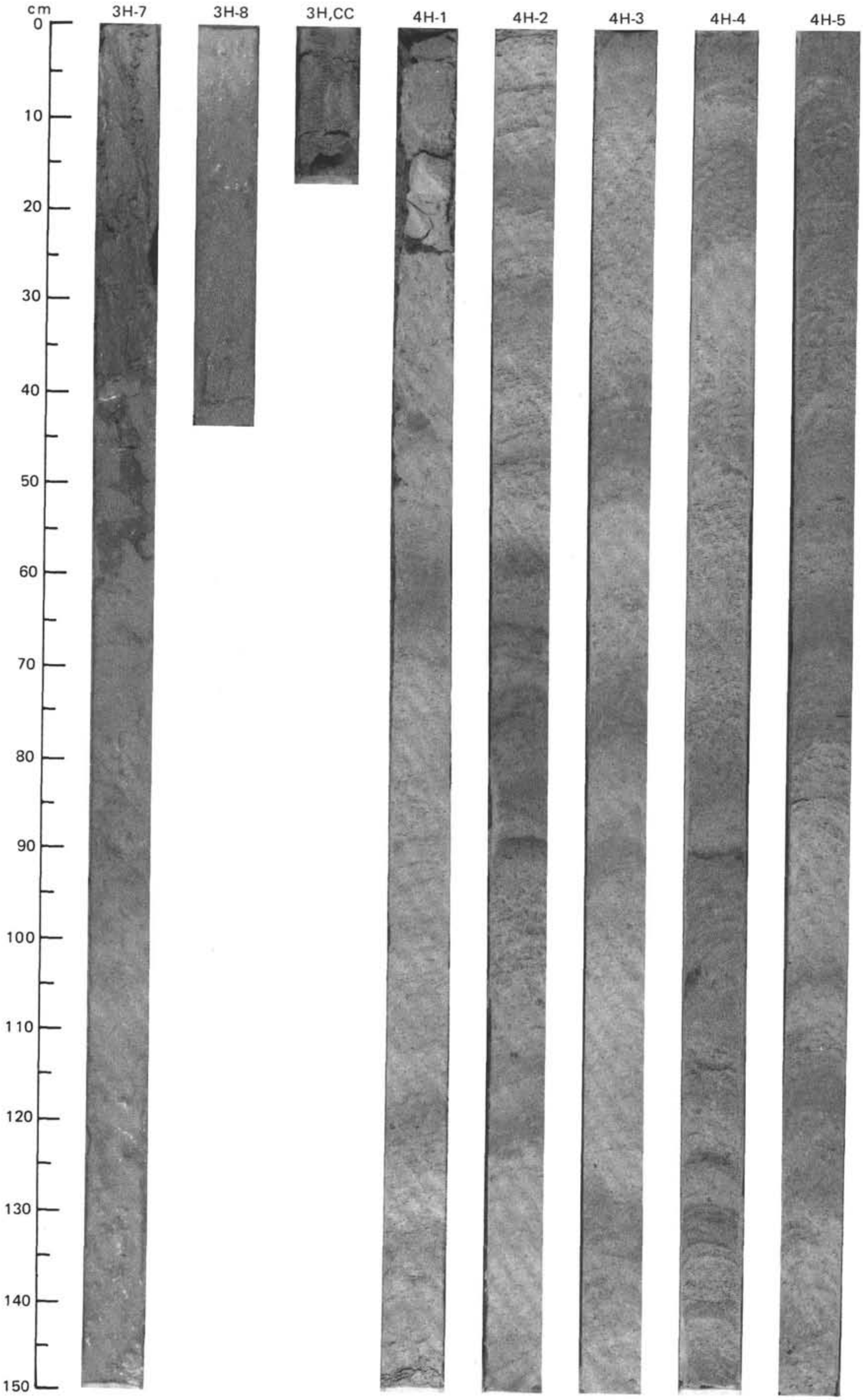
cm
0
10
20
30
40
50
60
70
80
90
100
110
120
130
140
150
3H-7
3H-8
3H,CC
4H-1
4H-2
4H-3
4H-4
4H-5

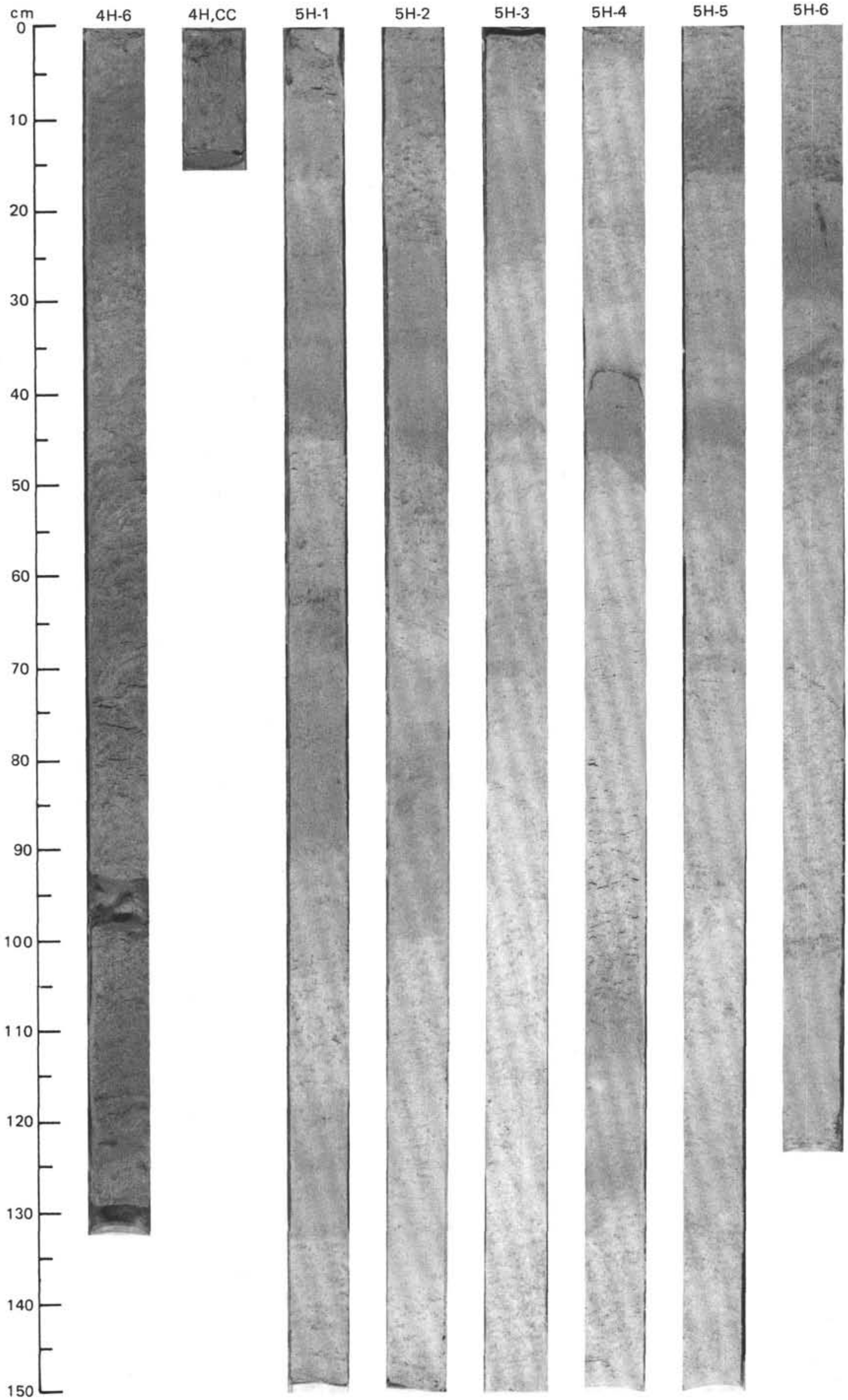
cm
4H-6
4H,CC
5H-1
5H-2
5H-3
5H-4
5H-5
5H-6
0
10
20
30
40
50
60
70
80
90
100
110
120
130
140
150

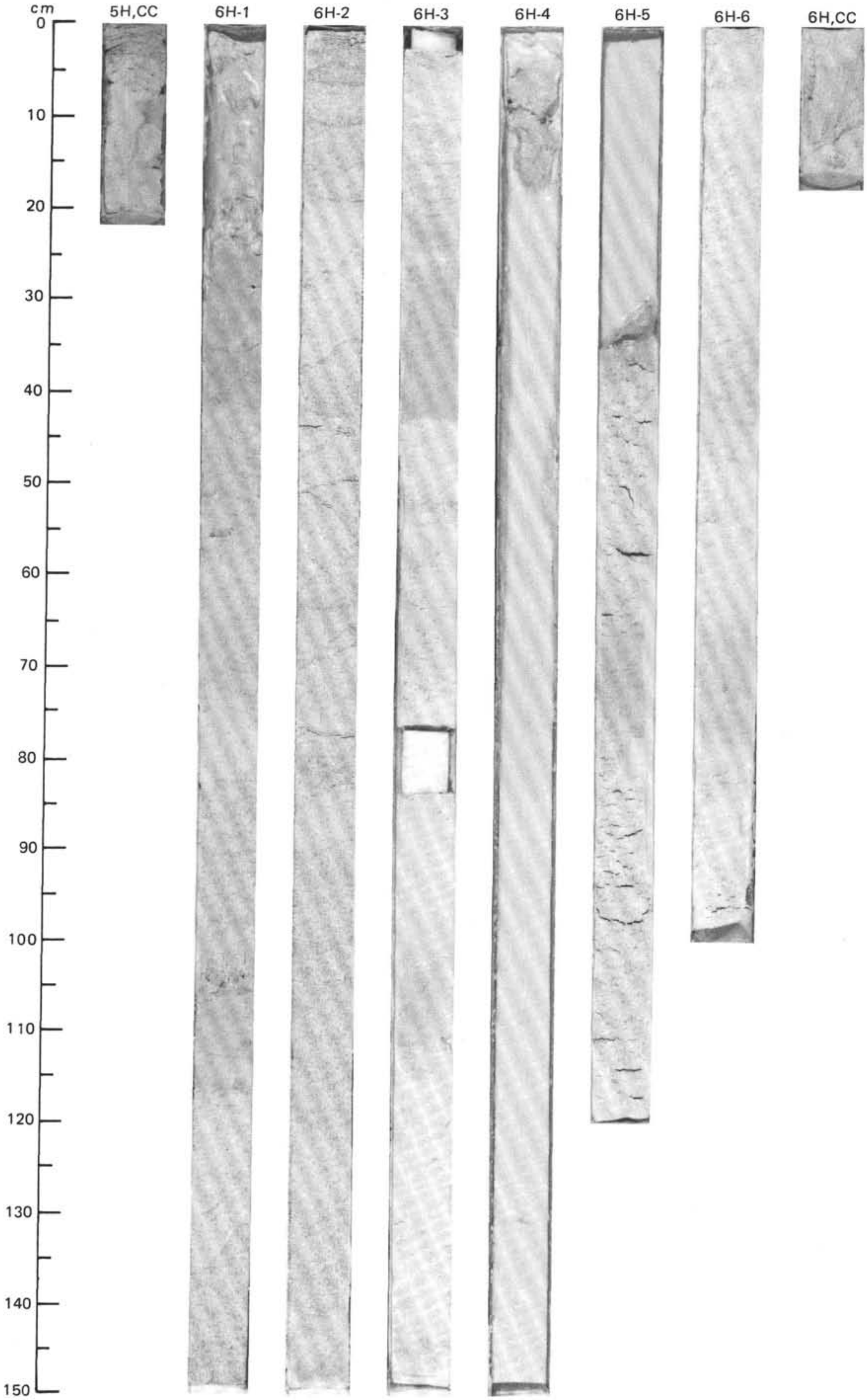
cm
0
10
20
30
40
50
60
70
80
90
100
110
120
130
140
150
5H,CC
6H-1
6H-2
6H-3
6H-4
6H-5
6H-6
6H,CC

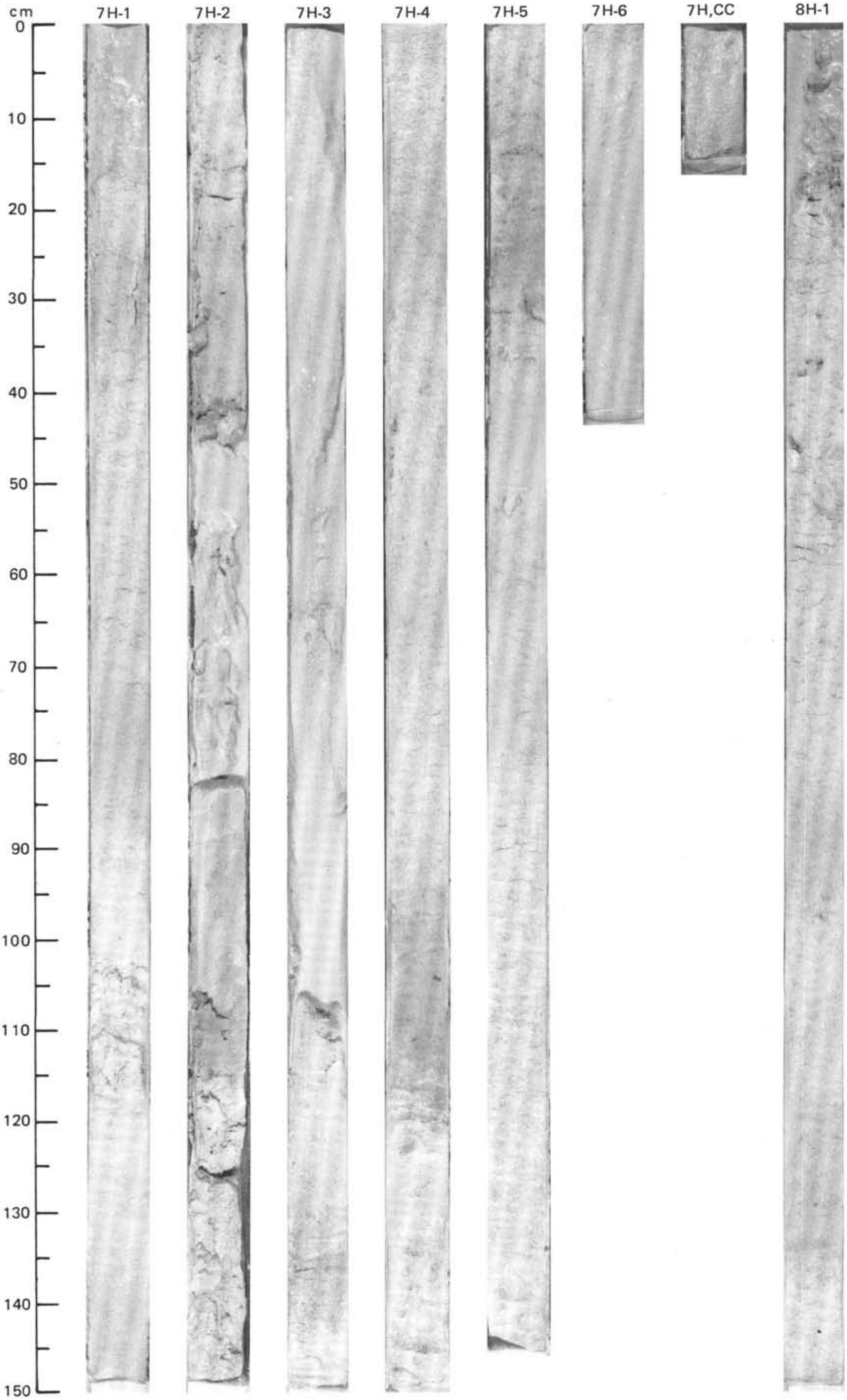
cm
0
10
20
30
40
50
60
70
80
90
100
110
120
130
140
150
7H-1
7H-2
7H-3
7H-4
7H-5
7H-6
7H,CC
8H-1

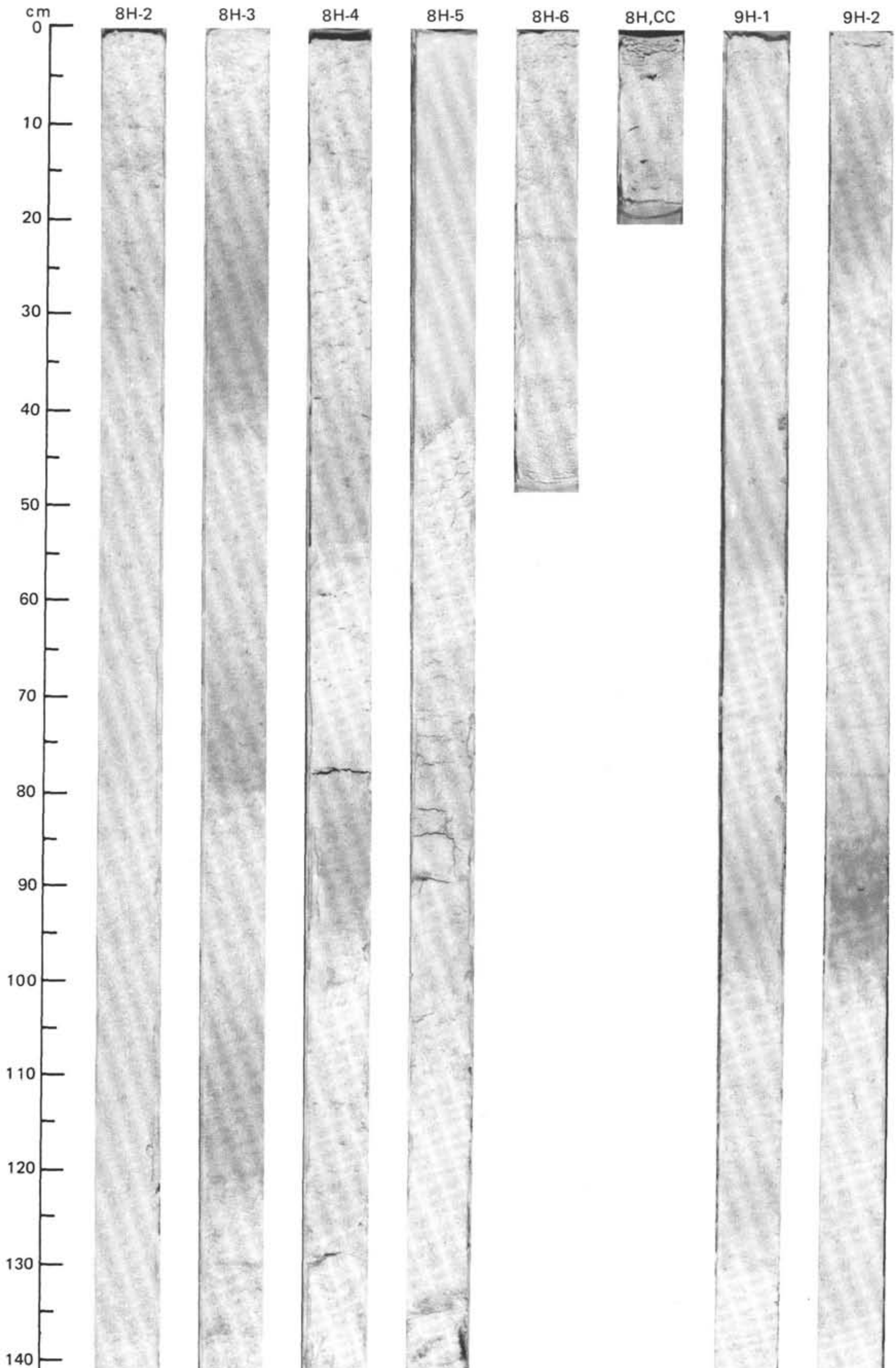
cm
0
10
20
30
40
50
60
70
80
90
100
110
120
130
140
150
8H-2
8H-3
8H-4
8H-5
8H-6
8H,CC
9H-1
9H-2

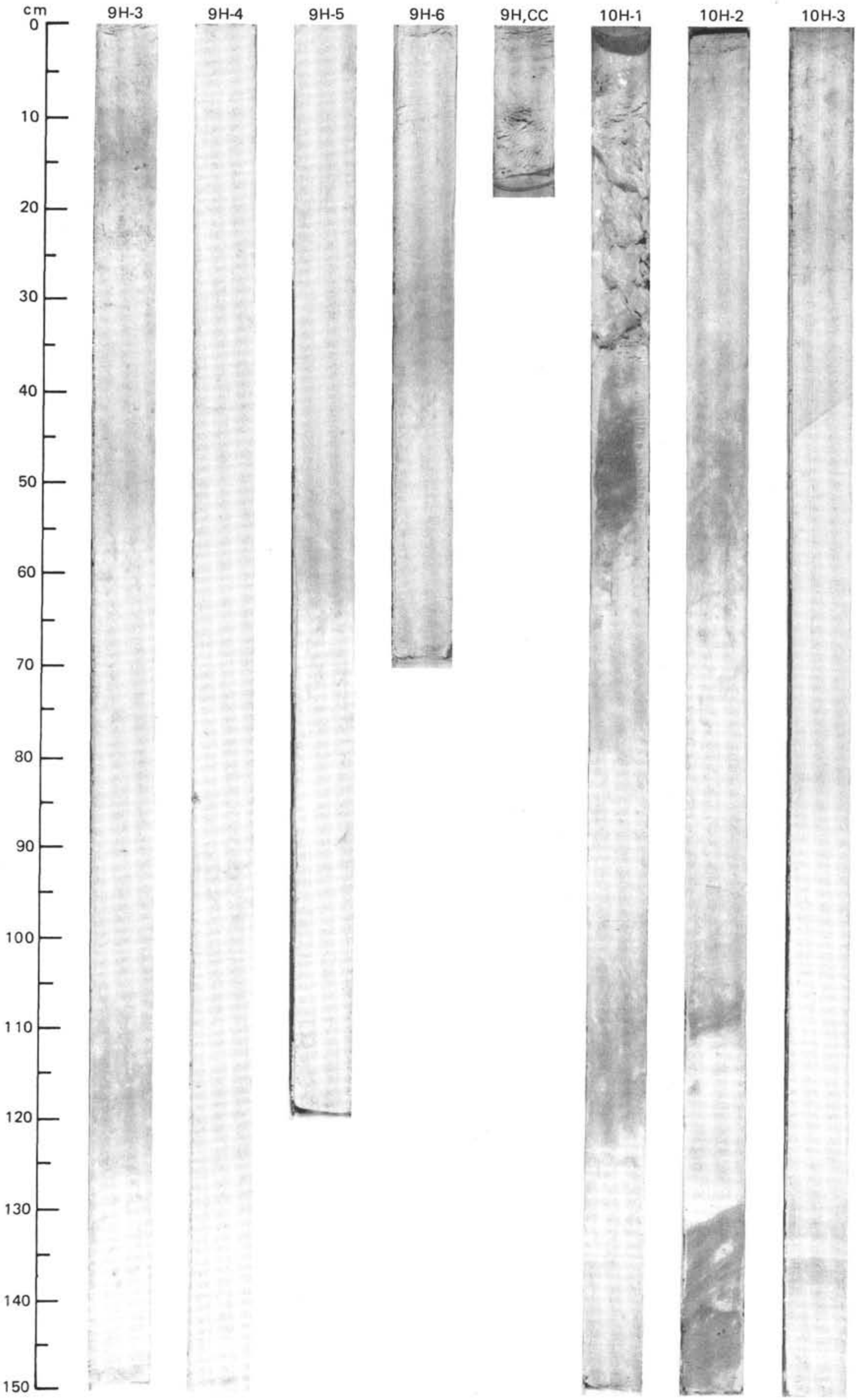
cm
0
10
20
30
40
50
60
70
80
90
100
110
120
130
140
150
9H-3
9H-4
9H-5
9H-6
9H,CC
10H-1
10H-2
10H-3

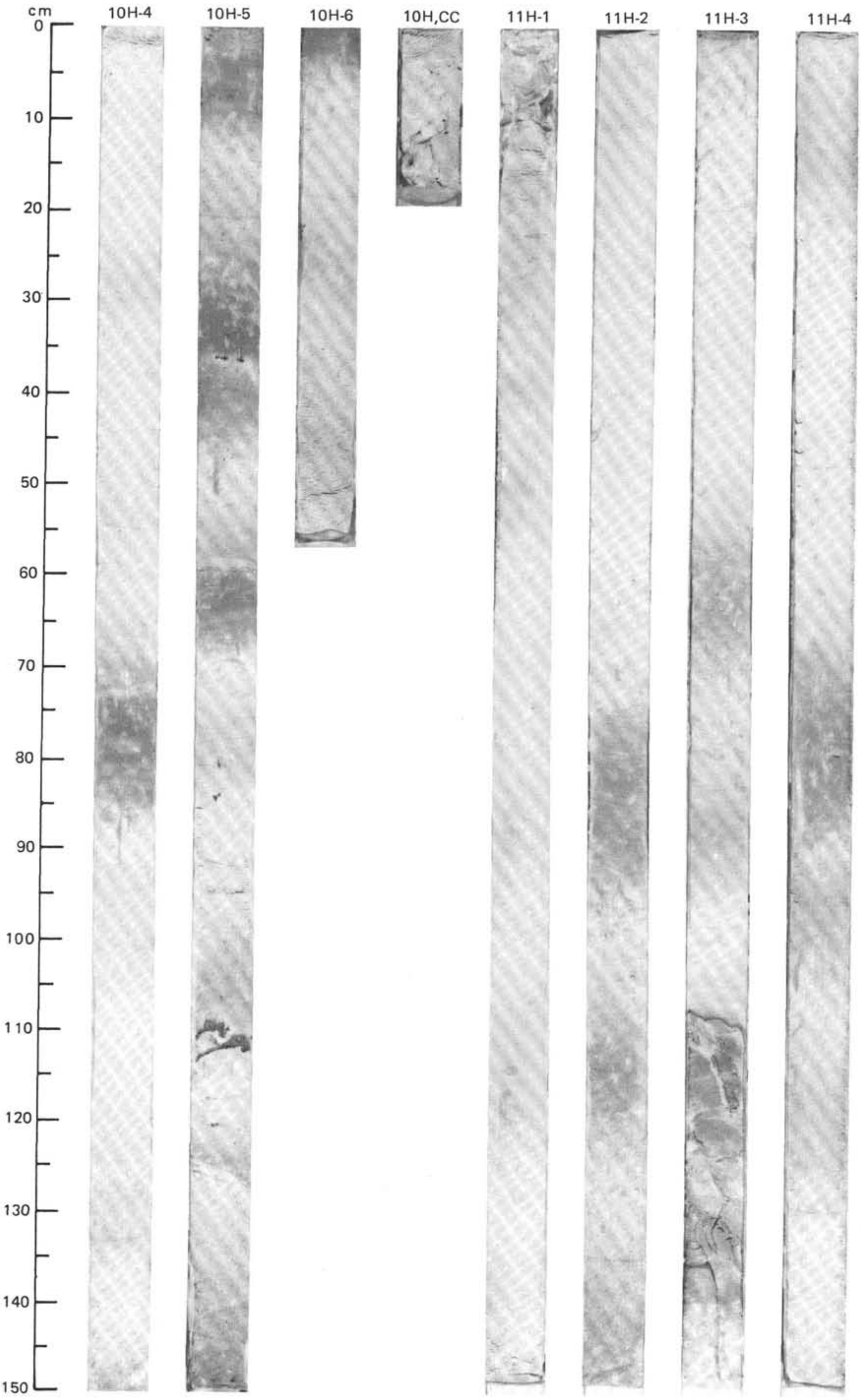
cm
0
10
20
30
40
50
60
70
80
90
100
110
120
130
140
150
10H-4
10H-5
10H-6
10H,CC
11H-1
11H-2
11H-3
11H-4

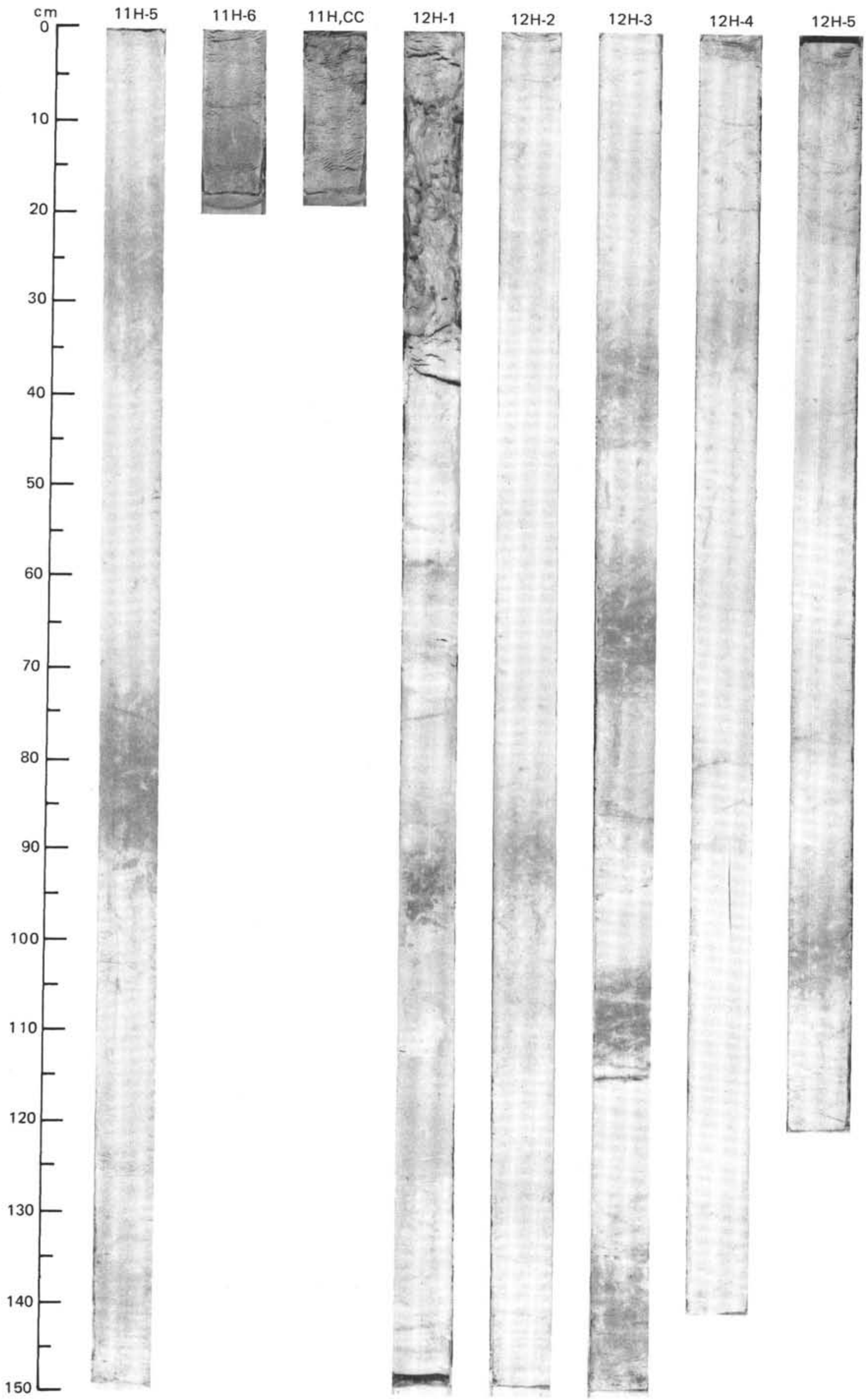
cm
0
10
20
30
40
50
60
70
80
90
100
110
120
130
140
150
11H-5
11H-6
11H,CC
12H-1
12H-2
12H-3
12H-4
12H-5

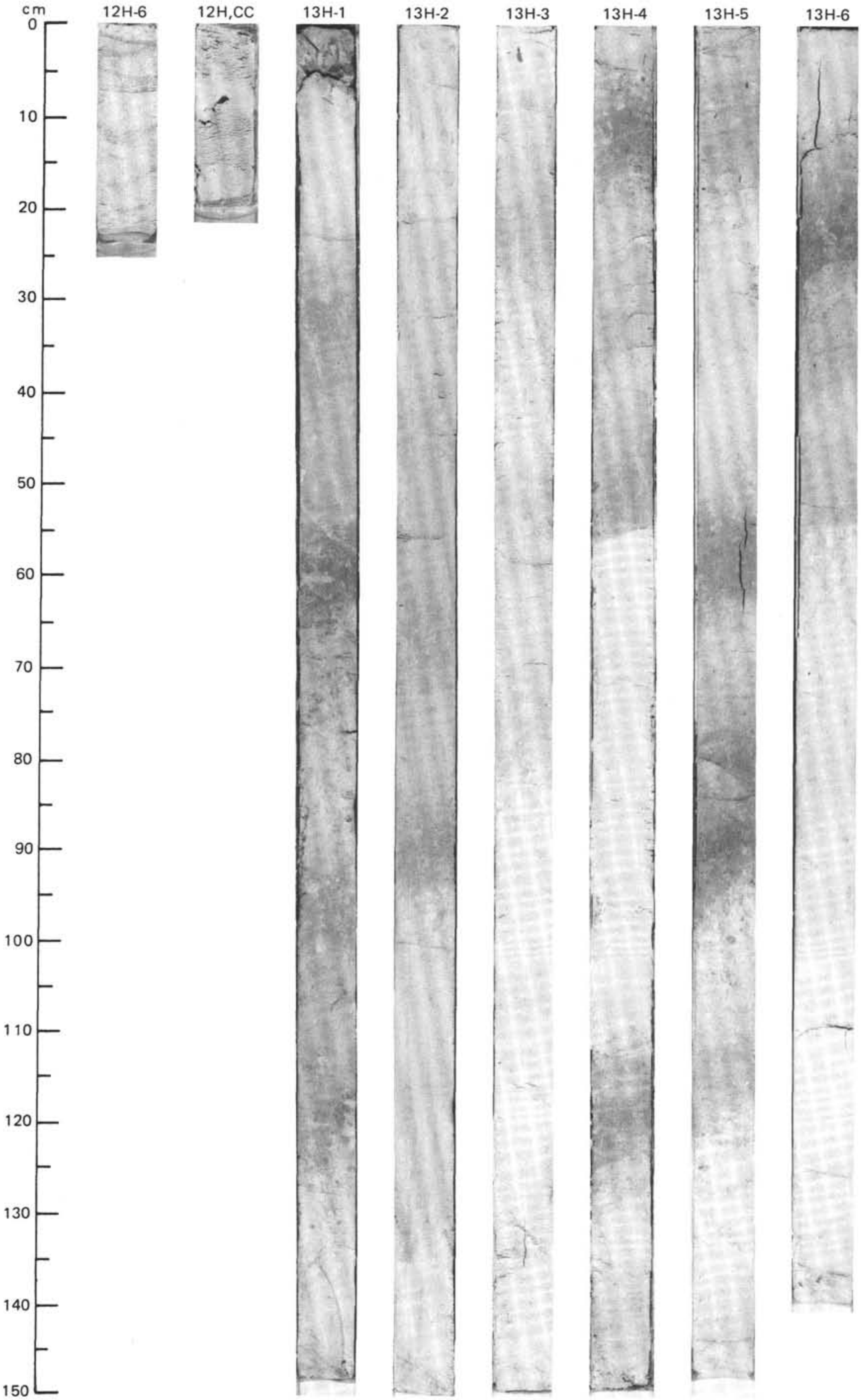
cm
0
10
20
30
40
50
60
70
80
90
100
110
120
130
140
150
12H-6
12H,CC
13H-1
13H-2
13H-3
13H-4
13H-5
13H-6

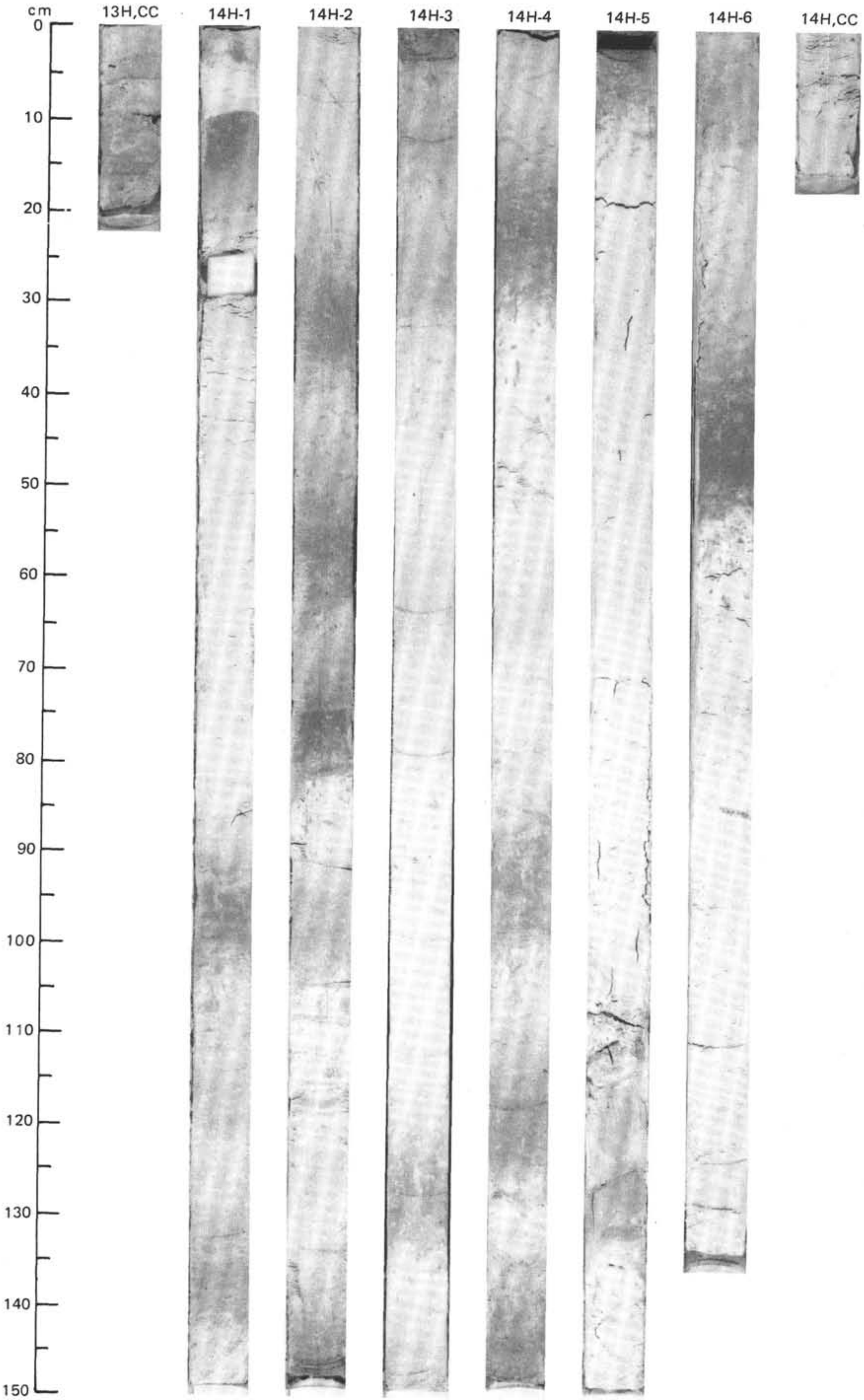
cm
0
10
20
30
40
50
60
70
80
90
100
110
120
130
140
150
13H,CC
14H-1
14H-2
14H-3
14H-4
14H-5
14H-6
14H,CC

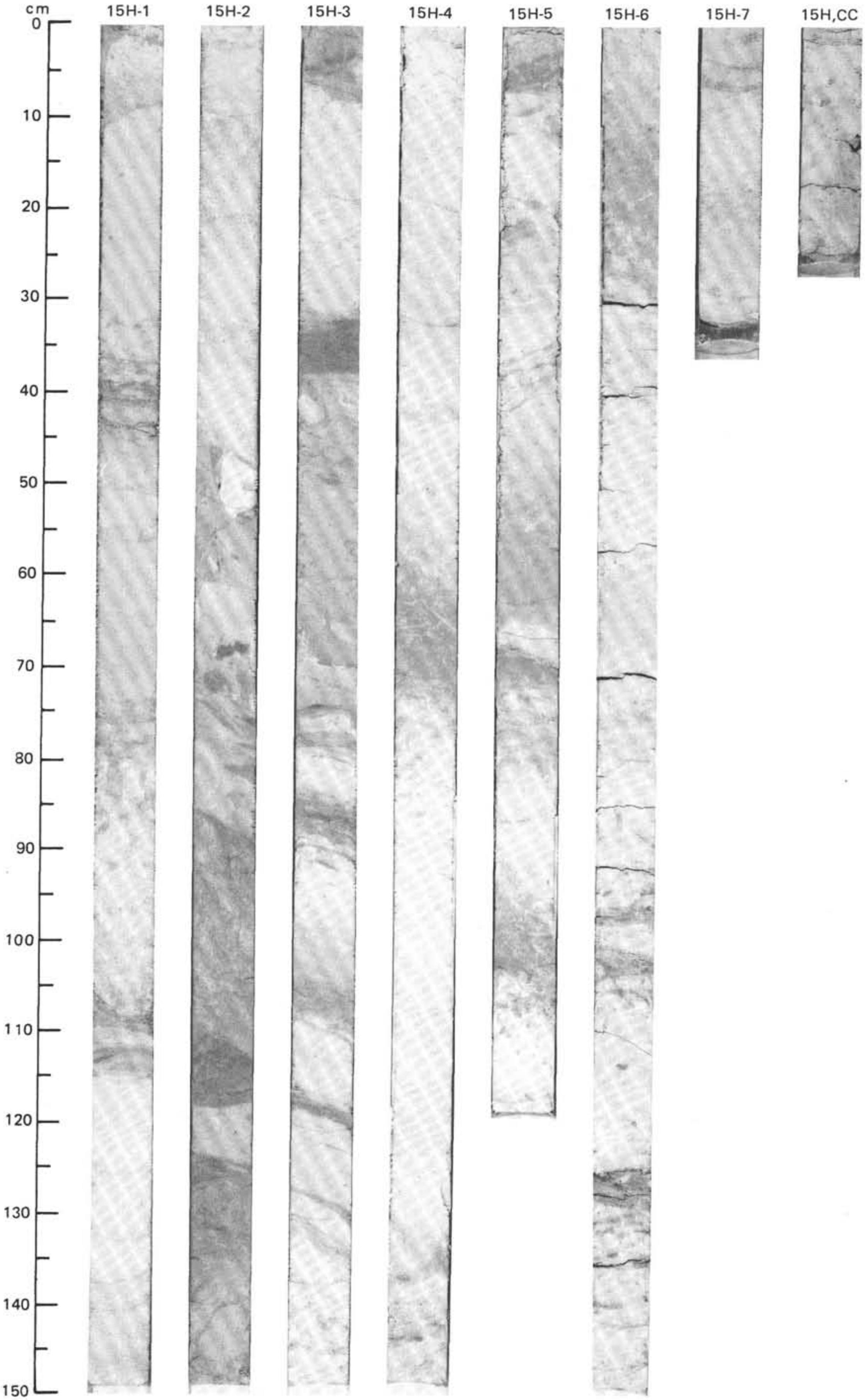
cm
0
10
20
30
40
50
60
70
80
90
100
110
120
130
140
150
15H-1
15H-2
15H-3
15H-4
15H-5
15H-6
15H-7
15H,CC

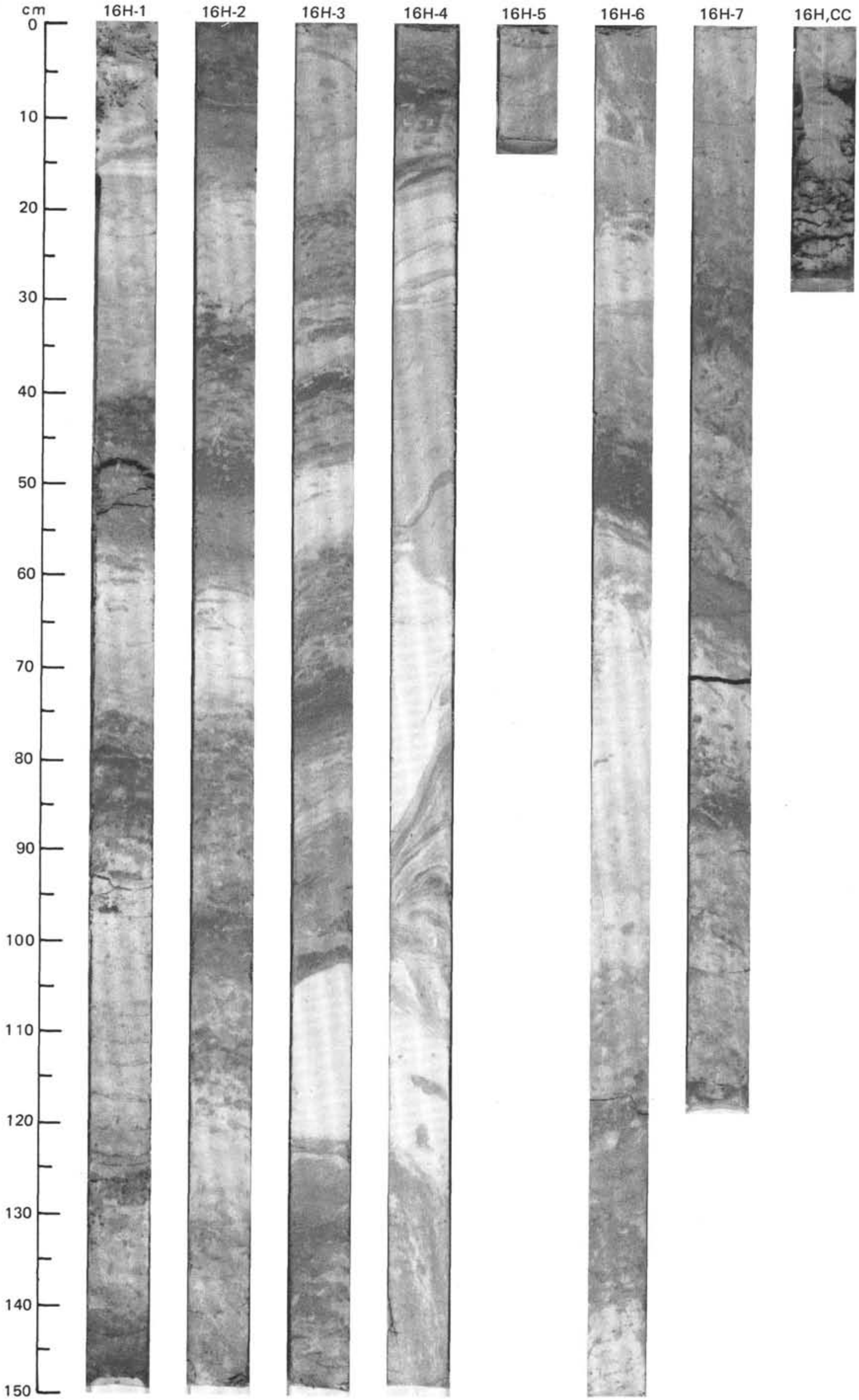
cm
0
10
20
30
40
50
60
70
80
90
100
110
120
130
140
150
16H-1
16H-2
16H-3
16H-4
16H-5
16H-6
16H-7
16H,CC

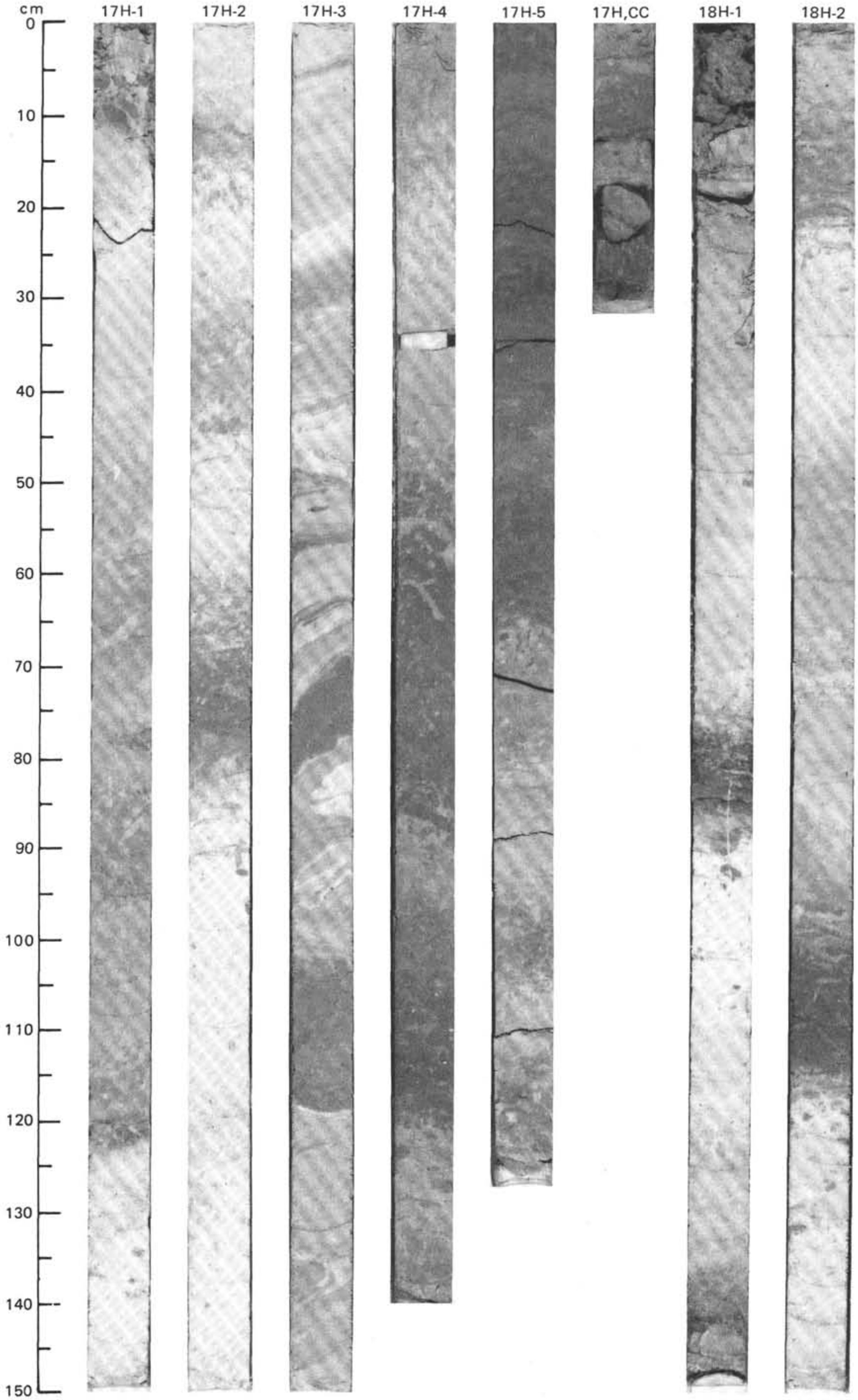
cm
0
10
20
30
40
50
60
70
80
90
100
110
120
130
140
150
17H-1
17H-2
17H-3
17H-4
17H-5
17H,CC
18H-1
18H-2

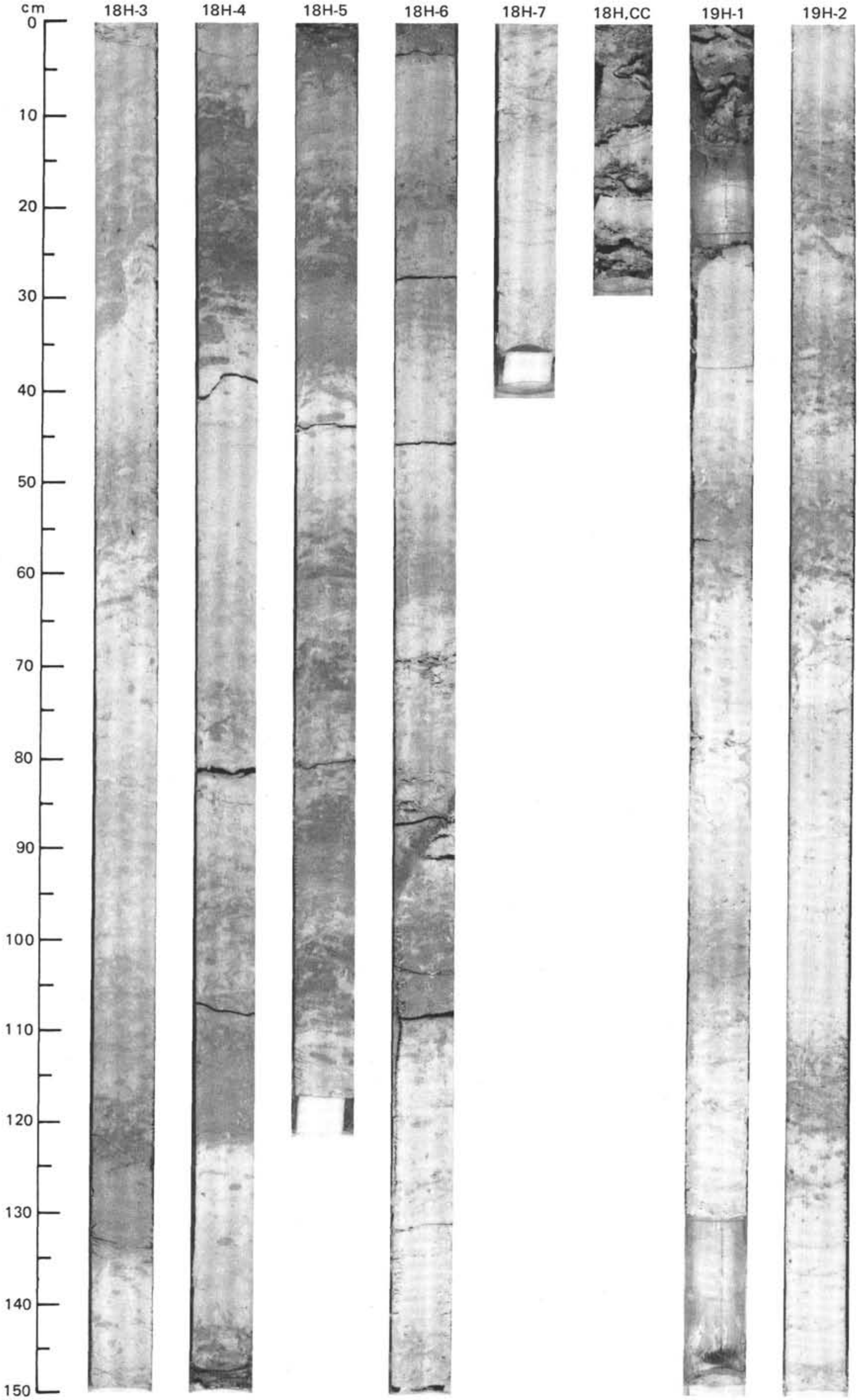
cm
0
10
20
30
40
50
60
70
80
90
100
110
120
130
140
150
18H-3
18H-4
18H-5
18H-6
18H-7
18H,CC
19H-1
19H-2

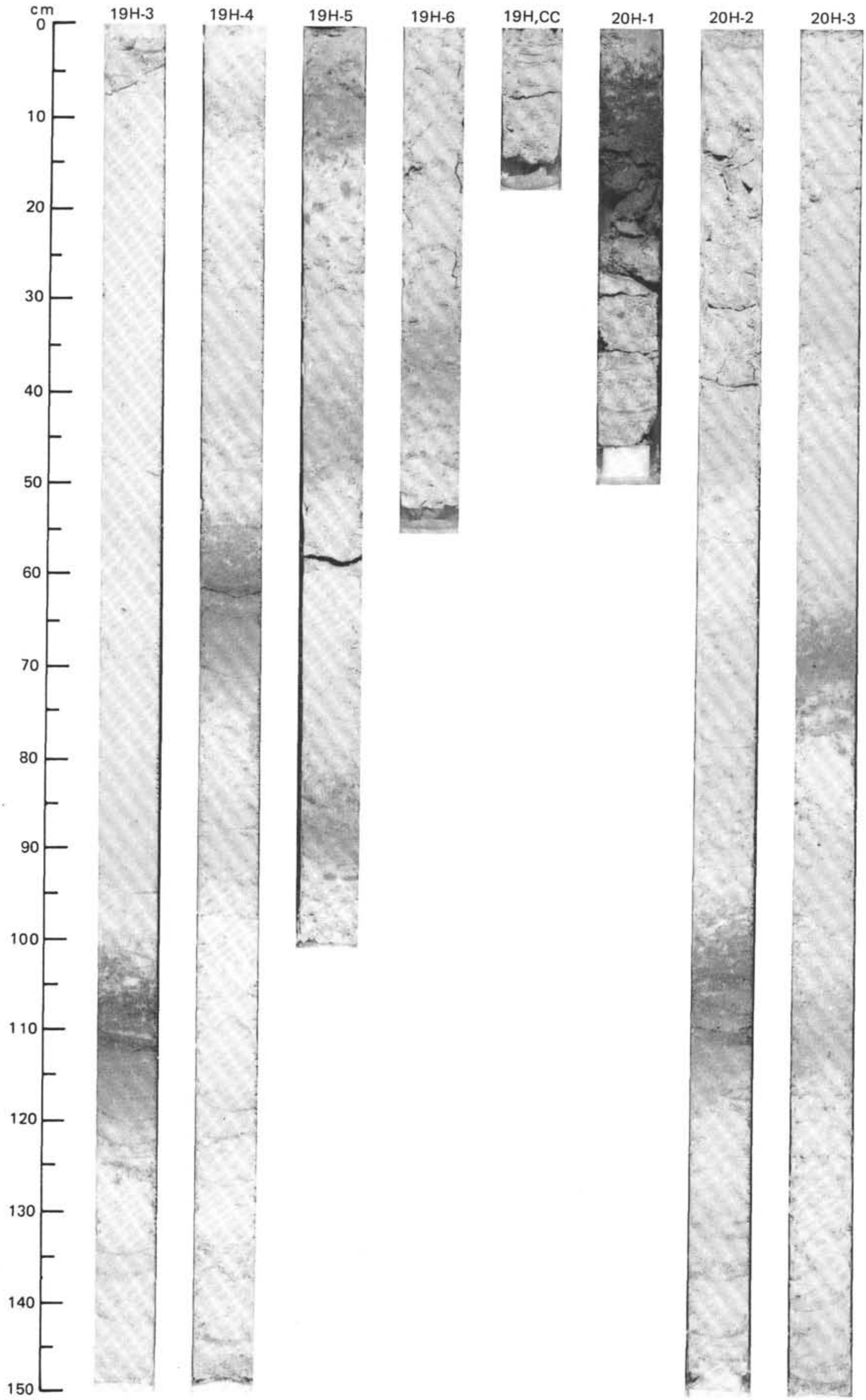
cm
0
10
20
30
40
50
60
70
80
90
100
110
120
130
140
150
19H-3
19H-4
19H-5
19H-6
19H,CC
20H-1
20H-2
20H-3

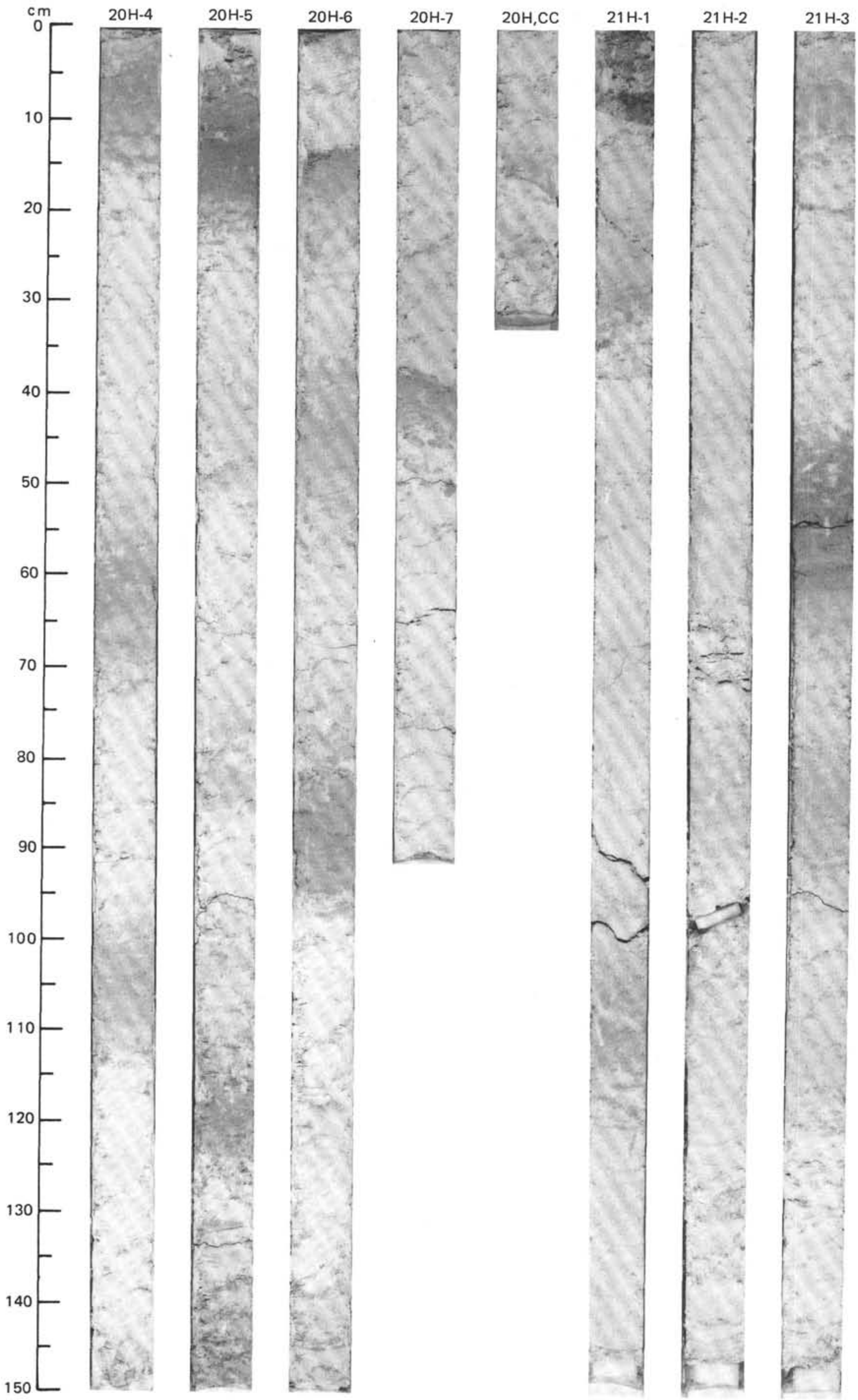
cm
0
10
20
30
40
50
60
70
80
90
100
110
120
130
140
150
20H-4
20H-5
20H-6
20H-7
20H,CC
21H-1
21H-2
21H-3

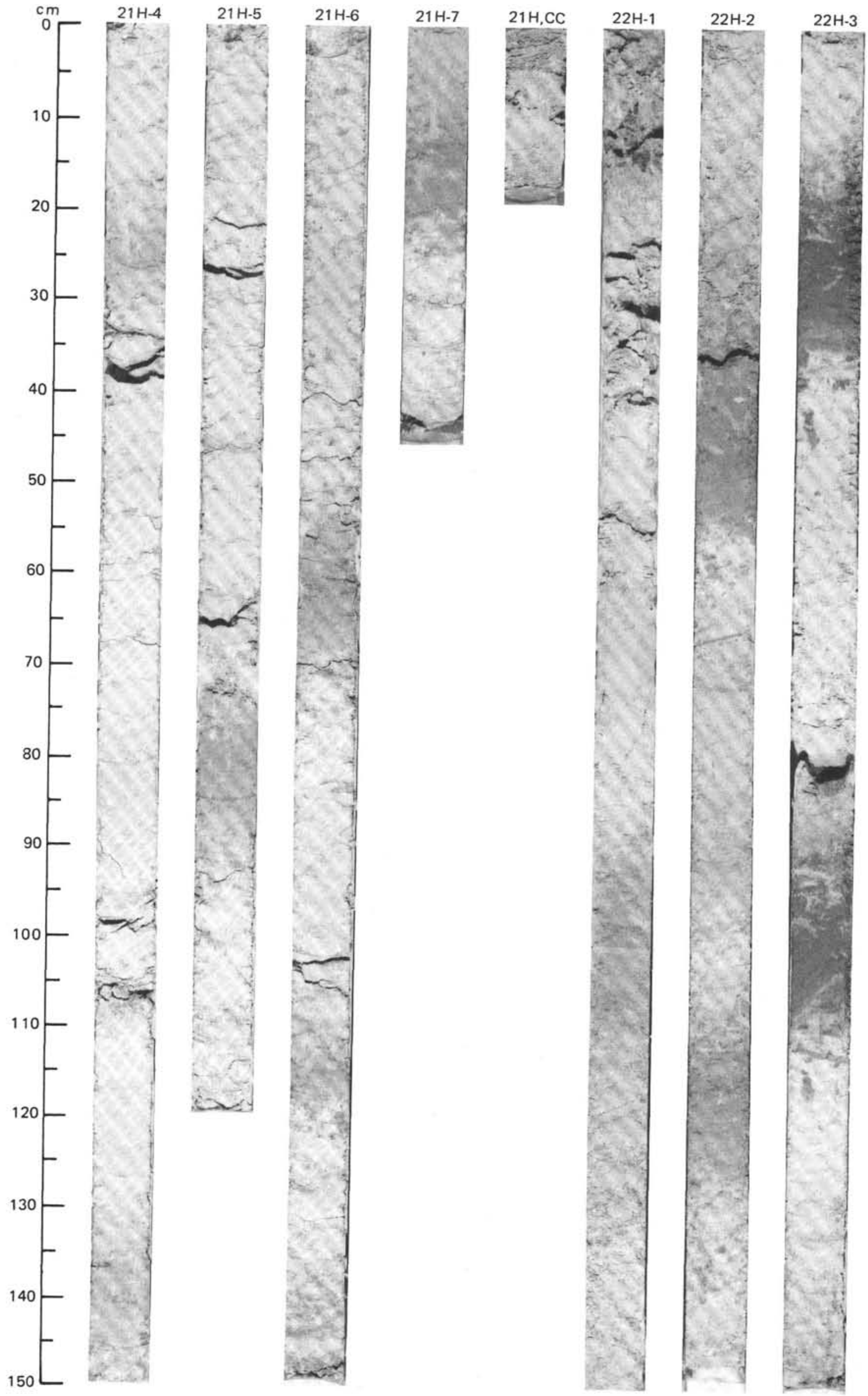
cm
0
10
20
30
40
50
60
70
80
90
100
110
120
130
140
150
21H-4
21H-5
21H-6
21H-7
21H,CC
22H-1
22H-2
22H-3

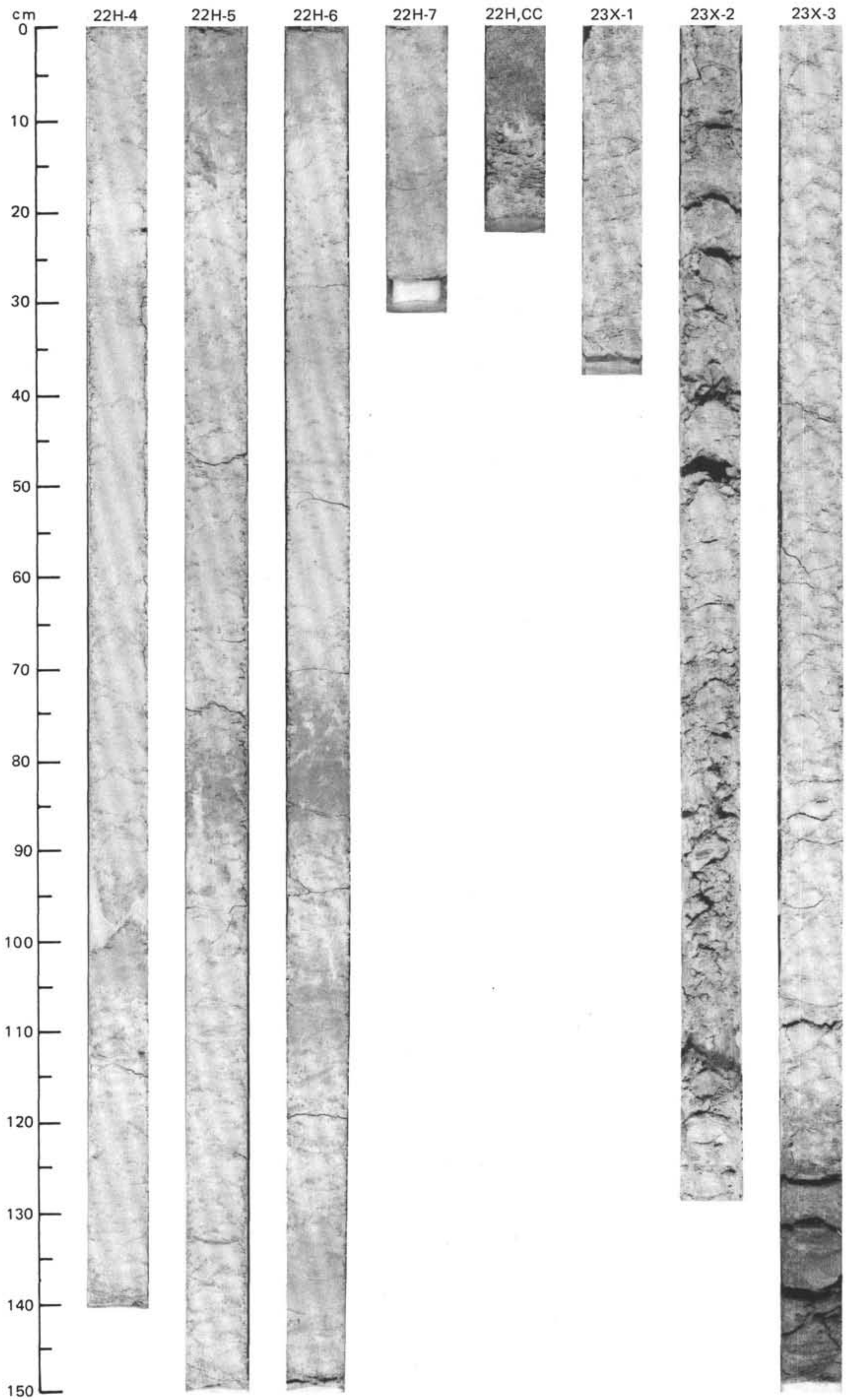
cm
0
10
20
30
40
50
60
70
80
90
100
110
120
130
140
150
22H-4
22H-5
22H-6
22H-7
22H,CC
23X-1
23X-2
23X-3

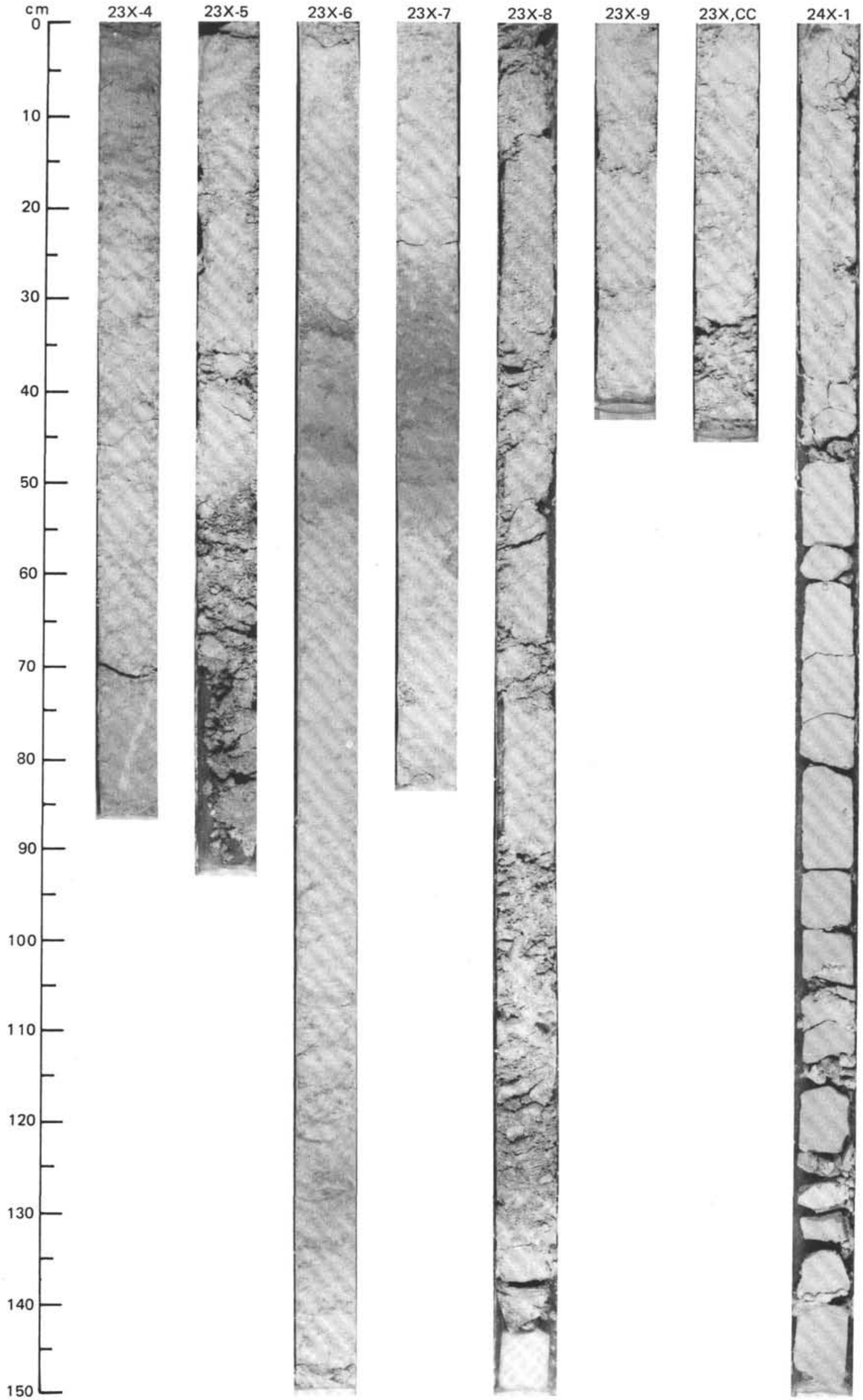
cm
0
10
20
30
40
50
60
70
80
90
100
110
120
130
140
150
23X-4
23X-5
23X-6
23X-7
23X-8
23X-9
23X,CC
24X-1

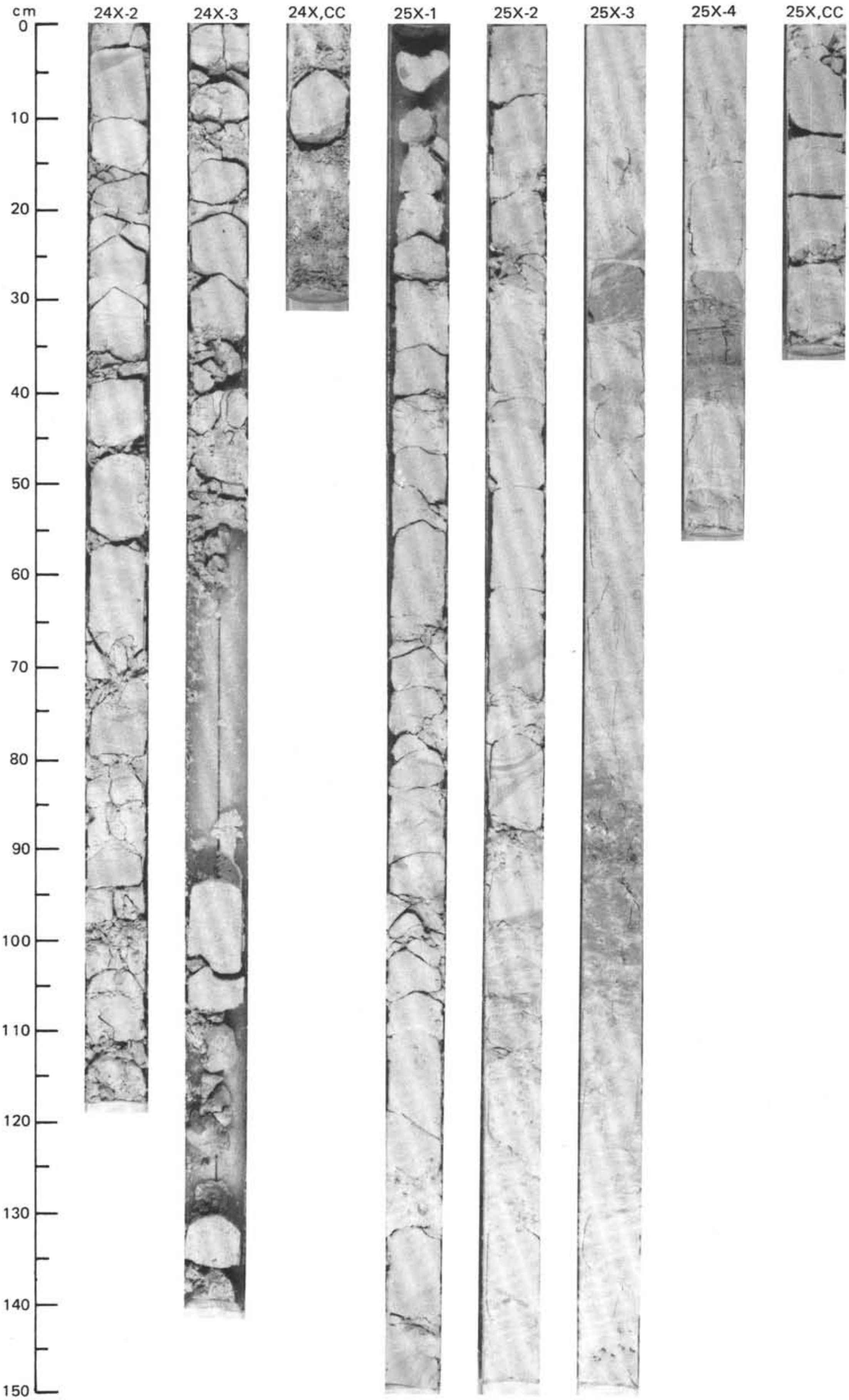
cm
0
10
20
30
40
50
60
70
80
90
100
110
120
130
140
150
24X-2
24X-3
24X,CC
25X-1
25X-2
25X-3
25X-4
25X,CC

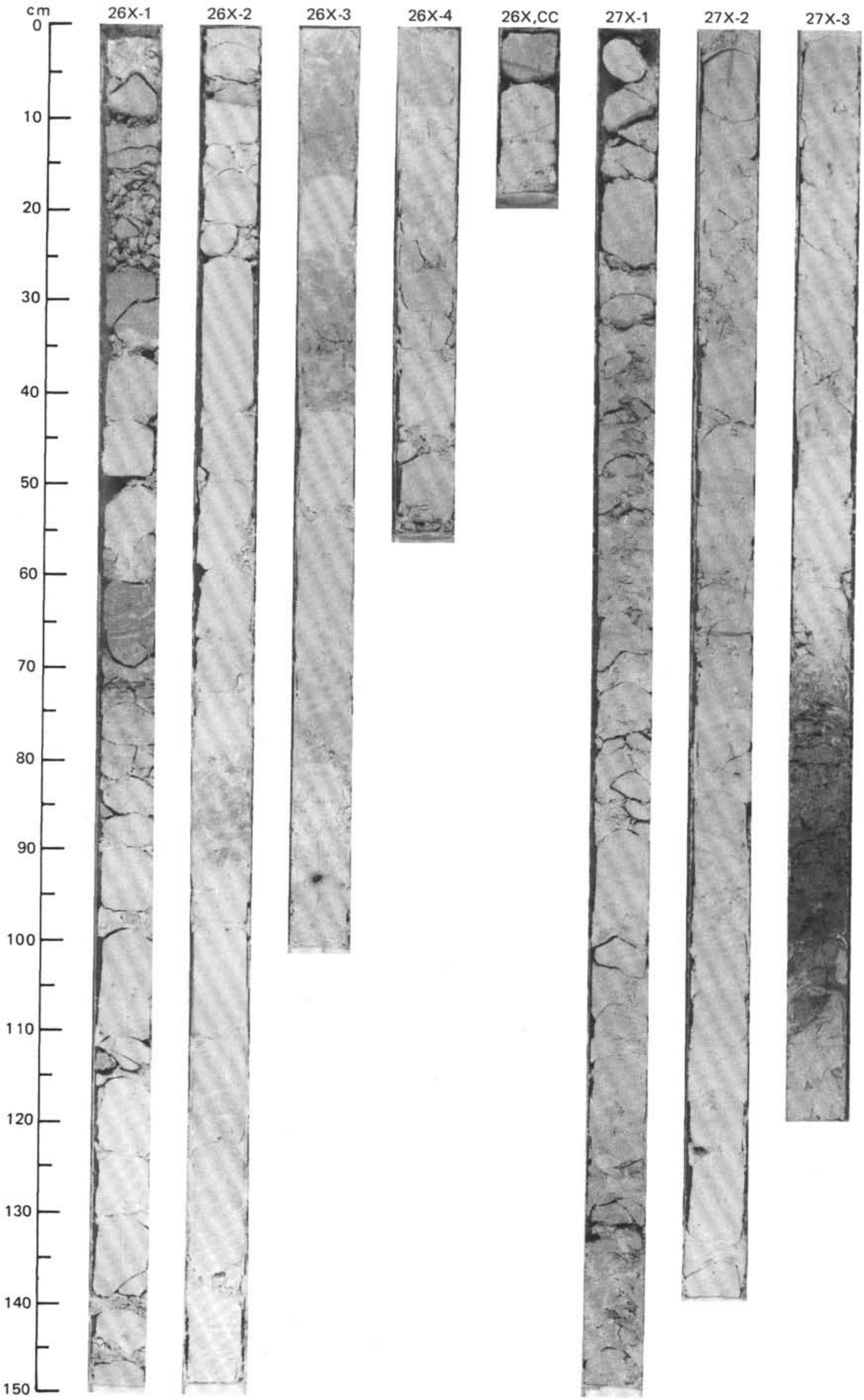
cm
0
10
20
30
40
50
60
70
80
90
100
110
120
130
140
150
26X-1
26X-2
26X-3
26X-4
26X,CC
27X-1
27X-2
27X-3

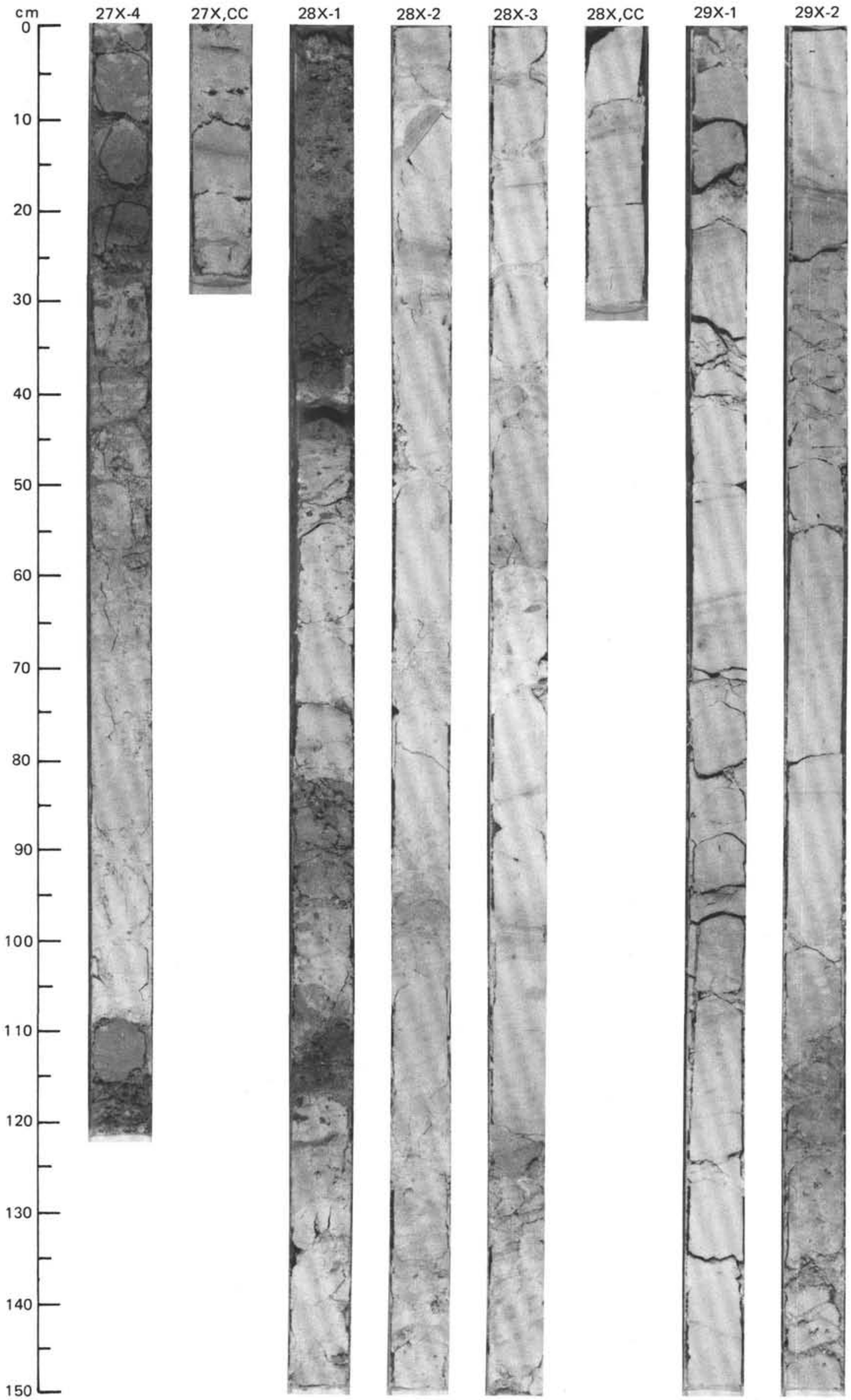
cm
0
10
20
30
40
50
60
70
80
90
100
110
120
130
140
150
27X-4
27X,CC
28X-1
28X-2
28X-3
28X,CC
29X-1
29X-2

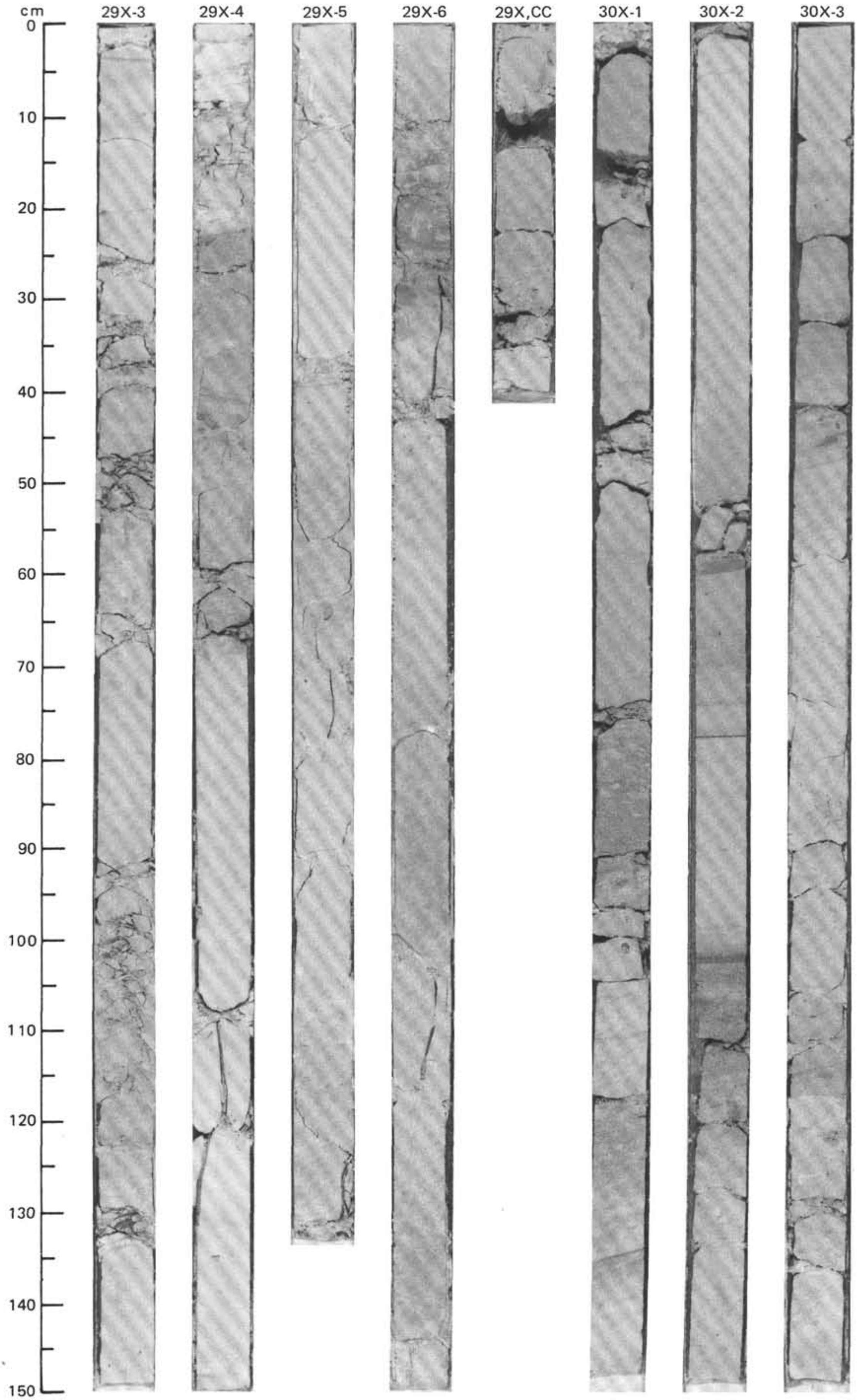
cm
0
10
20
30
40
50
60
70
80
90
100
110
120
130
140
150
29X-3
29X-4
29X-5
29X-6
29X,CC
30X-1
30X-2
30X-3

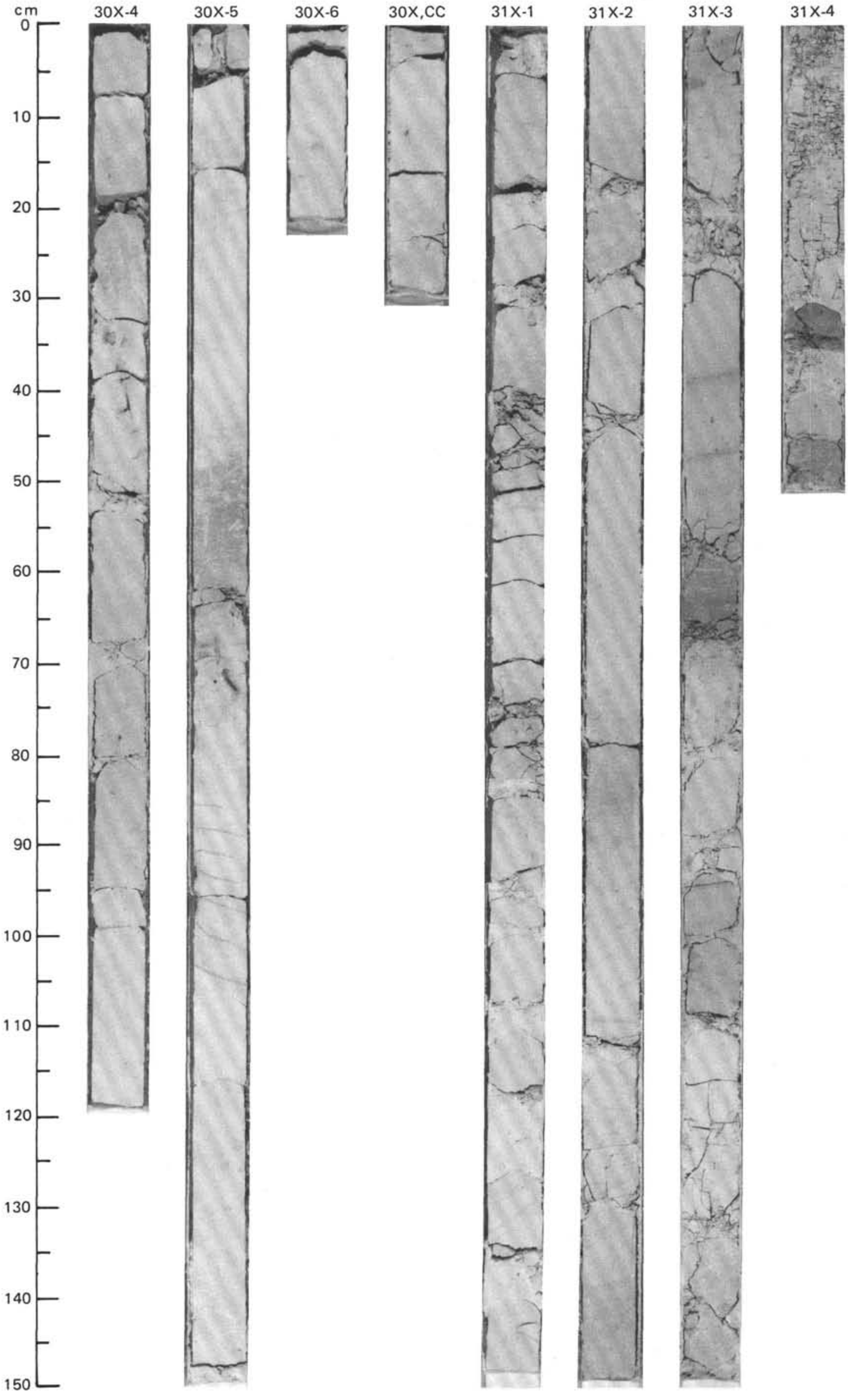
cm
0
10
20
30
40
50
60
70
80
90
100
110
120
130
140
150
30X-4
30X-5
30X-6
30X,CC
31X-1
31X-2
31X-3
31X-4

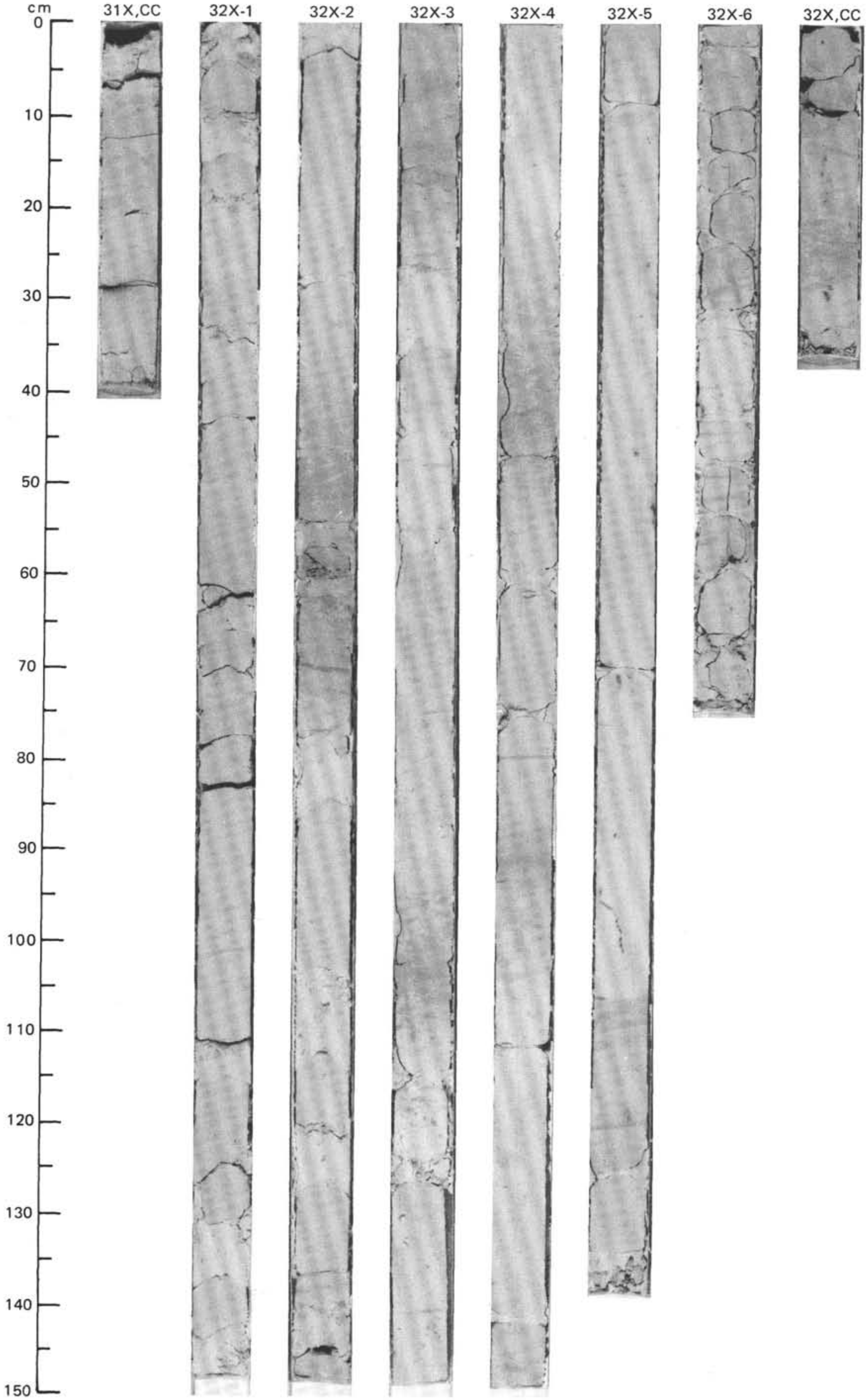
cm
0
10
20
30
40
50
60
70
80
90
100
110
120
130
140
150
31X,CC
32X-1
32X-2
32X-3
32X-4
32X-5
32X-6
32X,CC

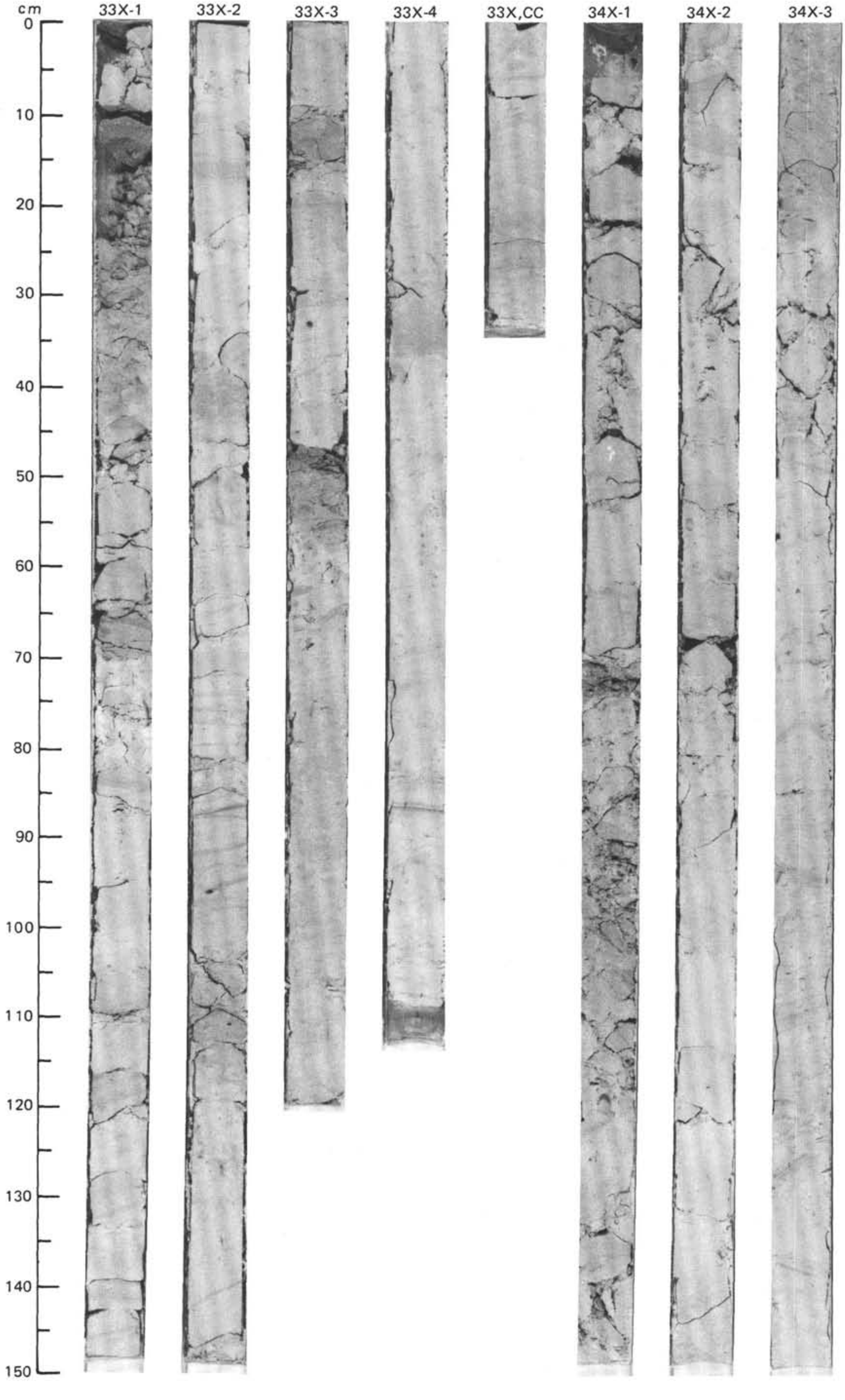
cm
33X-1
33X-2
33X-3
33X-4
33X,CC
34X-1
34X-2
34X-3
0
10
20
30
40
50
60
70
80
90
100
110
120
130
140
150

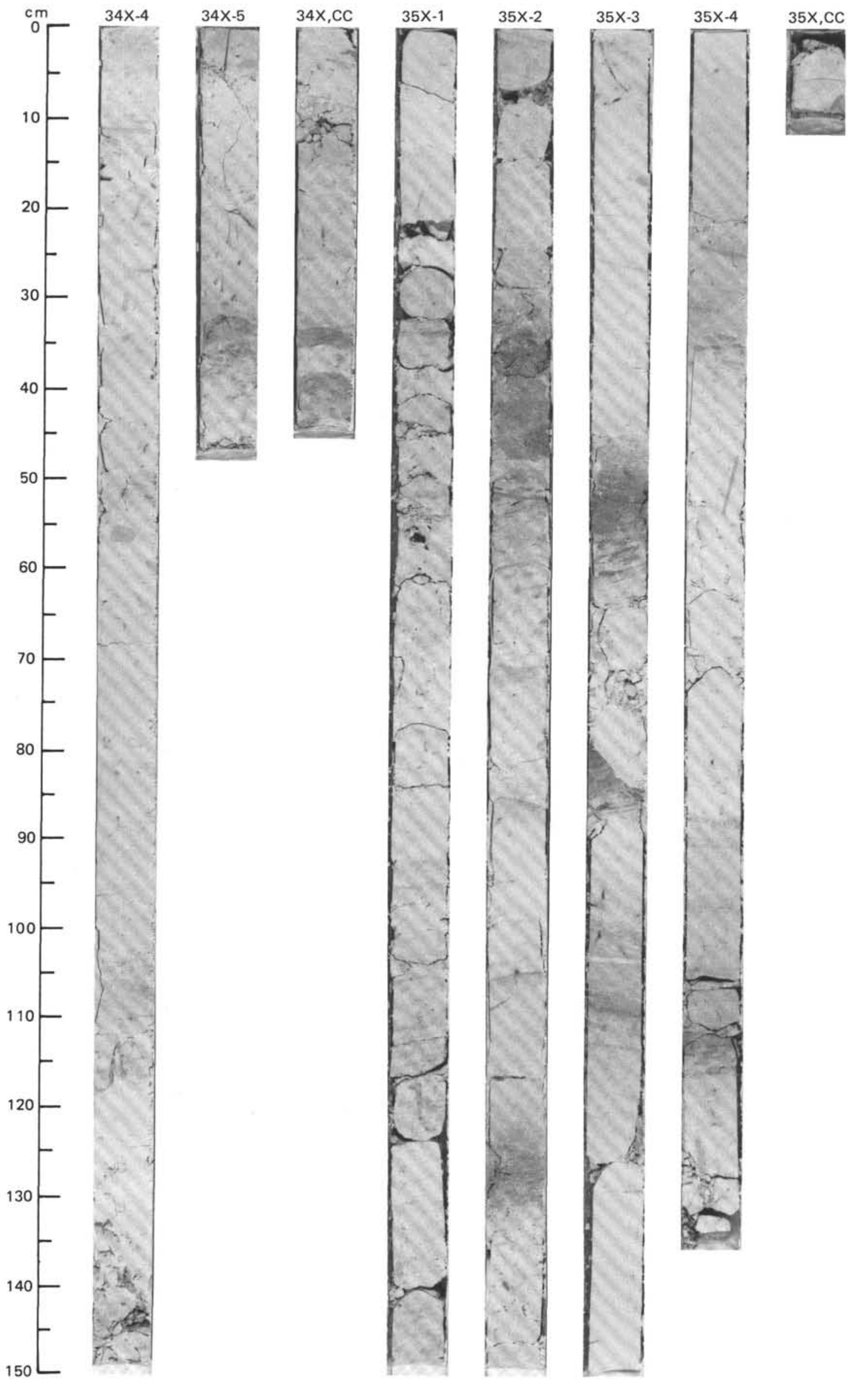
cm
0
10
20
30
40
50
60
70
80
90
100
110
120
130
140
150
34X-4
34X-5
34X,CC
35X-1
35X-2
35X-3
35X-4
35X,CC

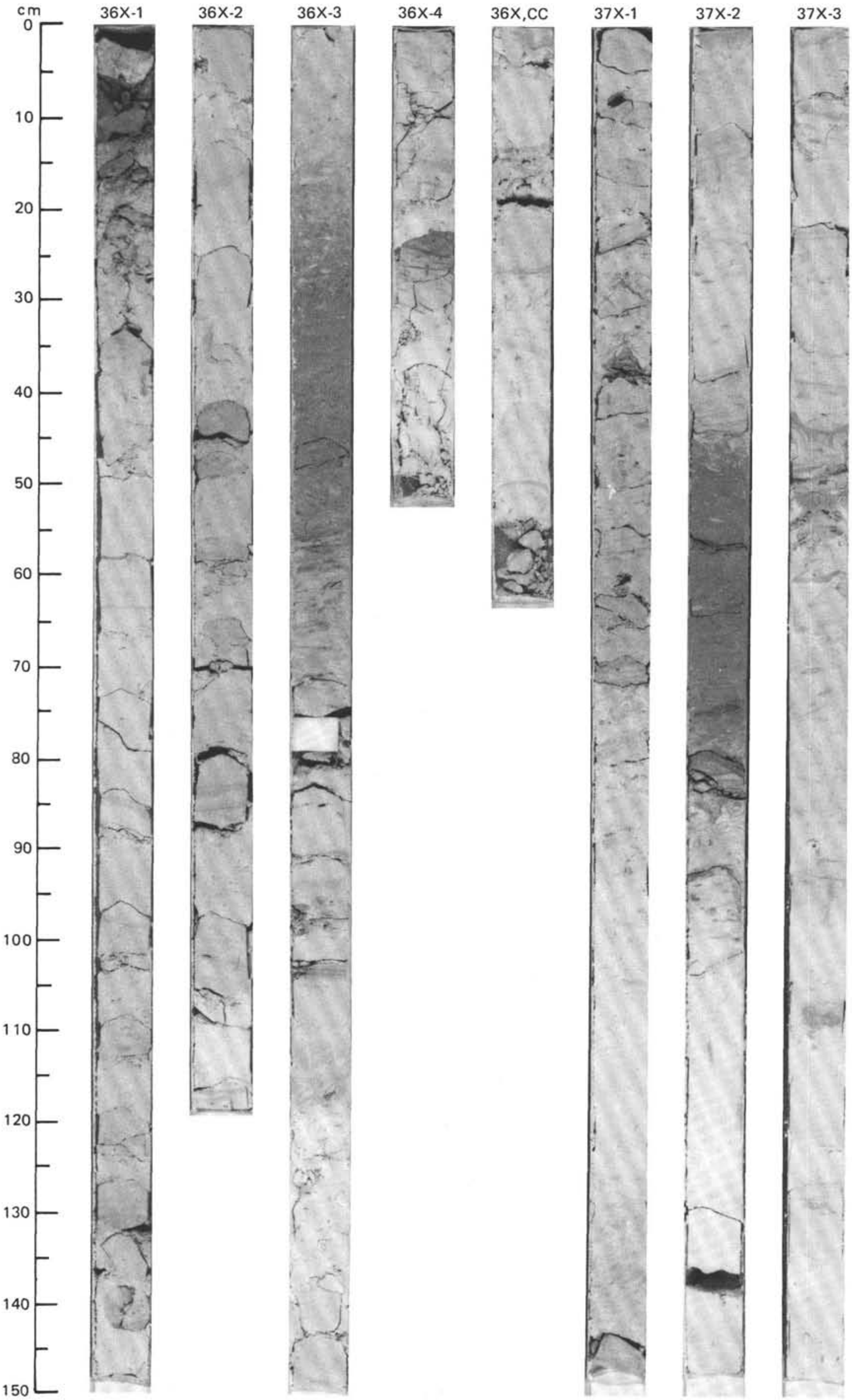
cm
0
10
20
30
40
50
60
70
80
90
100
110
120
130
140
150
36X-1
36X-2
36X-3
36X-4
36X,CC
37X-1
37X-2
37X-3

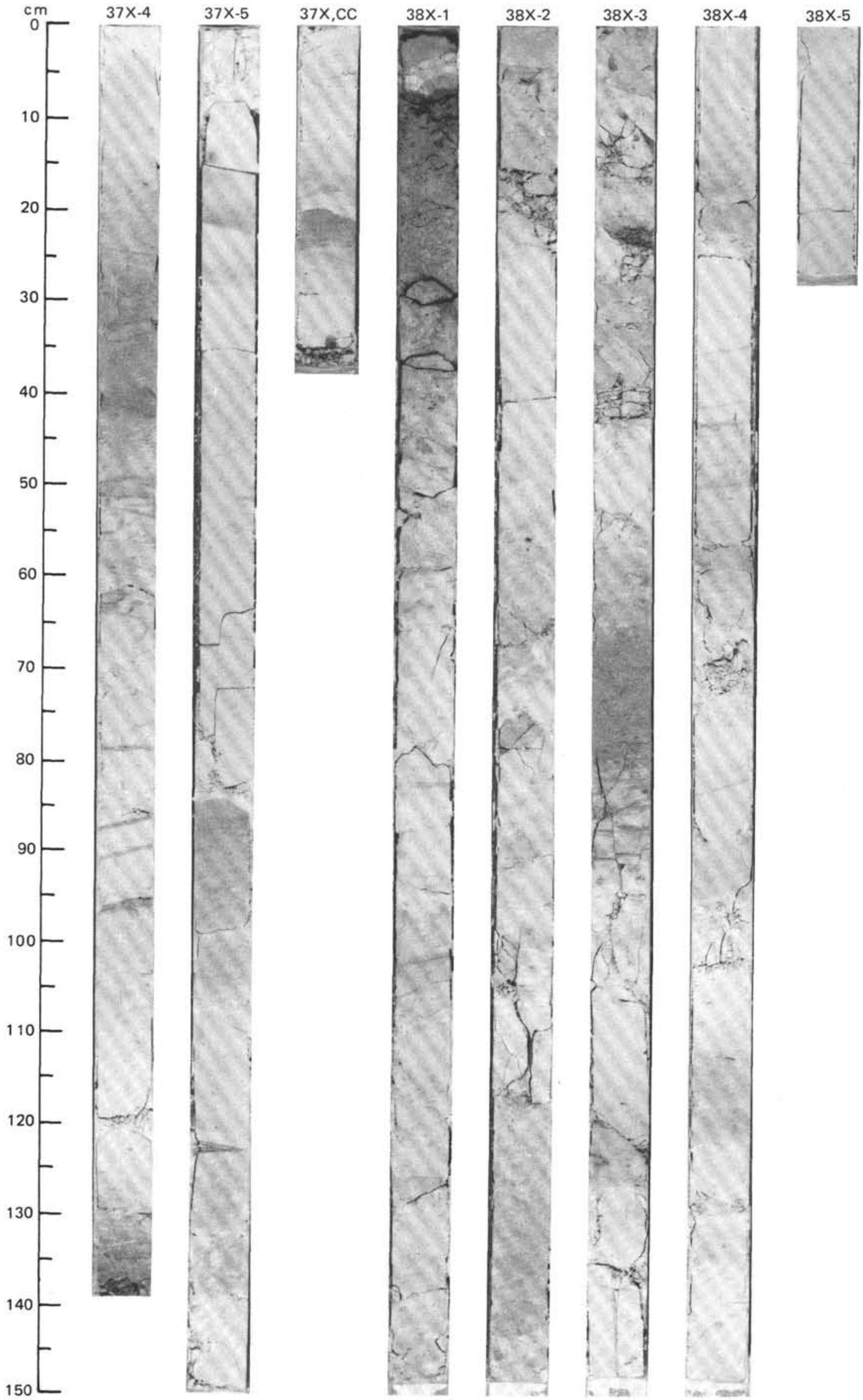
cm
0
10
20
30
40
50
60
70
80
90
100
110
120
130
140
150
37X-4
37X-5
37X,CC
38X-1
38X-2
38X-3
38X-4
38X-5

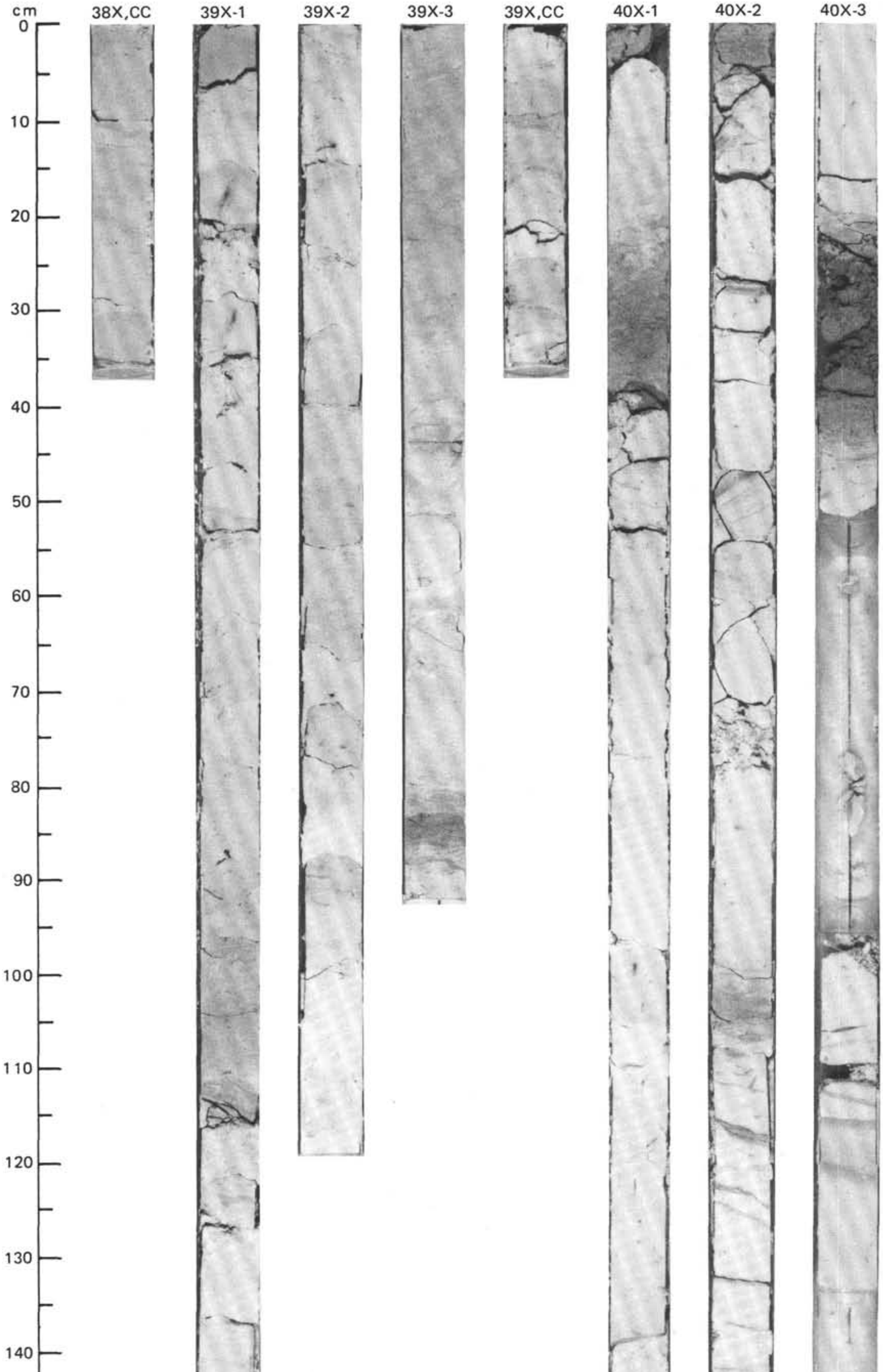
cm
0
10
20
30
40
50
60
70
80
90
100
110
120
130
140
150
38X,CC
39X-1
39X-2
39X-3
39X,CC
40X-1
40X-2
40X-3

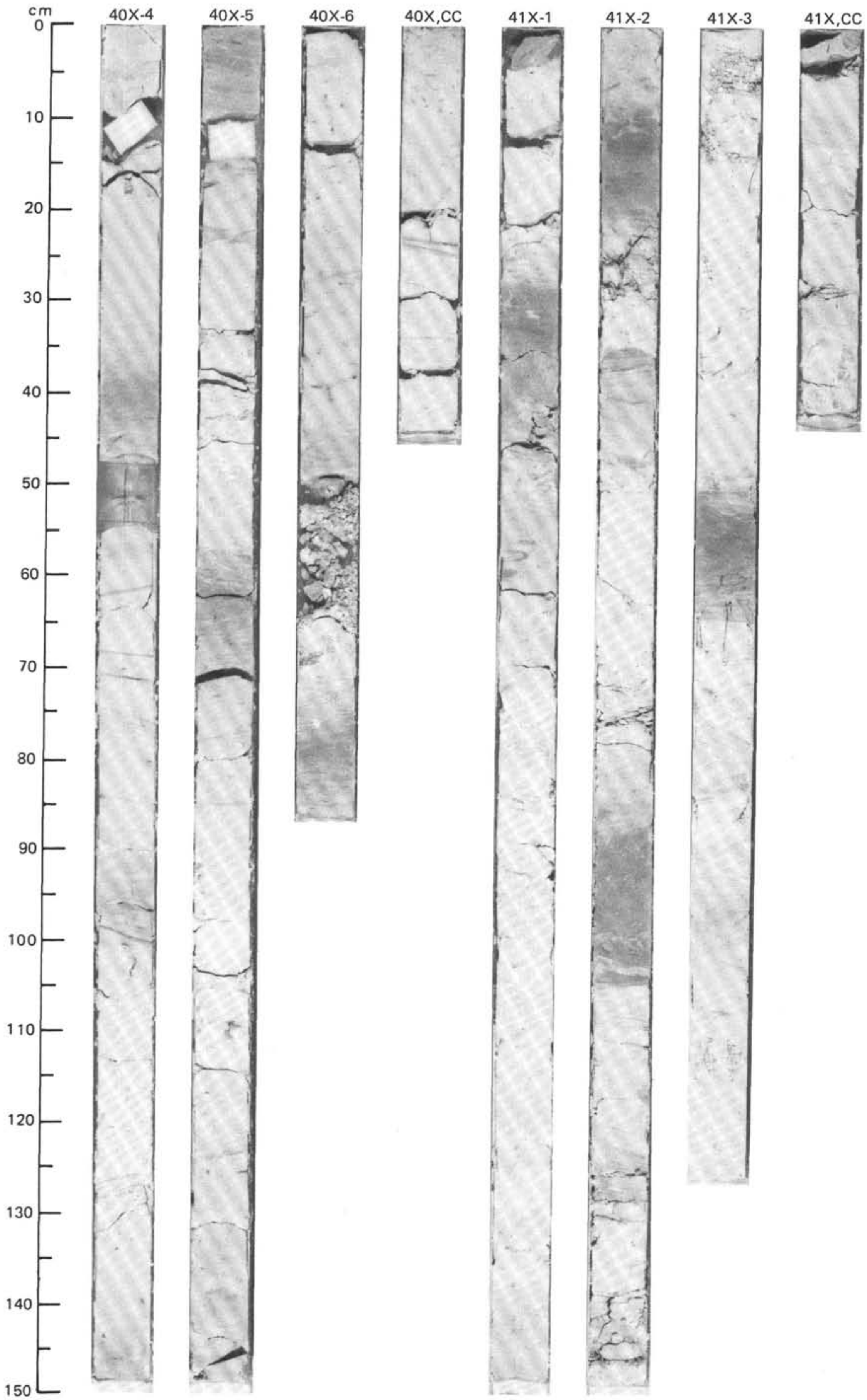
cm
0
10
20
30
40
50
60
70
80
90
100
110
120
130
140
150
40X-4
40X-5
40X-6
40X,CC
41X-1
41X-2
41X-3
41X,CC

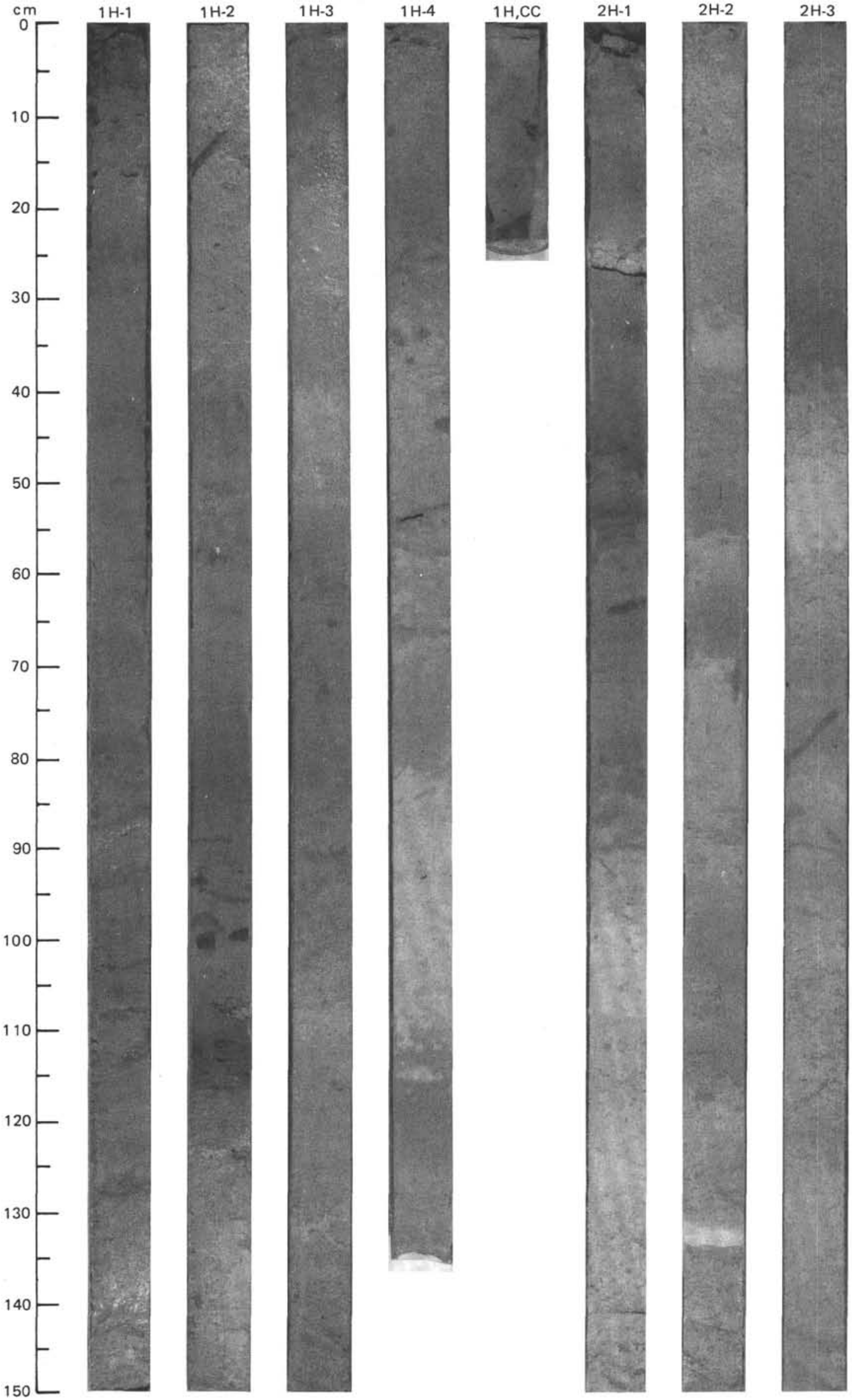
cm
1H-1
1H-2
1H-3
1H-4
1H,CC
2H-1
2H-2
2H-3
0
10
20
30
40
50
60
70
80
90
100
110
120
130
140
150

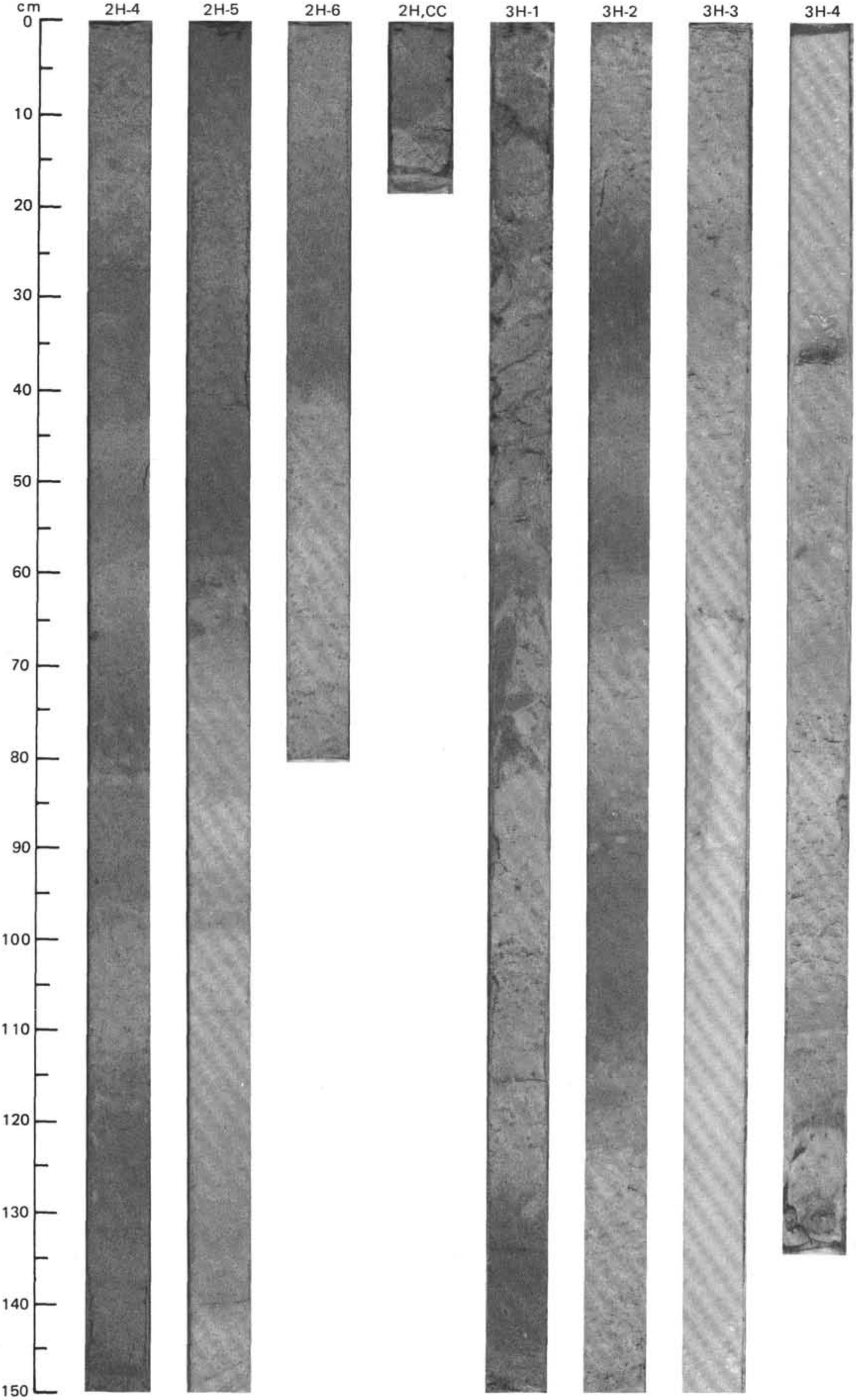
cm
0
10
20
30
40
50
60
70
80
90
100
110
120
130
140
150
2H-4
2H-5
2H-6
2H,CC
3H-1
3H-2
3H-3
3H-4

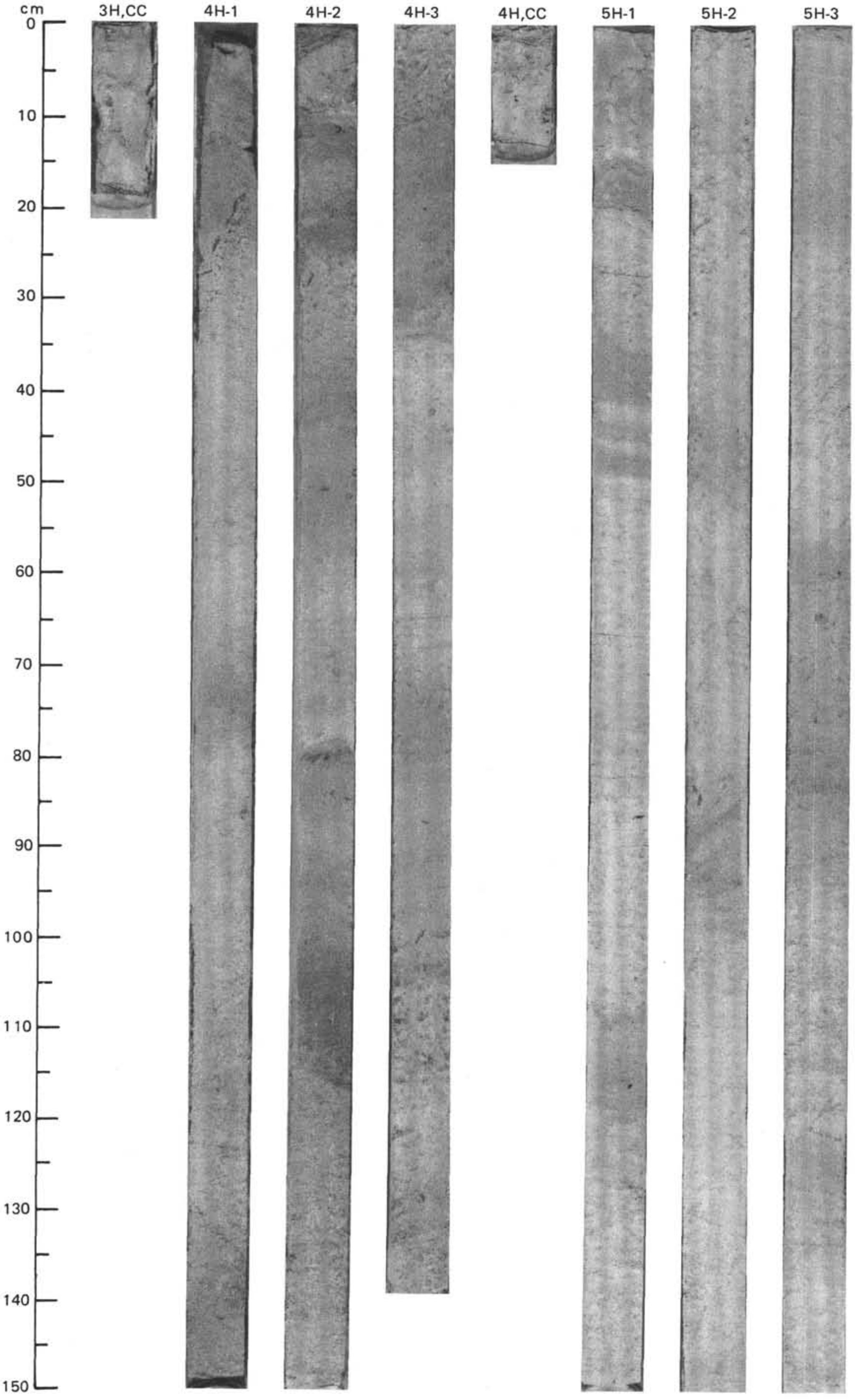
cm
0
10
20
30
40
50
60
70
80
90
100
110
120
130
140
150
3H,CC
4H-1
4H-2
4H-3
4H,CC
5H-1
5H-2
5H-3

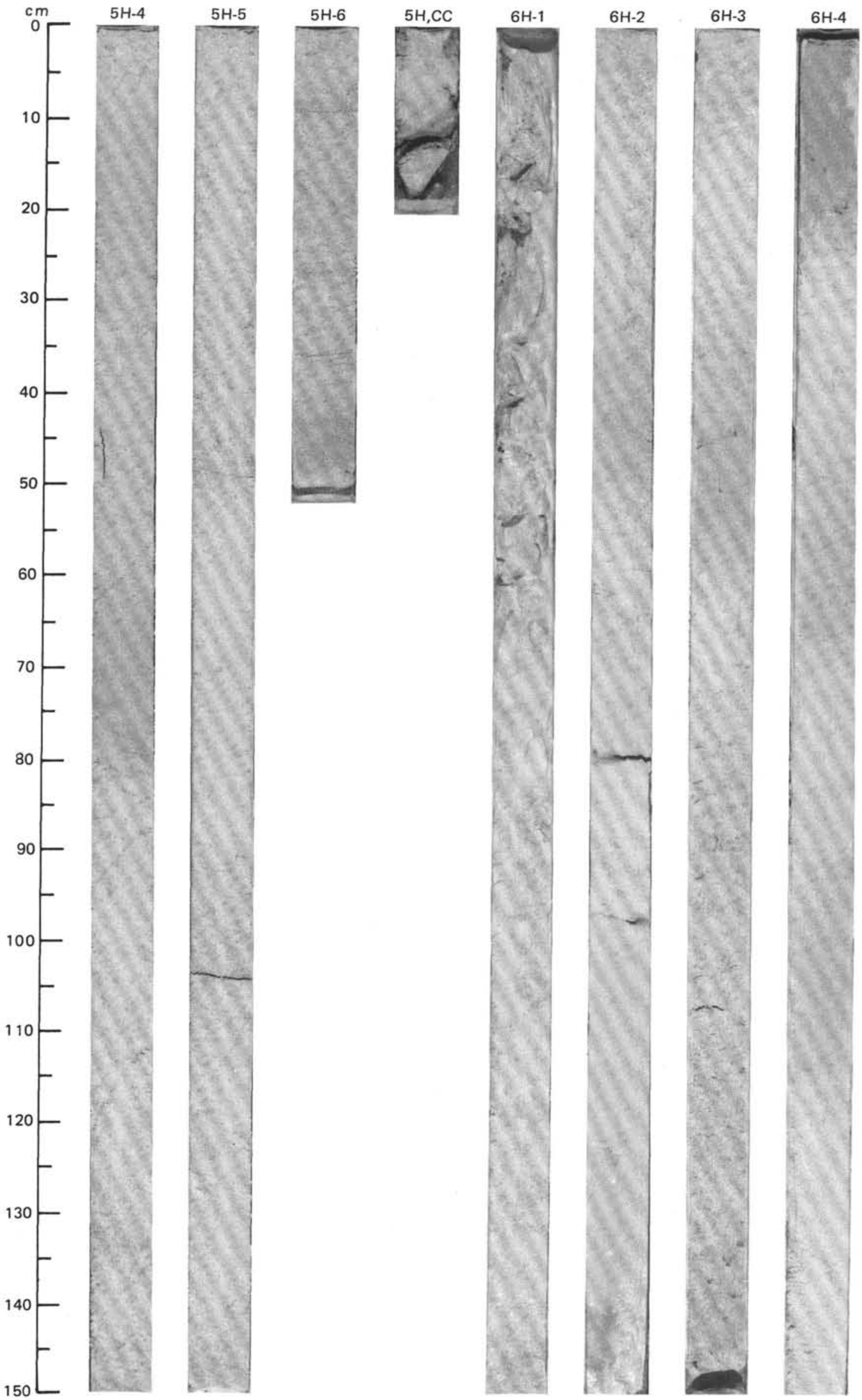
cm
0
10
20
30
40
50
60
70
80
90
100
110
120
130
140
150
5H-4
5H-5
5H-6
5H,CC
6H-1
6H-2
6H-3
6H-4

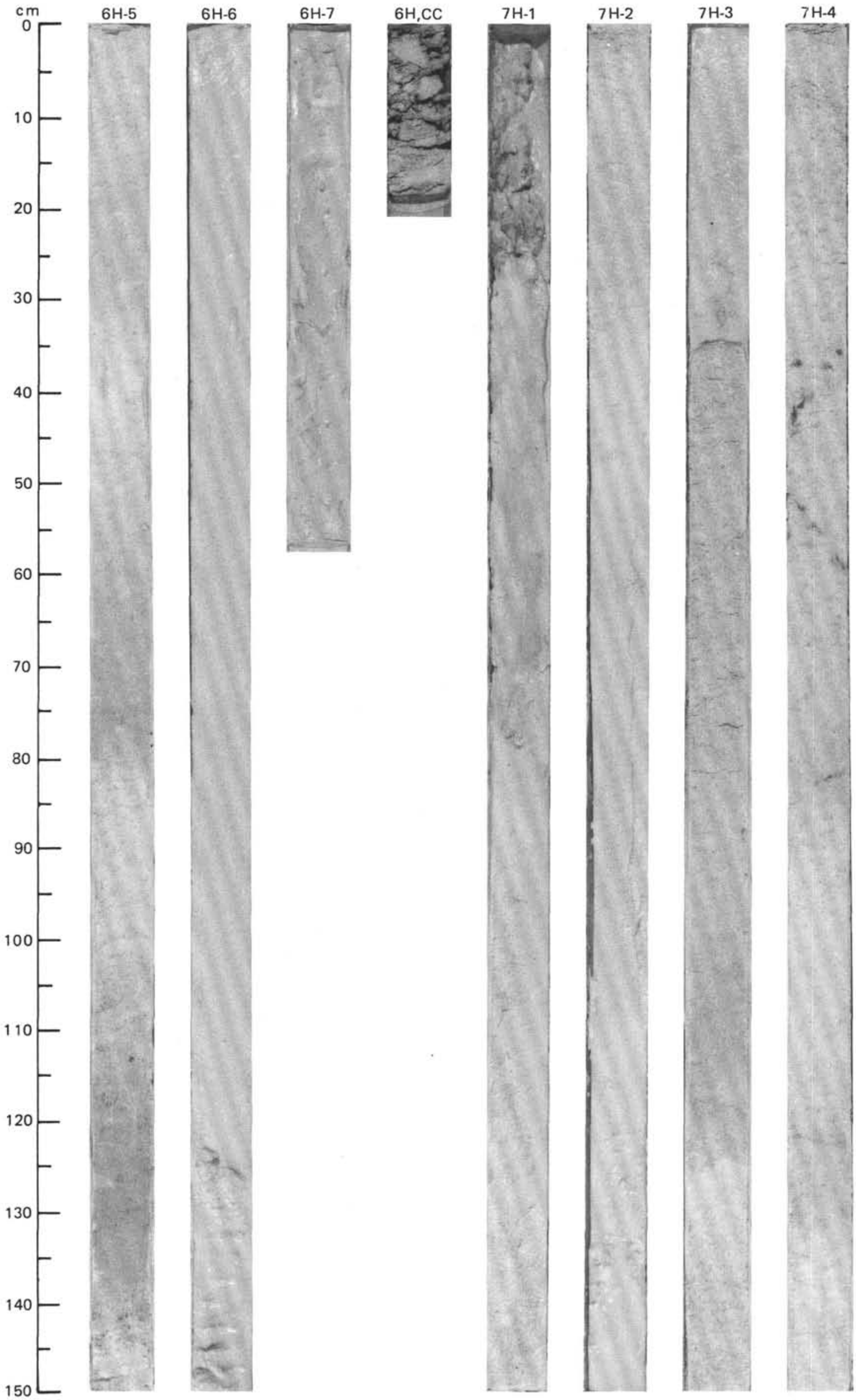
cm
0
10
20
30
40
50
60
70
80
90
100
110
120
130
140
150
6H-5
6H-6
6H-7
6H,CC
7H-1
7H-2
7H-3
7H-4

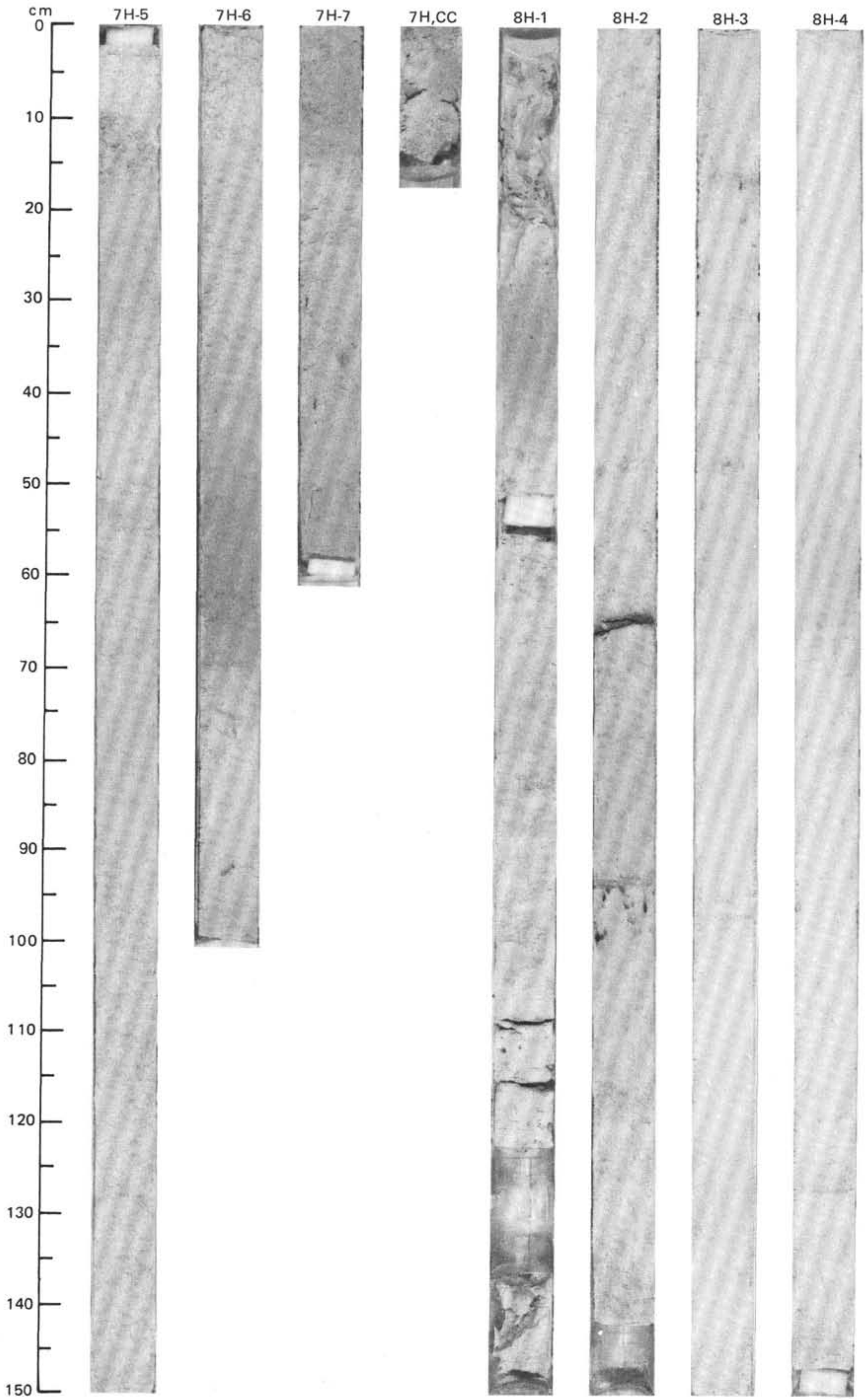
cm
0
10
20
30
40
50
60
70
80
90
100
110
120
130
140
150
7H-5
7H-6
7H-7
7H,CC
8H-1
8H-2
8H-3
8H-4

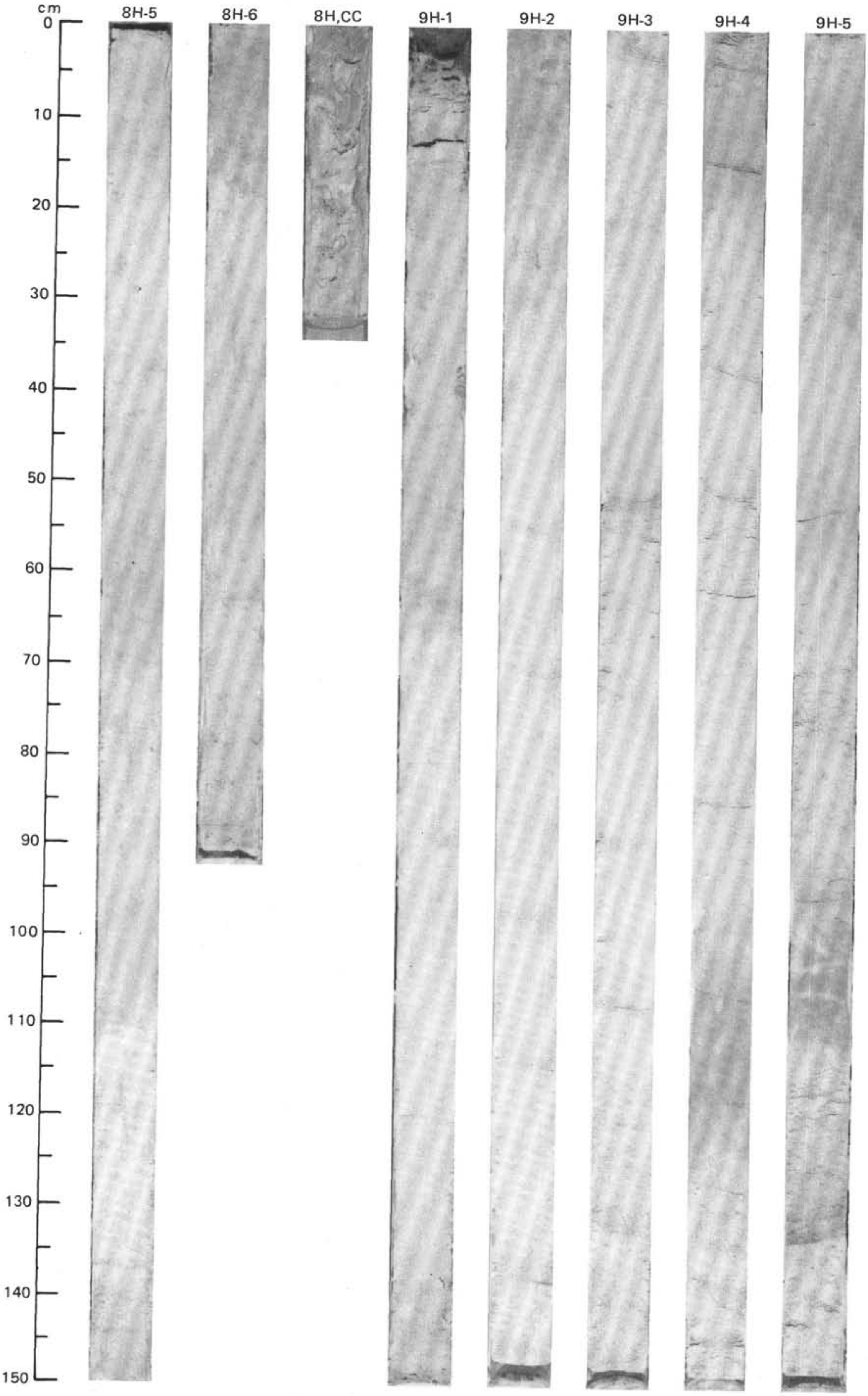
cm
0
10
20
30
40
50
60
70
80
90
100
110
120
130
140
150
8H-5
8H-6
8H,CC
9H-1
9H-2
9H-3
9H-4
9H-5

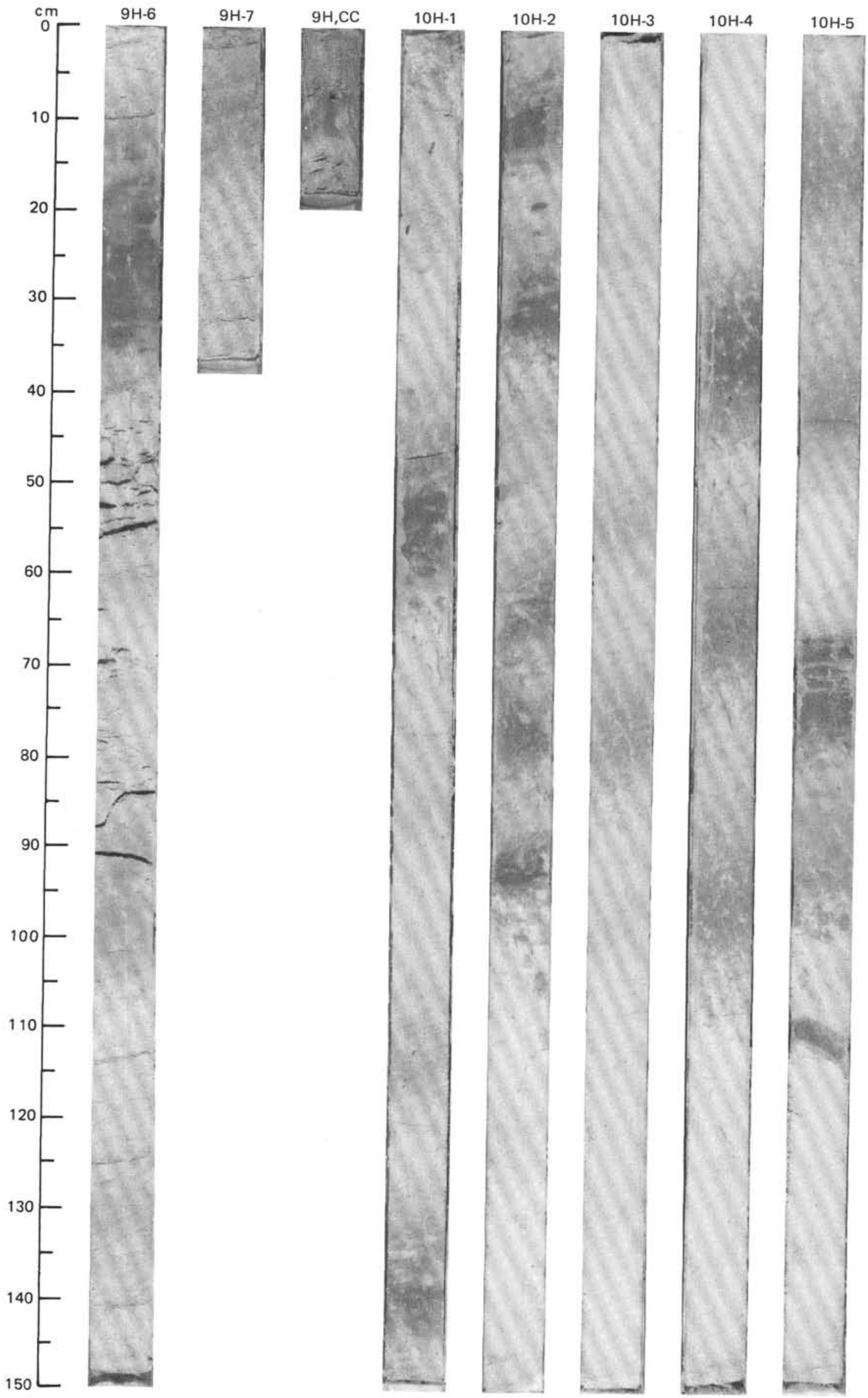
cm
0
10
20
30
40
50
60
70
80
90
100
110
120
130
140
150
9H-6
9H-7
9H,CC
10H-1
10H-2
10H-3
10H-4
10H-5

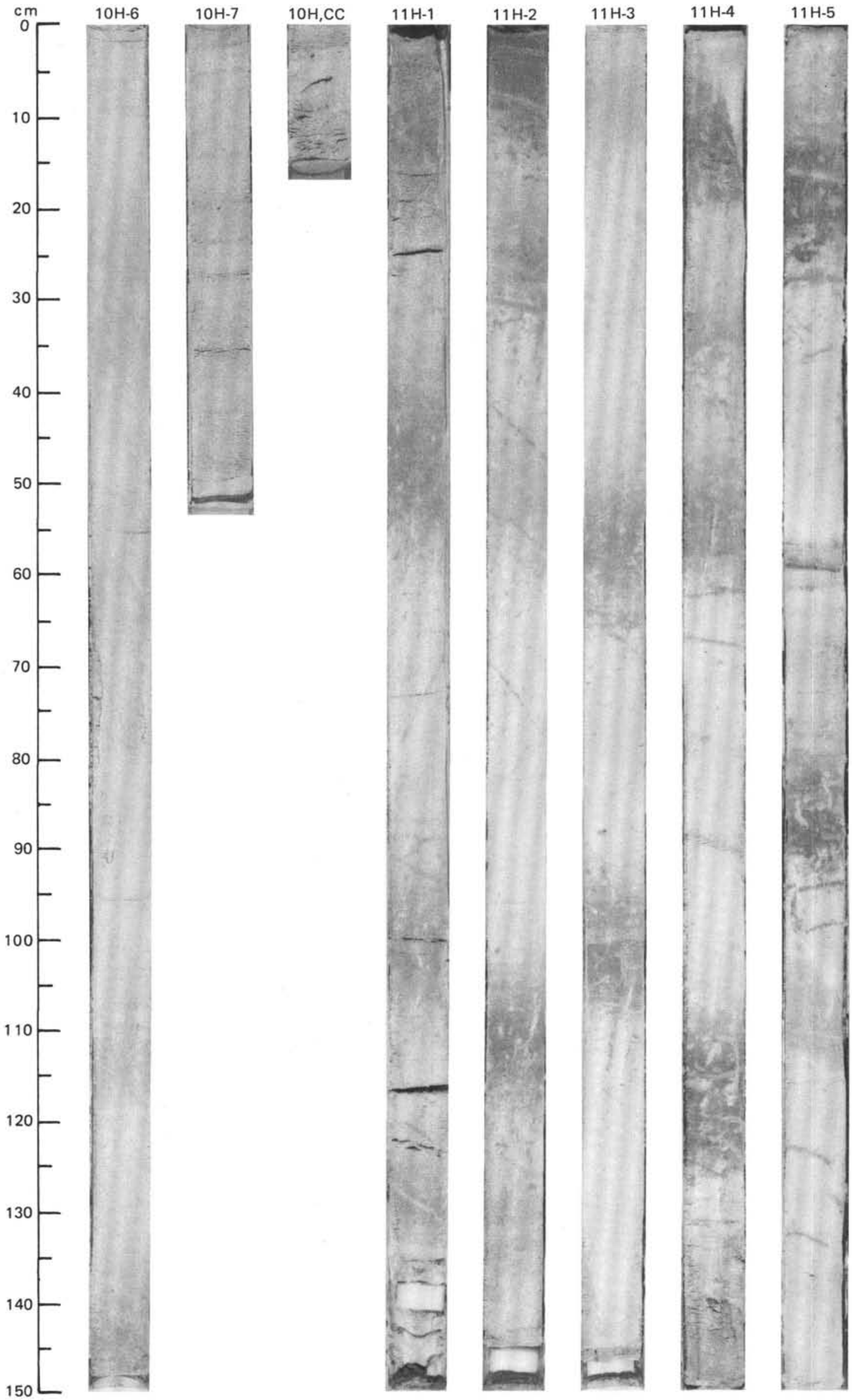
cm
0
10
20
30
40
50
60
70
80
90
100
110
120
130
140
150
10H-6
10H-7
10H,CC
11H-1
11H-2
11H-3
11H-4
11H-5

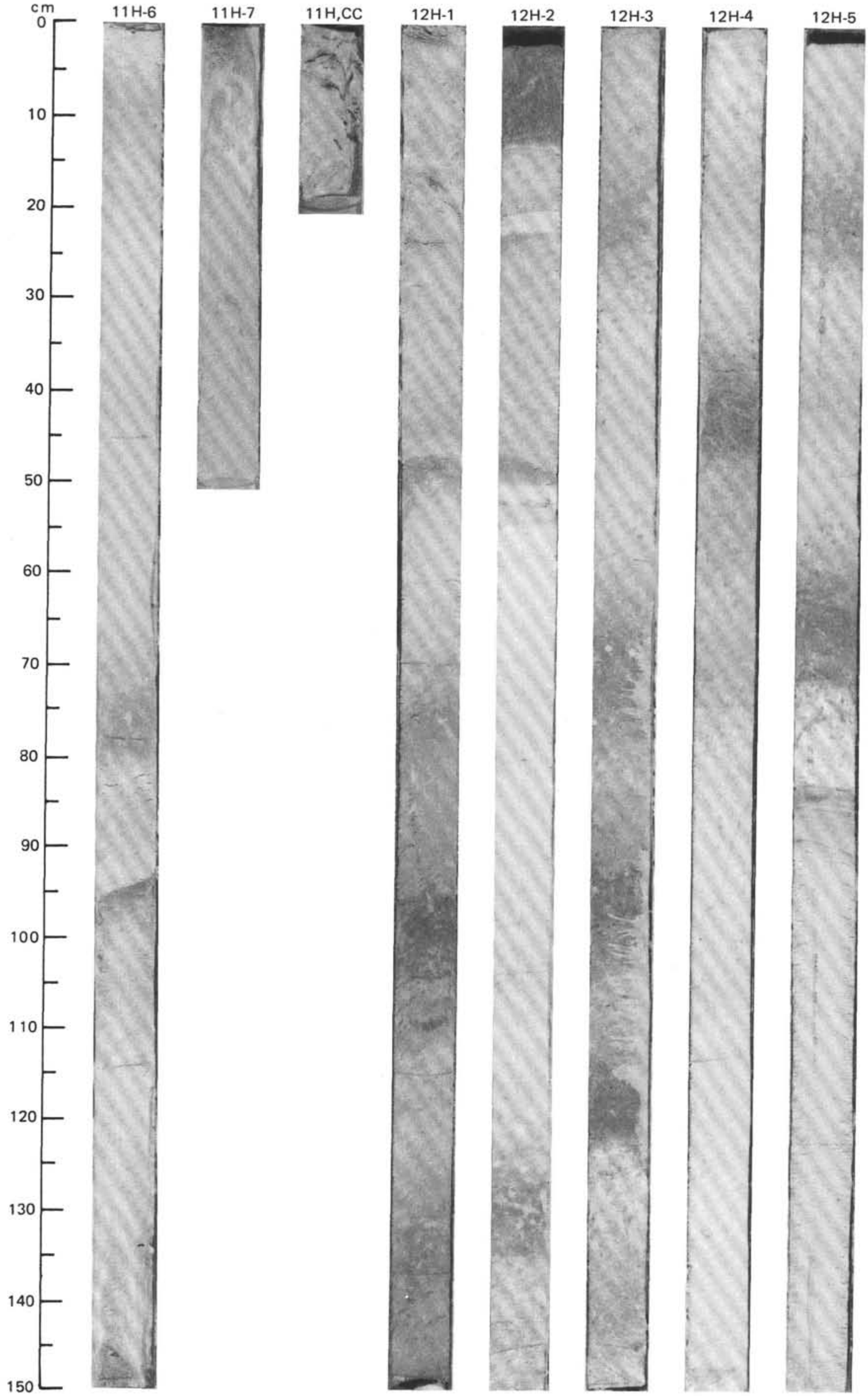
cm
0
10
20
30
40
50
60
70
80
90
100
110
120
130
140
150
11H-6
11H-7
11H,CC
12H-1
12H-2
12H-3
12H-4
12H-5

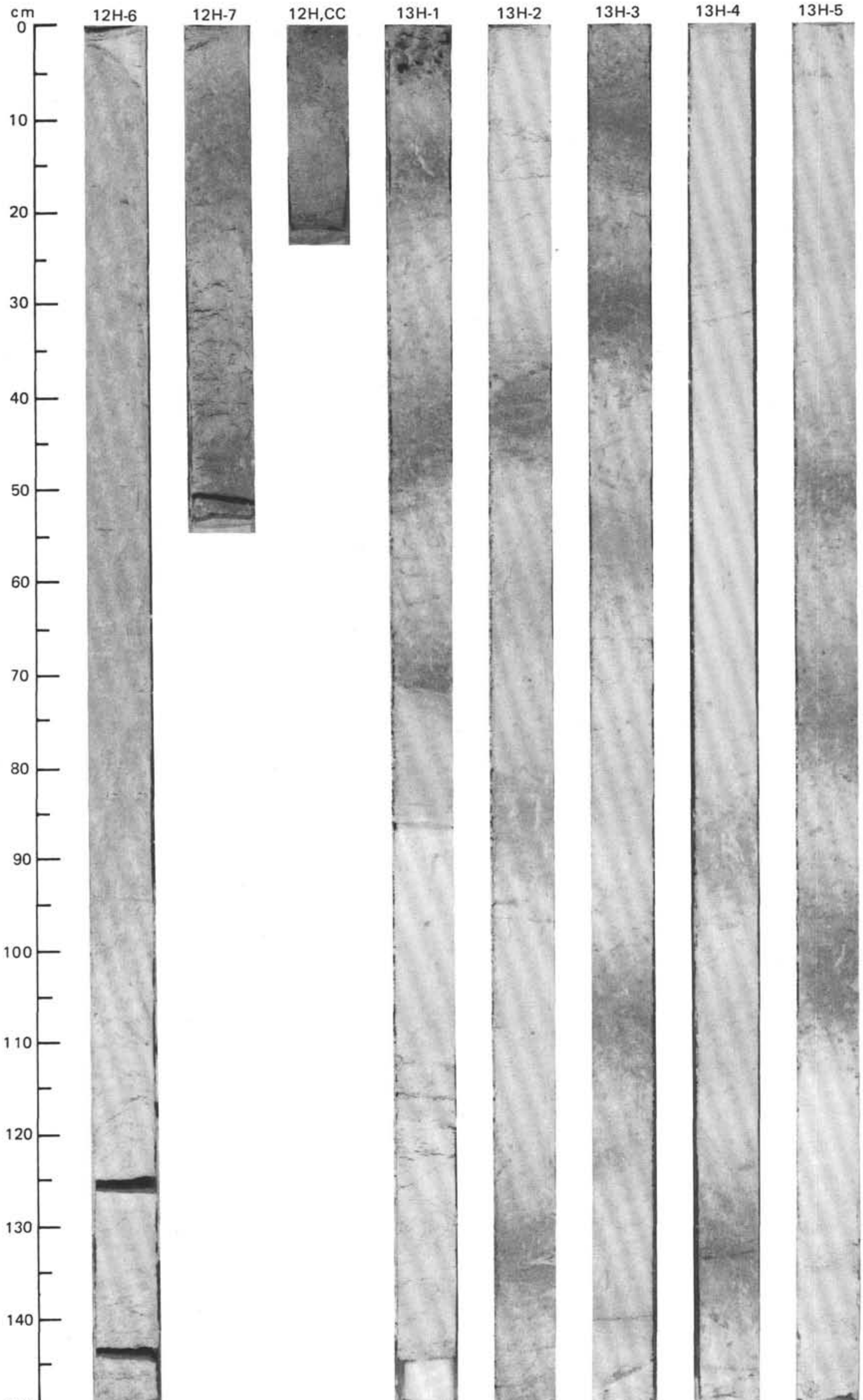
cm
0
10
20
30
40
50
60
70
80
90
100
110
120
130
140
150
12H-6
12H-7
12H,CC
13H-1
13H-2
13H-3
13H-4
13H-5

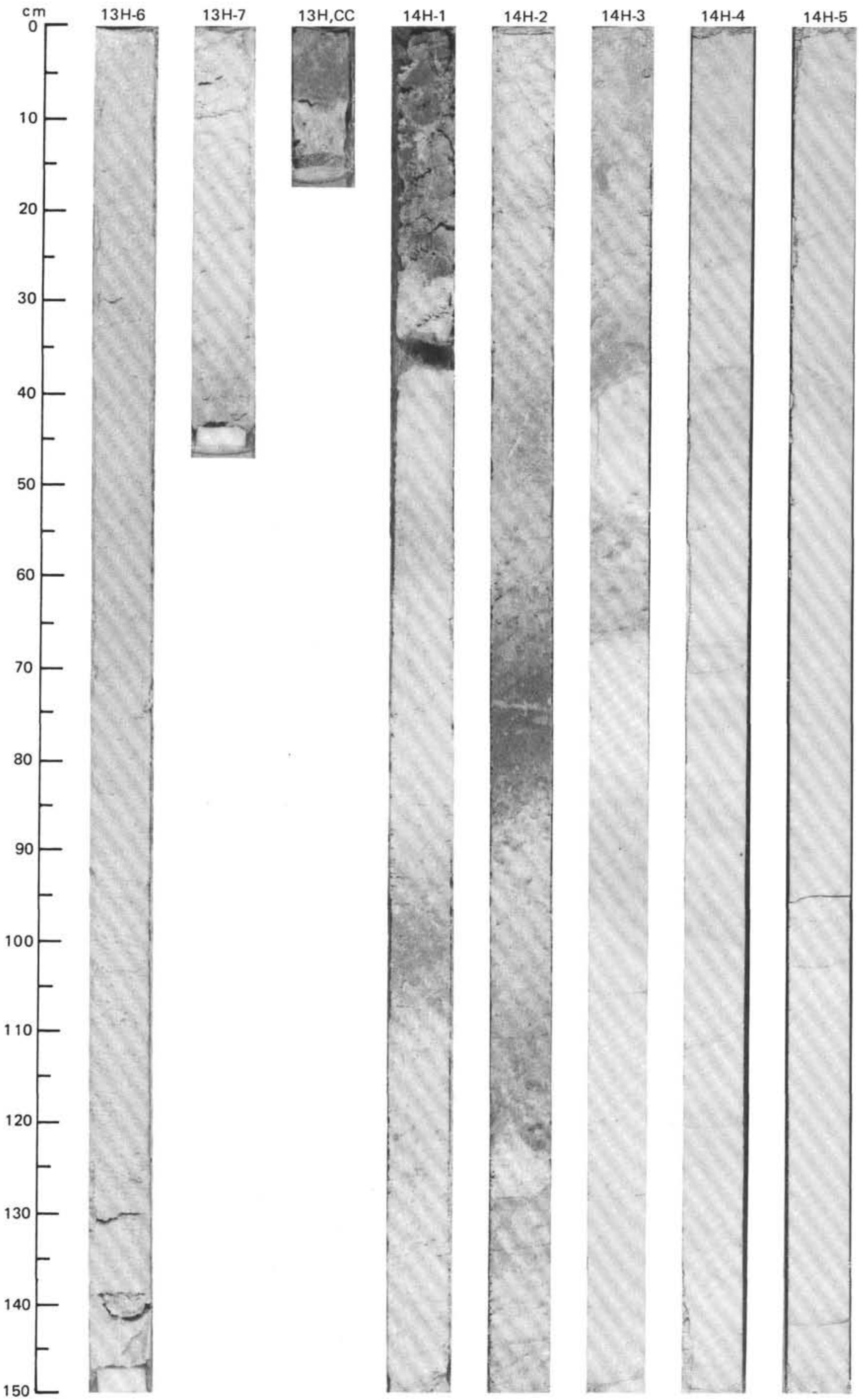
cm
0
10
20
30
40
50
60
70
80
90
100
110
120
130
140
150
13H-6
13H-7
13H,CC
14H-1
14H-2
14H-3
14H-4
14H-5

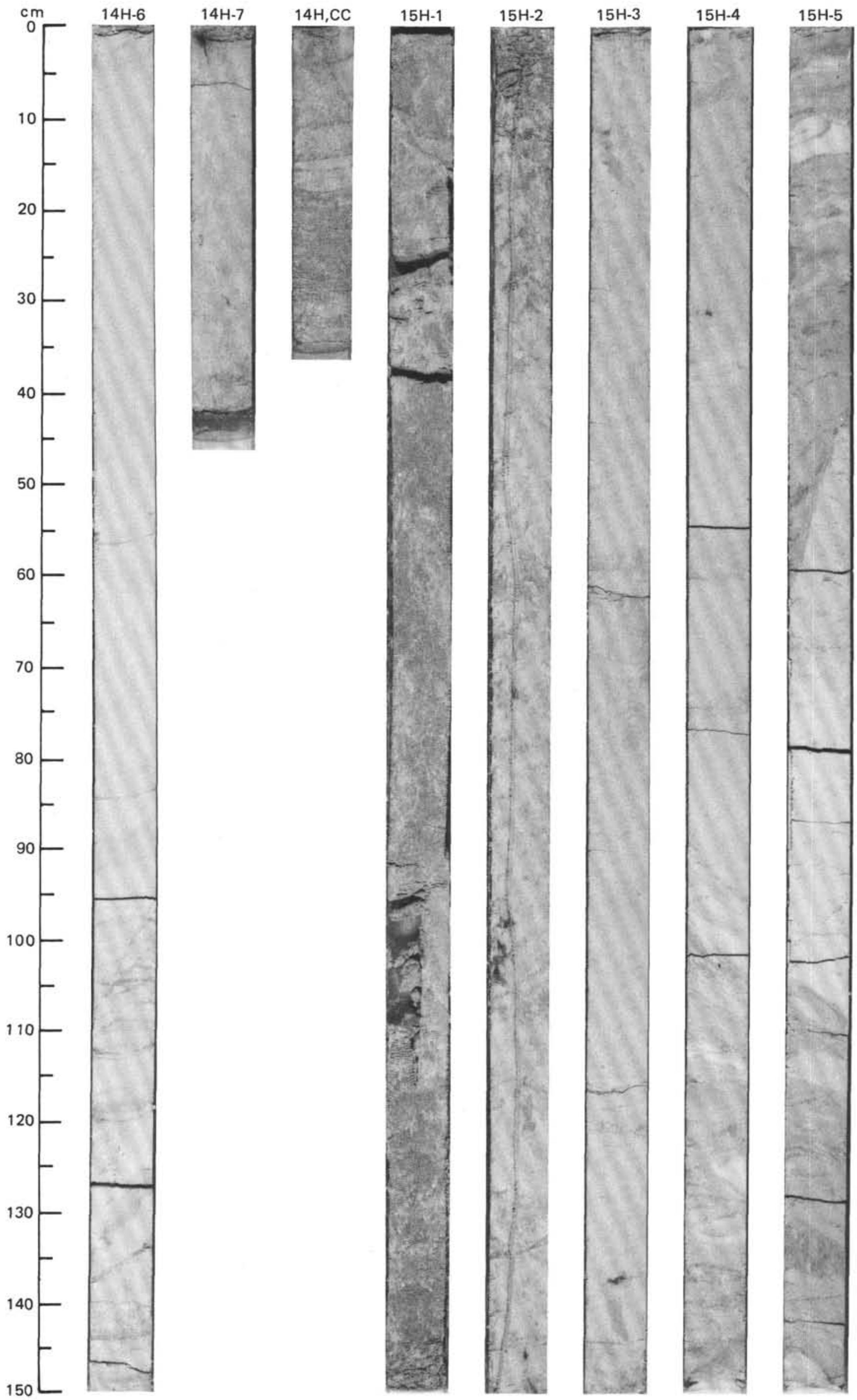
cm
0
10
20
30
40
50
60
70
80
90
100
110
120
130
140
150
14H-6
14H-7
14H,CC
15H-1
15H-2
15H-3
15H-4
15H-5

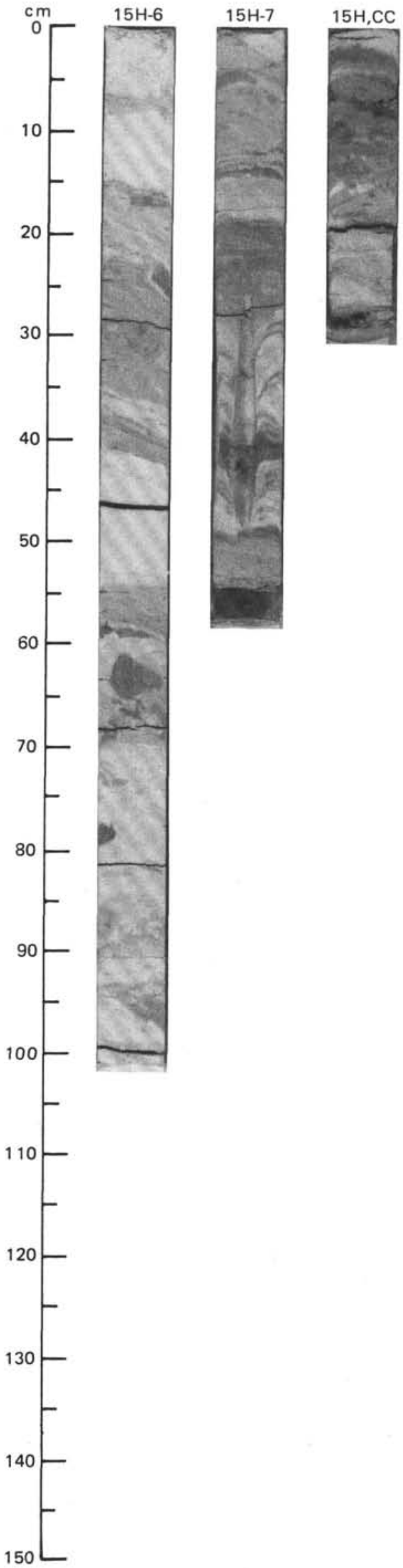
cm
15H-6
15H-7
15H,CC
0
10
20
30
40
50
60
70
80
90
100
110
120
130
140
150